UNIVERSITY OF SOUTHAMPTON

FACULTY OF MEDICINE

Cancer Sciences Unit

The contribution of ERAP1 & Natural Killer cells to the pathogenesis of Ankylosing Spondylitis

by

Dannielle Wellington

Thesis for the degree of Doctor of Philosophy

September 2016

UNIVERSITY OF SOUTHAMPTON

ABSTRACT

FACULTY OF MEDICINE

Cancer Sciences

Thesis for the degree of Doctor of Philosophy

THE CONTRIBUTION OF ERAP1 AND NATURAL KILLER CELLS TO THE PATHOGENESIS OF ANKYLOSING SPONDYLITIS

Dannielle Marie Wellington

Ankylosing Spondylitis (AS) is an autoimmune condition of the sacro-iliac region at the base of the spine. The pathogenesis of the disease is unknown despite strong genetic links with HLA-B27 and ERAP1. HLA-B27 is present in ~95% of AS patients and polymorphisms within ERAP1 have been shown to distinguish AS cases from controls. ERAP1 is an ER-resident aminopeptidase that trims peptides for binding to MHC Class I molecules, including HLA-B27, in antigen presentation to $CD8^+$ T cells. No specific peptides have been found to induce disease and the disease is unlikely to be $CD8^+$ T cell driven, suggesting that changes in the whole peptide repertoire may instead be important for disease generation through induction of other cell types. Natural Killer cells also interact with MHC Class I molecules through Killer immunoglobulin-like receptors and have been previously implicated in AS, with AS patients having higher percentages of natural killer cells in the peripheral blood than controls. Here I show that the sequence of the peptide bound to HLA-B27 can affect NK cell activation and begin to create a panel of amino acids at key positions that are activating or inhibitory. I have shown that AS-associated ERAP1 allotype combinations induce more NK cell activation than controls due to a reduction in cell surface FHC expression. Further to this I show how these changes in NK cell activation can alter the cytokine profile of the surrounding PBMC population. In addition I have looked into how different alleles of HLA-B27 are associated with disease and show that peptides bound to HLA-B*2709 can inhibit NK cell activation in an NK cell dependent manner, while peptide-B*2705 complexes bind NK cells in an ERAP1-independent manner. This work taken together provides some interesting possibilities to explain the events that lead to AS disease.

Table of Contents

List of Tables

List of Figures

DECLARATION OF AUTHORSHIP

I, ... [please print name]

declare that this thesis and the work presented in it are my own and has been generated by me as the result of my own original research.

[title of thesis] .....

.....

I confirm that:

1. This work was done wholly or mainly while in candidature for a research degree at this University;
2. Where any part of this thesis has previously been submitted for a degree or any other qualification at this University or any other institution, this has been clearly stated;
3. Where I have consulted the published work of others, this is always clearly attributed;
4. Where I have quoted from the work of others, the source is always given. With the exception of such quotations, this thesis is entirely my own work;
5. I have acknowledged all main sources of help;
6. Where the thesis is based on work done by myself jointly with others, I have made clear exactly what was done by others and what I have contributed myself;
7. [Delete as appropriate] None of this work has been published before submission [or] Parts of this work have been published as: [please list references below]:

Signed: .....

Date: .....

Acknowledgements

I would like to thank my supervisors Edd and Tim for constantly challenging me and pushing me through the past four years. This has not been easy and at times I have wanted to give up but I have come out the other end a better scientist, critical thinker and with more resilience than I could ever hope to have. Their approach to teaching me has led me to become an independent researcher and given me the experience and knowledge I need to tackle what comes next with confidence.

In addition, I would like to thank Salim for all of his invaluable support and help. Without being able to run to Salim when things weren't working I am sure this thesis would have been considerably smaller and much more unsubstantial. My thanks also go to Berenice who has been a sounding board for all of my silly ideas and questions in regards to those pesky NK cells, I appreciate the emails greatly.

Huge thanks go to Patrick, Leon and Nasia for their help, support and advice when it comes to all things protein purification and cloning. I would have been lost at sea without you all and I really appreciate all of the time and effort you have all taken with me. Thank you to Alastair for teaching me how to use Chimera and for providing the MHC I figure for my introduction.

Finally, I would like to thank my friends, family and partner for sticking with me while I have all but disappeared from your lives – especially this past year. I sincerely thank you and hope that you will all be waiting to see me again now I have finished. To my fellow PhD friends, these four years would have been impossible without you all and I know that this time together will bond us forever so I look forward to the fun times ahead and whatever may come in the future.

Abbreviations

ABC	ATP-binding cassette
ADCC	Antibody dependent cellular cytotoxicity
A-LAP	Adipocyte-derived leucine aminopeptidase
APC	Antigen presenting cell
AS	Ankylosing Spondylitis
$B27_2$	HLA-B27 homodimers
BCR	B cell receptor
BFA	Brefeldin A
BiP	Binding immunoglobulin protein
CEACAM	Carcinoembryonic antigen-related cell adhesion molecule
CLR	C-type lectin receptors
CRISPR	Clustered regularly interspaced short palindromic repeats
CTL	Cytotoxic T lymphocyte
DAP12	DNAX activation protein of 12kDa
DMEM	Dulbecco's modified eagle's media
dsRNA	Double stranded ribonucleic acid
EBV	Epstein Barr virus
EKO	ERAP1 knockout
ELISA	Enzyme linked immunosorbant assay
ER	Endoplasmic reticulum
ERAAP	ER aminopeptidase associated with antigen presentation
ERAP1	Endoplasmic reticulum aminopeptidase 1
FHC	Free heavy chain
FPLC	Fast protein liquid chromatography

GM-CSF	Granulocyte macrophage colony-stimulating factor
GWAS	Genome wide association study
HIV	Human Immunodeficiency virus
HLA	Human leukocyte antigen
hnRNP	Heterogeneous nuclear ribonucleoprotein
HPV	Human papilloma virus
HSV	Herpes Simplex virus
IBD	Inflammatory bowel disease
ICAM	Intercellular adhesion molecule
IFN	Interferon
Ig	Immunoglobulin
IL	Interleukin
ITIM	Immunoreceptor tyrosine-based inhibition motifs
kDa	Kilodaltons
KIR	Killer cell immunoglobulin like receptor
LAMP1	Lysosomal associated membrane protein
LMP	Low molecular weight protein
LPS	Lipopolysaccharide
MAC	Membrane attack complex
mAu	FPLC absorbance
MCP-1	Monocyte chemoattractant protein -1
MHC	Major histocompatibility complex
MHC I	MHC Class I molecules
MIP	Macrophage inflammatory protein
n.s.	Non-significant

NBD	Nucleotide binding domain
NCR	Natural killer cell receptor
NK	Natural Killer cell
NLR	Nod-like receptor
NSAID	Non-steroidal anti-inflammatory drug
PAMP	Pathogen-associated molecular pattern
pB27	Peptide HLA-B27 complexes
PBMC	Peripheral blood mononuclear cell
PCR	Polymerase chain reaction
PDI	Protein disulphide isomerase
P-LAP	Placental leucine aminopeptidase
PLC	Peptide loading complex
pMHC	Peptide MHC complex
RA	Rheumatoid arthritis
SCT	Single chain trimer
SHP-1	Src homology 2 domain tyrosine phosphatase -1
sICAM-1	Soluble intercellular adhesion molecule
SNP	Single nucleotide polymorphism
SpA	Spondyloarthritides
SSP-PCR	Short sequence primer PCR
TAP	Transporter associated with antigen processing
TCR	T cell receptor
TGFβ	Transforming growth factor β
Th (1/2/17)	$CD4^+$ T helper cell
TLR	Toll-like receptor

TNF	Tumour necrosis factor
TNFR	Tumour necrosis factor receptor
TRAIL	TNF-related apoptosis inducing ligand
Tregs	Regulatory T cells
UPR	Unfolded protein response
WT	Wild-type
β2m	Beta-2-microglobulin

Chapter 1: Introduction

1.1 Ankylosing Spondylitis

Ankylosing Spondylitis (AS) is a chronic autoimmune condition in which the immune system causes damage to the body, in particular the sacro-iliac region, however, the cause of this disease is currently unknown. It is one of a group of conditions known as Spondyloarthropathies (SpA) that includes psoriatic arthritis, reactive arthritis and arthritis complicating irritable bowel disease (IBD) (1). Its worldwide prevalence ranges up to 0.9% (2) and onset primarily occurs between 20-40 years of age, with a mean age of onset of 28.3 years. There is a sex bias with men more greatly affected than women at a 2-3:1 ratio. In addition, the disease pattern differs between the two sexes with the spine and pelvis most affected in males and a generally more severe disease progression. In contrast, women have symptoms more commonly in the knees, wrists, ankles, hips and pelvis and less severe involvement of the spine. Studies examining androgen receptor gene activity and X chromosome linkage analysis failed to identify an association to explain these differences (2). Genome wide association studies (GWAS) have shown that there is a strong association between AS and SNPs in *IL-23R* at chromosome 1p23, *ERAP1* at chromosome 5p15 and in the *MHC* genes on chromosome 6p (3, 4).

The earliest noticeable manifestation of the disease is sacroilitis, with additional involvement of peripheral joints and extra-articular structures. Investigation of the subchondral tissues revealed infiltration by plasma cells, lymphocytes, mast cells and macrophages causing the tissue to become granulomatous and leading to erosion and sclerosis of the joints. Over time, tissue is replaced by fibrocartilage and becomes ossified to create irreversible damage with the vertebrae becoming fused restricting movement. This process begins at the sacroiliac joint and can progress up the spinal column to form a long bony column that is commonly referred to as 'bamboo spine'. This phenomenon increases the chance of spinal fracture in patients that could lead to quadriplegia. Other complications include prostatis in males; aortic insufficiency and cardiac conduction disturbances in long term patients; and rarely amyloidosis, cauda equine syndrome and pulmonary fibrosis (2). AS is strongly associated with IBD with 70% of AS patients having microscopic terminal ileitis resembling Crohn's disease and 10% of IBD patients also suffering from AS (3).

Diagnosis of AS currently takes as long as ten years, mainly because the symptoms are shared by several other conditions, by which point irreversible damage of the tissue between the

vertebrae is likely to have occurred. Diagnosis is most commonly defined using the ASAS criteria for axial SpA. This is based on the presence of sacroiliitis on imaging together with at least one additional SpA feature, such as psoriasis, uveitis of HLA-B27 expression. In addition, as ~95% of AS patients are HLA-B27$^+$ diagnosis may be based on the patient being HLA-B27$^+$ together with the presence of two or more SpA features. However, these diagnostic criteria are only applicable in individuals with > 3 months back pain and an age of onset < 45 years. Based on these criteria the ASAS test has a sensitivity of 82.9% and specificity of 84.4%. The ASAS criteria is preferable to the previously used New York criteria since diagnosis was only possible if damage to the sacroiliac joint was observed by radiography (5).

Recently, Reeves *et al* have identified allotype combinations of ERAP1 that discretely identify AS patients from healthy controls (6). ERAP1 is an endoplasmic-reticulum (ER) resident aminopeptidase responsible for the N-terminal trimming of peptides for MHC Class I antigen presentation (7, 8). Potentially, the identification of the ERAP1 allotypes present in an individual could be used as a diagnostic method for disease but a larger cohort is required to confirm this as well as improvements in the ease of ERAP1 allotype sequencing from patients. The contributions of both HLA-B27 and ERAP1 to disease pathogenesis are key areas of focus in this work and will be discussed in greater detail below.

Current treatment for AS includes the use of non-steroidal anti-inflammatory drugs (NSAIDs) that suppress the inflammation associated with the disease (1). These treatments can be tailored to help individuals due to the range of effects they have, for example diflunisal provides rapid analgesic effects, while phenylbutazone helps to increase spinal motility. Importantly, these treatments target the symptoms rather than the cause and do not effect progression of the disease or prevent structural damage (2). Anti-TNFα treatment for AS, using the infliximab monoclonal antibody, was shown to regress disease activity in at least 50% of AS patients compared with only 9% of placebo controls. Within this study three patients had to stop treatment because of systemic tuberculosis, allergic granulomatosis of the lung, or mild leucopoenia, raising slight questions about the tolerance of this treatment (9). However, patients who tolerated treatment were followed up after three years of treatment and no further exclusions had occurred and disease progression was still controlled (10). Anti-TNFα treatment is now the first treatment for AS, but it is still unknown why this only works in ~50% of patients.

1.1.1 HLA-B27 association with AS

For over 40 years there has been a strong correlation between disease onset and presence of the MHC Class I molecule HLA-B27; however the nature of this link remains a mystery. The *HLA-B27* gene accounts for 37% of the total genetic risk of the disease (11) with >90% of AS patients being HLA-B27 positive but only 1-5% of the HLA-B27 positive population developing AS (1). All HLA-B27 subtypes evolved from HLA-B*2705 through nucleotide substitutions in exons 2 and 3, which respectively encode the α1 and α2 domains of the peptide-binding groove (4). There are currently 23 identified subtypes of HLA-B27 and those which are associated with disease differ by only one or two amino acids at the bottom of the peptide binding groove from those which do not cause disease (2). As an example, the two non-AS-associated alleles are shown compared to AS-associated HLA-B*2705, B*2703 and B*2704 (**Table 1:1**). HLA-B27 positive individuals are better at clearing viral infections like hepatitis C and HIV but cope less well with bacterial infections (4). This suggests that a bacterial infection could be a trigger for AS, potentially triggering an advanced immune response due to molecular mimecry.

Table 1:1: Allelic differences in HLA-B27

Subtype	Amino acid position				
	59	*77*	*114*	*116*	*152*
B*2705	Y	D	H	D	V
B*2703	**H**	D	H	D	V
B*2704	Y	**S**	H	D	**E**
B*2706	Y	**S**	**D**	**Y**	**E**
B*2709	Y	D	H	**H**	V

For an MHC class I molecule, HLA-B27 displays some unusual characteristics. It has a tendency to fold more slowly in the ER and has lower association with β2m that can lead to misfolding and an increase in the unfolded protein response (UPR) within cells. UPR acts to remove accumulated protein without adding to the stress already put on the ER, so that normal function can be resumed as soon as possible (12). In addition, HLA-B27 has a high tendency to dissociate from β2m resulting in the presence of free heavy chain (FHC) forms at the cell surface. These FHCs can remain singular or can aggregate through an unpaired cysteine residue at position 67 to form B27-homodimers ($B27_2$). $B27_2$ can interact with additional receptors compared with β2m-associated B27 (13), such as the NK receptor KIR3DL2 (14), as well as triggering the UPR in

the ER and increasing the secretion of inflammatory cytokines due to ER stress (15). It has been shown that there are a significantly increased number of FHC structures on monocytes from HLA-B27 positive patients with a Q730 in ERAP1 compared to patients with E730 (16).

1.1.2 ERAP1 association with AS

ERAP1 is the strongest non-MHC gene associated with AS, with an estimated population attributable risk of 26% (17), with this association only evident in HLA-B27$^+$ disease. First discovered in 1999 through a search of public databases for novel peptidases with sequence similarity to the already discovered placental leucine aminopeptidase (P-LAP), adipocyte-derived leucine aminopeptidase (A-LAP) was found to be made up of 941 amino acids, with a calculated molecular weight of 107kDa, and 43-45% homology with P-LAP at both the nucleotide and the amino acid level. This sequence contained an essential zinc binding motif, HEXXHX_{18}E, as well as the catalytic GAMEN motif (18). Subsequently, Cui *et al* identified the *ARTS-1* aminopeptidase as a protein that promotes tumour necrosis factor receptor-1 (TNFR1) shedding on human epithelial and endothelial cells through direct interaction with the TNFR1 extracellular domain. This aminopeptidase was also made up of 941 amino acids with a calculated molecular weight of 107kDa, and was later confirmed to be the same protein as A-LAP (19). In 2002, this protein was isolated from the ER lumen and shown to be capable of trimming various N-terminally extended peptides to a length suitable for MHC I loading. Due to this ER localisation it was suggested that the protein be renamed endoplasmic reticulum aminopeptidase 1 (ERAP1) (7). This is now the name used in all publications and has replaced the previous designations: A-LAP, ARTS-1, PILS, PILS-AP and APPILS.

ERAP1 is a member of the M1 family of zinc metalloproteases having 45-49% homology with other members of this family along with the highly conserved HEXXHX_{18}E motif (7, 20). It is the main aminopeptidase responsible for the trimming of antigenic peptides for presentation on MHC I within the ER (7, 21). In mice this protein is named the ER aminopeptidase associated with antigen presentation (ERAAP) and it shares 86% homology with ERAP1 (22). ERAAP is the only aminopeptidase which generates pMHC complexes in mice, but humans have a second aminopeptidase, ERAP2, which shares 51% identity (22). ERAP2 has complementary N-terminal specificity to ERAP1 and is thus proposed to have an accessory role in peptide trimming (23). The trimming function of ERAP1 was found to be critically dependent on the GAMEN motif within the catalytic domain through an E320A mutation that altered this motif to GAMAN and showed a

dramatically reduced trimming function (24). ERAP1 can be induced in a dose-dependent manner by IFNγ at a transcriptional level (7). ERAP1 has been found to have very specific length requirements with the greatest trimming efficiency on peptides between 9-14 amino acids. Interestingly, ERAP1 has very little or no activity against peptides shorter than the 8 or 9 residues that are required to fit into the peptide groove for MHC class I presentation (21).

Loss of ERAP1 expression through gene knockout in mice results in a ~30-40% reduction in H-2K^b and H-2D^b MHC I cell surface expression levels, respectively (25). In addition, the expression of the non-classical Qa-2 MHC molecule was reduced (26). No other ER-luminal aminopeptidase, including ERAP2, could compensate for the loss of ERAP1 and restore presentation of selected N-terminally extended peptides indicating the primary role of ERAP1 in generating MHC I binding peptide epitopes (8, 26). Analysis of the peptide repertoire in ERAP1 knockout cells showed an altered selection of peptides presented at the cell surface with some epitopes increased, some decreased and some novel peptides presented (8, 22, 25). Loss of ERAP1 increased the percentage of peptides longer than 9 residues from 24% to 42% and peptides longer than 10 residues from 16% to 57% (27). In addition, novel pMHC complexes were presented in the absence of ERAP1 that were structurally distinct from conventional pMHC complexes and elicited potent CD8$^+$ T cell and B cell responses (25, 28).

ERAP1 is a highly polymorphic protein with several common single nucleotide polymorphisms (SNPs) present in the population. These SNPs can affect the trimming function of ERAP1 and alter the peptide repertoire. Specifically, the polymorphisms R725Q/Q730E create a 'hyperfunctional' ERAP1 protein which can trim peptides past the point of 8 or 9 amino acids, thus making them too short for MHC I presentation; while the K528R polymorphism creates a 'hypofunctional' ERAP1 protein which is inefficient at cleaving peptides (29). ERAP1 cannot cleave N-terminal amino acids that are directly adjacent to a proline residue (X-Pro) but can cleave all other bonds (20). Intriguingly, this X-Pro sequence also cannot be transported by TAP into the ER (22). Genome wide association studies (GWAS) have found genetic links between ERAP1 and the autoimmune conditions AS (2, 3, 11), type I diabetes (30), psoriasis (31) and multiple sclerosis (32). ERAP1 has also been linked to human Papilloma virus (HPV) linked cervical carcinoma (33) (**Table 1:2**).

Table 1:2: Disease association of GWAS SNPs in ERAP1

SNP	Amino acid change	Disease association
rs3734016	E56K	HPV-associated cervical carcinoma
rs26653	R127P	Ankylosing spondylitis, HPV-associated cervical carcinoma
rs2287987	M349V	Ankylosing Spondylitis
rs30187	K528R	Ankylosing spondylitis, psoriasis, essential hypertension, multiple sclerosis
rs10050860	D575N	Ankylosing spondylitis, Behçet's disease
rs17482078	R725Q	Ankylosing spondylitis, Behçet's disease
rs27044	Q730E	Ankylosing spondylitis, HPV-associated cervical carcinoma

A number of GWAS studies identified several ERAP1 SNPs as associated with AS. A meta-analysis of these studies with 8,530 AS patients and 12,449 controls found five ERAP1 polymorphisms associated with AS susceptibility: rs27044 (Q730E); rs17482078 (R725Q); rs10050860 (D575N); rs30187 (K528R); and rs2287987 (M349V) (34). Investigation of the effect of these polymorphisms on ERAP1 function revealed R528, which has the strongest AS association together with E730, has reduced aminopeptidase activity compared to K528. The R725Q, M349V and Q730E mutations have also been shown to decrease ERAP1 activity, while the D575N mutation has been shown to increase trimming activity (35). How these polymorphisms confer their effects on peptide trimming are not known, however, positions 528 and 575 are located in domain III of ERAP1 and are thought to be important residues in transition of the enzyme from an open to a closed conformation. Positions 725 and 730 are located in domain IV within the proposed substrate binding pocket and may affect peptide specificity (36). Position 349 is located within the active site and although it is unlikely to interact with the peptide substrate directly it may alter the ability of the enzyme to form the correct catalytic conformation (29).

Since HLA-B27 and ERAP1 interact in the MHC I processing pathway it is likely that ERAP1 activity affects HLA-B27 expression or presence at the cell surface. The levels of cell surface HLA-B27 FHC varies in AS patients depending on the polymorphisms they have within ERAP1; however this does not correlate with the trimming activity of ERAP1. For example, E730 is a poor trimmer of peptide and shows increased FHC levels, but R528, which is also a poor trimmer, has little effect on FHC levels (6).

1.1.3 Animal models of AS disease

Slow progress in diagnosis, treatment and determination of the pathogenesis of AS could be largely attributed to the spinal location of the disease making it near impossible to obtain patient samples and the lack of a robust animal model of disease. There are currently 7 mice and 1 rat model of disease but none of these truly mimic the human disease (**Table 1:3**). Despite this, important information can be gleaned from these animal models. HLA-B27 transgenic mice do not develop spontaneous inflammatory disease unless in the absence of beta-2-microglobulin (β2m), suggesting that the disease may be associated with the homodimer form of HLA-B27 (37). In the rat B27/ β2m transgenic model, disease occurs in the presence of a high number of these genes and is not $CD8^+$ T cell dependent (38). These two models fail to confirm the role of antigen presentation or HLA-B27 folding in disease progression, but do suggest that Th17 play a role in AS pathogenesis due to the high expression of IL-17 in the rat B27/ β2m transgenic model coinciding with the onset of colitis (39). Animal models targeting TNF expression confirmed the role of TNF in disease and allowed investigators to determine that the strongest TNF effects were against stromal or fibroblast-like cells in arthritis models. Other models have targeted the ankylosis phenotype of disease or the inflammatory component (40). While these models all provide an insight into particular areas of disease, none can truly represent the disease and therefore the information on how pathogenesis begins remains a mystery.

Table 1:3: Animal models of AS

Model	Arthritis	Enthesitis	Spondylitis	Ankylosis
HLA-B27 $\beta2m^{-/-}$ tg mice	Destructive	Yes	No	Yes
HLA-B27 human β2m tg rats	Destructive	Yes	Yes	Yes
Murine ANKENT	Remodelling	Yes	No	Yes
Ank/ank mice	Remodelling	?	Yes	Yes
$TNF^{\Delta ARE}$ mice	Destructive	Yes	Yes	No
Human TNF tg mice	Destructive	Yes	Yes	No (Yes after anti-DKK-1 treatment)
Spontaneous AE in aging male, DBA/1 mice	Remodelling	Yes	No	Yes (inhibited by blocking of BMPs)
PGIA	Destructive	Yes	Yes	No

1.2 The Human Immune System

As an autoimmune disease, there is a large immune response in AS that drives the symptoms and spinal destruction. The human immune system is a complex, highly diverse system purposed with protecting the host from invading pathogens through destruction of the pathogen as well as any infected host cells, in addition to clearance of mutated and oncogenic cells to limit cancer generation. In autoimmune diseases this naturally protective system can become over activated against the host and cause large damage. The immune system consists of two arms, the innate and the adaptive response.

The innate system acts rapidly and without discrimination, while the adaptive system takes two to three days to generate a robust response specific to the pathogen encountered. The innate immune system is considered to have evolved earlier than the adaptive system as it is found in all multicellular organisms, whereas adaptive immunity is only present in vertebrates. This innate system distinguishes between self and non-self through pattern recognition receptors (PRRs) such as Toll-like receptors (TLRs), Nod-like receptors (NLRs) and C-type lectin receptors (CLRs), which recognise pathogen-associated molecular patterns (PAMPs) on invading pathogens. These PAMPs can vary between pathogens but are usually distinct for pathogen families and are not usually found in the host organism, for example; the general structure of lipopolysaccharides (LPS) and teichoic acids are shared by all gram-negative and gram-positive bacteria, respectively; unmethylated CpG is characteristic of bacterial DNA; double-stranded ribonucleic acid (dsRNA) is only found in dsRNA viruses; and mannans are conserved components of yeast walls. The recognition of PAMPs can lead to induction of signals that mediate inflammation (e.g. IL-1, TNFα, IL-6, type I IFNs), control the induction of effector functions (e.g. IL-4, IL-5, IL-10, IL-12, TGFβ and IFNγ), and function as a co-stimulatory signal for T cell activation (CD80/B7.1 and CD86/B7.2) (reviewed in (41)).

Innate immune cells derive from myeloid progenitor cells and differentiate into neutrophils, eosinophils, basophils, mast cells or monocytes. Monocytes can then further differentiate into macrophages and dendritic cells both of which are classed as professional antigen presenting cells (APCs). Macrophages are capable of engulfing and killing microbes; they recruit other myeloid cells to the site of infection and initiate the adaptive immune response through antigen presentation on major histocompatibility complex (MHC) class II molecules (42).

Adaptive immunity is mediated by T- and B-lymphocytes that direct a cell-mediated or antibody-mediated response, respectively. Both cells derive from a lymphoid progenitor and get their name from the site at which they mature: T cells in the thymus, B cell in the bone marrow. Both cell lines are highly adaptable due to somatic hypermutation and recombination of the variable (V), diversity (D) and junction (J) regions of the TCR and B cell receptor (BCR). The TCR is responsible for the activation of T cells. BCR ligation can activate B cells to produce antibodies that can then opsonise pathogens, highlight infected cells for destruction or activate complement. The adaptive immune system has immunological memory, an important feature in the case of re-infection with the same pathogen.

1.2.1 Innate Immune mediators implicated in AS

Neutrophils are the most abundant white blood cells in the body and are short-lived, highly mobile cells. They are phagocytes capable of ingesting microorganisms and killing them within phagosomes containing hydrolytic enzymes and reactive oxygen species. They also release granules containing proteins such as cathepsin, lactoferrin and defensins which kill the invading pathogen (43). The neutrophil-to-lymphocyte ratio has been suggested as a diagnostic tool for identification of AS disease as a higher ratio was found in patients compared to controls (44). This is a promising idea for diagnosis as it could be done with a simple blood test and therefore minimal disruption to the patient. This ratio could also be used to determine the patient response to anti-TNFα treatment.

Another innate defence mechanism is controlled by a group of blood proteins called complement. The complement cascade is activated in response to antibodies (classical pathway), serum proteins binding to mannose on bacterial cell surfaces (mannose-binding lectin pathway) or directly by bacterial cell surfaces (alternative pathway) (45). All three pathways lead to the cleavage of C3, the central component of complement, which functions as an opsonin, tagging pathogens and immune complexes for recognition and uptake, which is mediated by specific complement receptors on phagocytic cells. Subsequent activation of the terminal complement pathway, known as the membrane attack complex (MAC), leads to cell lysis (46). Complement activation in AS has been previously demonstrated by the detection of significantly elevated complement components or activation products including C3, C4 and C3d, and by the complement activation triggers including IgA, IgG, C-reactive protein (CRP), serum amyloid A, apolipoprotein A (47-50). Among these triggers, the cross-reactive antibodies against

autoantigens such as Klebsiella, when present in high titres, may activate the classical complement cascade (51). Recently, Yang *et al* showed that inhibition of the complement cascade reduced the progression of disease in a mouse model (52).

1.2.2 Natural Killer Cells

Lymphoid cells derive from a subpopulation of multipotent $CD34^{+}$ hematopoietic progenitor cells that give rise to B, T and NK cells. Commitment to the NK cell lineage is associated with the loss of CD34 and the acquisition of natural cytotoxicity receptors (NCRs) (53). NK cells express CD16 which facilitates antibody dependent cell cytotoxicity (ADCC) through detection of antibody coated targets, and CD56 which has a role in cell-cell adhesion and homing to sites of inflammation (54). Mature NK cells express a $CD56^{bright}$ $CD16^{-}$ or $CD56^{dim}$ $CD16^{+}$ phenotype with both subsets carrying out differing functions (55) (

Table 1:4). Human NK cells comprise around 10-15% of peripheral blood mononuclear cells (PBMCs) where they circulate for around 2 weeks (56). The majority of NK cells in the peripheral blood, ~90%, are the $CD56^{dim}$ $CD16^{+}$ subset which produce low levels of cytokines but possess an abundance of cytolytic granules for target cell lysis (57).

Transforming growth factor β (TGF-β) (58) and regulatory T cells (Tregs) can regulate NK cell functions in both humans and mice (59, 60). IL-15 and IL-2 are essential for driving NK cell development in the lymph nodes and bone marrow. These cytokines activate multiple intracellular pathways, including JAK/STAT, MAP kinase and PI3K, which in turn activate several transcription factors. Mice deficient in IL-15 production generate virtually no mature NK cells and normal NK cells die soon after transfer into these mice (61).

Table 1:4: Difference between $CD56^{bright}$ and $CD56^{dim}$ NK cells

	$CD56^{bright}$ $CD16^{-}$ NK cells	**$CD56^{dim}$ $CD16^{+}$ NK cells**
Location	Mostly hepatic sinusoid of the liver	Periphery
Effector functions	More adept at producing cytokines and contain less cytotoxic granules	Generally produce large quantities of cytotoxic granules and release minimal cytokines. ADCC
Receptor expression	CCR7. β2 (CD18) integrins, LFA-1 & Mac-1 and the β1 integrins, VLA-4 and VLA-5. CD31 and sialylated LeX structures.	CXCR1 and ChemRβ2 (CD18) integrins LFA-1 & Mac-1 and the β1 integrins, VLA-4 and VLA-5. CD31 and sialylated LeX structures.

NK cells express a wide range of additional receptors for activation and inhibition (**Figure 1.1**) that can be divided into three classes; the Ig-like receptors (KIRs, LILRs, LIRs); the lectin-like receptors (CD96/NKG); and the natural cytotoxicity receptors (NCRs) (NKp30, NKp44, NKp46) (62). Through their KIRs and the CD94/NKG2 system, NK cells can selectively attack target cells with reduced classical or non-classical MHC I expression, respectively (63). Some NK cells also express ILT-2 (LIR-1) a member of the ILT family with a broad specificity for MHC class I (MHC I), although these receptors are primarily expressed on dendritic cells and B cells (64).

NCRs are type I membrane proteins belonging to the immunoglobulin superfamily composed of an extracellular ligand binding domain, a trans-membrane domain and a short cytosolic domain. Upon receptor ligation, a charged residue in the trans-membrane domain associates with CD3ζ and/or FcεRγ to generate an activation signal for NK cells (65). NKp46 crosslinking on NK cell surfaces can lead to calcium ion mobilisation, cytotoxicity and cytokine release. NKp44 expression is induced by IL-2; making this receptor a marker of activated NK cells. NKp30 works in concert with NKp44 and NKp46 to induce cytotoxicity against a variety of target cells. The function of NCRs is normally down-regulated in the presence of a KIR-MHC class I interaction (66).

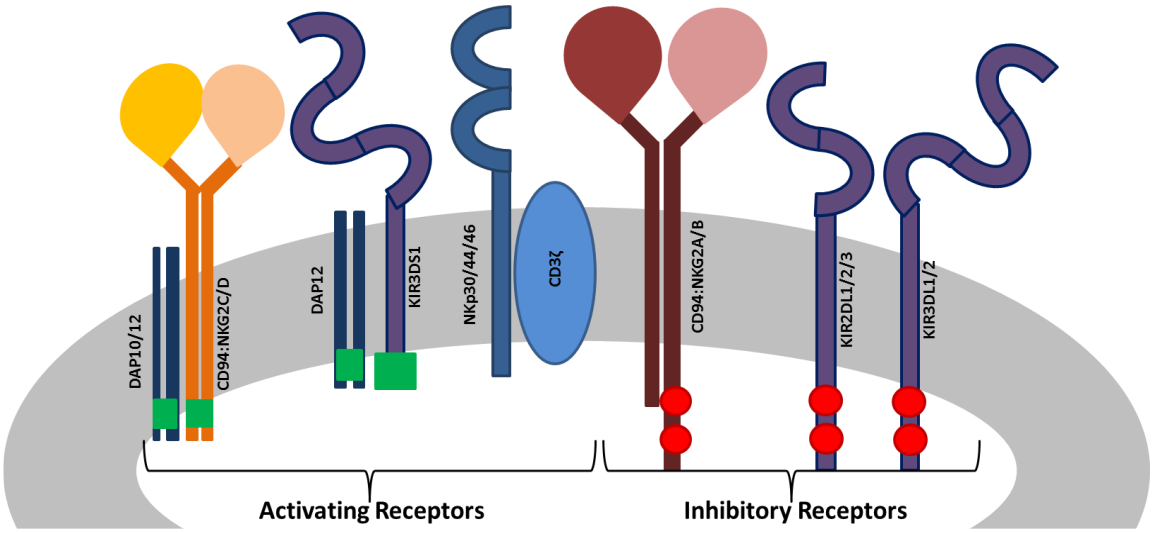

Figure 1.1: Natural Killer cell receptors

Natural Killer (NK) cells express a wide range of receptors that can inhibit or activate their function. Activating receptors generate signals through an ITAM (green box) in their short cytoplasmic tails binding to DAP10 or DAP12 (NKG2C/D and activating KIRs) or through CD3ζ (NKp receptors). Inhibitory receptors signal through ITIM sequences (red circle) in their long cytoplasmic tails. Receptor engagement leads to phosphorylation of these ITIM motifs resulting in the recruitment of the phosphotyrosine phosphatase SHP-1 that prevents activation of the cell.

NKG2 receptors are type II transmembrane proteins that form heterodimeric complexes with CD94, an accessory molecule required for signal transduction (67). There are seven known NKG2 family members (A-H) with some being activating and some inhibitory. NKG2A is inhibitory while NKG2C is activating, but both bind the non-classical Human leukocyte antigen (HLA) class I molecule, HLA-E, although the interaction with NKG2C is weaker. CD94:NKG2A is able to recognise the down-regulation of MHC class I molecules due to the loss of leader peptide-HLA-E complexes on the cell surface. These leader peptides are usually inhibitory to this receptor complex, with residues 5, 6 and 8 having a big influence on receptor binding (68). NKG2D is expressed on the cell surface as a homodimer and recognises non-classical MHC molecules (MICB and MICA) as well as other non-MHC molecules (ULBP1-6). It is typically up regulated in response to stresses such as viral infection or tumour formation (53). Expression of non-classical MHC I molecules are usually up-regulated following cellular stress (69), suggesting that if polymorphisms within ERAP1 or accumulation of HLA-B27 homodimers causes cellular stress the interactions of NKG2 receptors on NK cells may become important mediators of NK cell activation.

The KIR genes are found on human chromosome 19q13.4 in the leukocyte receptor complex closely packed together in a head to head orientation (70); predominantly expressed on $CD56^{dim}$ NK cells as well as a subset of T cells (71). They interact with HLA class I molecules on the surface of nearly all nucleated cells and the combination of inheritance of HLA and KIR is important for protection from both infection and predisposition to certain autoimmune diseases, such as rheumatoid arthritis (RA) and scleroderma (62). The KIR family contains at least 15 members, with every NK cell expressing up to six inhibitory and five activating receptors (64). They are named according to the number of extracellular Ig domains (KIR2D or KIR3D) and the length of their cytoplasmic tail (KIR2DL or KIR3DS). KIR expression influences the functional maturation of developing NK cells (57). KIR expression is mostly randomly determined by the KIR gene content, polymorphism and stochastic epigenetic regulation at the promoter level (72) meaning that a person may express KIRs for which they have no cognate ligand or fail to express the KIR required for interaction with an expressed MHC I molecule.

Inhibitory KIR proteins have a long cytoplasmic domain that contains at least two immunoreceptor tyrosine-based inhibitory motifs (ITIMs) and an extracellular HLA-binding portion made up of two or three domains. ITIMs recruit tyrosine phosphatases, specifically SH2 domain-containing protein tyrosine phosphatase (SHP)-1, to the plasma membrane for de-phosphorylation of tyrosine kinases to prevent activation of downstream signalling pathways (73, 74). Within the KIR family, activating receptors share structural similarities with the extracellular domains of inhibitory KIR but have short cytoplasmic tails with a positively charged residue (lysine or arginine) within the cytoplasmic domain allowing association with adaptor molecules, in particular DNAX activating protein 12 (DAP12) (64), for downstream signalling and activation of the NK cell (75). HLA class I molecules are recognised by a range of KIR receptors depending on their sequence or grouping (**Figure 1.2**). In addition, the ligand for some KIRs has yet to be elucidated and some HLA molecules have not yet been found to interact with any KIR. The genes for KIR3DL3 and KIR3DL2 define the centromeric and telomeric ends of the locus and, along with KIR3DP1 and KIR2DL4, are referred to as the framework genes which are present in every individual, although only expressed in some (76).

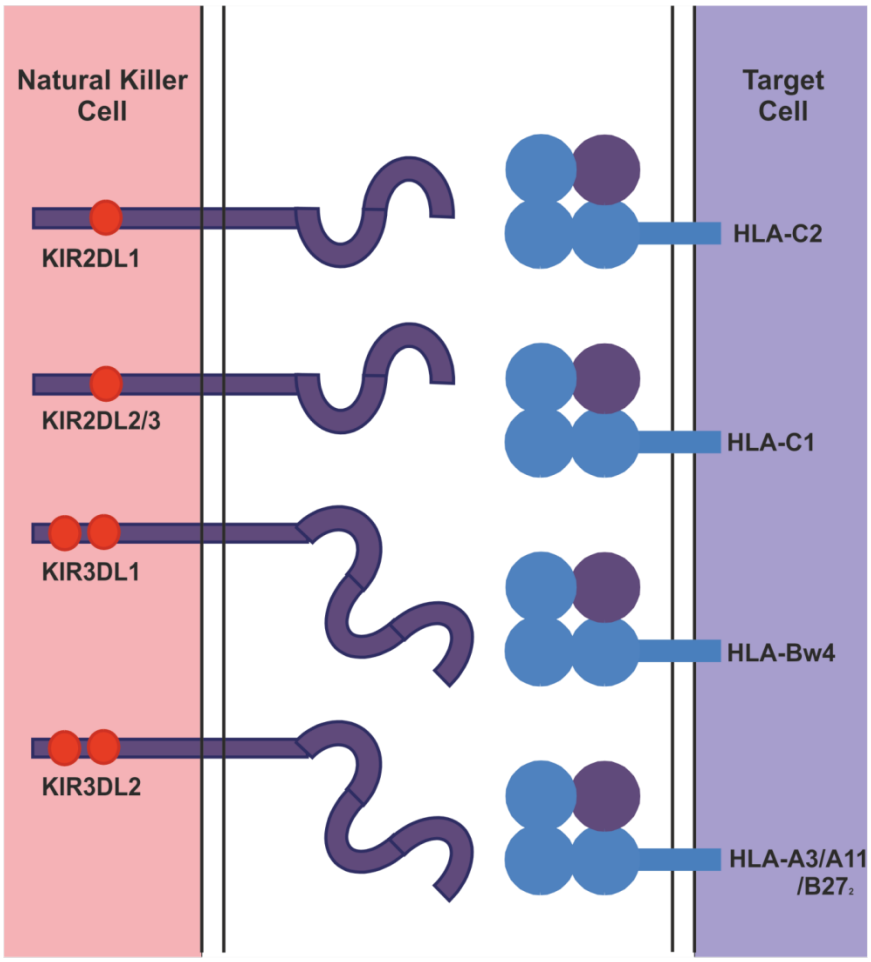

Figure 1.2: KIRs and their cognate HLA ligands

KIRs display specificity for their HLA Ligands, which is usually limited to one group of HLA. KIR2DL1 binds to members of the HLA-C1 group, such as HLA-Cw01, HLA-Cw08 and HLA-Cw13, while KIR2DL2/3 can interact with HLA-C2 group ligands, such as HLA-Cw02 and HLA-Cw05. KIR3DL1 recognises HLA-B molecules with the Bw4 motif (amino acids 77-83) such as HLA-B8, HLA-B15 and HLA-B27. It can also recognise HLA-A*03 and HLA-A*2402 as these contain the Bw4 motif. KIR3DL2 can bind to HLA-A3, HLA-A11 and HLA-B27 homodimers ($B27_2$).

The interaction of KIR3DL1, and potentially KIR3DL2, to HLA-B27, a Bw4 epitope molecule, is a potential driver of the autoimmune disease Ankylosing Spondylitis (AS). The KIR3DL1 gene is the most polymorphic member of the KIR family, with 78 alleles reported (70, 74). Within the HLA-B group, the amino acid at position 80 is integral for binding to KIR3DL1, a fact that is highlighted by the difference between the interaction of KIR3DL1 with Bw4 and Bw6 epitope HLA-B molecules. Bw4 epitope molecules have either an isoleucine (I) or threonine (T) residue at position 80, both of which can bind to KIR3DL1, while Bw6 epitope molecules have an asparagine (N) at this position and do not bind (77). Bw4 molecules with I80, such as HLA-B57, have greater avidity for KIR3DL1 than those with T80 (78). All HLA-B27 alleles have threonine at position 80,

with the exception of HLA-B*2702 and –B*2730 which have isoleucine (78). Different alleles of KIR3DL1 are expressed at different densities on the cell surface of NK cells, with some expressed highly (KIR3DL1*015-like), some dimly (KIR3DL1*005-like) and some completely absent (KIR3DL1*004); this can have an influence on the inhibition caused through HLA engagement (70).

The inhibitory KIR3DL1 and activating KIR3DS1 receptors differ by around 6-12 amino acids in the extracellular domain, depending on the KIR3DL1 allele. KIR3DS1, like other activating KIRs, has a lysine residue at position 328 which is involved in the interaction with the activating adaptor protein, DAP12 (79). DAP12-dependent activation occurs through recruitment of Syk/ZAP-70 tyrosine kinases by ITAMs (74). The HLA ligand for KIR3DS1 has yet to be determined but it is proposed to be the same as those of KIR3DL1 due to high amino acid and structural extracellular homology (>97%) to KIR3DL1 (80). The combination of HLA-Bw4 with isoleucine at position 80 and KIR3DL1/3DS1 genes are associated with slower progression to AIDS in HIV-1 infected patients (81, 82).

The KIR3DL2 framework gene is expressed by about 20-30% of circulating NK cells and 5% of T cells (mainly $CD8^+$) (83). KIR3DL2 has a cysteine residue at position 67 in the stem region that may promote covalent homodimerisation (64). KIR3DL2 binds to HLA-A03 and –A11 (84), as well as HLA-B27 homodimers ($B27_2$). Interactions between KIR3DL2 and HLA-A03 and –A11 are highly dependent on the peptide present while $B27_2$ interactions occur independently of peptide (83) and this binding to $B27_2$ is stronger than binding to HLA-A alleles (85). This receptor has also been shown to have an additional function as a sensor for PAMPs such as CpG oligodeoxynucleotides (70).

1.2.3 Involvement of NK cells in AS disease

There have been several conflicting reports and hypotheses put forward as to the contribution of NK cells in AS pathogenesis. A significantly higher percentage of NK cells have been found in the blood of AS patients (average 12.6%) compared to healthy controls (average 5.4%), including healthy controls expressing HLA-B27. This difference was irrespective of age, sex and treatment factors (86). The presence of the activating *KIR3DS1* gene was increased in SpA patients compared to healthy controls, while presence of the KIR3DL1 gene was significantly decreased (54, 87, 88). However, these findings were not repeated in a subsequent larger study (78) and they do not examine the level of expression observed in these individuals. The differences

between these studies may be due to the ethnic group of the population used, as differences in KIR gene expression are commonly seen between different populations. An increase has also been seen in KIR3DL2 expressing NK and $CD4^+$ T cells in SpA patients compared to healthy controls and RA patients, with this increase more pronounced in HLA-$B27^+$ SpA patients compared to HLA-$B27^-$ SpA patients (62). It was proposed that this interaction between HLA-B27 and KIR3DL2 provides a pro-survival signal to NK and T cells leading to their increased survival, proliferation and in the case of Th17 $CD4^+$ T cells increased IL-17 production (89, 90).

In some AS patients, the α-chain of the IL-2 receptor (CD25) was up regulated and significant expression of the adhesion molecule CEACAM-1 was observed on NK cells compared to controls, while no difference was observed for other common NK cell receptors. Homotypic CEACAM-1 interactions transduce inhibitory signals through the cytosolic ITIM sequences on NK cells, suggesting that AS patients utilise a mechanism of NK cell inhibition not frequently used by healthy controls. The AS patients in this study also exhibited increased levels of the chemotactic factors IL-8 and SDF-1 in their sera, factors which can in turn increase the expression of CEACAM-1. This led to the hypothesis from Azuz-Lieberman *et al,* that these chemotactants attract NK cells to the joints from where they can enter the highly vascular synovial membrane and increase their CEACAM-1 expression to allow homotypic binding to CEACAM-1 on the surface of polymorphonuclear cells and synoviocytes leading to inhibition of NK cells (86). In agreement with this, Scrivo *et al* showed that the functional activity of NK cells in SpA patients was decreased exhibiting reduced IFNγ production. They also showed that patients with greater disease activity had lower NK cell degranulation compared to less severe patients (91), potentially due to increased expression of CEACAM-1 on these cells.

IL-17 is a pro-inflammatory cytokine that stimulates fibroblasts, endothelial cells, macrophages and endothelial cells to produce IL-1, IL-6, TNFα, NOS-2, metalloproteases and several chemokines. It can also recruit and activate neutrophils (92). The frequency of KIR3DL2$^+$ Th17 $CD4^+$ T cells was shown to be increased in AS patients with increased levels of IL-17 in both the serum and synovial fluid of these patients (89). In addition to their association with AS, these cells and IL-17 have been implicated in the pathogenesis of other autoimmune conditions including psoriasis, RA, multiple sclerosis and IBD (93, 94).

1.2.4 T cells

For T cell activation, TCRs recognise MHC molecules on the surface of cells and decide, based on the peptide presented, whether the cell is infected or healthy and act appropriately. In addition to TCR ligation, T cells require a second co-stimulatory signal such as CD28 binding to CD80 and CD86 and a third cytokine signal, usually IL-2, for activation (41). Within the T cell family there are two distinct subsets which express either CD4 or CD8, both of which act as co-receptors with the TCR (95). These co-receptors are acquired during T cell maturation in the thymus, a process that every T cell must complete to become mature. T cells mature from $CD25^-$ $CD44^+$ -> $CD25^+$ $CD44^+$ -> $CD25^+$ $CD44^-$ -> $CD25^-$ $CD44^-$ -> $CD4^-$ $CD8^{LO}$ -> $CD4^+$ $CD8^+$ before undergoing positive selection to express only CD4 or CD8. $CD4^+$ T cells, which recognise peptide bound to MHC class II molecules, are further differentiated into Th1, Th2 or Th17 cells. Each of these has distinct effects against different pathogens and secretes a range of different cytokines (95).

The large classification and differentiation found within the T cell family allows the adaptive immune response to be exquisitely tailored to the specific pathogen encountered. $CD8^+$ T cells recognise peptides bound to MHC class I molecules (pMHC) on the surface of to the host or from an invading pathogen. If the peptide is not native to the host, the $CD8^+$ T cell will become activated and release cytotoxic granules into the immunological synapse between the two cells that act to perforate and lyse the host cell. In this way, these T cells can limit the spread of infection from cell to cell (95).

1.2.5 Involvement of T cells in AS disease

Due to the involvement of HLA-B27 and ERAP1 in AS disease, the most likely cellular candidate for generation of AS disease would be expected to be $CD8^+$ T cells as these cells interact with HLA-B27 and engage peptides generated by ERAP1. In accordance with this, elevated levels of $CD8^+$ T cells have been reported in the blood of AS patients (96). However, despite the suggestion that $CD8^+$ T cells in AS patients may be activated against aggrecan (97), a critical component of cartilage, further evidence of this link is absent and an explanation for the increase in this immune cell population has not been forthcoming.

$CD4^+$ T cell numbers have also been shown to be elevated in the blood of AS patients (98, 99). In particular, the Th1 and Th17 cell populations have been shown to be expanded in AS patients (100). AS previously mentioned, the $KIR3DL2^+$ Th17 $CD4^+$ population has been shown to

be expanded also (89). This increase in Th17 cells is generally associated with a decrease in Treg cell populations, leading to a skewed Th17/Treg balance that may drive the pro-inflammatory disease progression seen with AS (101, 102). No conclusive explanation for the generation of AS disease by these increased $CD4^+$ T cell populations has so far been shown, although strong evidence from their association with other autoimmune diseases (94) suggests that Th17 cells may play an important role. However, if these cells are important in the pathogenesis of AS, they are still part of the adaptive immune response and therefore an early innate mediator may be involved to initiate the T cell responses and expansions seen.

1.3 Project aims

The focus of this project will be to explore how HLA-B27, ERAP1 and NK cells interact together with the aim of discovering whether changes in peptide repertoire, due to ERAP1 polymorphisms, or HLA-B27 cell surface expression can influence NK cell activation through KIR3DL1 or KIR3DL2. Establishing whether there is a connection between these three elements, which have previously been associated with AS disease, may help to provide insight into the pathogenesis of the disease or reveal diagnostic or therapeutic markers that could be used in the future. In particular the project will address the following questions:

- How do changes in the peptide repertoire alter KIR3DL1 engagement and therefore NK cell activation?
- Do ERAP1 polymorphic variants induce different levels of NK cell activation?
- Why are certain alleles of HLA-B27 associated with AS disease while similar alternative alleles are not?
- Could ERAP1 be used as a diagnostic marker for disease?
- Could NK cells be the driving force for the pathogenesis of AS?

Chapter 2: Materials & Methods

2.1 KIR Genotyping of donors

Short sequence primer polymerase chain reaction (SSP-PCR) was used to identify KIR3DL1^{+} individuals from a selection of genomic DNA (gDNA) samples previously collected by Dr Emma Reeves for her PhD thesis and subsequent publications (6, 29). gDNA was generated from a PBMC population, with consent from each individual (donors 1, 2 and 3) for use in both the original intended study and the subsequent work shown here. Individuals were tested for the presence of both KIR3DL1 and KIR3DS1. KIR3DS1 was included in the experiment in order to exclude donors that express this receptor as if these two receptors do share a common ligand there may be a confounding effect.

KIR3DS1 and KIR3DL1 primer pairs, in addition to a primer pair for the internal positive control (IPC) that binds to the heavy chain of MHC class I molecules (**Table 2:1**), were added to 5µl dNTPs, 5µl 10x KOD HotStart buffer, 4µl $MgSO_4$, 1µl KOD hotstart DNA polymerase (Novagen) and 100ng gDNA; as previously described by Vilches *et al* (103). Samples were run on a BIOER XP Thermocycler (Alpha laboratories) and consisted of an initial step of denaturation at 95°C followed by 40 cycles of 20 s at 95°C, 10 s at 61°C and 5 s at 70°C. PCR products were analysed by electrophoresis in 2% agarose gel stained with ethidium bromide and visualized on an UV transilluminator using a gel documentation system (Gel225 DocXR BioRad) to check the presence or absence of gene-specific amplicons (**Figure 2.1**).

Table 2:1: Primer sequences for KIR SSP-PCR genotyping

Target	Name	Sequence
KIR3DL1 forward	Ftt624	5'-TCCATCGGTCCCATGATGTT
KIR3DS1 forward	Fg624	5'-CATCGGTTCCATGATGCG
KIR3DL1/S1 reverse	Rt697	5'-CCACGATGTCCAGGGGA
IPC283 forward	FDRA360	5'-GAGGTAACTGTGCTACGAACAGC
IPC283 reverse	RDRA595	5'-GGTCCATACCCCAGTGCTTGAGAAG

gDNA from donors 1 & 2 contains the gene for KIR3DL1 but not KIR3DS1. gDNA from donor 3 showed the presence of the KIR3DS1 gene but the absence of KIR3DL1 gene. Based on these results, donor 1 was chosen as a potential PBMC donor for subsequent experiments.

However, before a conclusive choice of donor could be made, it was necessary to confirm that this donor expresses an allele of KIR3DL1 that is present on the cell surface, as some alleles of KIR3DL1 are not (104).

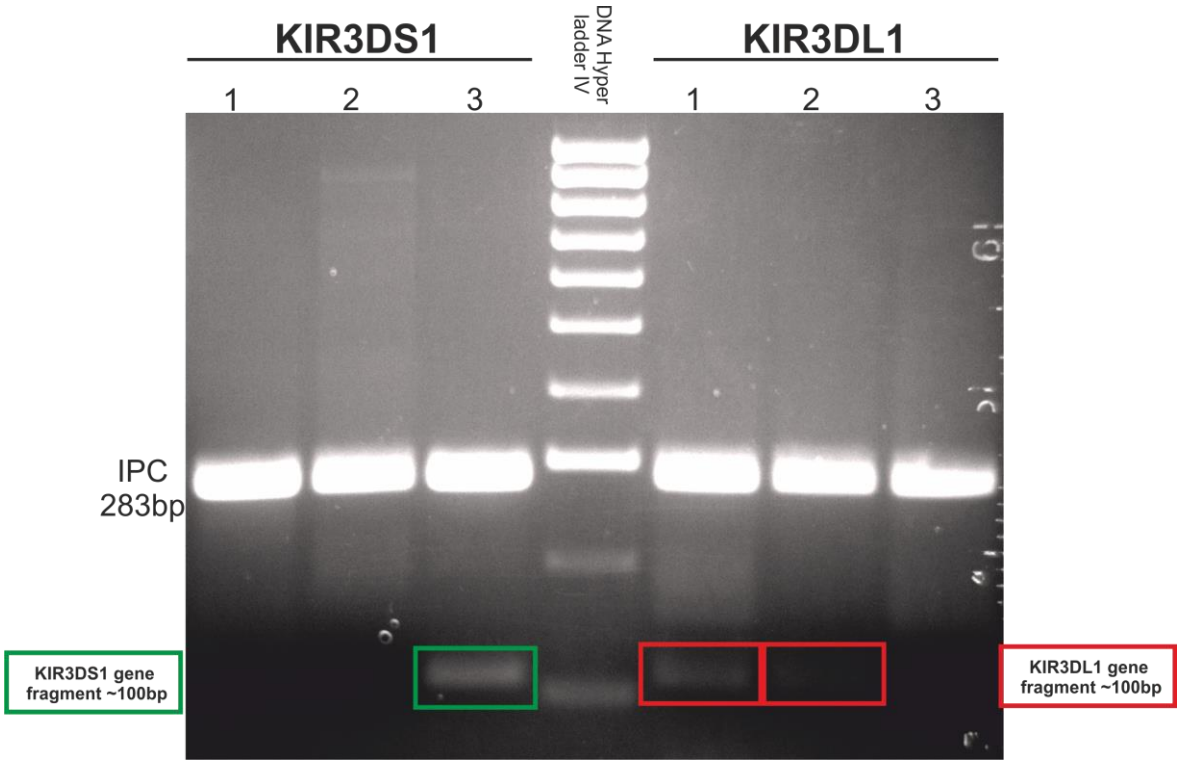

Figure 2.1: KIR genotyping DNA gel

PCR products from the KIR genotyping SSP-PCR were run on a 2% agarose gel and bands were visualised. The internal positive control (IPC) can be seen in all samples at ~283bp. The KIR3DS1 gene fragment can only be seen in donor 3, while the KIR3DL1 fragment is present in both donors 1 and 2, but absent in donor 3.

PBMCs from donor 1 were collected from a fresh blood sample taken with consent and isolated using Ficoll-hypaque density centrifugation (Amersham Biosciences). $15x10^6$ PBMCs were aliquoted into individual cryovials, supplemented with foetal calf serum (FCS) + 20% DMSO and frozen at -80°C until needed. To confirm the cell surface expression of KIR3DL1 in this donor, one vial of PBMCs was thawed in warm FCS and then re-suspended at 10^6 cells per ml in RPMI media supplemented with 10% FCS (PAA), 100mM penicillin & streptomycin (Sigma-Aldrich) and 200mM L-glutamine (Sigma-Aldrich). Recombinant human IL-15 (rhIL-15) was added to the cells at a concentration of 0.5ng/ml to stimulate NK cell growth and expansion of this lymphocyte population. 200,000 cells were plated per well into a 96-well U-bottom plate and left overnight in a 37°C, 5% CO_2 incubator.

The following day, the 96-well plate was spun at 1500rpm for 2 minutes to pellet the cells, supernatant was removed and the cells were washed twice in FACS wash buffer (PBS containing 2% FBS and 0.1% NaN_3). Subsequently, cells were incubated with the following antibodies for 45 minutes at 4°C before being washed twice with FACS wash buffer and then being analysed using the Canto II Flow cytometer (BD Biosciences) (**Figure 2.2**). αCD56-FITC (Biolegend) and αCD3-PerCP (Biolegend) were used to identify the target NK cell population as $CD3^-CD56^{dim}$. The DX9 clone of αCD158e1-BV421 (Biolegend) against KIR3DL1 (subsequently called DX9) was used to identify this population. The DX31 clone of αCD158k-PE (Biolegend) against KIR3DL2 was used to identify the proportion of $KIR3DL2^+$ NK cells.

KIR3DL1 was expressed on the cell surface of approximately 16% of $CD3^-$ $CD56^{dim}$ NK cells (**Figure 2.2a**). Of this $KIR3DL1^+$ population, around one third of cells also express KIR3DL2. This is in addition to the 20% of NK cells that express KIR3DL2 in the absence of KIR3DL1. Despite being a framework gene present in all individuals, KIR3DL2 is only expressed on the cell surface of certain individuals (76). These data confirm that donor 1 expresses an allele of KIR3DL1 found at the cell surface in addition to showing cell surface expression of KIR3DL2 making them an ideal donor to investigate the role of these two receptors.

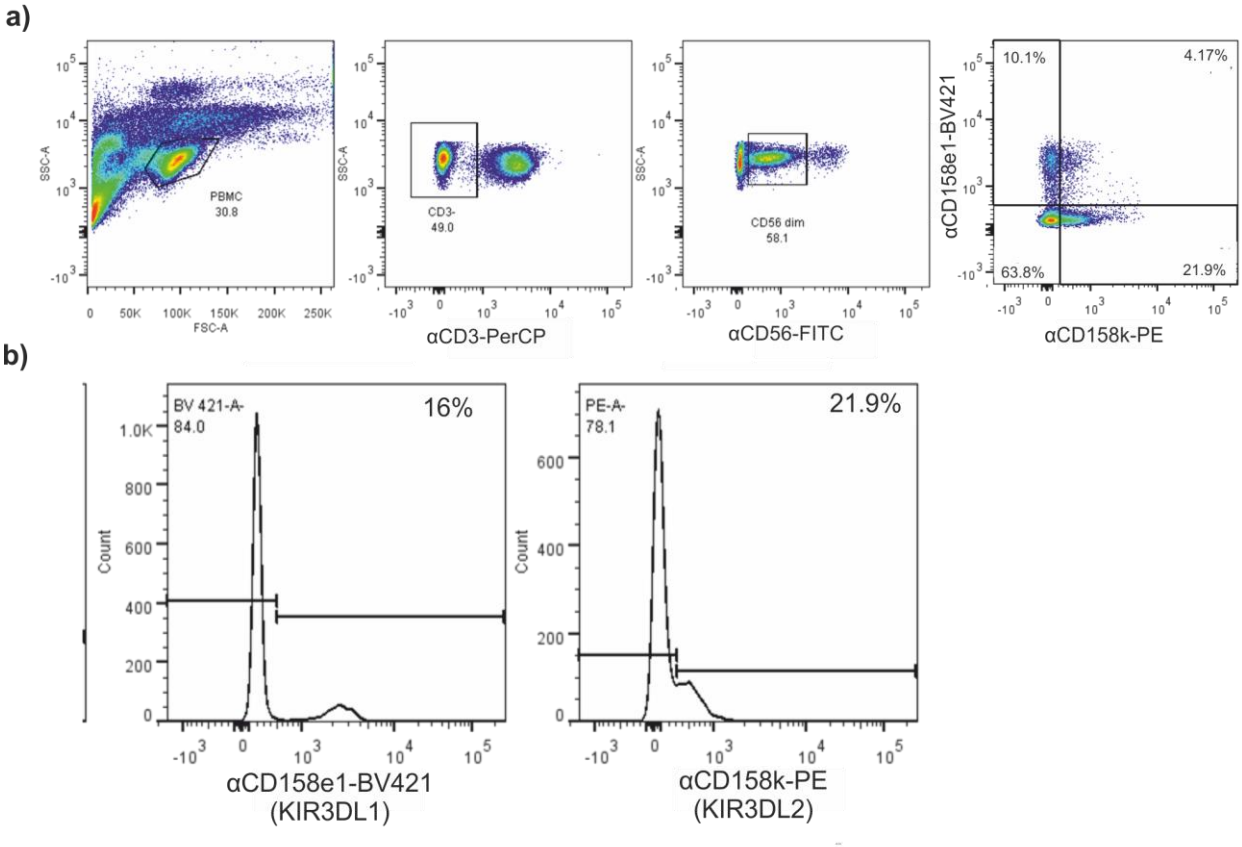

Figure 2.2: Donor 1 KIR expression

PBMCs from donor 1 were incubated overnight with 0.5ng/ml rhIL-15 before being surface stained in order to determine the proportion of KIR3DL1^{+} and KIR3DL2^{+} NK cells. This antibody panel represents the panel used in LAMP1 assays, as described later. (a) The lymphocyte population was gated on using the FSC v SSC dot plot. KIR-expressing NK cells are identified as CD3-PerCP negative and CD56-FITC dim. This NK cell population is then further identified as KIR3DL1 (CD158e1-BV421) and/or KIR3DL2 (CD158k-PE) positive for further analysis. (b) The PBMC population used for all consequent experiments were isolated from a single donor who expresses KIR3DL1 on ~15% and KIR3DL2 on ~21% of NK cells.

2.2 Cell culture and transfection

The adherent HeLa cell line was either transiently or stably transfected using FuGene 6 reagent (Promega). These cells were cultured in RPMI (Lonza) supplemented with 10% FCS (PAA), 100mM penicillin & streptomycin (Sigma-Aldrich) and 200mM L-glutamine (Sigma-Aldrich). 2ml of cells were plated in a 6-well dish (Corning) at 10^5 cells per ml for 24 hours before transfection to allow cells to grow to a confluency of ~50-70%. For transfection, 3µg of FuGene 6 was added to 97µl of serum-free media and incubated for 5 minutes before addition of 1µg DNA (3:1 ratio of FuGene: DNA), incubation for 15 minutes and then addition to cells in a dropwise fashion. Cells for transient transfection were left for 24 hours before harvesting. Cells for stable transfection were left for 24 hours before addition of antibiotic: 1mg/ml Geneticin (G418) (Gibco) or 0.5mg/ml Hygromycin (Invivogen).

The 721.221 (.221) cell line is a B lymphoblastoid cell line that was generated by *γ*-ray-induced mutagenesis in the HLA complex (105). These cells are HLA-null and express only very low levels of HLA-C (105). .221 cells are a suspension cell line and so it was necessary to transfect in a different way with stable transfection achieved by using Nucleofection. These cells were also cultured in RPMI (Lonza) supplemented with 10% FCS (PAA), 100mM penicillin & streptomycin (Sigma-Aldrich) and 200mM L-glutamine (Sigma-Aldrich). Using the Amaxa Nucleofection kit V (Amaxa), $2x10^6$ cells were re-suspended in Solution V combined with nucleofector solution and added to 5µg DNA in a cuvette. The cuvette was placed into the nucleofector machine and program A-24 was run. Transfected cells were added to 1ml pre-warmed media and left for 24 hours before addition of antibiotic (same as above).

2.3 Plasmid minigene construction

Minigene constructs were designed to deliver specific peptides into HeLa target cells for cell surface expression on HLA-B27 for LAMP1 assays. These minigene constructs consist of a peptide sequence preceded by an endoplasmic reticulum (ER) signal sequence within the pcDNA3 vector. The ER signal sequence used, 'MRYMILGLLALAAVCSA', is derived from the human adenovirus C serotype 6 virus. To generate this, long primers of the both the ER signal sequence and the peptide sequence with an EcoRI and XbaI restriction site either end were designed for each peptide required (Sigma Aldrich) (**Table 2:2**).

Table 2:2: Primer sequences for minigene constructs

Peptide sequence	Primer sequences
FRYNGLIHR	For: 5'-AATTATGAGGTACATGATTTTAGGCTTGCTCGCCCTTGCGGCAGTCTGCAGCGCGTTCCGCTACAACGGACTGATTCACCGCTAG-3' Rev: 5'- CTAGCTAGCGGTGAATCAGTCCGTTGTAGCGGAACGCGCTGCAGACTGCCGCAAGGGCGAGCAAGCCTAAAATCATGTACCTCAT-3'
FRYNGLIKR	For: 5'- AATTATGAGGTACATGATTTTAGGCTTGCTCGCCCTTGCGGCAGTCTGCAGCGCGTTCCGCTACAACGGACTGATTAAACGCTAG-3' Rev: 5'- CTAGCTAGCGTTTAATCAGTCCGTTGTAGCGGAACGCGCTGCAGACTGCCGCAAGGGCGAGCAAGCCTAAAATCATGTACCTCAT-3'
FRYNGLIER	For: 5'- AATTATGAGGTACATGATTTTAGGCTTGCTCGCCCTTGCGGCAGTCTGCAGCGCGTTCCGCTACAACGGACTGATTGAACGCTAG-3' Rev: 5'- CTAGCTAGCGTTCAATCAGTCCGTTGTAGCGGAACGCGCTGCAGACTGCCGCAAGGGCGAGCAAGCCTAAAATCATGTACCTCAT-3'
FRYNGLRHR	For: 5'- AATTATGAGGTACATGATTTTAGGCTTGCTCGCCCTTGCGGCAGTCTGCAGCGCGTTCCGCTACAACGGACTGAGACACCGCTAG -3' Rev: 5'- CTAGCTAGCGGTGTCTCAGTCCGTTGTAGCGGAACGCGCTGCAGACTGCCGCAAGGGCGAGCAAGCCTAAAATCATGTACCTCAT-3'
LRNQSVFNF	For: 5'- AATTATGAGGTACATGATTTTAGGCTTGCTCGCCCTTGCGGCAGTCTGCAGCGCGCTCAGAAACCAGAGTGTGTTTAACTTCGGTAG-3' Rev: 5'- CTAGCTACCGAAGTTAAACACACTCTGGTTTCTGAGCGCGCTGCAGACTGCCGCAAGGGCGAGCAAGCCTAAAATCATGTACCTCAT-3'
SRLRNQSVFNF	For: 5'- AATTATGAGGTACATGATTTTAGGCTTGCTCGCCCTTGCGGCAGTCTGCAGCGCGTCCAGGCTCAGAAACCAGAGTGTGTTTAACTTCGGTAG-3' Rev: 5'- CTAGCTACCGAAGTTAAACACACTCTGGTTTCTGAGCCTGGACGCGCTGCAGACTGCCGCAAGGGCGAGCAAGCCTAAAATCATGTACCTCAT-3'
ARFQHGHSR	For: 5'- AATTATGAGGTACATGATTTTAGGCTTGCTCGCCCTTGCGGCAGTCTGCAGCGCGGCGAGGTTCCAGCACGGGCACAGCAGGTAG-3' Rev: 5'- CTAGCTACCTGCTGTGCCCGTGCTGGAACCTCGCCGCGCTGCAGACTGCCGCAAGGGCGAGCAAGCCTAAAATCATGTACCTCAT-3'
ARFEQLISR	For: 5'- AATTATGAGGTACATGATTTTAGGCTTGCTCGCCCTTGCGGCAGTCTGCAGCGCGGCGAGGTTCGAGCAGCTGATCAGCAGGTAG-3' Rev: 5'- CTAGCTACCTGCTGATCAGCTGCTCGAACCTCGCCGCGCTGCAGACTGCCGCAAGGGCGAGCAAGCCTAAAATCATGTACCTCAT-3'
RRLPVPRAK	For: 5'- AATTATGAGGTACATGATTTTAGGCTTGCTCGCCCTTGCGGCAGTCTGCAGCGCGAGGAGGTTGCCGGTGCCGAGGGCGAAGTAG-3' Rev: 5'- CTAGCTACTTCGCCCTCGGCACCGGCAACCTCCTCGCGCTGCAGACTGCCGCAAGGGCGAGCAAGCCTAAAATCATGTACCTCAT-3'
QRLKEYRSK	For: 5'- AATTATGAGGTACATGATTTTAGGCTTGCTCGCCCTTGCGGCAGTCTGCAGCGCGCAGCGGCTGAAGGAGTACAGGAGCAAGTAG-3' Rev: 5'- CTAGCTACTTGCTCCTGTACTCCTTCAGCCGCTGCGCGCTGCAGACTGCCGCAAGGGCGAGCAAGCCTAAAATCATGTACCTCAT-3'

Primers were dissolved at 1µg/µl and phosphorylated at each end using the T4 kinase PK protocol (NEB). The corresponding 5' and 3' primer for each peptide were then combined and annealed by placing the primers in boiling water and allowing the water to cool to room temperature. The accepting vector, pcDNA3, was digested with EcoRI and XbaI (Promega) and the minigene primers were ligated into pcDNA3 at a molar ratio of 3:1 overnight using T4 ligase (NEB). The following day ligated vectors were transformed into JM109 competent *E.Coli* bacteria (made in house). DNA was mini-prepped (Promega PureYield plasmid miniprep system), confirmed by sequencing (Source Bioscience) and then maxi-prepped (Qiagen Qiafilter Plasmid Maxi kit) to obtain a large stock of DNA at 1µg/µl suitable for transient transfection.

For additional experiments showing that mutation of the amino acids at positions 7 and 8 could alter NK cell activation, mutants of these minigenes were created using site-directed mutagenesis (SDM) PCR. Short primers were designed to mutate existing minigenes at positions 7 and 8 and ordered from Sigma Aldrich (**Table 2:3**). These primers were added to 5µl dNTPs, 5µl 10 x KOD hotstart buffer, 4µl $MgSO_4$, 1µl KOD hotstart DNA polymerase (Novagen) and 100ng minigene DNA and run for 20 cycles on a BIOER XP Thermocycler (Alpha laboratories); 95°C 20secs, 55°C 10secs, 70°C 2mins 20secs. PCR products were incubated with 1µl DpnI (NEB) for 1.5

hours at 37°C. DpnI is a restriction enzyme that digests methylated DNA and is used to remove template DNA following PCR. PCR DNA was purified through addition of 10µl NaAc, 50µl dH_2O and 250µl 100% Ethanol (-20°C) and centrifugation at 13,000rpm for 20 minutes (4°C). Following this, the DNA pellet was washed once with 70% ethanol, 13,000rpm for 5 minutes (4°C). Purified DNA was transformed into JM109 competent *E.Coli* bacteria (made in house). DNA was mini-prepped (Promega PureYield plasmid miniprep system), confirmed by sequencing (Source Bioscience) and then maxi-prepped (Qiagen Qiafilter Plasmid Maxi kit) to obtain a large stock of DNA at 1µg/µl suitable for transient transfection.

Table 2:3: Primer sequences for mutating existing minigene constructs

Peptide sequence	Minigene template	Primer sequences
FRYNGLPSR	FRYNGLIHR	For: 5'- GCTACAACGGACTGCCGAGCCGCTAG -3' Rev: 5'- CTAGCGGCTCGGCAGTCCGTTGTAGC -3'
FRYNGLISR	FRYNGLIHR	For: 5'- GCTACAACGGACTGATCAGCCGCTAG -3' Rev: 5'- CTAGCGGCTGATCAGTCCGTTGTACG -3'
FRYNGLHSR	FRYNGLIHR	For: 5'- GCTACAACGGACTGCACAGCCGCTAG -3' Rev: 5'- CTAGCGGCTGTGCAGTCCGTTGTAGC -3'
FRYNGLRSR	FRYNGLRHR	For: 5'- GCTACAACGGACTGAGGAGCCGCTAG -3' Rev: 5'- CTAGCGGCTCCTCAGTCCGTTGTAGC -3'
FRYNGLRAR	FRYNGLRHR	For: 5'- GCTACAACGGACTGAGGGCGCGCTAG -3' Rev: 5'- CTAGCGCGCCCTCAGTCCGTTGTAGC -3'
FRYNGLDAR	FRYNGLIHR	For: 5'- GCTACAACGGACTGGACGCGCGCTAG -3' Rev: 5'- CTAGCGCGCGTCCAGTCCGTTGTAGC-3'
FRYNGLLAR	FRYNGLIHR	For: 5'- GCTACAACGGACTGCTGGCGCGCTAG -3' Rev: 5'- CTAGCGCGCCAGCAGTCCGTTGTAGC -3'
FRYNGLVAR	FRYNGLIHR	For: 5'- GCTACAACGGACTGGTGGCGCGCTAG -3' Rev: 5'- CTAGCGCGCCACCAGTCCGTTGTAGC -3'
ARFQHGIHR	ARFQHGHSR	For: 5'- CGAGCAGCTGATCCACAGGTAGCTAGAGGG -3' Rev: 5'- CCCTCTAGCTACCTGTGGATCAGCTGCTCG-3'
ARFQHGIKR	ARFQHGHSR	For: 5'- CGAGCAGCTGATCAAGAGGTAGCTAGAGGG -3' Rev: 5'- CCCTCTAGCTACCTCTTGATCAGCTGCTCG-3'
RRLPVPIHK	RRLPVPRAK	For: 5'-CGGTGCCGATCCACAAGTAGCTAGAGGG-3' Rev: 5'- CCCTCTAGCTACTTGTGGATCGGCACCG-3'
RRLPVPIKK	RRLPVPRAK	For: 5'- CGGTGCCGATCAAGAAGTAGCTAGAGGG -3' Rev: 5'-CCCTCTAGCTACTTCTTGATCGGCACCG -3'

2.4 NK cell degranulation (LAMP1) assay

Activation of NK cells can be measured through detection of lysosomal-associated membrane protein-1 (LAMP1/CD107a) at the cell surface. LAMP1 lines the membrane of cytolytic granules and was shown to be significantly up regulated on the surface of activated NK cells compared to un-stimulated cells (106) and is used as a marker of cytotoxic $CD8^+$ T cell degranulation (107). PBMCs from donor 1 were thawed from -80°C as above (2.1 KIR Genotyping of donors), stimulated with 0.5ng/ml rhIL-15 (Peprotech), plated at 200,000 cells per well and incubated overnight at 37°C. This assay was run using both .221 and HeLa cells as target cells that were treated differently before use in the assay:

- **.221 cells**: Cells were pulsed with 10µM exogenous peptide overnight at 26°C. For harvesting, cells were washed once in RPMI.
- **HeLa cells**: Cells were plated at 10^5 cells/ml in a 6-well dish and incubated for 24 hours at 37°C before transfection, as described (**2.2 Cell culture and transfection**). For harvesting, cells were incubated with 0.5M EDTA for ~5 minutes to release the contacts with the plate and washed once with RPMI.

For the LAMP1 assay, target cells were harvested and re-suspended with donor PBMCs at an effector-to-target ratio of 5:1 in fresh RPMI medium. 1/400 αLAMP1-APC (eBioscience) was present in the culture. If .221 target cells were previously pulsed with peptide, peptide was again added at a concentration of 10µM. All cells were incubated for 4 hours at 37°C, with 6µg/ml BFA (GolgiPlug, BD Biosciences) added after 1 hour.

At the end of the 4 hours, cells were washed twice in FACS wash buffer and then incubated with αCD56-FITC, αCD3-PerCP, αKIR3DL1-BV421 and αKIR3DL2-PE for one hour at 4°C. Cells were washed twice more before acquisition on the Fortessa X-20 flow cytometer (BD Biosciences). The strategy for identifying the $CD3^-CD56^{dim}$ NK cell population, followed by the four KIR3DL1 and/or KIR3DL2 expressing populations was identical to that shown in **Figure 2.2**. Three experimental repeats from one plate were run per experiment and, unless otherwise stated, three experiments were run on separate days. Data was analysed by one- or two-way ANOVA and Tukey's multiple comparisons test (GraphPad Prism).

Data was analysed using Treestar FlowJo software to identify the percentage of $LAMP1^+$ cells and this value was then normalised as a percentage of the control condition, i.e. .221 cell or HeLa $ERAP1^{-/-}$ B*2705 value. This standardisation was required due to high variability in the

percentage of $LAMP1^+$ cells or for when one experiment could not accommodate all samples, as in the case of the 15 ERAP1 allotypes (**Figure 4.2**) or 13 ERAP1 allotype combinations (**Figure 4.4**). High variability in the assay was common as blood donations from donor 1 to collect PMBCs were given on average once every three months. Therefore, any changes in the health of donor 1 could impact first how many PBMCs were isolated from different collections, but also the activation state of their immune cells. Confirmation of the validity of the standardisation approach came from a LAMP1 assay looking at the response of NK cells to .221 cells with different HLA molecules (**Figure 2.3**). When the $LAMP1^+$ population was plotted there was high variability, however when each result was expressed as a percentage of the $LAMP1^+$ population seen with .221 cells there was a clear and reproducible pattern.

Antibody blocking of KIR3DL1, HLA-B27 or FHC was required to determine the interactions involved in the results seen in **Figure 4.4**. For KIR3DL1 blocking, PBMCs were incubated for one hour at 37°C in the presence of 2µg/ml DX9 antibody prior to the protocol described above. The ME.1 antibody against pHLA-B27 complexes and the HC10 antibody against free heavy chains were used to block target cells for one hour before harvest and inclusion into the LAMP1 assay, as described above. Cells were also blocked with the appropriate control IgG in exactly the same conditions: IgG1 for DX9, IgG2a for ME.1 and HC10.

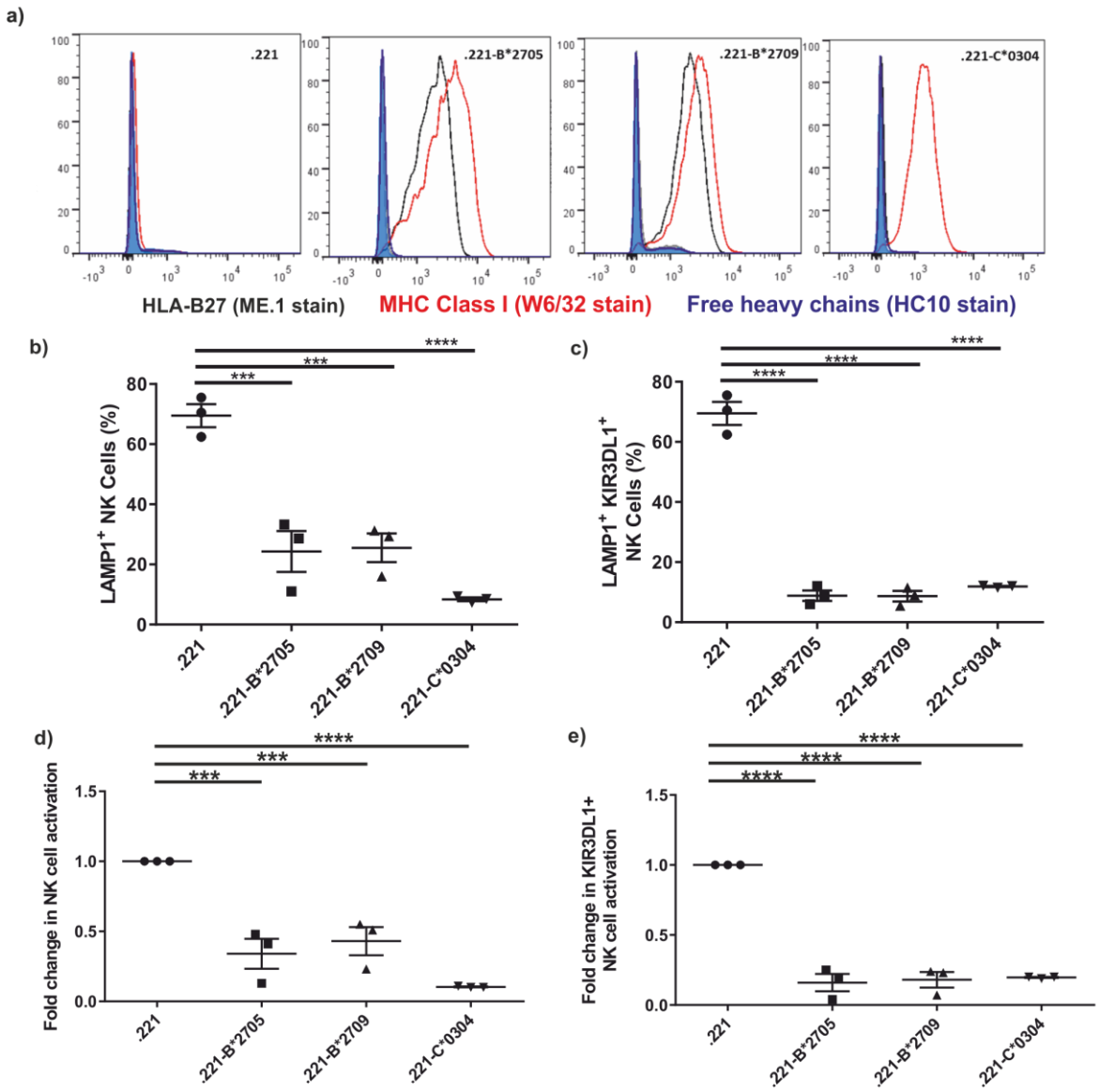

Figure 2.3: Addition of HLA to 721.221 cells inhibits NK cell activation

(a) 721.221 (.221) and .221-B*2705, .221-B*2709 and .221-C*0304 cells were stained for their MHC cell surface expression using the ME.1 antibody for HLA-B27 (black), W6/32 for MHC class I molecules (red) and HC10 for free heavy chain expression (blue). (b) These cells were used as target cells in LAMP1 assays of NK cell activation. In the whole NK cell population, addition of HLA-B*2705 ($p>0.001$), -B*2709 ($p>0.001$) and –C*0304 ($p>0.0001$) significantly inhibited NK cell activation as shown by a reduction in the LAMP1+ population. (c) This inhibition was repeated and more striking in the KIR3DL1$^+$ NK cell population ($p>0.0001$ for all HLA). (e) When the data was expressed as a fold change in NK cell activation compared to .221 cells alone, the statistical analysis remained the same. (f) For the KIR3DL1$^+$ NK cell population, a switch to fold change had no effect on the analysis of results either. N=3, Data analysed by one-way ANOVA and Tukey's multiple comparisons test.

2.5 Brefeldin A Peptide stabilisation assay

Brefeldin A (BFA) peptide stabilisation assays can be used to show the stabilisation of peptide-MHC (pMHC) complexes on the cell surface across a number of hours. High affinity pMHC complexes will remain stable on the surface for longer than lower affinity complexes (108). BFA can be used to prevent the export of new pMHC complexes from the ER to the cell surface (109). In order to accumulate class I molecules on the cell surface, 10^6 721.221, 721.220 or T2 cells were cultured overnight at 26°C, as previously described (110).

The 721.221 (.221) cell line is a B lymphoblastoid cell line that was generated by *γ*-ray-induced mutagenesis in the HLA complex (105). These cells are HLA-null and express only very low levels of HLA-C. The 721.220 cell line is a mutant of the .221 cell line that does not express the chaperone protein tapasin, lowering the affinity of pMHC complexes through a lack of peptide quality control in the ER (111). The T2 cell line is derived from fusion of a B-LCL cell line with CEMR.3 cells, with both copies of CEMR.3 chromosome 6 deleted. Chromosome 6 contains all of the HLA genes, including TAP1 and TAP2 (112) meaning that in these cells there is a vast reduction in the available peptides for MHC binding due to a lack of transport of peptides from the cytosol into the ER. These three cell lines were cultured in RPMI media supplemented with 10% FCS (PAA), 100mM penicillin & streptomycin (Sigma-Aldrich) and 200mM L-glutamine (Sigma-Aldrich).

Accumulated surface class I molecules were peptide-loaded by adding 20µM exogenous peptide from DMSO stock solutions to overnight cultures at 26°C. GL Biochem generated each exogenous peptide: FRYNGLIHR, FRYNGLIER, FRYNGLIKR & FRYNGLRHR. The following day, at each time point (6, 4, 2, 1 or 0.5 hours) 10^5 cells were taken, combined with BFA (1/1000 dilution in RPMI) (GolgiPlug, BD Biosciences) and moved to a 96-well dish and placed in a 37°C incubator. At the end of 6 hours, two further aliquots of cells were taken and added to the 96-well plate from the 37°C incubator.

All cells in the plate were washed twice with FACS wash buffer before incubation with the 0.5mg/ml ME.1 antibody for the detection of peptide-HLA-B27 complexes at the cell surface for 45 minutes at 4°C. Cells were again washed twice before incubation with the secondary antibody anti-Mouse-PE (0.5mg/ml, 30 minutes, 4°C) for detection. Cells were once more washed twice and then analysed on a Canto I Flow cytometer (BD Biosciences).

The average of three experimental repeats were shown for each experiment and, unless otherwise stated, three individual experiments were run on different days. Data was analysed

using Treestar FlowJo software. The mean fluorescence intensity (MFI) of PE was recorded and used to create an X:Y graph (GraphPad Prism). At each time point the MFI was compared to the MFI from 0 hours to create a percentage of maximal binding which was then plotted on another X:Y graph. A grouped histogram for the percentage of maximal binding at 4 hours was also plotted before analysis by two-way ANOVA and Tukey's multiple comparisons test. Data is presented in chapter 3.

2.6 Compilation & bioinformatics analysis of peptide database

To assess the contribution of changes at positions 7 and 8 (P7 or P8) of 9 amino acid peptides (9mer) to KIR3DL1 engagement on NK cells, a database of all the peptides previously eluted from HLA-B27 was compiled. From this database, 9mer peptides that were exclusively found in only one of four cell lines (HeLa, C1R05, P50, LG2) were identified for further analysis, resulting in 416 peptides (appendix B). All of these peptides had arginine at position 2, P2 is the anchor position for HLA-B27 molecules and generally only arginine or glutamine are accepted at this position.

Following the identification of these peptides, the amino acids present at P7 and P8 were analysed. As the number of peptides left for analysis was too small for any typical statistical test another approach was adopted. The percentage of peptides with a particular amino acid at each position was determined compared to the total number of peptides for that cell line. If this percentage was less than 10% that amino acid was deemed under-represented in that cell line. If the percentage was more than 25% it was deemed to be over-represented by that cell line. While this approach is largely subjective it does allow comparisons and conclusions to be made that can then be tested experimentally.

2.7 Recombinant human KIR3DL1 binding

Recombinant KIR can be used to determine the level and strength of KIR binding to HLA molecules on the cell surface. Recombinant human KIR3DL1 (rhKIR3DL1) (RnD systems) was reconstituted at 100µg/ml in PBS and then combined with an equal volume of protein-A-AF488 (1/100) (Invitrogen) and stored overnight at 4°C. Protein A can bind up to four rhKIR3DL1 molecules creating fluorescent tetrameric complexes that can be analysed by flow cytometry. HeLa ERAP1$^{-/-}$ cells were transiently transfected with HLA-B*2705 and an ERAP1 allotype combination as previously described (**2.2 Cell culture and transfection**) before inclusion in the assay.

The following day 10^5 HeLa or .221 target cells were harvested as above and combined with 50µl of the rhKIR3DL1-protein-A complex for 1 hour at room temperature. Once again, HeLa cells were incubated at 37°C for 1.5 hours following EDTA harvest before inclusion into this assay. Cells were washed twice in FACS wash buffer, re-suspended in FACS wash buffer, acquired on a FACS Fortessa X-20 flow cytometer (BD biosciences) and analysed using FlowJo software (Treestar). The MFI of AF488 was measured for each condition and expressed as a percentage of the control condition; data was presented on a histogram and analysed by one-way ANOVA and Tukey's multiple comparisons test (GraphPad Prism). Remaining target cells were surface stained in an HLA-B27 expression screen, as described (2.8 HLA-B27 expression screen), and, for cells transiently transfected with ERAP1, a Western blot was run to confirm presence of ERAP1 protein.

2.8 HLA-B27 expression screen

HeLa target cells and .221 cells, usually leftover from LAMP1 assays or rhKIR3DL1 assays although sometimes independently, were screened for their HLA-B27 cell surface expression to determine the levels of both pHLA-B27 complexes using the ME.1 antibody and FHC using the HC10 antibody. In addition, some cells were stained for total MHC Class I expression using the W6/32 antibody. HeLa cells were left at 37°C for 1.5 hours following harvest in order to recover their MHC expression following EDTA harvest, as EDTA has been proposed to strip the surface of MHC molecules (personal communication with Dr Louise Boyle, University of Cambridge). .221 cells were stained immediately following harvest.

Prior to staining cells were washed twice with FACS wash buffer. Washed cells were incubated with 0.5mg/ml ME.1 or HC10 antibody diluted in FACS wash buffer for 45 minutes at 4°C. Cells were then washed twice and re-suspended in 0.5mg/ml anti-Mouse-PE secondary antibody for 30 minutes at 4°C. Cells were again washed twice and the acquired on a Fortessa X-20 flow cytometer. Flow cytometry data was analysed by Treestar FlowJo software. In general, FACS histograms with the MFI for each condition are displayed. Additionally the MFI was normalized across three experiments to compare expression to the untransfected control and plotted on a histogram (GraphPad Prism). Triplicate MFI reading data was obtained and at least 3 independent experiments were conducted.

2.9 Western blotting for ERAP1

Remaining transfected HeLa ERAP1$^{-/-}$ cells from rhKIR3DL1 binding assays were probed for their ERAP1 expression to confirm transfection. Cells were spun at 2000rpm for 3 minutes, washed once in PBS and re-suspended in NP-40 lysis buffer at 50µl/10^6 cells. NP-40 lysis buffer consists of 1% NP-40, 150mM NaCl and 50mM Tris pH8.0 supplemented with 1% PMSF and 1% IAA to inhibit proteases. Cells were incubated on ice for 30 minutes and then spun at 13,000rpm for 10 minutes at 4°C. The supernatant was discarded and the cell pellet was re-suspended in loading sample buffer before 10µl was loaded onto a 10% SDS-PAGE gel. Following completion of the gel, the proteins were transferred onto a nitrocellulose membrane (Amersham), running for 1 hour 15 minutes at 26V.

Transferred membranes were blocked overnight at 4°C in 0.5% milk in 0.1% PBS/Tween. Polyclonal goat anti-human ERAP1 antibody (1:500, AF2334 RnD Systems) was added to the membrane and incubated for 1 hour before being washed three times with 0.1% PBS/Tween. Donkey anti-goat IgG (1:5000, Santa Cruz) was added to the membrane and incubated for 1 hour before being washed three times with 0.1% PBS/Tween. For detection of ERAP1 bands, membranes were incubated with SuperSignal West Femto chemoluminescent substrate (Thermo Scientific) for 5 minutes in the dark before visualisation on a BioRad Fluor-S Multi Imager camera (BioRad).

To confirm accurate protein loading, HC10 antibody against FHC of MHC I was used as a loading control. Blots were stripped by incubation with stripping buffer (1M Tris-HCl pH6.8, 20% SDS, β-mercaptoethanol) for 30 mins and then washed three times with 0.1% PBS/Tween before being re-probed with mouse anti-human HC10 antibody (1:500, made in house) for 1 hour and then washed three times with 0.1% PBS/Tween. Rabbit anti-mouse IgG (1:5000, Abcam) was added to the membrane and incubated for 1 hour before being washed three times with 0.1% PBS/Tween. For detection, membranes were incubated with SuperSignal West Femto chemoluminescent substrate (Thermo Scientific) for 5 minutes in the dark before visualisation on a BioRad Fluor-S Multi Imager camera (BioRad).

2.10 RnD Sytems Proteome profiler kit

To look at the cytokines and chemokines released from PBMCs following incubation with ERAP1 transfected HeLa ERAP1$^{-/-}$ target cells, I initially used a human cytokine array proteome profiler kit from RnD Systems. This kit simultaneously looks at 36 different cytokines and chemokines in a single dot blot to show whether each analyte is present and, crudely, how much of each is available. 50,000 HeLa ERAP1$^{-/-}$ target cells previously transfected with ERAP1 variants (**2.2 Cell culture and transfection**) and HLA-B*2705 were incubated with 200,000 PBMCs (5:1 ratio) for 24 hours before the cells were spun down and the supernatant was collected. The PBMCs had been previously stimulated overnight with 0.5ng/ml rhIL-15 (Peprotech).

The supernatant from the cell cultures was combined with the human cytokine array detection antibody cocktail and then added to the pre-prepared dot blots overnight at 4°C, as per the manufacturer's instructions. Membranes were washed, incubated with streptavidin-HRP for 30 minutes at room temperature and then washed again before detection. For detection, membranes were incubated with SuperSignal West Femto chemoluminescent substrate (Thermo Scientific) for 3 minutes in the dark before visualisation on a BioRad Fluor-S MultiImager camera (BioRad). The image was then analysed using ImageJ software dot blot analysis to measure the density of each dot. This density was plotted on a grouped histogram (GraphPad Prism) (**Figure 4.8**).

2.11 RnD Systems Luminex multiplex assay

Luminex multiplex assays can simultaneously look at several cytokine and chemokine targets in one assay through detection of multiple fluorescent beads labelled with target antibodies. A panel of 16 analytes was designed based on the results of the Proteome profiler kit (**Figure 4.8**) as described in chapter 4 and a magnetic multiplex assay kit was purchased from RnD systems. 10^5 HeLa ERAP1$^{-/-}$ cells were transiently transfected with HLA-B*2705 and an ERAP1 allotype combination (**2.2 Cell culture and transfection**) before harvest and incubation with $4x10^5$ PBMCs (previously stimulated with 0.5ng/ml rhIL-15 overnight) for 24 hours at 37°C. Following this, the supernatant for each condition was collected and used directly in the assay. Experimental conditions looked at the baseline levels of cytokine/chemokine production following incubation of target cells and PBMCs, as well as looking at the effect of blocking KIR3DL1, pB27 complexes or FHCs and the depletion of NK cells from the PBMC population.

As per the manufacturer's instructions, the magnetic beads provided with the kit were incubated with supernatant for 2 hours at room temperature, washed three times, incubated with the Biotin antibody cocktail for 1 hour at room temperature, washed three times, incubated with Streptavidin-PE for 30 minutes at room temperature and washed a further three times before being read using the Bio-Rad analyser (BioRad).

The concentration of each analyte was expressed on histograms (GraphPad Prism) and the fold change seen in each analyte compared to a control condition of the C1 allotype combination (add *00 info) was shown on a heatmap (Microsoft Excel) (**Figure 4.12**). One experiment was completed with each supernatant run in duplicate on one day. Data was analysed by t-test, one- or two-way ANOVA and Tukey's multiple comparisons test.

2.11.1 Antibody blocking conditions

As described previously for the LAMP1 assay (2.4), some transfected HeLa ERAP1$^{-/-}$ target cell and PBMC cultures were blocked with antibody during the 24 hours of incubation. 2ug/ml DX9 antibody against KIR3DL1, ME.1 antibody against pHLA-B27 complexes or HC10 antibody against FHC complexes was included in the cell cultures.

2.11.2 NK cell depletion

Using CD56 magnetic beads (MACS Miltenyi Biotech) the NK cell population was depleted from the whole PBMC population by magnetic depletion. 3x10^7 PBMCs were combined with CD56 microbeads, as per the provided datasheet, for 15 minutes before addition of the cells to a LD column. The NK cells with anti-CD56 magnetic beads bound were sequestered in the column and the flow through containing the NK cell-depleted PBMC population was collected.

Samples from both pre-sorted and post-sorted PBMC populations were run on the Fortessa X-20 flow cytometer (BD Biosciences) and analysed by FlowJo analysis software (Treestar) (**Figure 2.4**). This NK cell depleted population was then used in the Luminex assay as described above.

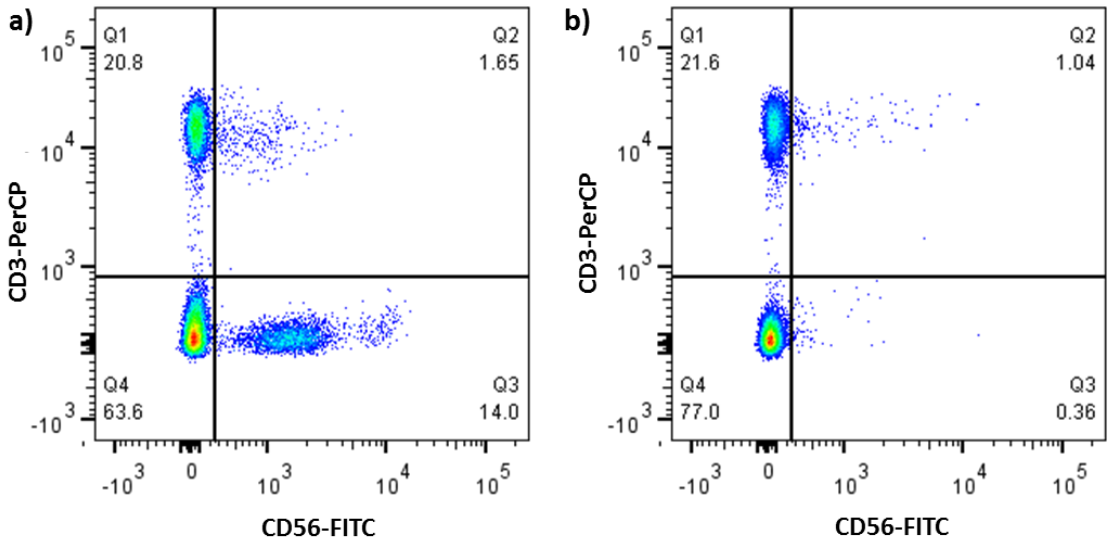

Figure 2.4: NK cell depletion from the PBMC population

The NK cell population was depleted from the whole PBMC population using CD56 magnetic beads and depletion was checked by flow cytometry. (a) Before sorting the PBMC population contained 14% $CD3^-$ $CD56^+$ NK cells and 1.65% $CD3^+CD56^+$ NKT cells. (b) Following magnetic depletion the $CD3^-CD56^+$ NK population was reduced to 0.36% and the NKT population was reduced to 1.04%.

2.12 HLA-B27 single chain trimer construction

Single chain trimer (SCT) constructs were designed to generate pB27 protein complexes that could be used for crystallisation or as recombinant protein for investigation into KIR3DL1 engagement. SCT protein consists of a peptide-b2m-HLA Class I heavy chain on one long polypeptide chain with linker regions between each domain (**Figure 2.5**) (113). Additionally, the peptide can be disulphide trapped into the peptide-binding groove to create a more stable construct (114). Four SCT constructs were designed: LF9-β2m-HLA-B*2705 (LF9-05), SF11-β2m-HLA-B*2705 (SF11-05), LF9-β2m-HLA-B*2709 (LF9-09) and SF11-β2m-HLA-B*2709 (SF11-09). LF9 is short for the 9mer peptide LRNQSVFNF; SF11 is short for the natural N-terminally extended form of LF9, SRLRNQSVFNF. The amino acid sequence for the LF9-05 construct can be found in **Figure 2.6** with the amino acid that is altered between HLA-B*2705 and –B*2709, D116, highlighted in red. Primers and PCR conditions for each step can be found in **Table 2:4** and **Table 2:5**, respectively.

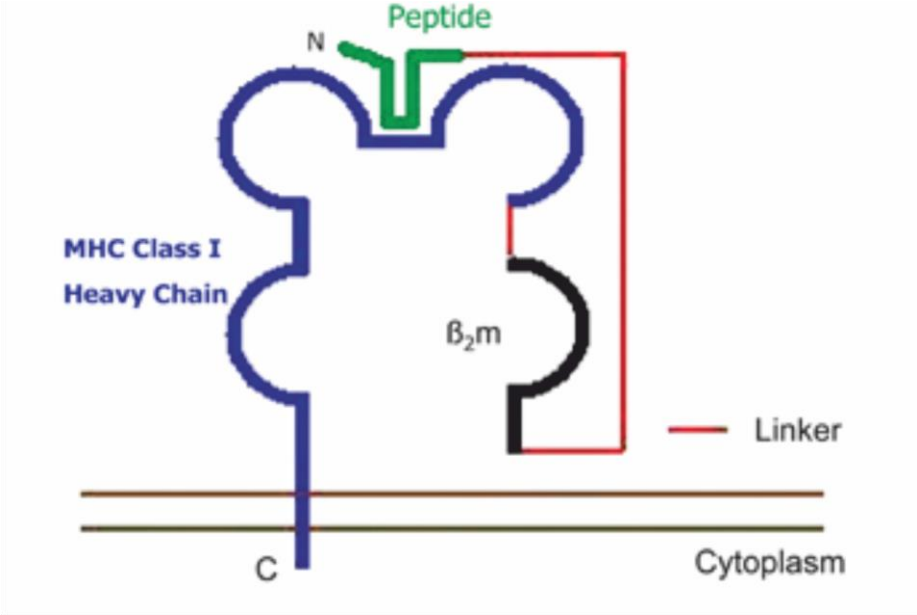

Figure 2.5: Single chain trimer structure

A single chain trimer (SCT) consists of an MHC Class I heavy chain (blue), β2m (black) and a peptide (green) all connected on one polypeptide chain by linker regions (red). Expression of the SCT protein leads to correct folding of the structure and expression at the cell surface.

L R N Q S V F N F G C G A S G G G G S G G G G S I Q R T P K I Q V Y S R H P A E N G K
S N F L N C Y V S G F H P S D I E V D L L K N G E R I E K V E H S D L S F S K D W S F Y
L L Y Y T E F T P T E K D E Y A C R V N H V T L S Q P K I V K W D R D M G G G G S G G
G G S G G G G S G G G G S G S H S M R Y F H T S V S R P G R G E P R F I T V G Y V D D
D T L F V R F D S D A A S P R E E P R A P W I E Q E G P E Y W D R E T Q I C K A K A Q
T D R E D L R T L L R Y Y N Q S E A G S H T L Q N M Y G C D V G P D G R L L R G Y H Q
D A Y D G K D Y I A L N E D L S S W T A A D T A A Q I T Q R K W E A A R V A E Q L R A
Y L E G E C V E W L R R Y L E N G K E T L Q R A D P P K T H V T H H P I S D H E A T L
R C W A L G F Y P A E I T L T W Q R D G E D Q T Q D T E L V E T R P A G D R T F Q K
W A A V V V P S G E E Q R Y T C H V Q H E G L P K P L T L R W E P S S Q S T V P I V G
I V A G L A V L A V V V I G A V V A A V M C R R K S S G G K G G S Y S Q A A C S D S A
Q G S D V S L T A S R G K P I P N P L L G L D S T

Figure 2.6: Amino acid sequence for LF9-mβ2m-B*2705 SCT

The amino acid sequence for the LF9-m05 SCT construct shows the peptide sequence (green), mouse β2m sequence (blue) and HLA-B*2705 sequence (yellow) linked by two linker regions (grey). The aspartic acid (D) residue which is mutated to histidine (H) is highlighted in red.

Table 2:4: Primer sequences for SCT construction

PCR Target	No.	Primer sequence
Amplify SIINFEKL-mβ2m	1 2	5'-aagcttatggctcgctcggtgacc-3' 5'- ctcatggagtgggagccactacctccaccaccggatc-3'
Amplify HLA-B*2705	3 4	5'-cggtggtggaggtagtggctcccactccatgagg-3' 5'- aagctttcaggtggagtccaatcc-3'
SIINFEKL to LRNQFEKL	5 6	5'-ctgaccggtttgtatgctctcagaaaccagttcgaaaaacttggatgc-3' 5'-gcatccaagtttttcgaactggtttctgagagcatacaaaccggtcag-3'
LRNQFEKL to LRNQSVFNF	7 8	5'-gtatgctctcagaaaccagagtgtgtttaacttcggatgcggtgctagcgg-3' 5'- ccgctagcaccgcatccgaagttaaacacactctggtttctgagagcatac-3'
Move SCT from pcDNA3 to pET28a and remove transmembrane domain	9 10	5'-ccatgggcctcagaaaccagagtgtg-3' 5'- ctcgaggggacggtggactgg-3'
LRNQSVFNF to SRLRNQSVFNF	11 12	5'-ccggtttgtatgcttccaggctcagtttcc-3' 5'- ggtttctgagcctggaagcatacaaaccgg-3'
D116H B*2705 to B*2709	13 14	5'-gggtaccaccaggacgcctacgagggc-3' 5'-gcctcgtaggcgtcctggtggtaccc-3'

To construct LF9-05, an existing SCT from our lab, SIINFEKL-mb2m-H2-K^b was used as the template. The SIINFEKL-mb2m portion of this SCT was amplified using primers 1 and 2. The HLA-B*2705 gene was amplified from an existing pcDNA3 vector using primers 3 and 4. Amplification was checked by running 5µl of each PCR product on a 1% agarose gel before combining 5µl of each product into a new PCR reaction with primers 1 and 4 to generate SIINFEKL-mβ2m-B*2705. The resulting PCR product was run on a 1% agarose gel, gel extracted (Promega PureYield plasmid miniprep system) and ligated into the PCR Blunt II TOPO vector (Invitrogen Zero blunt TOPO PCR cloning kit) before transformation into JM109 competent *E.Coli* bacteria. Correct ligation was checked by double digest of each colony with XhoI and HindIII restriction enzymes (Promega) and the insert was gel extracted to obtain cut SCT DNA. This DNA was then ligated into pcDNA3 overnight using T4 ligase (NEB), followed by transformation into JM109 bacteria. DNA was miniprepped (Promega PureYield plasmid miniprep system), confirmed by sequencing (Source Bioscience) and maxi-prepped (Qiagen Qiafilter plasmid maxi kit) to obtain a good stock of DNA.

Table 2:5: PCR conditions for SCT construction

PCR Step	PCR Conditions
Amplification of SIINFEKL-mβ2m	(95°C 20 secs, 57°C 10 secs, 70°C 12 secs) x 35 cycles
Amplification of HLA-B*2705	(95°C 20 secs, 57°C 10 secs, 70°C 40 secs) x 35 cycles
Generation of SIINFEKL-mβ2m-B*2705	(95°C 20 secs, 57°C 10 secs, 70°C 45 secs) x 35 cycles
SIINFEKL to LRNQFEKL and LRNQFEKL to LRNQSVFNF	(95°C 20 secs, 65°C 10 secs, 70°C 3 mins 15 secs) x 24 cycles
Amplify SCT from pcDNA3 to move to pET28a	(95°C 20 secs, 55°C 10 secs, 70°C 35 secs) x 18 cycles
Extension of LF9 to SF11 and change from HLA-B*2705 to –B*2709	(95°C 20 secs, 60°C 10 secs, 70°C 3 mins) x 25 cycles

SIINFEKL peptide was exchanged for LRNQSVFNF in a two-step process, with LRNQFEKL as an intermediate. Primers 5 and 6 were used for step one (SIINFEKL to LRNQFEKL) and primers 7 and 8 were used for step two (LRQNFEKL to LRNQSVFNF). At both stages PCR products were treated with 1µl DpnI for 1.5 hours and DNA was purified through addition of 10µl NaAc, 50µl dH_2O and 250µl 100% Ethanol (-20°C) and centrifugation at 13,000rpm for 20 minutes (4°C). Following this, the DNA pellet was washed once with 70% ethanol, 13,000rpm for 5 minutes (4°C). Purified DNA was transformed into JM109 competent *E.Coli* bacteria (made in house). DNA was mini-prepped (Promega PureYield plasmid miniprep system) and accurate exchange of peptides was confirmed by sequencing (Source Bioscience).

For the large-scale protein production required for crystallisation, the SCT was moved to the pET28a plasmid by amplifying the section from the pcDNA3 vector using primers 9 and 10 and ligating it into the Blunt II TOPO vector (Invitrogen Zero blunt TOPO PCR cloning kit). At the same time the transmembrane domain of HLA-B*2705 was excluded, as this must be completed for generation of soluble protein within bacteria. LF9-05 minus the transmembrane domain was successfully cloned into the Blunt II TOPO vector, as confirmed by sequencing (Source Bioscience). However, attempts to move this construct to the pET28a vector failed. Due to these cloning problems we made the complete SCT-pET28a vector from GenScript. The ordered plasmid contained LF9-05 within the pET28a vector (NcoI and XhoI insertion site).

The other SCT constructs were made from this LF9-05 template using primers 11 and 12 to extend the peptide from LF9 to SF11 and primers 13 and 14 to exchange the Aspartic acid (D) (-B*2705) at position 116 to Histidine (H) (-B*2709). All constructs were confirmed by sequencing

(Source Bioscience) and maxi-prepped (Qiagen Qiafilter plasmid maxi kit) to generate a good stock of DNA.

2.13 SCT Protein production

For production of SCT protein, each construct was transformed into BL21 bacteria with a RIPL codon. Each construct was subjected to a small scale IPTG induction, a large scale IPTG induction, purification of inclusion bodies and, finally, refolding of the SCT prior to protein purification by FPLC. Each stage is described in more detail below.

2.13.1 Small scale IPTG induction

From the transformed BL21 RIPL plate, 4 colonies were picked and cultured overnight in 2ml LB + KCS antibiotics (kanamycin, chloramphenicol, streptomycin). The following day, 100µl was added to 5ml LB + KCS antibiotics and left in a 37°C shaker until the bacteria had reached the exponential growth phase (~1 hour), at which point 1/1000 1mM IPTG was added to the bacteria and it was left to grow for 4 hours. A sample of bacteria before and after IPTG induction was run on a 15% SDS PAGE gel for 15 minutes at 60V and then 45 minutes at 250V. Confirmation of the induction of SCT protein prompted the next stage of protein generation, large scale IPTG induction.

2.13.2 Large scale IPTG induction

One colony positive for SCT production, as shown by small scale IPTG induction, was then selected to be grown up for large-scale IPTG induction. 500µl bacteria was added to 65ml LB + KCS antibiotics and left in a 37°C shaker overnight. The following day, 30ml of this culture was added to two 1L pre-warmed LB + KCS antibiotics flasks (total 2L prep per colony) and left until the OD600 reached 0.5-0.8A at which point the OD600 for each flask was noted. IPTG (1mM) was added at a ratio of 1/1000 to the bacteria for 4 hours, at the end of which the OD600 was noted again for each colony. For each colony samples from before and after IPTG induction were run on a 15% SDS-PAGE gel for 15 minutes at 60V and then 45 minutes at 250V to confirm the induction of SCT protein production. Bacteria was harvested through centrifugation of the culture media at

8000rpm, 4°C for 10 minutes (Sorvall RC6 centrifuge, SLA-3000 rotor), washed once in PBS and spun at 4000g, 4°C for 15 minutes (Heraeus Multifuge X3R). The liquid was disposed of and the bacterial pellet was frozen at -20°C until required.

2.13.3 Purification of inclusion bodies

Following large scale protein production, protein is enclosed within inclusion bodies inside the bacteria and these inclusion bodies must be purified. Bacterial pellets containing inclusion bodies were purified using 5ml of BugBuster (primary amine free) extraction reagent (Novagen) per gram of bacterial pellet, with 20µl of 1000kU/ml Lysozyme per gram of pellet, 50µl of 2mg/ml DNAse I per gram of pellet and 50µl of 1M $MgCl_2$ per gram of pellet. Tubes were placed on rollers for 40 min with 10mM DTT added after 30 min before the solution was centrifuged at 26,900g, 4°C for 15 minutes (Sorvall RC6 centrifuge, SS-34 rotor). This process was then repeated using an equal volume of BugBuster and 1mM DTT, and finally the pellet was washed twice with 25ml of 1/10 BugBuster in dH_2O, placed on rollers for 10 minutes and then centrifuged at 38,720g, 4°C for 15minutes (Sorvall RC6 centrifuge, SS-34 rotor).

The pellet was solubilised in 8M Urea, 50mM MES (pH 6.5), 0.1mM EDTA and 1mM DTT on rollers overnight, and spun at 18000rpm, 4°C for 20minutes (Sorvall RC6 centrifuge, SS-34 rotor) the following day. The supernatant was collected and aliquoted for storage at -20'C. Using the molecular weight and extinction coefficient of each construct, the Nanodrop (Thermo Scientific) was used to determine protein concentration and an SDS-PAGE gel was run with samples from each step to confirm the presence of inclusion bodies and level of purification.

2.13.4 Refolding SCT protein

Purified inclusion bodies contain unfolded protein and so protein must be folded before purification. Approximately 30mg of purified inclusion body protein per 500ml refold buffer was added by drop diffusion to the solution on a magnetic stirrer in three injections at 0, 10 and 24 hours. Initially, the refold buffer consisted of 100mM Tris-HCl (pH 8.4), 400mM L-Arginine HCl, 2mM EDTA, 0.5mM reduced glutathione, 0.5mM oxidised glutathione and 0.5mM PMSF. The refold solution was left for 24 hours following the final injection and was then concentrated in an Amicon concentrator to <10mls for fast protein liquid chromatography (FPLC) (Nasia Kontouli).

Following some poor yields following protein purification the ratio of reduced to oxidised glutathione was investigated (**Figure 2.7**). It was found that a ratio of 5:1 reduced: oxidised glutathione gave the greatest yield of monomeric protein compared to dimeric protein and so this ratio was utilised in subsequent refold reactions.

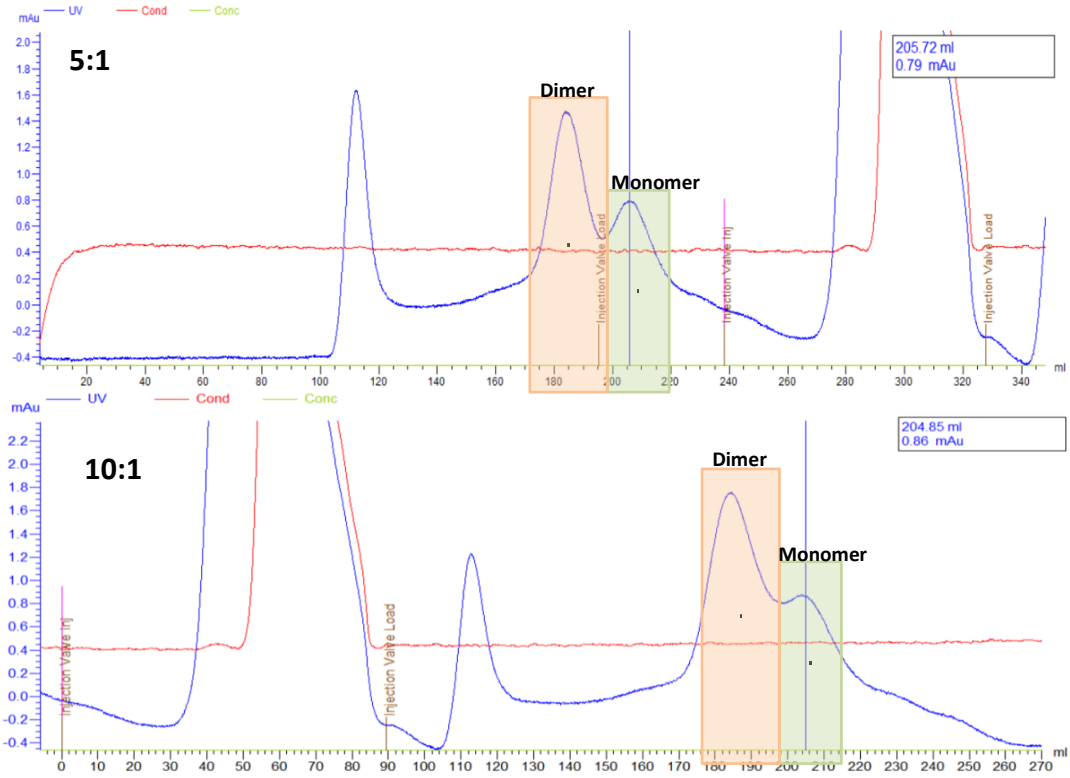

Figure 2.7: Optimisation of refold conditions for SCT

The refold conditions for the previous refolds has used reduced and oxidised glutathione at a 1:1 ratio, to try and optimise refold conditions for better monomer purification I altered this ratio to 5:1 and 10:1 reduced to oxidised. 60ml refold buffers were set up and 4mg protein was added over 48 hours before 5ml was loaded onto an AKTA Prime FPLC, Superdex 200 HiLoad 26/60 column. (a) At a 5:1 ratio there was a more pronounced monomer peak but the dimer peak was still higher. (b) At a 10:1 ratio the monomer peak was lower than that of 5:1 and the dimer peak was larger.

2.13.5 Purification of refolded SCT protein

Purification of the SCT was done using an AKTA Prime FPLC, Superdex 200 HiLoad 26/60 column. 15mg LF9-05 SCT protein was added to 250ml refold buffer and then concentrated to ~7ml before injection onto the AKTA Prime FPLC, Superdex 200 HiLoad 26/60 column (**Figure 2.8a**). There is a large overlap of dimers in the monomer peak, which would make it difficult to purify just the monomer fraction. In addition, the absorbance (mAu) of the peaks, a marker of expected protein concentration, was very low and so it is unlikely that enough protein could be recovered for crystal trials. A reducing SDS-PAGE gel was run for each peak, un-concentrated refold buffer and the concentrated SCT before injection onto the column (**Figure 2.8c**). Fractions from peaks 2 and 3 showed a band at ~48kDa, the correct size for the SCT, but in the peak 2 fraction there was an additional band at ~100kDa which likely represents the dimer of SCT. Fractions from the monomer peak were also run on a separate reducing SDS-PAGE gel with a band at ~48kDa representing the SCT protein.

The aggregation seen with this first refold was a problem seen with subsequent refold and purification attempts. Addition of more protein or an increase in refold buffer volume gave no better results. Cysteine 67 of HLA-B27 was mutated to Serine in an attempt to prevent dimerization, as this is the residue responsible for the formation of $B27_2$, although these are only thought to occur in the absence of peptide and β2m (13). This change had little effect on the aggregation and purification of a purely monomeric population was still impossible.

To determine at which stage this aggregation occurs, a 1L refold was set up with 60mg LF9-09 SCT protein. 10ml of un-concentrated refold solution was loaded onto the AKTA Prime FPLC, Superdex 200 HiLoad 26/60 column and showed that the monomer peak was almost equal to the dimer peak, but as this was an un-concentrated sample the mAu was very low (**Figure 2.9a**). Next, 300ml of the refold buffer was concentrated to ~8.5ml and loaded onto the same column (**Figure 2.9b**). The monomer peak had completely disappeared, which is especially visible in the zoomed in image of the dimer and monomer peaks (**Figure 2.9c**). The remaining 700ml refold buffer was concentrated to 250ml and 5ml of this was loaded onto the same column (**Figure 2.9d**). The monomer peak was still clearly visible in this sample; however when this 250ml was further concentrated to ~5.5ml and loaded onto the same column the monomer peak had disappeared (**Figure 2.9e**).

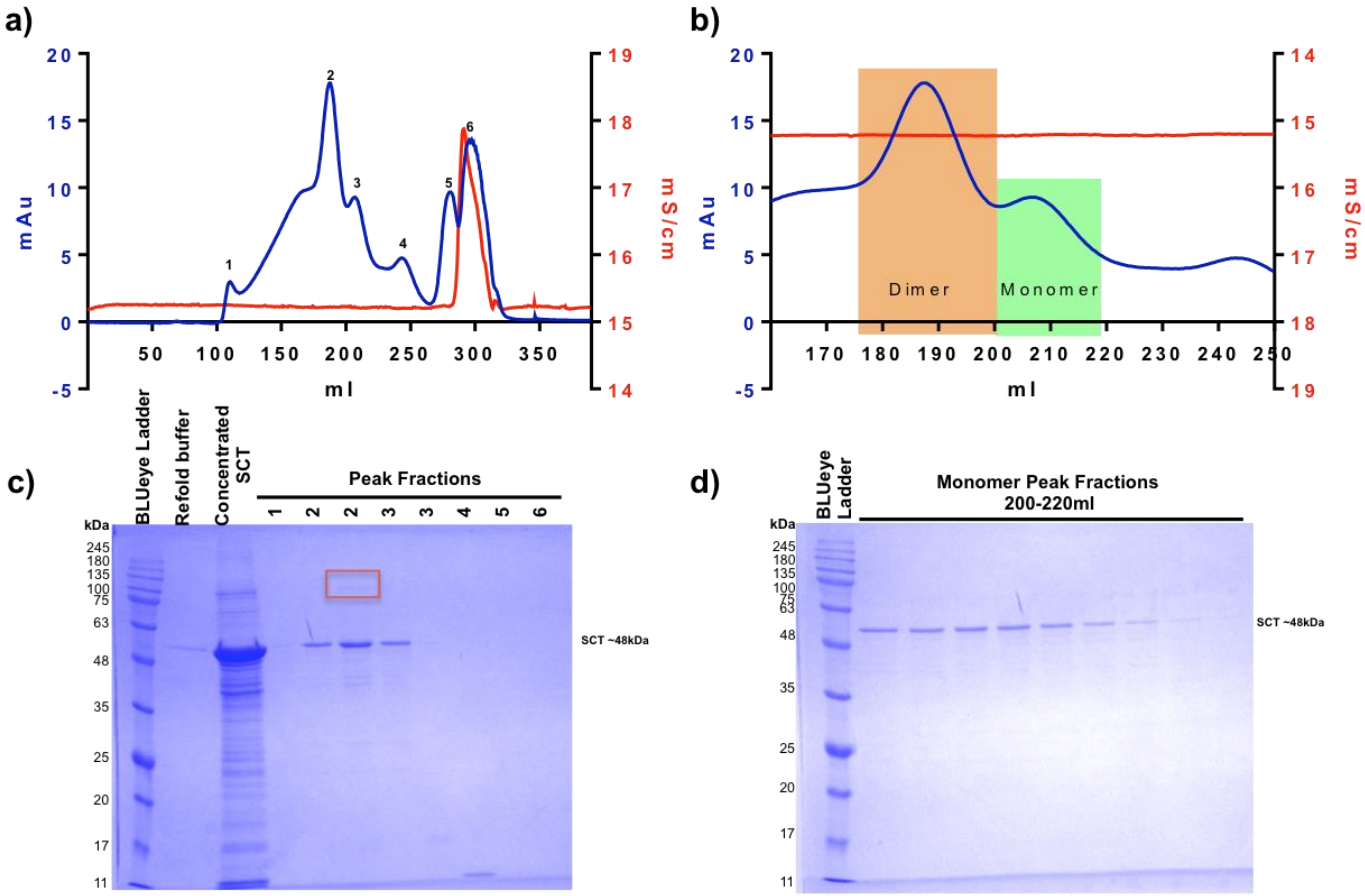

Figure 2.8: Purification of LF9-hb2m-B*2705 SCT with FPLC

LF9-hβ2m-B*2705 SCT was expressed in BL21 RIPL bacteria to create soluble protein enclosed in inclusion bodies. Inclusion bodies were then purified and 15mg protein was added to a 250ml refold buffer solution across 2 days. The refold solution was concentrated to ~7ml and then injected onto AKTA Prime FPLC, Superdex 200 HiLoad 26/60 column. (a) The chromatogram trace shows a high peak for dimers (peak 2), a smaller monomer peak (peak 3) and some aggregates (peak 1). The absorbance (mAu) of all peaks was low suggesting low protein levels were loaded onto the column. (b) Zoomed in visual of dimer and monomer peaks shows large overlap between these two groups. (c) Fractions from each peak seen on the chromatogram were loaded onto a 15% reducing SDS-PAGE gel along with some concentrated and un-concentrated refold buffer. There is a clear band at the expected size for SCT (~48kDa) in fractions from peaks 2 and 3. In peak 2, there is an additional feint band at ~100kDa (highlighted in red), representing SCT dimers. (d) All monomer peak fractions were also run on a separate 15% reducing SDS-PAGE gel and the SCT band can be seen in most fractions.

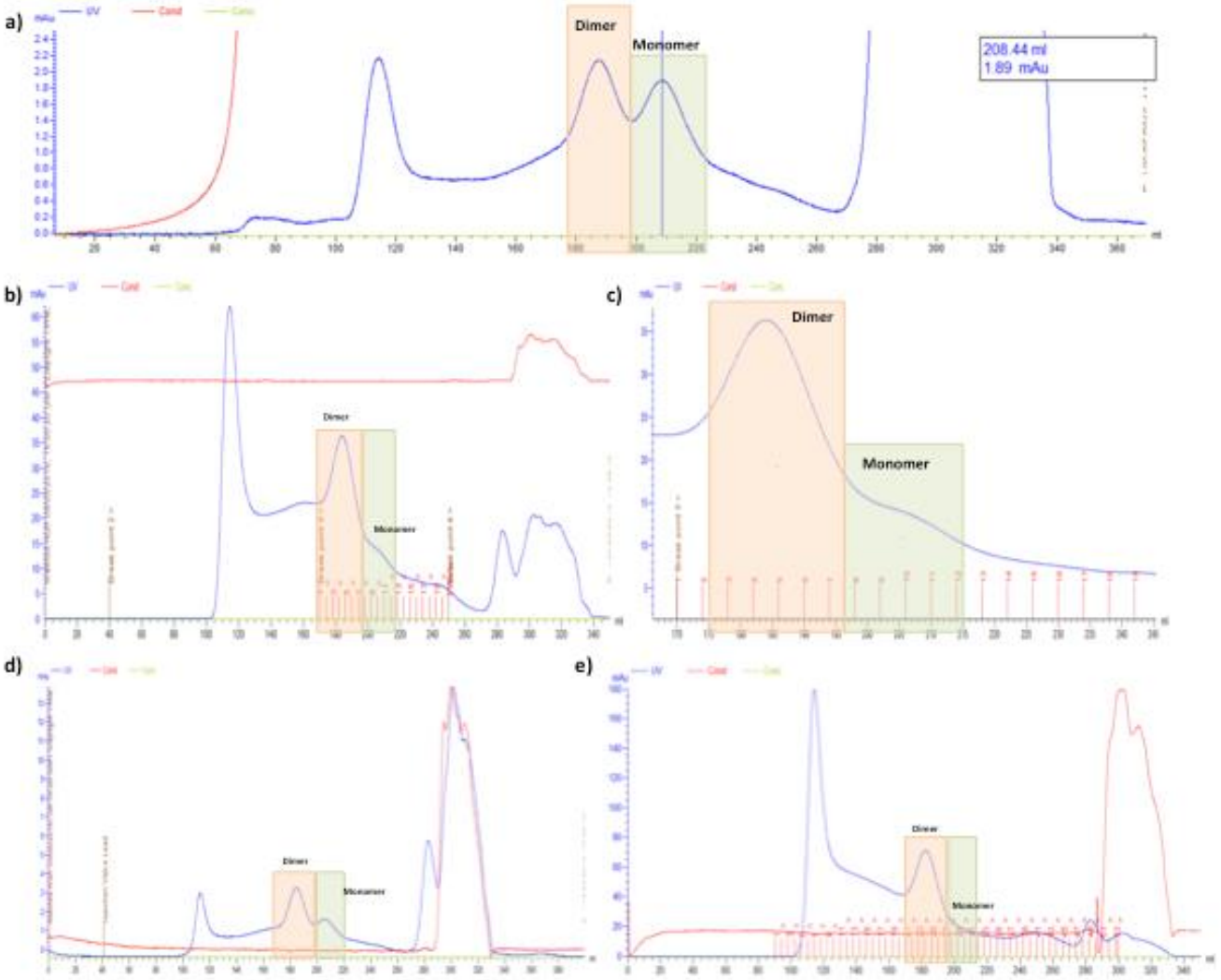

Figure 2.9: Purification of LF9-hb2m-B*2709 SCT with FPLC

LF9-hβ2m-B*2709 SCT was expressed in BL21 RIPL bacteria to create soluble protein enclosed in inclusion bodies. Inclusion bodies were then purified and 60mg protein was added to a 1L refold buffer solution across 2 days. (a) 10ml of un-concentrated refold buffer was loaded onto an AKTA Prime FPLC, Superdex 200 HiLoad 26/60 column. The monomer peak was almost equal to the dimer peak, but as this was an un-concentrated sample the mAu is very low. (b) 300ml of the 1L refold was concentrated to ~8.5ml and loaded onto the same column. There was a large dimer peak, minimal shoulder monomer peak and a large amount of aggregates. (c) Zoomed in view of dimer and monomer peaks shows minimal monomer peak and low mAu. (d) The remaining 700ml was concentrated to 250ml and 5ml of this was loaded onto the column. At this point there is a clear monomer peak although the dimer peak is still dominant. (e) The 250ml was further concentrated to ~5.5ml and loaded onto the column. At this point the monomer peak has completely disappeared and been replaced by a large aggregate peak.

Chapter 3: Peptide preferences of KIR3DL1

3.1 Introduction

The balance between activation and inhibition of NK cells is tightly controlled by a collection of receptors, with disruption of the engagement between one receptor and its ligand being enough to skew the balance one way or the other. Particularly important within the context of this work is the relationship between the Ig-like KIRs and MHC I; with this work focussing on the interaction between KIR3DL1 and HLA-B27.

Initially, a lack of MHC I on the cell surface was believed to induce NK cell activation through KIRs, however, it is now known that the sequence of the peptide bound to MHC I plays a role in skewing the balance between activation and inhibition. KIR3DL1 interaction with HLA-Bw4 has been shown to be dependent on the amino acids at positions 7 and 8 (P7:P8) of a 9 amino acid peptide (115). Using the peptide FRYNGLIHR, part of the 60S ribosomal protein L28, bound to HLA-B*2705, Peruzzi *et al* showed that mutation of the amino acids at these positions increased target cell lysis by an NK cell clone from around 20% (P7I: P8H) to 80% (P7I: P8E), 90% (P7I: P8K) and 50% (P7R: P8H) (115). A recent crystal structure, by Vivian *et al*, showing KIR3DL1 interacting with HLA-B57 showed that important contacts are made between all three domains to various parts of the HLA; the D0 domain formed one interface, while the D1-D2 intersection formed a second. Tyr200, Glu282 and Leu166 from domains 1 and 2 of KIR3DL1 were found to be important in forming contacts with P8 and P9 of the bound 9mer peptide (116). The binding interfaces of this KIR supports a more rigid binding formation between KIR and HLA as the D0 domain acts as an additional stabiliser for binding. These interactions were a combination of van der Waals and water-mediated H-bonds, suggesting that the biochemical composition of the amino acids at these positions could also affect correct KIR3DL1 engagement (116).

HLA-B27 was chosen as the MHC I molecule to interact with KIR3DL1 for this work as it has been implicated in the pathogenesis of AS (117, 118). How the peptide sequence can alter KIR3DL1 engagement when bound to this MHC I molecule could be important in the pathogenesis of AS as ERAP1, which trims peptides in the ER and has been strongly associated with AS, may alter the peptide repertoire presented at the cell surface (25). ERAP1 is a highly polymorphic protein and several variant combinations have been shown to discretely distinguish between AS cases and controls (6). ERAP1 variants associated with controls generally have moderate trimming function creating peptides of the correct length for MHC I binding, while those more

associated with AS are either hypo- or hyper-functional (6). Therefore, differences in ERAP1 activity may alter the peptide repertoire and hence the relative abundance of particular P7 and P8 amino acids and may alter the balance of NK cell activation between inhibition and activation.

3.2 Hypothesis

AS-associated ERAP1 variants will produce a peptide repertoire with different P7 and P8 residues compared to non-AS associated ERAP1 variants and promote greater NK cell activation.

This work will provide insight into which amino acids prevent strong KIR3DL1 engagement and can be used as a guide to predict whether a peptide repertoire generated by ERAP1 variants may have a positive or negative effect on NK cell activation.

3.3 Aims

- Develop a model system for looking at the interaction between KIR3DL1 and HLA-B27 bound peptides
- Create a peptide database to investigate the abundance of P7:P8 amino acids bound to HLA-B27
- Use the peptide database to identify combinations of P7:P8 which have the potential to inhibit or activate NK cells through KIR3DL1
- Use model system to determine the NK cell activation in response to these new peptides

3.4 Results

3.4.1 Exogenous FRY peptides do not alter NK cell activation in LAMP1 assays

Previously, Peruzzi *et al* showed that mutation of different amino acids in the naturally occurring FRYNGLIHR peptides could alter lysis of RMA-S-B27 cells by the NK clone 2w-14/C1R. In particular, changes in the amino acids at positions 7 and 8 (P7 + P8) increased lysis from ~20% with the wild-type (WT) FRYNGLIHR (FRY-IH) peptide to ~90% with the FRYNGLIKR (FRY-IK) peptide (115). To investigate whether P7 and P8 positions affected NK cell activation through the induction of cytolysis we used the LAMP1 assay of NK cell activation (103). In order to confirm that the LAMP1 assay produced similar results to those seen by Peruzzi *et al,* thus making it a suitable assay to look at the effect of P7:P8 peptide mutations on NK cell activation through KIR3DL1, I chose 3 peptide sequences used in addition to the WT FRY-IH peptide. FRY-IK induced ~90% lysis, FRY-IE induced ~80% lysis and FRY-RH ~50% lysis of the RMA-S-B27 cells.

221-B*2705^{+} target cells were pulsed with 20μM exogenous peptide overnight at 26°C before inclusion in LAMP1 assays the following day (2.4 NK cell degranulation (LAMP1) assay). There was significant inhibition of NK cell activation following incubation with .221-B*2705 cells compared to .221 cells ($p<0.001$), which was more pronounced in the KIR3DL1^{+} population, corresponding with what was previously seen in **Figure 2.3** (**Figure 3.1**). However, addition of exogenous peptide generated no significant difference in NK cell activation compared to no peptide addition controls in both the NK cell population and the KIR3DL1^{+} population. This lack of difference in NK cell activation was unexpected and suggested that there was a problem with stabilisation of HLA-B27 with exogenous peptide.

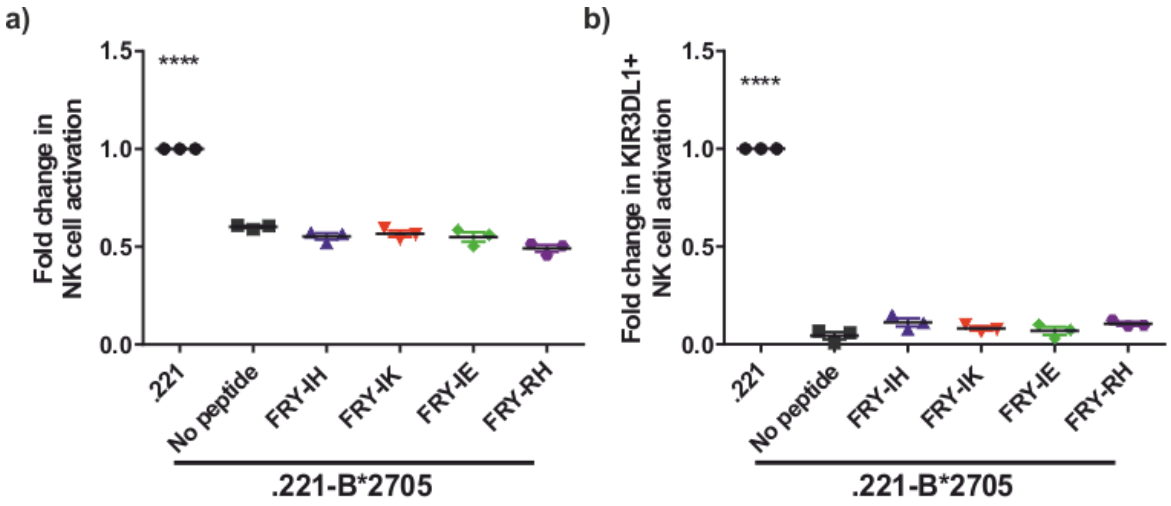

Figure 3.1: Exogenous FRY peptide loading onto .221-B*2705 has no effect on NK cell activation

.221-B*2705 cells were pulsed overnight with exogenous peptide at 26°C. 20µM of either WT FRY peptide (FRYNGLIHR) or P7:P8 mutated FRY peptide (FRY-xx) was pulsed overnight prior to the addition of PBMCs for a LAMP1 assay. There was a significant inhibition of both the whole NK cell population (a) and KIR3DL1+ NK cell population (b) with .221-B*2705 cells compared to .221 cells ($p>0.0001$). However, the addition of peptide made no significant difference to the activation of the NK cells. Triplicate data from 3 experiments run on different days. Data analysed by one-way ANOVA and Tukey's multiple comparisons test.

3.4.2 Exogenous FRY peptides do not stabilise HLA-B*2705

To investigate the stabilisation of exogenous peptide on B*2705 I used BFA peptide stabilisation assays to measure the cell surface expression of peptide-HLA-B27 complexes on the cell surface across 6 hours following peptide pulsing of.221-B*2705 cells. It was expected that the exchange of exogenous high affinity peptide for lower affinity peptides naturally presented on the cell surface would increase the stabilisation of HLA-B27, which could be observed by an increase in cell surface ME.1 staining and a slower drop-off rate from the cell surface.

However, there was no increase in HLA-B27 staining on the cell surface observed above levels seen with no exogenous peptide loading following pulsing with any of the four peptides (**Figure 3.2**). In addition, the loading of a high affinity peptide would be expected to stabilise the MHC I at the cell surface for longer leading to a reduction in the rate at which MHC I decreases at the cell surface in the presence of BFA. Despite the addition of high affinity peptides, no stabilisation of the MHC I was observed above that seen for no peptide control (**Figure 3.2**).

To optimise this exogenous peptide loading I altered the concentration of FRY-IH pulsed onto .221-B*2705 cells and found that 10µM was the optimal concentration for binding as it

showed the highest initial ME.1 staining (HLA-B27 expression) (**Figure 3.3a**). Across a 3 hour BFA decay, there was a slight increase in HLA-B27 staining following addition of 10µM FRY-IH (**Figure 3.3b**), but when these data was expressed as a percentage of maximal binding at zero hours there was no discernible difference in decay rate between no peptide and FRY-IH (**Figure 3.3c**).

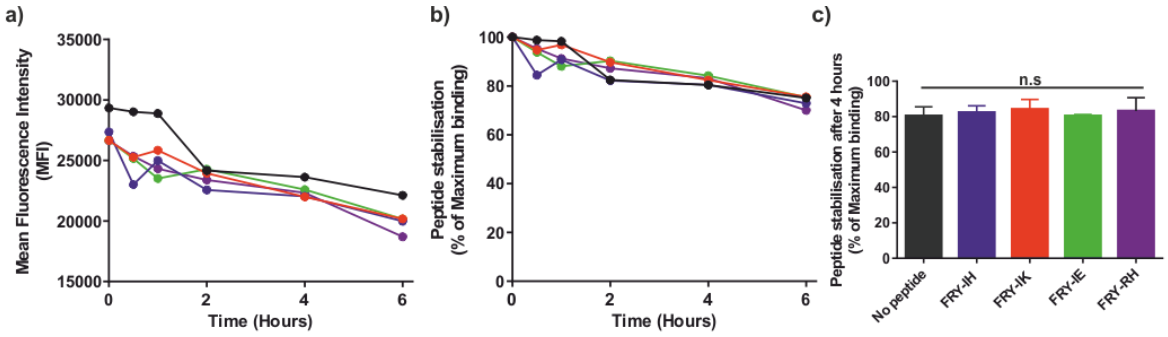

Figure 3.2: Exogenous FRY peptides do not stabilise cell surface HLA-B*2705

20µM exogenous FRY peptide was pulsed over .221-B*2705 cells at 26°C overnight and then moved to 37°C for 0-6 hours in a BFA decay assay. At each time-point the level of peptide-HLA-B27 staining on the cell surface was measured by staining the cells with the ME.1 antibody. There was no marked difference in HLA-B27 staining with any of the exogenous peptides compared to the addition of no peptide (a,b). Across 4 hours there was no significant difference in HLA-B27 expression on the cell surface (c). N=3, Data analysed by one-way ANOVA and Tukey's multiple comparisons test.

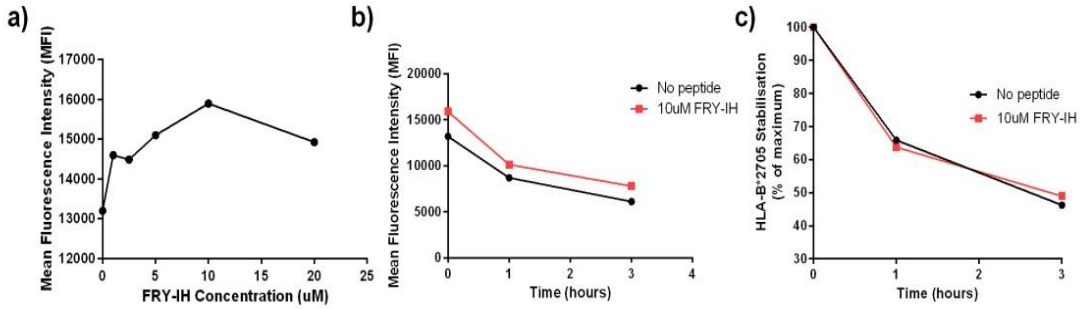

Figure 3.3: Optimisation of exogenous FRY peptide binding to HLA-B*2705

(a) The optimal concentration for exogenous peptide pulsing onto the .221-B*2705 cells was determined by titration of peptide pulsed overnight at 26°C from 0µM to 20µM. Following ME.1 staining of cells, 10µM was shown to be optimal for peptide stabilisation as this gave the highest initial MFI. (b) 10µM WT FRY peptide was used in a 3 hour BFA decay and showed some increase in MFI compared to no peptide. (c) However, when the MFI from (b) was expressed as a percentage of maximal binding there was no difference in HLA-B27 stabilisation.

These data suggests that the FRY peptide has a lower-affinity for HLA-B*2705 than the naturally bound peptides and is therefore not displacing presented peptides at the cell surface. To investigate this further I looked for alternative target cells with a reduction in high affinity peptides and used 721.220 (.220) and T2 cells in BFA peptide stabilisation assays. The .220 cell line has no expression of tapasin; tapasin is a chaperone protein that is a part of the peptide loading complex in the ER to facilitate the loading of high-affinity peptides onto MHC I for antigen presentation (111) and the T2 cell line is TAP deficient; TAP is the transporter of peptides from the cytosol into the ER and another part of the peptide-loading complex (119). This T2 cell line is derived from fusion of a B-LCL cell line with CEMR.3 cells, with both copies of the CEMR.3 chromosome 6 being deleted in the process. Chromosome 6 contains all of the HLA genes, including the TAP1 and TAP2 genes (112). Both of these two cell lines therefore should have less high affinity peptides on the cell surface, creating a higher potential for exogenous peptide loading.

The cell surface expression of HLA-B27 was measured over 6 hours following overnight peptide pulsing at 26°C. There was a minimal increase in stabilisation following the addition of exogenous peptide to .220-B*2705 cells but only after 2 hours (**Figure 3.4a-c**). None of these differences were significant at four hours, suggesting minimal exogenous peptide stabilisation. There was a good level of stabilisation with the addition of FRY-IH, -IK and –IE on T2-B*2705 cells **(Figure 3.4d-e**). But this result was variable across different experiments and when the data was combined there was no significant difference between the addition of exogenous peptide and no peptide addition after 4 hours (**Figure 3.4f**)

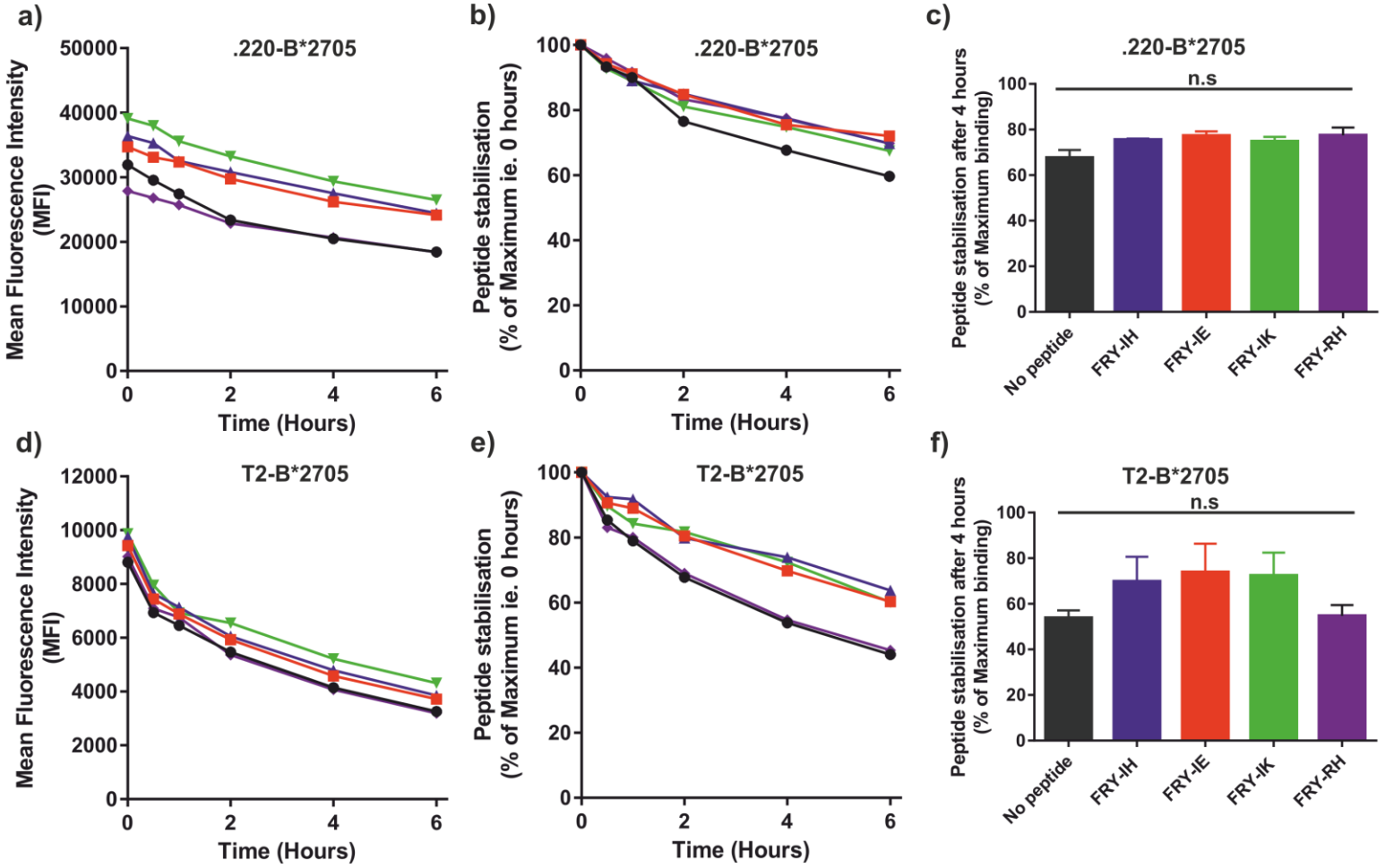

Figure 3.4: Exogenous stabilisation of FRY peptides on .220 and T2 cells

721.220 (.220) and T2 cells were used with exogenous FRY peptides in BFA decays to determine whether increased stabilisation of HLA-B27 could be observed. .220 have depleted MHC class I and are tapasin negative. Loading of exogenous peptide onto .220-B*2705 cells showed minor stabilisation of FRY-IH (blue), FRY-IE (red) and FRY-IK (green) (a,b) but this was not significant across four hours (c). The TAP-deficient T2-B*2705 cell line showed some stabilisation with FRY-IH (blue), FRY-IE (red) and FRY-IK (green) (d,e). This difference was clear after 4 hours but the results were not significant (c). N=3, Data analysed by one-way ANOVA and tukey's multiple comparisons test.

3.4.3 Transfected peptides bound to HLA-B*2705 alter NK cell activation

To overcome the problems with exogenous peptide loading onto HLA-B27, an alternative system using minigene constructs for each peptide was developed. A minigene construct consists of the peptide sequence attached to the 'MRYMILGLLALAAVCSA' ER signal sequence from the Human adenovirus C serotype 6 virus, within the pcDNA3 vector. This is transiently transfected into HeLa target cells, within which, following translation, the peptide is transported to the ER and the signal sequence cleaved leaving just the peptide available for MHC I binding and presentation at the cell surface. To reduce the pool and affinity of peptides already available within the HeLa cells, I used HeLa ERAP1$^{-/-}$ cells previously created in our lab with CRISPR. The cells were also transiently transfected with HLA-B*2705 as HeLa cells do not naturally express this MHC I allele. Within our lab we have tried to create a stable HLA-B*2705 expressing HeLa ERAP1$^{-/-}$ cell line several times, but expression of the HLA is lost after 1-2 weeks each time and the cells do not survive past this point. Following transient transfection I routinely get 50-70% HLA-B27^{+} cells, as determined by flow cytometry during every experiment. At any point, if no HLA-B27 expression is seen the corresponding condition is excluded from analysis.

Minigenes expressing the WT FRY-IH peptide, FRY-IK, -IE & –RH were created (2.3 Plasmid minigene construction) and used in LAMP1 assays to determine NK cell activation (2.4 NK cell degranulation (LAMP1) assay). In the whole NK cell population FRY-IH showed some inhibition compared to HeLa ERAP1$^{-/-}$ B*2705 (HeLa EKO 05) cells (n.s.) (**Figure 3.5a**). This inhibition was significant compared to FRY-IK ($p<0.05$), which showed the highest activation level. FRY-IE and FRY-RH showed minimal difference compared to HeLa EKO 05 cells. In the KIR3DL1^{+} population, in support of data previously shown by Peruzzi *et al* (115), FRY-IK and FRY-RH induced significantly higher NK cell activation than FRY-IH ($p<0.05$) (**Figure 3.5b**). As it was previously shown that FRY-IE induced ~80% target cell lysis it was surprising that in this system FRY-IE showed minimal effect on NK cell activation and instead acted in much the same way as HeLa EKO 05 cells.

With the exception of FRY-IH in the displayed histograms, which still had similar inhibition to HeLa EKO 05 despite the reduction, the MFI of HLA-B27 staining is equal for each minigene, suggesting that it is the sequence of the peptide rather than a reduction in HLA-B27 at the cell surface that is affecting NK cell activation (**Figure 3.5c-d**). In addition, despite some variability, there were no significant differences in FHC levels on the cell surface suggesting that the peptides have similar affinity for HLA-B*2705 (**Figure 3.5c-e**).

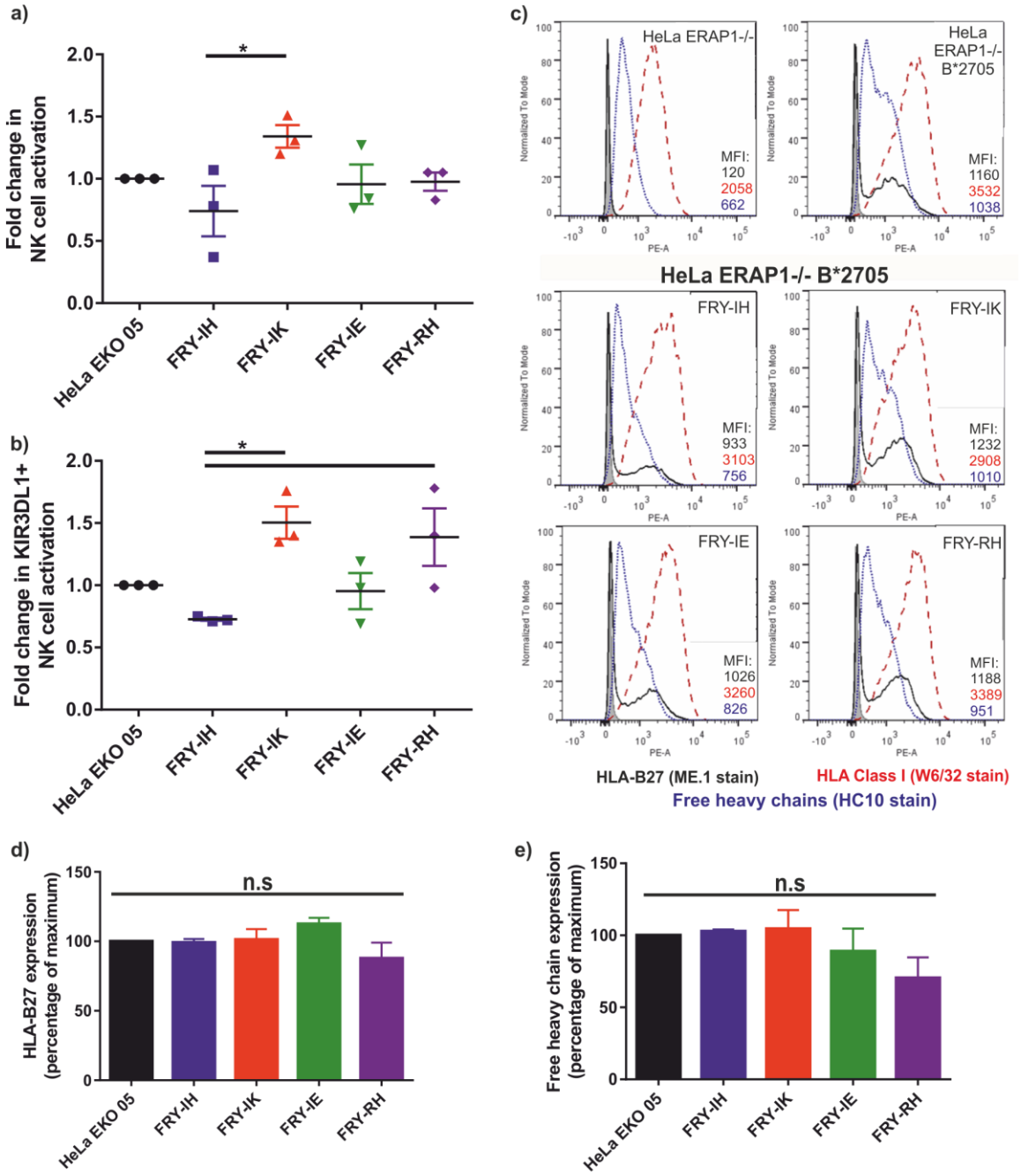

Figure 3.5: P7:P8 mutations alter NK cell activation

Using peptide minigenes, HLA-B*2705 and FRY peptides were transiently transfected into HeLa ERAP1$^{-/-}$ (EKO) cells for LAMP1 assays. (a) FRY-IH significantly inhibits NK cell activation compared to FRY-IK ($p<0.05$), while no other peptide has any significant effect. (b) In the KIR3DL1^{+} population, FRY-IH significantly inhibited NK cell activation compared to FRY-IK ($p<0.05$) and FRY-RH ($p<0.05$). (c) Following transfection HeLa EKO targets were MHC screened for MHC class I, HLA-B27 and FHC expression. (d,e) There was no significant difference in HLA-B27 or FHC cell surface expression with any of the peptide minigenes. N=3, Data analysed by one-way ANOVA and Tukey's multiple comparisons test.

3.4.4 Transfected peptides bound to HLA-B*2705 do not alter rhKIR3DL1 binding

In the LAMP1 system the whole PBMC population is used, and thus NK cells that express a range of receptors – both activating and inhibitory. This makes the results more physiologically relevant but in the context of this work it is important to confirm that the changes we are seeing are due to KIR3DL1 engagement specifically. To confirm the previous results I measured KIR3DL1 binding to HLA-B*2705 on minigene transfected cells using recombinant human KIR3DL1 (rhKIR3DL1) protein and combined this with protein A overnight (2.7 Recombinant human KIR3DL1 binding). This protein A is conjugated to an AF488 molecule allowing direct detection of this protein by flow cytometry. Addition of protein A creates tetramer complexes with four rhKIR3DL1 molecules attached to one protein A molecule; again creating a more physiologically relevant system as this represents clustering of receptors at the cell surface.

The binding of KIR3DL1 onto HLA-B*2705 expressing FRY minigenes was determined by allowing tetramerised rhKIR3DL1 to bind to transfected HeLa target cells for 1 hour, before the MFI was measured by flow cytometry. Higher binding of rhKIR3DL1 to target cells represents a stronger interaction with this MHC I. There was very little difference between rhKIR3DL1 binding with each peptide minigene, with all differences being non-significant (**Figure 3.6**).

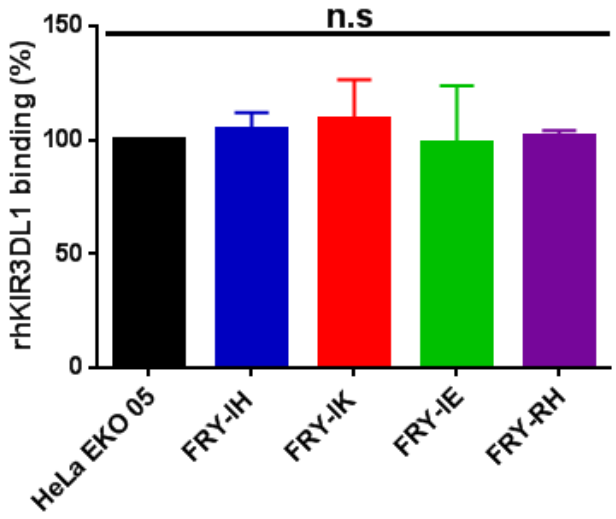

Figure 3.6: Binding of rhKIR3DL1 is not altered with FRY peptides

Using peptide minigenes, HLA-B*2705 and FRY peptides were transiently transfected into HeLa EKO cells for 24 hours prior to binding of recombinant human KIR3DL1 (rhKIR3DL1) for 1 hour. There is no significant difference in rhKIR3DL1 binding with any minigene compared to HeLa ERAP1$^{-/-}$ B*2705 cells. N=3, Data analysed by one-way ANOVA and Tukey's multiple comparisons test.

3.4.5 Modelling predicts that peptide conformation may affect NK cell engagement

To better understand how the differences in peptide sequence may effect engagement of KIR3DL1 structural modelling was used to map each FRY peptide onto HLA-B*2705 and determine the fit in the peptide binding groove using the Chimera program (Resource for Biocomputing, Visualization, and Informatics at the University of California, San Francisco supported by NIGMS P41-GM103311) (**Figure 3.7a**). When each peptide is superimposed the arginine at position 7 (R7) extends out of the F-pocket of the peptide binding groove further than the WT isoleucine (I7) which may sterically hinder engagement of KIR3DL1 by preventing the KIR from getting close enough to HLA-B*2705 to make contact (**Figure 3.7b**). Additionally, lysine at position 8 (K8) extends out the peptide-binding groove further than histidine (H8), which may explain the increase in NK cell activation with FRY-IK; KIR3DL1 cannot get close enough to generate interactions between domains 1 and 2 of KIR3DL1 and P8/P9 of the peptide. Glutamic acid at position 8 (E8), FRY-IE, changes the direction the amino acid chain without affecting the length, potentially explaining why there is minimal change in NK cell activation through KIR3DL1 with this peptide.

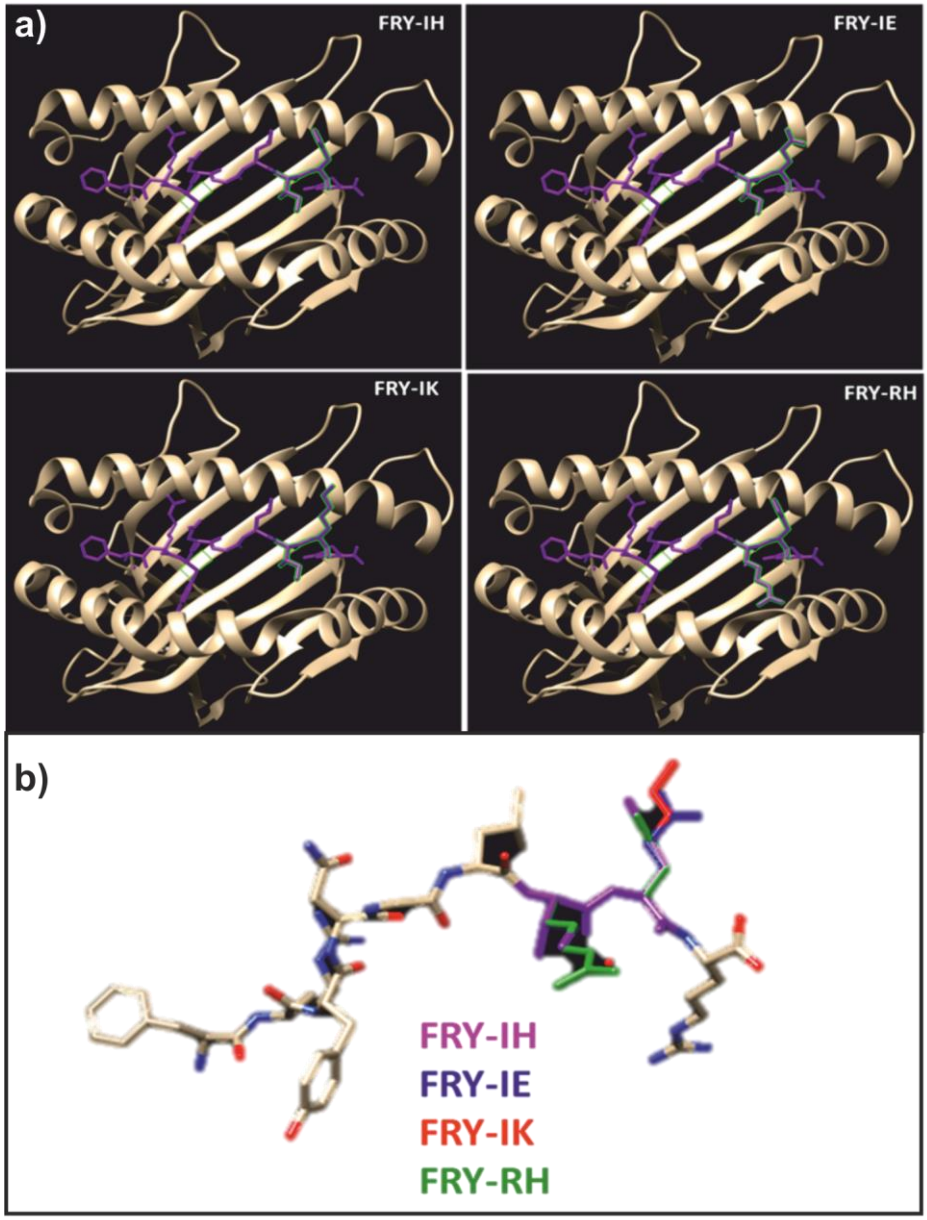

Figure 3.7: Modelling of FRY peptides onto HLA-B*2705

(a) Using the Chimera program, the FRY peptides were modelled onto HLA-B*2705 to show the most likely conformation of each peptide within the peptide binding groove. Amino acids at position 7 & 8 are shown in green. (b) When the peptides are superimposed there is a clear extension of the peptide with P7R (FRY-RH, green) and P8K (FRY-IK, red). These extensions may prevent the binding of the peptide into the F-pocket of the peptide binding groove, or may prevent strong KIR engagement by extending out of the peptide binding groove to prevent the formation of KIR:MHC interactions.

3.4.6 Changes in the peptide repertoire of HeLa cells alters NK cell activation

In the previous section I confirmed that peptide sequence could alter the activation of NK cells through KIR3DL1 using HeLa ERAP1$^{-/-}$ target cells. Before continuing to use these cells in further experiments I wanted to examine how simple changes to MHC I expression and antigen presentation machinery affected NK cell activation. From the WT HeLa cell line I generated the following stable cell lines: HeLa B*2705^{+}, HeLa ICP47^{+} and HeLa B*2705^{+} ICP47^{+}. In addition, HeLa ERAP1$^{-/-}$ (EKO) cells, previously created in our lab using CRISPR, and transiently transfected HeLa ERAP1$^{-/-}$ B*2705 cells were used as target cells for LAMP1 assays (2.4 NK cell degranulation (LAMP1) assay).

Addition of HLA-B*2705 to HeLa cells inhibited NK cell activation but this was not significant in either the whole NK cell population (**Figure 3.8a**) or the KIR3DL1^{+} population (**Figure 3.8b**). Inhibition was expected due to the increase in cell surface MHC I expression (**Figure 3.8c**) providing more targets for inhibitory NKR engagement. However, the lack of significance seen likely reflects the role of additional inhibitory receptors in the interaction between HeLa cells and NK cells.

Addition of ICP47 inhibits TAP thereby preventing movement of proteasome-derived peptides from the cytoplasm into the ER (120). This reduces the number of peptides available in the ER for MHC I binding, thus reducing the expression of high affinity pMHC complexes on the cell surface, and potentially inducing NK cell activation. In the whole NK cell population, as expected, HeLa ICP47 cells ($p<0.001$) and HeLa B*2705 ICP47 cells ($p<0.05$) significantly activated NK cells compared to the HeLa cell line (**Figure 3.8a**). In the KIR3DL1^{+} population, HeLa ICP47 cells again significantly activated NK cells ($p<0.001$), however, the addition of HLA-B*2705 to these cells prevented any significant increase in NK cell activation (**Figure 3.8b**). In fact HeLa B*2705 ICP47 cells induced significantly less NK cell activation than HeLa ICP47 cells alone ($p<0.001$) despite showing similar levels of cell surface MHC I (**Figure 3.8c**). This suggests that even a low number of HLA-B27 molecules on the cell surface can prevent NK cell activation.

Loss of ERAP1 from HeLa cells reduced NK cell activation in the whole NK cell population (**Figure 3.8a**) but this was not true in the KIR3DL1^{+} population (**Figure 3.8b**). This was surprising because the loss of ERAP1 drastically alters the peptide repertoire (25). The natural ERAP1 in HeLa cells has been shown to have SNPs associated with poor trimming activity and potentially shows a hypo-trimming phenotype. The loss of this ERAP1 has potentially allowed the formation of better

pMHC complexes that can engage KIR3DL1 better than those normally found on the cell surface. Addition of HLA-B*2705 to these cells further reduced NK cell activation ($p<0.01$) in both populations. Comparison of HeLa ERAP1$^{-/-}$ cells with HeLa ERAP1$^{-/-}$ B*2705 cells showed significant inhibition upon addition of HLA-B*2705 in the KIR3DL1^{+} population ($p<0.001$). As the HeLa ERAP1$^{-/-}$ cells could only be transiently transfected, only ~50% of cells express HLA-B*2705 in the MHC screen data shown (**Figure 3.8c**). Across all repeats ~50-70% of transfected cells were seen. If it was possible to generate a stable cell line with 100% of cells expressing HLA-B*2705 I would expect to see greater inhibition of NK cell activation because the addition of HLA-B*2705 to HeLa ERAP1$^{-/-}$ cells did increase inhibition.

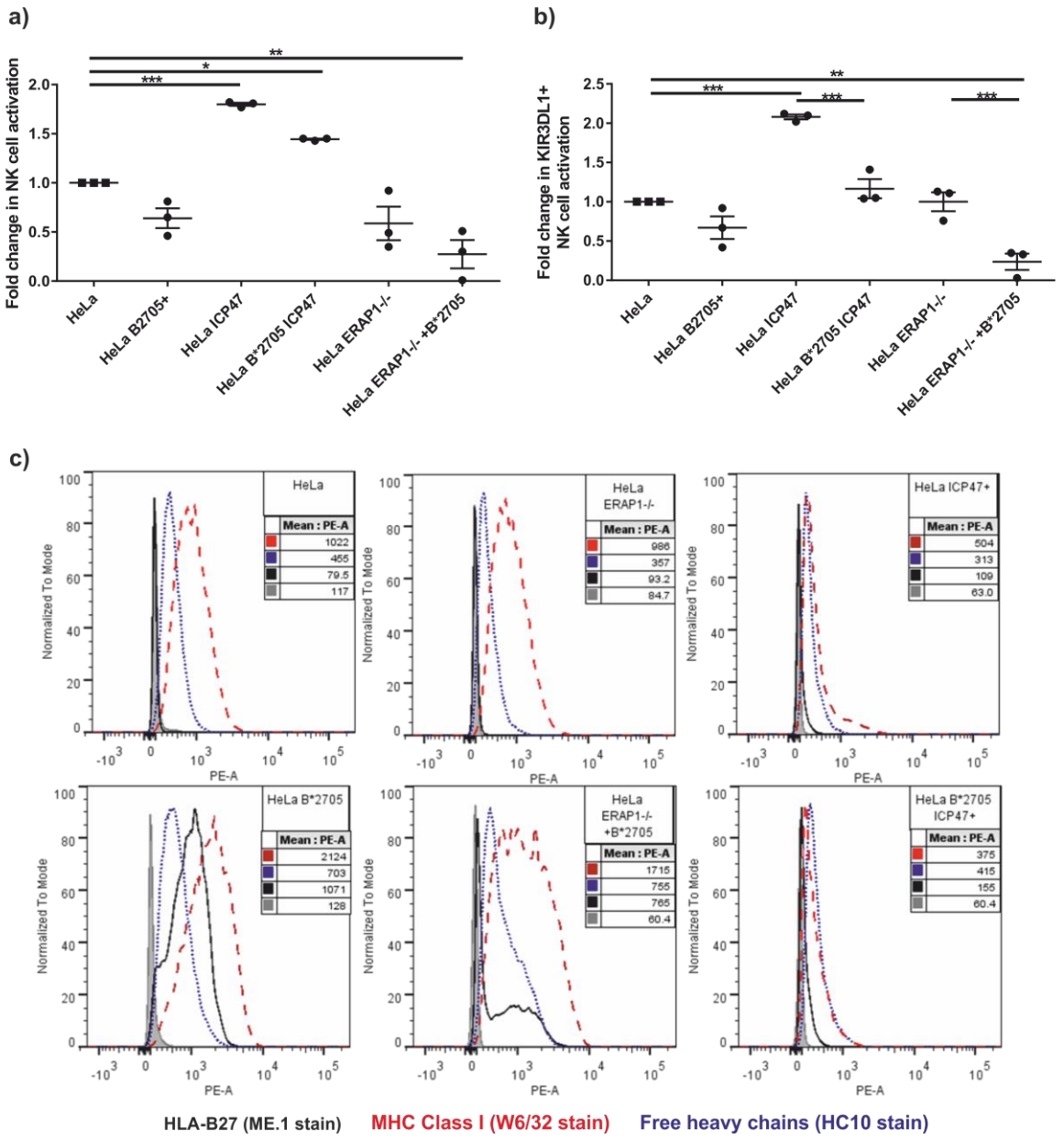

Figure 3.8: Changes in peptide repertoire alter NK cell activation against HeLa cells

HeLa cells were stably transfected with HLA-B*2705 and/or the TAP inhibitor ICP47 and HeLa ERAP1$^{-/-}$ cells previously made in the lab using CRISPR were transiently transfected with HLA-B*2705 to generate several cell lines with altered MHC I antigen presentation. These cells were used as target cells in a LAMP1 assay. (a) In the whole NK cell population, there was significant activation of NK cells with HeLa ICP47 cells ($p<0.001$) and HeLa B*2705 ICP47 ($p<0.05$). There was significant inhibition of NK cells with HeLa ERAP1$^{-/-}$ B*2705 cells ($p<0.01$). (b) In the KIR3DL1^{+} NK cell population, there was significant activation of NK cells with HeLa ICP47 ($p<0.001$) and inhibition with HeLa ERAP1$^{-/-}$ B*2705 cells ($p<0.01$). When comparing HeLa ICP47 and HeLa B*2705 ICP47 cells there was a significant reduction in NK cell activation upon addition of HLA-B*2705 to the cells ($p<0.01$). HeLa ERAP1$^{-/-}$ cells do not show much difference in NK cell activation compared to HeLa cells in this population, but upon addition of HLA-B*2705 there is a significant reduction in NK cell activation compared to HeLa ERAP1$^{-/-}$ cells ($p<0.001$). N=3, Data analysed by one-way ANOVA and Tukey's multiple comparisons test.

3.4.7 HLA-B27 peptide database shows changes in amino acid distribution between cell lines with expression of polymorphic variants of ERAP1

Having shown that the HeLa LAMP1 assay can be used to identify the difference in NK cell activation with peptide variants, the next stage was to identify some potential P7:P8 mutations or combinations which could also alter KIR3DL1. To do this, a bioinformatics data mine of all peptide sequences eluted from HLA-B27 was carried out (2.6 Compilation & bioinformatics analysis of peptide database). These studies have examined the peptidomes from different HLA-B27 expressing cell lines with known ERAP1 sequences and SNP expression. While this allows us to predict the likely allotype and thus it's trimming phenotype, further analysis would be required to unequivocally identify the full coding sequence of each expressed allotype of ERAP1. The use of ERAP1 as a distinguishing feature of the peptide repertoire eluted from each cell line allowed us to determine whether AS-associated ERAP1 allotypes were more likely to produce peptides with lower KIR3DL1 inhibition. The list of references from which these peptide sequences were acquired can be found in appendix B.

An independent investigation of the functional interaction of AS-associated ERAP1 polymorphisms in HLA-B27 by Garcia-Medel *et al,* looked at the contribution of AS-protective or AS-associated SNPs on the stability of peptides at the cell surface and the HLA-B*2704 peptidome. While this study would potentially provide a wealth of information on ERAP1 polymorphisms and the presented peptidomes, it did not show the contribution of individual cell lines, instead choosing to do three pairwise comparisons (121). For this reason this study was not included in the peptide analysis.

All other studies that identified peptide sequences eluted from HLA-B27 in a single cell line were considered for analysis. These peptides were all found in one of four cell lines: HeLa, C1R05, P50 or LG2. The HeLa cell line was originally derived from a cervical carcinoma and is an adherent, epithelial-derived, human cell line commonly used in the laboratory. The P50 and LG2 cell lines are Epstein-Barr virus (EBV)-transformed lymphoblastoid cell lines (122). C1R05 is a transfectant of the lymphoid HLA class I-defective Hmy2.C1R cell line (123), expressing HLA-B*2705. The SNPs for each cell line are found in **Table 3:1: Peptide database characteristics**, along with a trimming prediction for peptides based on data previously found in our lab by Dr Emma Reeves (6, 29). The full list of peptides and the literature they were found in can be found in appendix B.

Table 3:1: Peptide database characteristics

Cell Line	ERAP1 single nucleotide polymorphisms	ERAP1 trimming prediction	N. peptides
C1R05	R127P, K528R, Q730E	Substrate-dependent, hypo-trimmer	101
HeLa	K528R, Q730E	Substrate-dependent, hypo-trimmer	215
LG2	M349V, Q730E	Substrate-dependent, hypo-trimmer	54
P50	R127P, M349V, K528R, D575N, R725Q, Q730E	Hypo-trimmer	46
			416

Analysis of peptides eluted from HLA-B27 revealed 1083 different peptides with arginine at position 2 (P2) ranging from 6 amino acids to 14 amino acids; arginine at P2 is a known anchor residue for HLA-B27 (124). Of these, 764 were 9 amino acids in length (9mers) and 418 9mers were unique to only one cell line from the four cell lines. The final amino acid residue of a peptide is also an anchor residue for 9mer peptides bound to HLA-B27 and only a fraction of amino acids are found at this position (124). **Figure 3.9** shows the distribution of P9 amino acids both per amino acid (**Figure 3.9a**) and per cell line (**Figure 3.9b**). The differences in P9 amino acids may reflect differences in the allele of HLA-B27 found in each cell line as this can affect the P9 anchor residue, but as expected based on previous data the most abundant amino acids at this position are phenylalanine, lysine, leucine and tyrosine (125).

P7 and P8 of a 9mer peptide has previously been shown to be important for engagement of KIR3DL1, with changes to these amino acids affecting NK cell activation (115). Both of these positions are not thought to make strong contacts with HLA-B27 (116) suggesting that any variability seen will not be due to the preferential binding of each HLA-B27 allele. The amino acid at position 7 was analysed and expressed per amino acid (**Figure 3.10a**) and per cell line (**Figure 3.10b**). Interestingly, every amino acid was represented by at least one cell line. The relative presence of each amino acid was compared to the green P50 cell line, as this expressed the strongly AS-associated 5SNP ERAP1 allotype (*001). Amino acids that were represented in P50 cells in ≤10% were considered to be under-represented, while those present in ≥25% peptides were considered to be highly represented. Alanine (A), glutamic acid (E), histidine (H), isoleucine (I), proline (P), glutamine (Q) and threonine (T) were under-represented in the P50 cell line (c). Arginine (R) and methionine (M) were highly expressed by P50 cells. Cysteine (C), aspartic acid (D) and glycine (G) were absent in P50 cells, although C and G were only found in C1R05 and HeLa cells, respectively, and at very low abundance. Interestingly, the amino acids I and R at position 7 have previously been shown to affect KIR3DL1 engagement (Peruzzi *et al* and above) with P7:I allowing good KIR3DL1 engagement, whereas P7:R prevents KIR3DL1 engagement (115).

At position 8, phenylalanine (F), lysine (K), glutamine (Q), arginine (R) and serine (S) were under-represented and Aspartic acid (D), histidine (H), isoleucine (I) and tyrosine (Y) were absent from P50 cells (**Figure 3.11**). Proline (P) was highly expressed in P50 cells. E, K and H amino acids at position 8 were also shown to have differential effects on KIR3DL1 engagement (Peruzzi *et al* (115) and above) with P8:H the natural amino acid of the FRY peptide, and inhibitory, while mutation to P7:K prevents inhibition through KIR3DL1. Interestingly, although E was shown to increase target cell lysis it did not have any effect on inhibition of KIR3DL1 NK cells in the LAMP1 assay.

This peptide database analysis provides some interesting observations about the abundance of different amino acids at P7 and P8, potentially suggesting some novel P7:P8 combinations which may have differential KIR3DL1 engagement in the same way as the FRY peptides (Peruzzi *et al* (115) and above). Based on these results, a selection of P7 and P8 combinations that were reduced, absent or over-represented in the P50 cell line were selected. To keep this work physiologically relevant, these chosen combinations were compared to peptides listed in the database to find naturally occurring P7:P8 combinations that would represent each of these conditions. Altogether, PS, IS, HS, RS, RA, DA, LA and VA P7:P8 mutants were chosen for further analysis. RA and RS were expected to prevent inhibition through KIR3DL1, i.e. induce NK cell activation, while all other combinations were predicted to engage KIR3DL1 leading to NK cell inhibition.

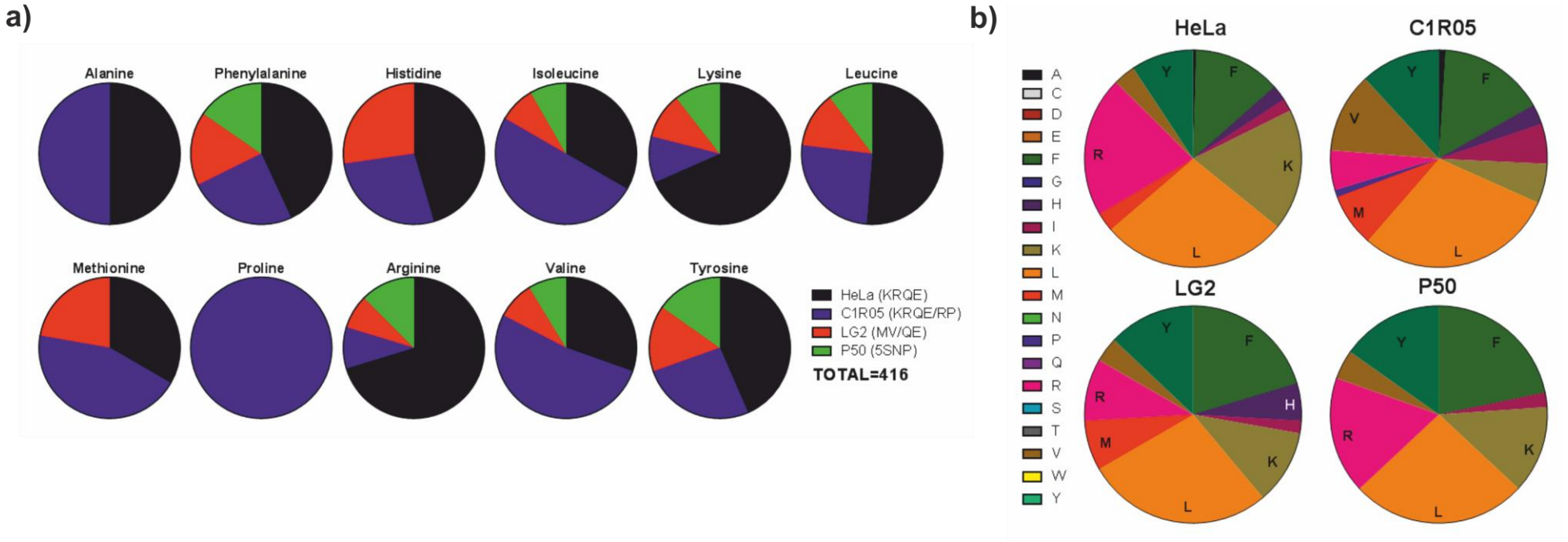

Figure 3.9: Distribution of amino acids at position 9

From the peptide database created, the distribution of the amino acid at the anchor position 9 was examined on an individual basis (a) and in each cell line (b). As expected for HLA-B27 peptides, leucine, lysine, phenylalanine, arginine and tyrosine were the most abundant in all cell lines.

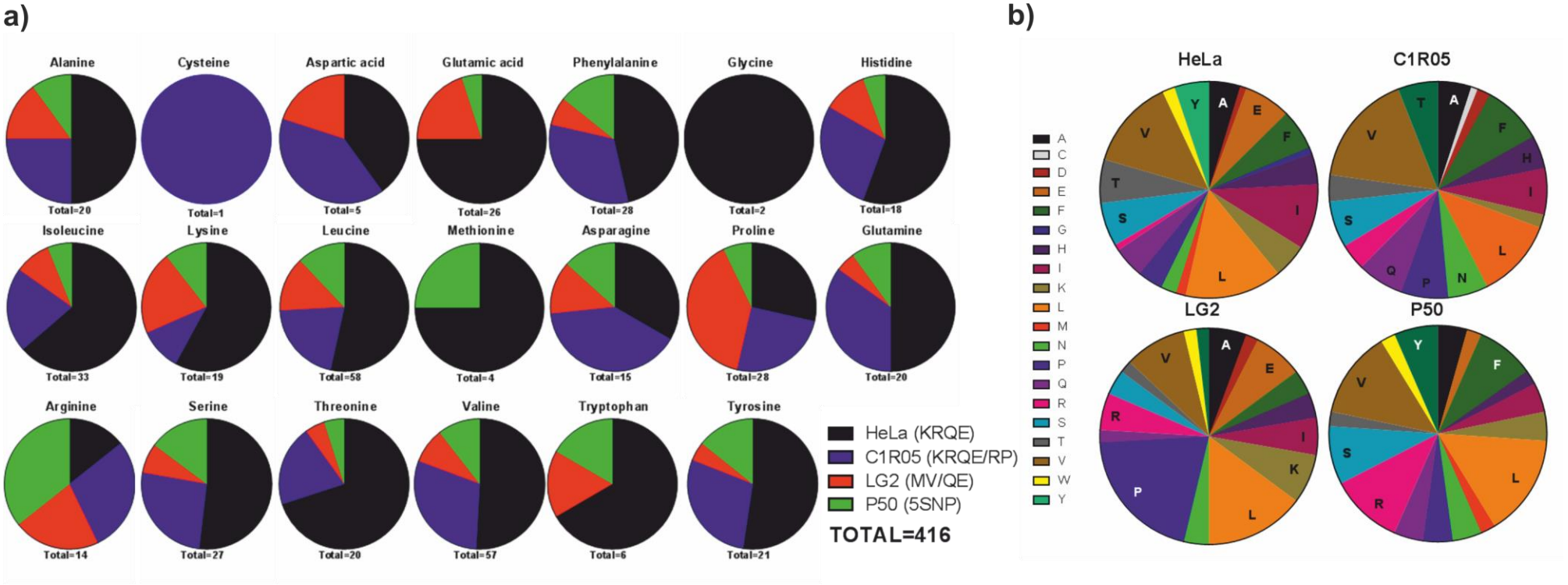

Figure 3.10: Distribution of amino acids at position 7

From the peptide database created, the amino acid distribution at position 7 was examined on an individual basis (a) and in each cell line (b). Compared to the P50 cell line, which has AS-associated polymorphisms in ERAP1, there is a visible increase of arginine at P7. There is a decrease in histidine, isoleucine and serine. In addition, aspartic acid, cysteine and glycine are absent in peptides from the P50 cell line.

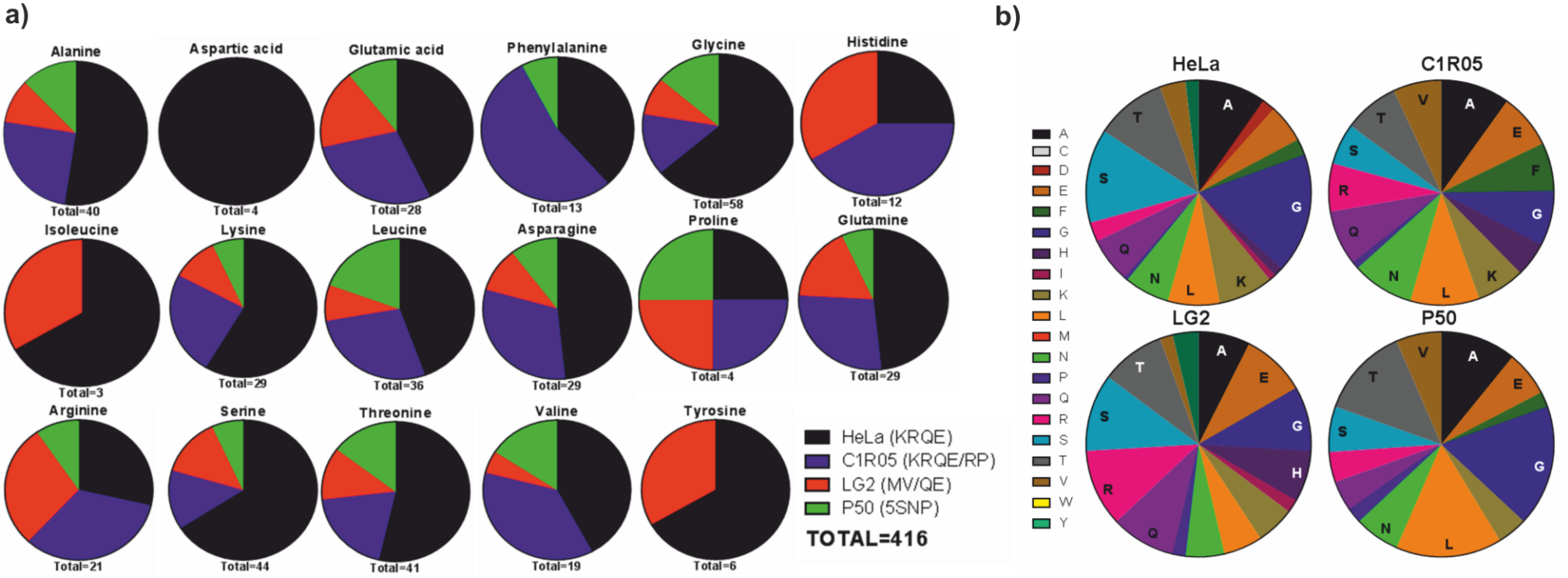

Figure 3.11: Distribution of amino acids at position 8

From the peptide database created, the amino acid distribution at position 8 was examined on an individual basis (a) and for each cell line (b). Compared to the P50 cell line, which has AS-associated polymorphisms in ERAP1, there is a decrease in serine, glutamic acid and lysine while aspartic acid, histidine, tyrosine and isoleucine are absent.

3.4.8 P7:P8 combinations from database analysis induce changes in NK cell activation

To generate the P7:P8 combinations selected from the peptide database, SDM-PCR was used to mutate the existing FRY-IH or –RH minigenes (2.3 Plasmid minigene construction) and these new mutant minigenes were used to examine their effects on NK cell activation (**Figure 3.12**). In comparison to HeLa ERAP1$^{-/-}$ B*2705 there were no significant differences with any of the mutant peptide minigenes in the whole NK cell population (**Figure 3.12a**). However, in the KIR3DL1^{+} population there were some clear differences with FRY-IS and FRY-VA showing some NK cell inhibition ($p<0.05$ compared to FRY-HS or FRY-RS) (**Figure 3.12b**). Interestingly, in some repeats of the experiment, FRY-HS and FRY-RS increased NK cell activation, but as this was not consistent across experiments it was not a significant result. These changes were expected for FRY-IS, -VA and RS, but the activation occasionally seen in the presence of FRY-HS was not predicted. There were no significant differences in HLA-B27 expression or FHC expression on the cell surface suggesting that any differences in NK cell activation were due to peptide sequence and not changes in the chemistry of HLA-B27 on the cell surface (**Figure 3.12c-e**).

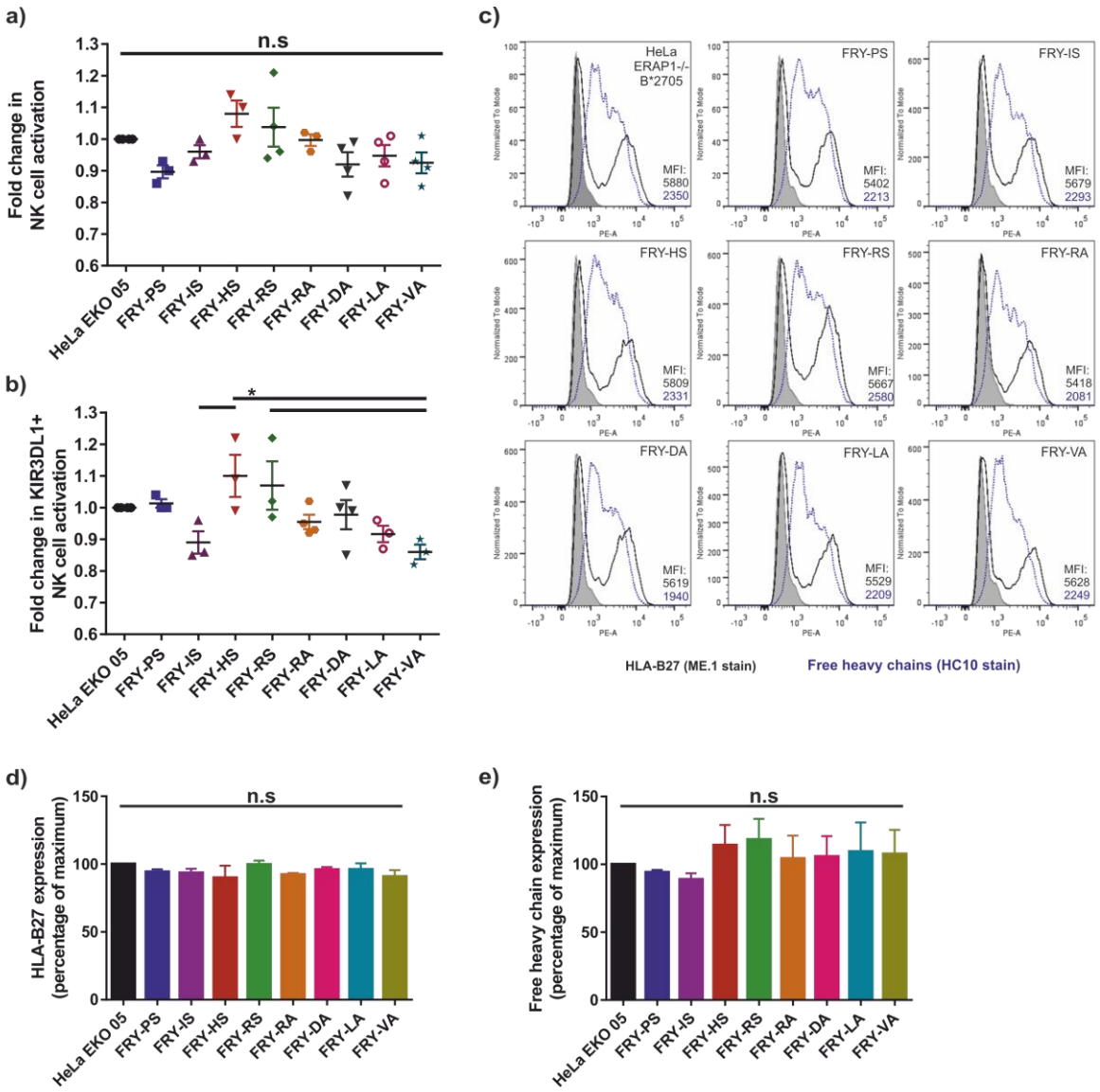

Figure 3.12: The effect of P7:P8 mutations on NK cell activation

Based on the peptide database analysis, P7 and P8 combinations were chosen for further investigation. All chosen combinations were found to occur naturally in at least one peptide in the database. 8 new minigenes were designed to alter the P7/P8 amino acids of WT FRY peptide and transfected into HeLa EKO cells along with HLA-B*2705. These cells were then used in a LAMP1 assay (a,b) and MHC screen (c, d, e). FRY-VA and FRY-IS significantly inhibited KIR3DL1^{+} NK cell activation compared to FRY-RS and FRY-HS ($p>0.05$). LA also inhibited but this was not significant. There was no significant difference in the HLA-B27 or FHC levels at the cell surface with any of the minigenes. N=3, Data analysed by one-way ANOVA and Tukey's multiple comparisons test.

3.4.9 P7:P8 combinations from database analysis do not alter rhKIR3DL1 binding

To confirm that the changes in NK cell activation seen in the LAMP1 assay (**Figure 3.12**) were due to KIR3DL1 engagement of different P7:P8 combinations, the binding of rhKIR3DL1 to cells transfected with each new mutant minigene was measured. Binding of rhKIR3DL1 to HLA-B27 shows some variability following mutant minigene transfection but no changes were significant (**Figure 3.13**). This result was expected due to the lack of differences seen with the FRY peptides (**Figure 3.6**), and was most likely due to the presence of natural HLA on the HeLa cells, as was seen before. However, further testing of this may reveal significant changes.

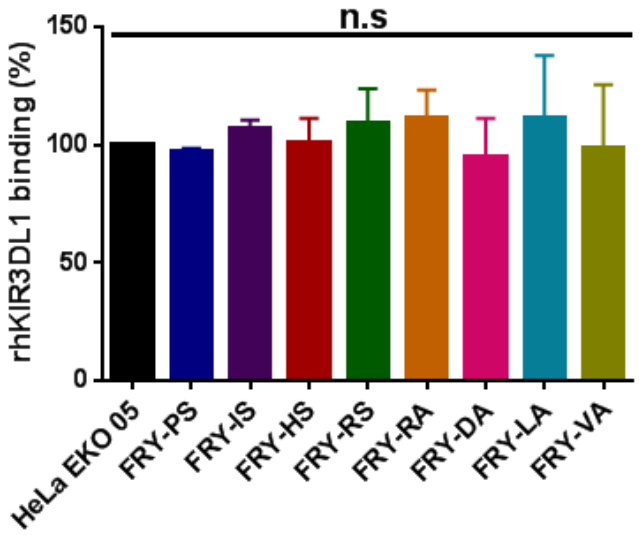

Figure 3.13: Binding of rhKIR3DL1 is altered in response to FRY P7:P8 mutant minigenes

Using peptide minigenes, HLA-B*2705 and FRY peptides were transiently transfected into HeLa EKO cells for 24 hours prior to binding of recombinant human KIR3DL1 (rhKIR3DL1) for 1 hour. FRY-IS has increased rhKIR3DL1 binding compared to HeLa ERAP1$^{-/-}$ B*2705 cells and this peptide was previously shown to be inhibitory (n.s). No changes were significant. N=2, Data analysed by one-way ANOVA and Tukey's multiple comparisons test.

3.4.10 Modelling of P7:P8 combinations from database analysis suggest structural differences in peptide binding affect KIR3DL1 engagement

To better understand the possible effects of mutating the P7 and P8 residues each new peptide was mapped onto HLA-B*2705 using the Chimera program with those with P8S (**Figure 3.14a**) and P8A (**Figure 3.14b**) grouped. FRY-RS extends out of the peptide-binding groove, as previously shown in the context of FRY-RH, which was shown to be non-inhibitory. FRY-HS also extends away from the peptide backbone, which may explain why these peptides are not inhibitory because they cannot form close contacts with KIR3DL1 to allow inhibition. In the peptides with P8A, only FRY-RA shows extension out of the groove while the others have little effect on how the peptide sits. In the LAMP1 assay, all of the P8A peptides were in some way inhibitory, with the exception of FRY-RA which was at around the same level as HeLa ERAP1$^{-/-}$ B*2705 cells (**Figure 3.12**). These data suggests that the differences in KIR3DL1 engagement may be due to structural differences

rather than changes in amino acid biochemistry. However, crystal structures would be needed to further elucidate this.

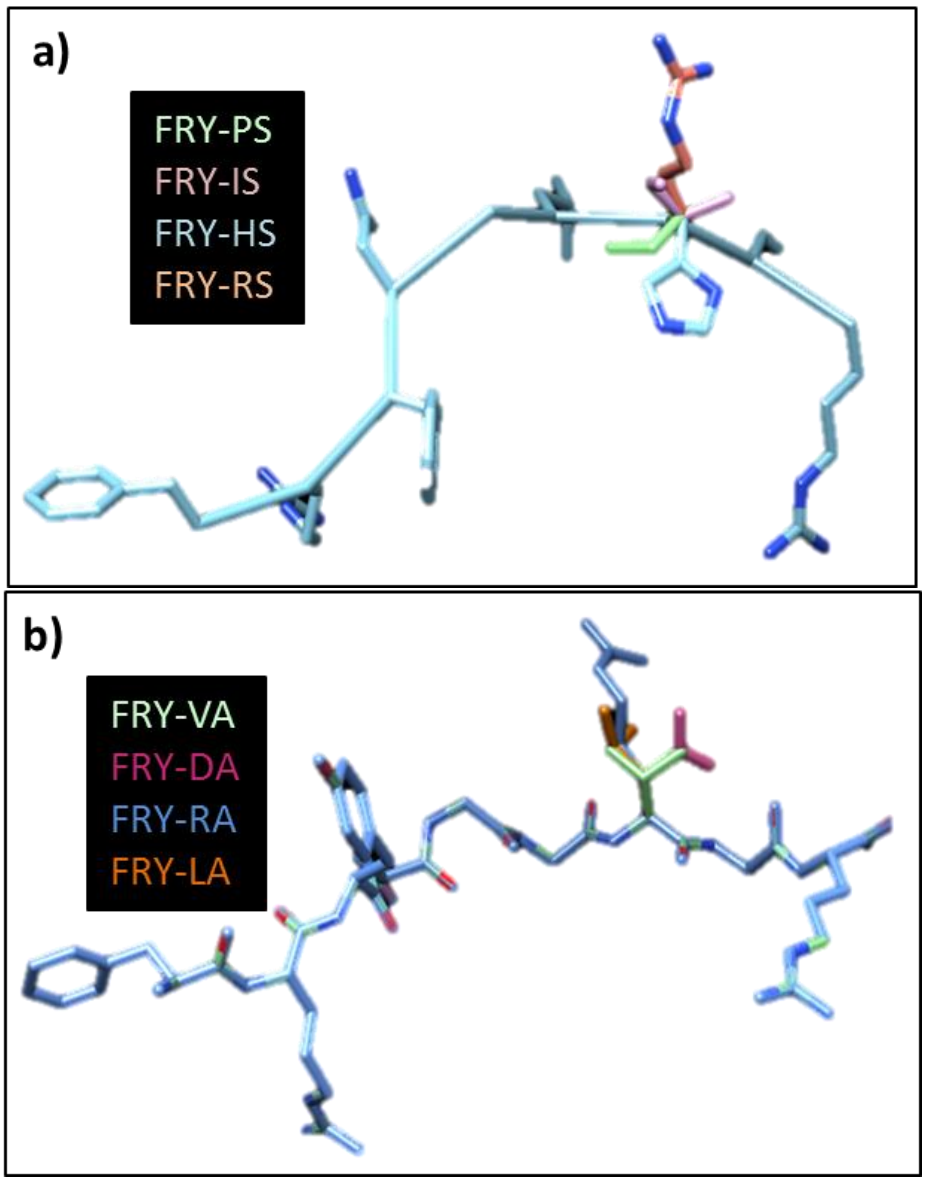

Figure 3.14: Modelling of FRY P7:P8 mutant peptides onto HLA-B*2705

The mutated FRY peptides were modelled for binding conformation of each peptide onto HLA-B*2705 binding groove using Chimera. Amino acids at position 7 & 8 are shown in a different colour for each peptide. (a) Mutant peptides with Serine at position 8. (b) Mutant peptides with Alanine at position 8.

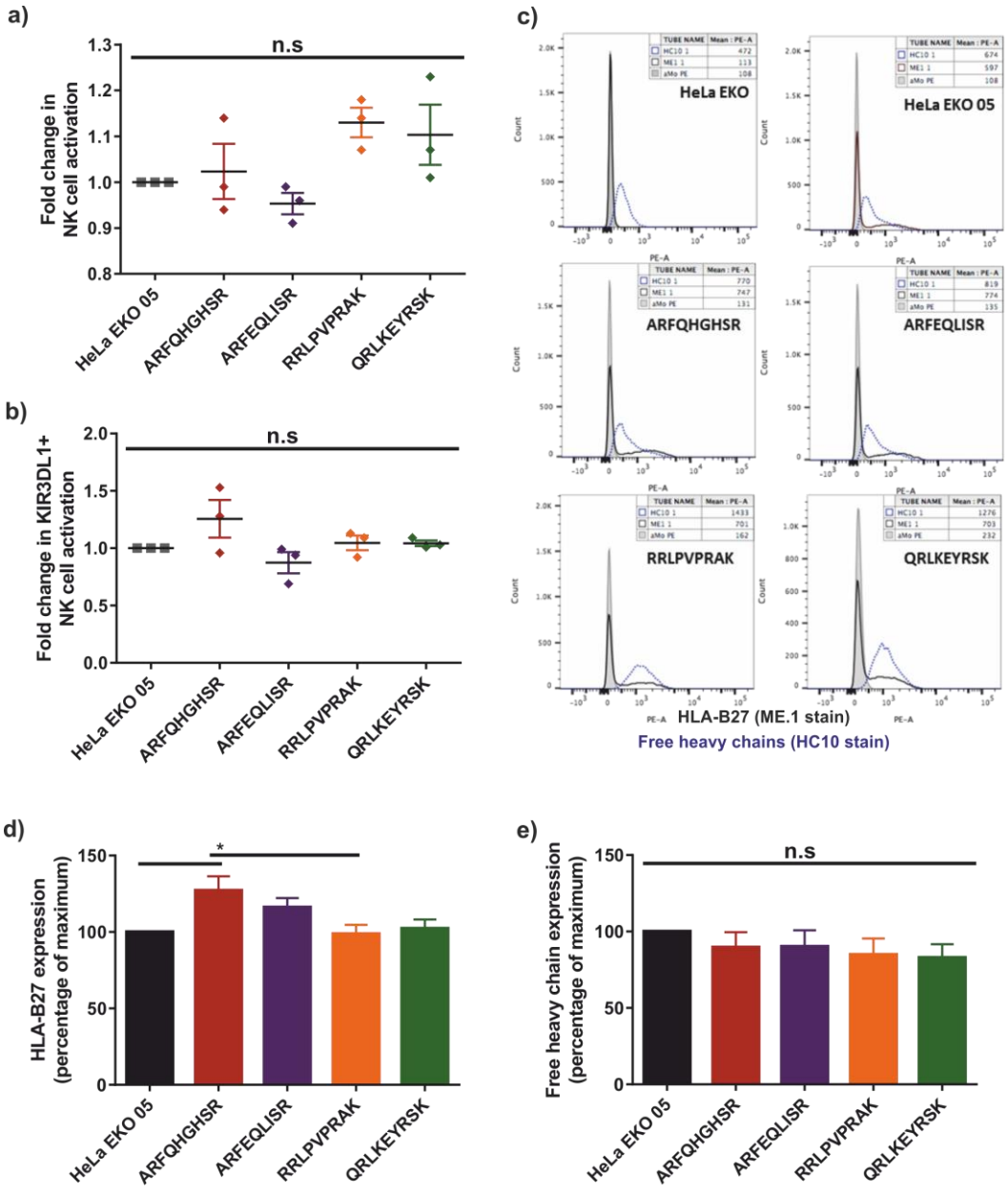

Figure 3.15: Natural peptides with selected P7:P8 residues alter NK cell activation

Natural peptide ligands for HLA-B*2705 were selected from the peptide database based on their P7:P8 residues and how these residues behaved in the FRY model peptide study previously shown. Peptide minigenes were made and transiently transfected into HeLa EKO cells, along with HLA-B*2705, for 24 hours. As previously seen, P7I:P8S (ARFEQLISR, purple) showed slight inhibition of NK cell responses in both the whole NK cell population (a) and the KIR3DL1-specific population (b). P7H:P8S (ARFQHGHSR, red) showed minimal activation of NK cells, and P7R:P8A & P7R:P8S showed an increase in activation in the whole NK population but no changes from the addition of no peptide minigene in the KIR3DL1 population. There was increased HLA-B27 expression on the cell surface following transfection with ARFQHGHSR and ARFEQLISR peptide minigenes, potentially suggesting that these peptides have a high affinity for B*2705 (c, d). There was no change in FHC expression following transfection with any peptide minigenes (c, e). N=3, Data analysed by one-way ANOVA and Tukey's multiple comparisons test.

3.4.11 Native peptides with P7:P8 combinations from database analysis mimic changes in NK cell activation seen previously

As mentioned, mutant FRY minigenes used in the previous set of experiments were chosen based on P7:P8 combinations naturally found in peptides from the peptide database. To assess whether the rest of the peptide backbone was important in KIR3DL1 engagement and therefore NK cell activation, new minigenes from identified peptide sequences corresponding to the P7:P8 combinations found in the peptide database were generated: ARFQHG**HS**R, ARFEQL**IS**R, RRLPVP**RA**K and QRLKEY**RS**K (2.6 Compilation & bioinformatics analysis of peptide database). These minigenes were transfected then into HeLa ERAP1$^{-/-}$ cells along with HLA-B*2705 and used in a LAMP1 assay (2.4 NK cell degranulation (LAMP1) assay) (**Figure 3.15**).

In the previous experiment (**Figure 3.12**), the P7:P8 combinations from these new peptides showed HS to be activating (in most cases), IS inhibitory and RA & RS to have little effect compared to the addition of no peptide. In this experiment we can see a similar pattern of NK cell activation with the corresponding peptides (n.s) (**Figure 3.15a-b**) suggesting that the backbone has no effect on KIR3DL1 engagement. The MHC screen for these transfected cells showed low percentages of HLA-B27 expression following transfection (~10-30%) compared to those usually seen (~50%) suggesting that these peptides have a lower affinity for HLA-B*2705 than the Fry peptides (**Figure 3.15c**). When the MFI of each transfection condition is normalised and displayed as a percentage of HeLa ERAP1$^{-/-}$ B*2705 expression there was a significant increase in ARFQHGHSR compared to HeLa ERAP1$^{-/-}$ B*2705 cells and RRLPVPRAK transfected cells ($p<0.05$) (**Figure 3.15d**). No significant differences were seen in FHC expression with any peptide (**Figure 3.15e**).

3.4.12 Native peptides with P7:P8 combinations from database analysis do not alter rhKIR3DL1 engagement

The binding of rhKIR3DL1 to cells transfected with these new minigenes shows some variability in binding to HLA-B27 following mutant minigene transfection (Figure 3.16). But this variability was not consistent across two experiments and so no significant differences were observed. Once again, this is most likely due to the presence of other HLA on the surface of the HeLa cells preventing enough rhKIR3DL1 binding for consistent results as seen in Figure 3.6 and Figure 3.13.

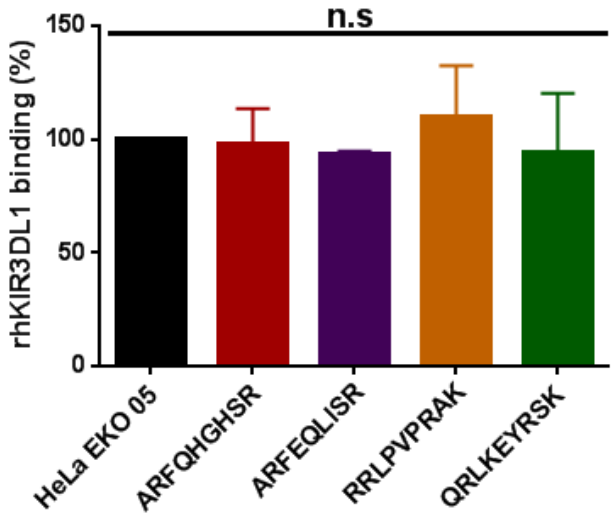

Figure 3.16: Binding of rhKIR3DL1 is altered in response to FRY P7:P8 mutant minigenes

Using new peptide minigenes, HLA-B*2705 and FRY peptides were transiently transfected into HeLa EKO cells for 24 hours prior to binding of recombinant human KIR3DL1 (rhKIR3DL1) for 1 hour. No significant differences were seen with any peptides. Although the two intermediate NK cell activators RRLPVPRAK and QRLKEYRSK showed intermediate rhKIR3DL1 binding which may explain the results seen in the LAMP1 assay. N=2, Data analysed by one-way ANOVA and Tukey's multiple comparisons test.

3.4.13 Native peptides with P7:P8 combinations from database analysis mimic changes in NK cell activation seen previously more greatly in HeLa B*2705 cells

The new peptide minigenes were transfected into the ERAP1 competent HeLa B*2705 cell line and then included in LAMP1 assays (2.4 NK cell degranulation (LAMP1) assay) and a HLA-B27 screen (2.8 HLA-B27 expression screen) (**Figure 3.17**). In the whole NK cell population some slight differences in NK cell activation could be seen, with RRLPVPRAK being slightly inhibitory (**Figure 3.17a**). However, the previously activating ARFQHGHSR was only activating 50% of the time and the previously inhibitory ARFEQLISR only inhibitory in 50% of cases. None of these differences were significant and this was repeated in the KIR3DL1^{+} NK cell population (**Figure 3.17b**). There were no changes in HLA-B27 or FHC cell surface expression following transfection with any peptide (**Figure 3.17c-d**). These changes were generally as predicted but further experiments would be required to confirm this.

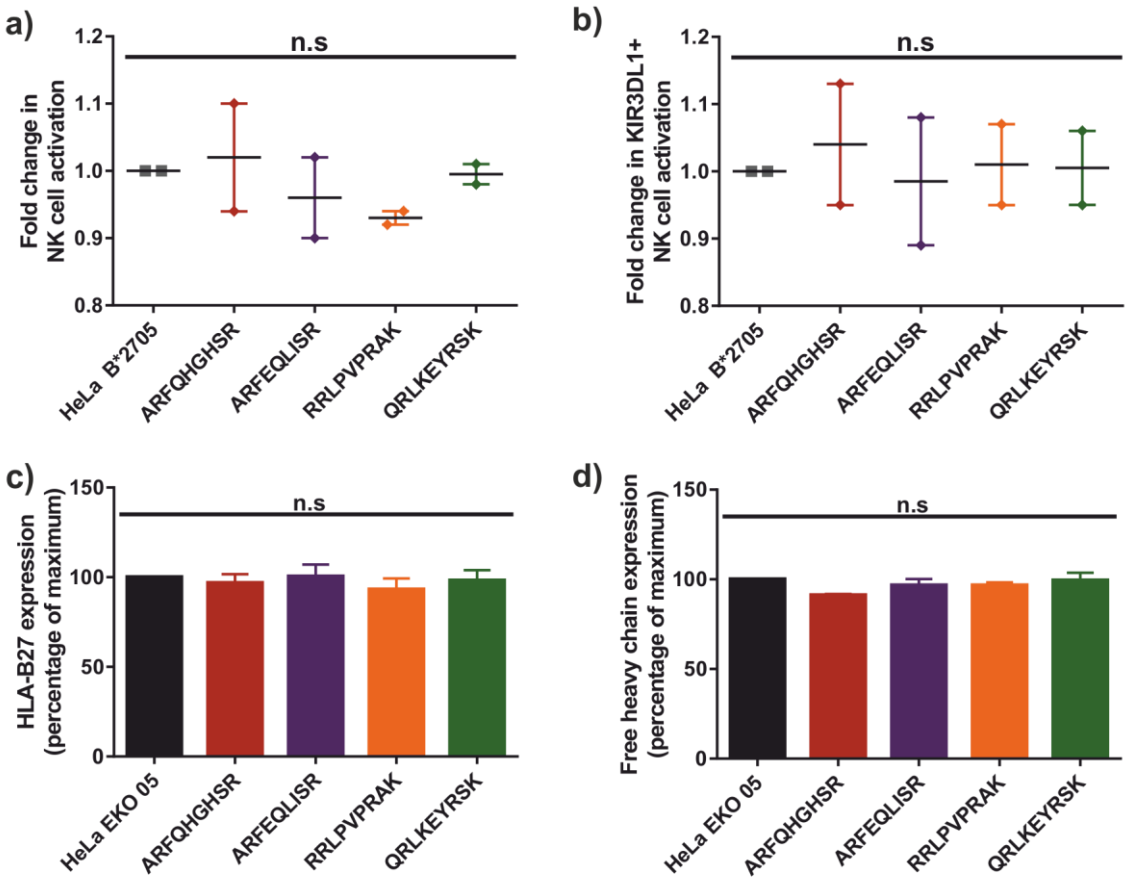

Figure 3.17: NK cell activation to new peptides in HeLa B*2705 cells

Natural peptide ligands for HLA-B*2705 with differing P7:P8 residues previously shown to induce a range of NK cell activation were transiently transfected into HeLa B*2705 cells for LAMP1 assays (a-b). There were no significant differences in NK cell activation in either the whole NK cell population or in the KIR3DL1^{+} population. (c) No significant changes were seen in the cell surface expression of HLA-B27. (d) No significant differences were seen in the cell surface expression of FHC. N=2, data analysed by one-way ANOVA and Tukey's multiple comparisons test.

3.5 Discussion

The NK cell receptor KIR3DL1 was previously shown to have preferences for specific amino acids at positions 7 and 8 of a 9mer peptide (115). Since this article came out 20 years ago there has been little additional work done into these preferences, with the exception of work by Fadda *et al* that looked into the binding preferences of KIR3DL1 for HIV epitopes (126). This group showed that KIR3DL1 could recognise some HIV-1 epitopes bound to HLA-B*5701 but not others. In addition they showed that P3 and P9 of a specific 10mer epitope were crucial for this KIR3DL1 engagement, with P3T to P3N and/or P9G to P9D completely abrogating HLA-B*5701 tetramer binding to KIR3DL1^{+} Jurkat cells. This work again proves that KIR3DL1 engagement is dependent on the sequence of the bound peptide but, as this work only looked at binding of a HLA-B*5701 tetramer to KIR3DL1^{+} cells, the functional consequences of these differences in KIR engagement on the NK cell remain unknown. This work aimed to further identify the peptide preferences of KIR3DL1 by looking at the interaction between this receptor and peptides bound to HLA-B*2705. As well as looking at whether ERAP1 polymorphisms can alter KIR3DL1 binding by exploiting these differences.

Initial work aimed to reproduce data shown by Peruzzi *et al* showing that alteration of P7:P8 residues of FRYNGLIHR peptide affects target cell lysis by an NK cell clone (115). 721.221 cells were chosen as the target cell for LAMP1 assays based on the dramatic NK cell inhibition seen upon addition of HLA (**Figure 2.3**). It was proposed that exogenous peptide could be pulsed over these cells to create specific pMHC complexes at the cell surface (127). Unfortunately, any attempts to stabilise exogenous peptides onto HLA-B*2705 failed to work, despite optimisation and the use of alternative, related, target cell lines .220 and T2. HLA-B27 pMHC complexes on the cell surface will generally express high affinity peptides and exchange of these existing pMHC complexes with new peptides is difficult (personal communication with Prof. Tim Elliott). Potentially our exogenous FRY peptides do not have a high enough affinity for HLA-B27 to displace those already present.

In an attempt to find an alternative target cell we looked into the use of 293T, mouse ERAAP$^{-/-}$ fibroblasts, K89 antigen presenting cells and HeLa cells and found that HeLa cells gave the best data with both a discernible difference in NK cell activation and a shift in B27 expression following addition of HLA-B27 (data not shown). We used HeLa cells that naturally express their

own HLA molecules in addition to those we add in. There are conflicting reports for the HLA expression of HeLa cells, but they have been serologically typed as HLA-A3, -A28, -Bw15 and –Bw35 expressing (128) and genetically typed as HLA-A68 (a subtype of A28), -B75 (a subtype of B15) and negative for B35 (129). None of these alleles are HLA-Bw4 epitopes and so are unlikely to have an impact on any conclusions we draw from the KIR3DL1 data. However, they will interact with other KIRs and affect NK cell activation.

In our lab we have previously used peptide minigenes to deliver peptides into the ER to examine N-terminal trimming of peptides by ERAP1 (29). The use of these minigenes provided a system with which to measure the activation of NK cells in response to different peptide sequences. HeLa ERAP1$^{-/-}$ cells were chosen as the target cells for the following experiments because the loss of ERAP1 was expected to create a lower affinity peptide repertoire on the cell surface and prevent any trimming of our minigenes. The WT FRY-IH peptide was shown to be slightly inhibitory, which was significant compared to FRY-IK and FRY-RH, both of which were activating. These results represent what was previously seen by Peruzzi *et al* (115); thus confirming the use of this system as a suitable model as changing just the peptide sequence was enough to alter NK cell activation, although this system is by no means fully optimised. In this way we can see that despite the presence of additional HLA and KIRs, altering just one thing can alter NK cell activation.

Despite causing around 80% target cell lysis in the Peruzzi *et al* article, FRY-IE failed to show any differences in NK cell activation as measured by expression of LAMP1. This result is hard to explain, however, NK cells have many mechanisms of activation and target cell killing so it may be that FRY-IE induces target cell killing in a mechanism other than the release of cytolytic granules. For example, activated NK cells, including following IL-15 stimulation, can express TNF-related apoptosis-inducing ligand (TRAIL) that can induce apoptosis of target cells through caspase-8 (130).

Having shown that HeLa ERAP1$^{-/-}$ cells could be used as target cells in LAMP1 assays in the previous experiments it was important to assess how alterations in antigen presentation machinery within these cells altered NK cell activation. Wild-type HeLa cells inhibited NK cell activation following HLA-B*2705 transfection, an expected result due to an increase of cell surface MHC I. Blocking of TAP, which transports proteasome-derived peptides from the cytoplasm into the ER, induced dramatic NK cell activation. This was again, an expected result due to a reduction

in cell surface MHC I following a reduction in the number of peptides available for MHC I presentation.

However, surprisingly, knockout of ERAP1 from HeLa cells slightly increased NK cell inhibition and addition of HLA-B*2705 into these cells made this inhibition significant compared to WT HeLa cells. This change in NK cell activation is surprising because it is thought that loss of ERAP1 would reduce the number of good, high affinity pMHC complexes on the cell surface (25). However, the ERAP1 naturally found in HeLa cells is a polymorphic variant that has been shown to be a substrate-dependent hypo-trimmer (personal communication with Dr Emma Reeves). This suggests that loss of this dysfunctional hypo-trimming ERAP1, which is not very good at trimming peptides, actually generates a repertoire of peptides that are actually more stable and higher affinity. This change suggests that peptides generated by a hypo-trimming ERAP1 allotype are actually worse than those created when no ERAP1 is present, in this context at least. This potentially suggests that ERAP1 may aid in the loading of peptides onto MHC I or sequesters peptides that should otherwise bind to MHC I. These results mean that in all experiments where we have used these HeLa ERAP1$^{-/-}$ B*2705 cells as control target cells, and thus the mark by which we determine fold change in activation, the added peptides must induce a dramatic effect on an already inhibitory peptide repertoire.

The use of HeLa ERAP1$^{-/}$ cells and peptide minigenes for looking at how changes in peptide sequence affect NK cell activation provides a platform from which to investigate the amino acid preferences of KIR3DL1 in more detail. Instead of randomly picking amino acid substitutions, natural P7:P8 combinations were identified from natural peptides eluted from the cell surface bound to HLA-B27. These peptides were identified from cell lines with known SNPs in ERAP1 providing a potential link between AS-disease associated ERAP1 variants and HLA-B27 (2.6 Compilation & bioinformatics analysis of peptide database).

These peptides were shown to have the canonical P9 anchor residues expected for HLA-B27 bound peptides. But when looking at the P7 or P8 amino acid distributions some differences could be seen when comparing the other cell lines to the P50 cell line. The P50 cell line has been shown to have the five SNPs most commonly associated with AS disease within its ERAP1, making it highly likely that the ERAP1 found in these cells would be AS-associated. Of course, the subjective comparison of the distribution of amino acids compared to this cell line is not a robust method for identification of any true pattern, but the number of peptides in the database is not

sufficient for any conclusive statistical analysis. Nonetheless, several amino acids were identified that are over or under-represented in the P50 cell line. By taking this information and going back to the peptide database 8 naturally occurring P7:P8 combinations were identified that represented the results of the analysis. For example, P8S was reduced and P7R was increased in the P50 cell line. The 8 P7:P8 combinations chosen were mutated into the FRY backbone as this had been shown to induce significant differences in NK cell activation.

Most P7:P8 mutant minigenes showed slight differences in NK cell activation, with FRY-VA, -IS and –LA inducing inhibition, while FRY-HS and –RS induced increased NK cell activation. The inhibition seen with –IS was unsurprising as both P7I and P8S were reduced in the P50 cell line. Inhibition with FRY-VA and –LA was more surprising as, in the peptide analysis, despite both of these P7 amino acids being represented least by P50 they were equally represented in C1R05 and LG2, respectively. Activation of NK cells in the presence of FRY-RS could have been predicted as P7R has previously been shown to be activating. However, the activation seen with FRY-HS was surprising as both P7H and P8S were under-represented in the P50 cell line. These results show that while the peptide database was a useful tool for identifying a selection of P7:P8 combinations with a range of effects on NK cell activation, it is not robust enough to accurately predict the response of NK cells.

Examination of the way these peptides fit into the HLA-B*2705 peptide binding groove showed that FRY-RS and FRY-RA extend away from the peptide binding groove, as was previously seen with FRY-RH. As mentioned before, this extension could prevent the KIR getting close enough to form the contacts required for strong inhibition. All of the other P7:P8 combinations do not seem to alter the structure in any dramatic way, with the exception of FRY-HS. The P7H of FRY-HS extends further into the peptide-binding groove F-pocket than any other amino acid side chain. Potentially this could create a bulge in how the peptide sits in the groove, which may then prevent KIR3DL1 being able to make contacts with both the peptide and the MHC. This presents the possibility that P7H in itself is not activating and does not hinder the contacts the peptide makes to KIR3DL1; it is instead a case of steric hindrance with the peptide extending too far out of the groove at this F-pocket for all of the necessary contacts to be formed.

The use of P7:P8 combinations within the context of the FRY backbone was useful for identifying combinations that can be activating or inhibitory. However, due to evidence that the P3 amino acid can affect KIR3DL1 engagement (126), it was important to ensure that we could see the same

changes in NK cell activation in the context of the whole natural peptide backbones. Going back to the peptide database four peptides with P7:P8 combinations which exhibited a range of effects on NK cell activation in the previous step were chosen: -HS = activating, -IS = inhibitory, -RA = expected to be activating, but no effect and –RS expected to be activating, but no effect. As previously seen, P7H:P8S (ARFQHGHSR) was activating in most repeats of the experiment while P7I:P8S (ARFEQLISR) was inhibitory. However, these results were not significant. Once again, P7R:P8A (RRLPVPRAK) and P7R:P8S (QRLKEYRSK) showed no differences in NK cell activation compared to when no peptide was added. There was a significant increase in HLA-B27 expression with ARFQHGHSR peptide suggesting that this is a high affinity peptide that can stabilise HLA-B27 on the cell surface which was surprising considering the small differences seen in the NK cell activation assays. As previously mentioned, HeLa ERAP1$^{-/-}$ B*2705 cells induce high inhibition of the NK cell population before addition of any extra peptides. Potentially, without the FRY backbone, which we know shows a large range of NK cell activation when P7 or P8 is altered, the natural peptides are already too similar to peptides already presented on the cell surface for any significant differences to be seen.

rhKIR3DL1 has previously been used to show how the binding affinity of pMHC complexes can vary depending on the ERAP1 polymorphisms present within the cell (131). In this study, they were looking at the impact of changes in the whole peptide repertoire, in contrast with our system, which aimed to look at the effect of only one peptide. The differences seen in this study were quite minimal and highly variable, suggesting that, with additional repeats, we may eventually see a result here. The HeLa cells used for this experiment express several other HLA molecules on the cell surface; however none of these are known to bind to KIR3DL1. While these HLA alleles do not directly engage KIR3DL1, the interaction between KIR3DL1 and HLA-B*2705 may be compromised by the presence of several other HLA alleles competing for space at the cell surface.

In this system, the presence of additional MHC on the surface of HeLa cells seems to have prevented any distinguishable rhKIR3DL1 binding. Most likely, the presence of additional MHC has limited the levels of HLA-B*2705 on the cell surface to a similar level in each condition, meaning that no differences could be seen with any peptide. However, the limited numbers of minigene-HLA-B27 complexes that get to the cell surface are sufficient enough to have an effect on NK cell activation, as previously seen. Crystal structure modelling of each FRY peptide onto HLA-B*2705 provides an idea as to why FRY-IK and –RH do not engage KIR3DL1, with P7R and P8E

extending out the peptide binding groove. This extension could prevent the correct binding of KIR3DL1 by preventing formation of the contact residues between the HLA and KIR. In particular, Tyr200, Glu282 and Leu166 from domains 1 and 2 of KIR3DL1 form contacts with P8 and P9 of the bound 9mer peptide (116). If these contacts cannot be fully formed, engagement of the KIR is prevented and no inhibitory signal is transmitted.

One of the biggest problems with this rhKIR3DL1 binding assay is the avidity and efficacy of the recombinant protein. KIR3DL1 is thought to be the hardest KIR to work with and the generation of recombinant protein or crystal structures can be troubling (personal communication with Professor Jamie Rossjohn, Monash University). The recombinant protein used in these assays is currently the only commercially available protein, which again suggests that it is difficult to manufacture. That is not to say that this recombinant protein doesn't work, but the efficacy is called into question. Data in chapter 5 shows the use of rhKIR3DL1 against .221 cells only expressing HLA-Bw4 epitopes and gives clear data to suggest good binding of rhKIR3DL1, suggesting that in a system without additional HLA rhKIR3DL1 could give a good result.

This work aimed to create a model system for looking at the interaction between KIR3DL1 and HLA-B27. While a system for this has been shown here, and successfully used to replicate data shown previously (115), it is not a good model system and further optimisation or perhaps the use of a different cell line would need to be investigated. However, through the use of this system, P7:P8 combinations elucidated by the peptide database analysis were tested and the preference of KIR3DL1 for each of these ascertained. Based on the peptide database comparison of the predicted AS-associated ERAP1 containing P50 cell line and the other cell lines, it has been shown that AS-associated ERAP1 variants will produce a peptide repertoire with different P7:P8 residues. In addition, these differences appear to slightly induce NK cell activation, thus providing evidence to support our hypothesis.

This work will be useful in the future, especially as a current collaboration with Prof. Arie Admon, Tel Aviv, aims to identify the sequence of each peptide repertoire bound to HLA-B27 following transfection with stable variants of ERAP1. Using the bioinformatics approach shown here, we may be able to investigate the distribution of amino acids at P7 and P8 and make predictions about their effect on NK cell activation through KIR3DL1.

3.6 Future Directions

In the previously described work a system for looking at the amino acid preferences of KIR3DL1 that bypasses the need to pulse exogenous peptides onto HLA-B27 was shown to identify changes in KIR3DL1 engagement. In the future this system could be used to establish an accurate picture of these amino acid preferences. By creating this panel we would be able to look at any HLA-Bw4 bound peptide and predict the strength of KIR3DL1 engagement. This information could be important in the search for immunogenic peptides both in the context of HIV-1 infection and in the pathogenesis of Ankylosing Spondylitis.

The minigene system of loading peptides onto HLA-B27 works well, but the activation of NK cells is often not significantly altered. This is most likely due to the additional receptors on both the target cells and NK cells altering activation of the NK cells. To confirm that it is in fact peptide-B27 complexes interacting with KIR3DL1 causing the changes in NK cell activation I would use a reporter cell line. The Jurkat cell line can be stably transduced to express KIR3DL1 attached to CD3ζ, when the KIR is engaged downstream signalling leads to IL-2 expression that can then be measured by ELISA. This system would prevent any confounding effect of additional receptors and should hopefully reveal the true binding preferences of KIR3DL1.

Colleagues in my lab, along with collaborators, are working to elucidate the sequence of peptides expressed on the cell surface in cells with different ERAP1 allotypes present. Once this work has been completed, the KIR3DL1 panel could be used to identify whether each peptidome would be a strong or weak KIR3DL1 engager. Potentially providing insight into how NK cells would respond to each peptidome, and thus each ERAP1 variant.

Most immediately, I have created mutated minigenes of the new peptides that have altered P7:P8 residues to P7I and P8H or P8K. These were created with the hope of showing whether P8S or P8H is more inhibitory in the case of ARFEQLISR and that P7R:P8A is truly an intermediate KIR3DL1 engager. This would also be useful for identifying the effect of the rest of the peptide backbone on KIR3DL1 engagement.

While this work has used the minigene system as a method to investigate how KIR3DL1 responds to different peptides bound to HLA-B27 it is possible that this system or indeed the method of exogenous peptide pulsing could be used to identify the KIR3DL1 response to other HLA-Bw4 molecules, such as HLA-B57. This work was focussed on HLA-B27 as the wider aims of the project concern the pathogenesis of AS, but in terms of learning more about KIR3DL1 biology and its preferences this system could be utilised in the presence of another HLA.

Chapter 4: NK cell response to ERAP1 variants

4.1 Introduction

AS is a chronic autoimmune disease of the sacroiliac region with an unknown pathogenesis despite strong, and long known, genetic links with HLA-B27 (117, 118) and ERAP1 (3, 4, 11). Both HLA-B27 and ERAP1 intersect in the MHC class I antigen presentation pathway suggesting that the presentation of pMHC complexes at the cell surface may be important in the pathogenesis of this disease. ERAP1 is an ER-resident aminopeptidase responsible for the trimming of peptides to the correct length for MHC I binding and antigen presentation (7, 8, 20, 21) and is highly polymorphic with several known SNPs identified within its coding sequence; variability within the population is common (29). Previously in our lab, we have shown that the combination of polymorphic variants expressed by an individual can discretely distinguish between AS cases and healthy controls (6). The consequence of these ERAP1 combinations on cell surface expression of HLA-B27 was investigated in the previous study but the functional consequences of the altered peptide repertoire on immune cells is unknown.

ERAP1 polymorphic variants alter the repertoire of peptides presented at the cell surface either through over-trimming peptides past the point of 8-9 amino acids for binding to MHC I ("hyperfunctional" variants) or by inefficient trimming ("hypofunctional" variants) (6, 132). It is predicted that a "hyperfunctional" ERAP1 variant would reduce the number of peptides normally presented by trimming them past the point of MHC I binding, potentially allowing the presentation of novel peptides. While "hypofunctional" variants of ERAP1 are predicted to present longer peptides, again altering the repertoire, however the repertoire is likely to have significantly longer peptides being presented; similar to that observed in the absence of ERAP1 (25).

Recently ERAP1 was shown to be highly polymorphic consisting of haplotypes made up of combinations of at least one SNP. This study identified 9 naturally occurring ERAP1 haplotypes based on these five previously characterised SNPs. Alleles M349V and M349V/D575N/R725Q were able to trim a target peptide as efficiently as wild-type (WT) ERAP1, while other alleles, including 5SNP (containing all 5 associated SNPs), R725Q/Q730E and K528R/R725Q, generated less than 30% of the mature peptide compared with WT ERAP1. Further analysis of ERAP1 in AS individuals showed that ERAP1 association with AS cannot just be considered on an individual SNP basis. Instead, when both chromosomal copies of ERAP1 (allotypes) were identified in individuals,

complete stratification of AS patients from controls was observed (6, 29). On-going work in our lab seeks to determine the peptidome in the presence of different ERAP1 variants which would provide useful information as to how these polymorphic variants alter the peptide repertoire at the cell surface.

NK cells have been implicated in the pathogenesis of AS, with a significantly higher percentage of NK cells in the peripheral blood of AS patients compared to healthy controls, including HLA-B27$^+$ controls (86). Another study found that the functional activity of NK cells in SpA patients was decreased, exhibiting reduced IFNγ production (91). These studies suggest that NK cells may play a role in the pathogenesis of AS. NK cells interact with HLA-B27 through two receptors: KIR3DL1 and KIR3DL2. KIR3DL1 can interact with all HLA-Bw4 epitopes and additionally binds to FHC & $B27_2$ structures of HLA-B27 (70, 133). KIR3DL2 binds to HLA-A3 and –A11 in the presence of peptide but can additionally bind to $B27_2$ (90, 133). The work presented here will focus on the interaction of these KIRs, NK cells, HLA-B27 and ERAP1, determining whether changes in the peptide repertoire or cell surface expression of HLA-B27 due to ERAP1 polymorphisms can alter NK cell activation.

4.2 Hypothesis

ERAP1 polymorphisms alter the cell surface expression of HLA-B27 on the cell surface and/or the activation of NK cells in response to interactions between HLA-B27 and KIR3DL1 and/or KIR3DL2.

4.3 Aims

- Determine the cell surface expression of HLA-B27 following transfection of target cells with ERAP1 allotypes and allotype combinations
- Determine the NK cell response to ERAP1 allotypes and allotype combinations

4.4 Results

4.4.1 ERAP1 allotypes do not significantly alter HLA-B27 or FHC expression on the cell surface of HeLa ERAP1-/- cells

ERAP1 is a highly polymorphic protein with at least 13 naturally occurring allotypes found in the general population (6) (**Table 4:1**). To determine whether these 13 allotypes had any effect on the cell surface expression of HLA-B27 and FHC, HeLa ERAP1$^{-/-}$ cells were transiently transfected with HLA-B*2705, as stable transfection was unachievable, and an ERAP1 allotype (*001-*013) and a HLA-B27 screen was run (2.8 HLA-B27 expression screen) (**Figure 4.1**). No significant changes in HLA-B27 expression were seen with any ERAP1 allotype. However, *001-*005 showed generally more HLA-B27 expression than the rest. No significant changes were seen in FHC expression with any ERAP1 allotype, although there was some slight variability across the allotypes.

Table 4:1: ERAP1 allotypes

ERAP1 allotypes	Frequency	
	Controls (n=38) n (%)	Cases (n=34) n (%)
*001	8 (21)	15 (44)
*002	17 (44.5)	1 (3)
*003	1 (2.5)	1 (3)
*004	0	1 (6)
*005	4 (11)	10 (29)
*006	0	2 (6)
*007	0	2 (6)
*008	1 (2.5)	0
*009	0	1 (3)
*010	2 (5)	0
*011	4 (11)	0
*012	0	1 (3)
*013	1 (2.5)	0

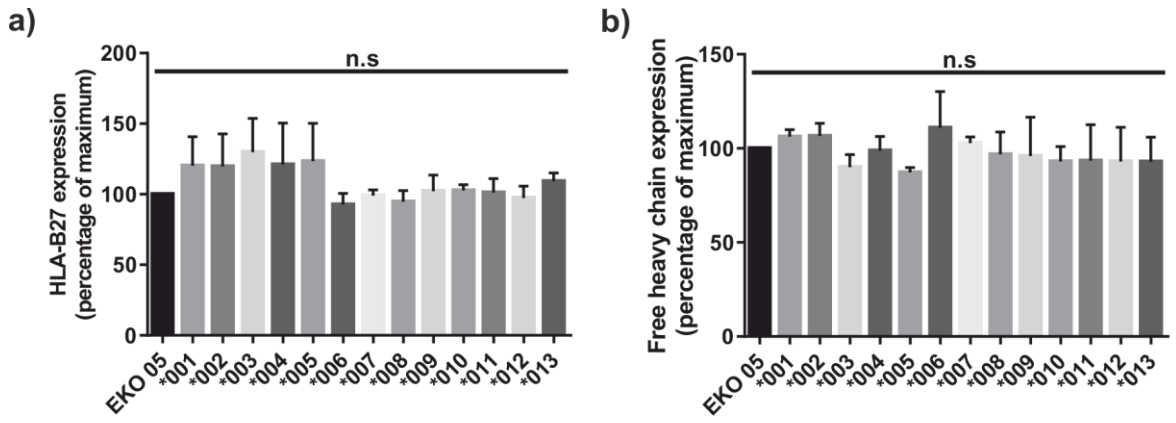

Figure 4.1: HLA-B27 and FHC expression with different ERAP1 allotype

Individual ERAP1 allotypes were transiently transfected into HeLa ERAP1$^{-/-}$ cells along with HLA-B*2705 before surface staining for their HLA-B27 and FHC cell surface expression. (a) No significant differences were visible with any allotype compared to HeLa ERAP1$^{-/-}$ B*2705 cells (HeLa EKO 05) or any other condition, although there was some slight increase with the *001-*005 allotypes. (b) No significant differences were seen in FHC expression following transfection with any allotype. N=3, data analysed by one-way ANOVA and Tukey's multiple comparisons test.

4.4.2 ERAP1 allotypes do not alter NK cell activation

ERAP1 and HLA-B*2705 transfected HeLa ERAP1$^{-/-}$ cells were next used as target cells in LAMP1 assays (NK cell degranulation (LAMP1) assay) to determine the NK cell activation state in response to different ERAP1 allotypes (**Figure 4.2**). No significant differences in NK cell activation were seen with any allotype in the total NK cell population, the KIR3DL1^{+}, the KIR3DL2^{+} or the KIR3DL1/2^{+} populations. However, in the KIR3DL1/2^{-} population, *013 induced increased NK cell activation compared to *001 & *004 ($p<0.01$) and *002 & *003 ($p<0.05$). This result was higher than the others in each of the three repeats of the experiment, suggesting that this is a real result. However, further work would be required to elucidate this fully and to determine why this may be the case. These ERAP1 allotypes were distributed across both case and control groups with little preference for either group (6), which would suggest that a lack of difference in HLA-B27 cell surface expression or NK cell activation is expected.

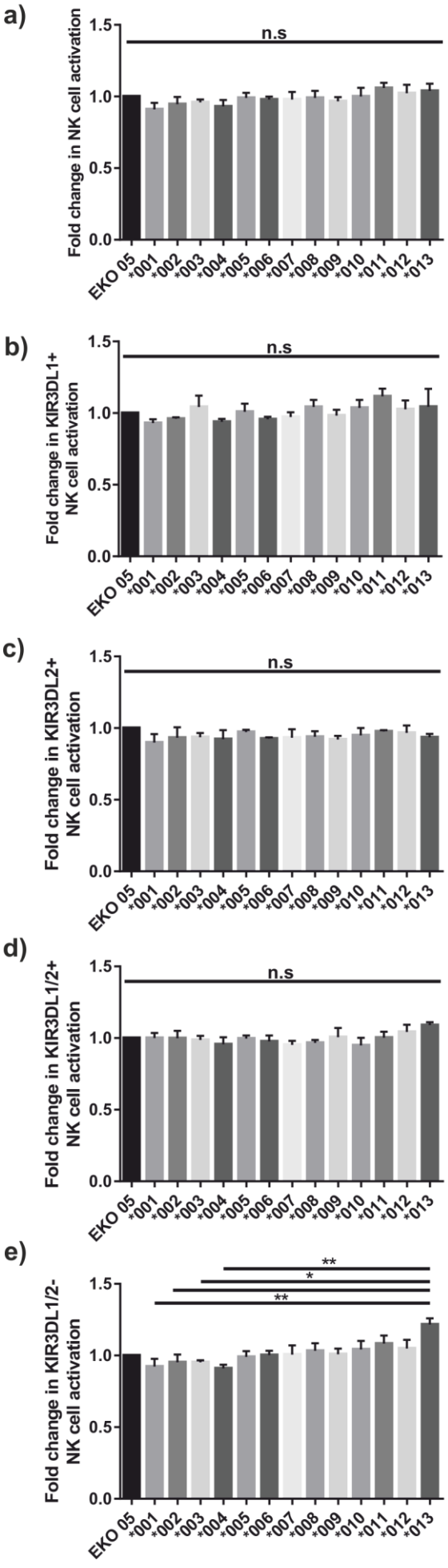

Figure 4.2: NK cell response to individual ERAP1 allotypes

ERAP1 allotypes were transiently transfected into HeLa ERAP1$^{-/-}$ cells along with HLA-B*2705 and these cells were used as the target cell in LAMP1 assays. (a) In the whole NK cell population, there were no significant differences in NK cell activation with any allotype. (b) In the KIR3DL1^{+} NK cell population, there were no significant differences. (c) In the KIR3DL2^{+} population, there were no significant differences in NK cell activation. (d) In the KIR3DL1/2^{+} NK cell population, there were no significant differences with any allotype. (e) In the KIR3DL1/2^{-} NK cell population, *013 significantly activated NK cells more than *004 and *001 ($p<0.01$) & *002 and *003 ($p<0.05$).

N=3, data analysed by one-way ANOVA and Tukey's multiple comparisons test.

4.4.3 AS-associated ERAP1 allotype combinations express significantly less FHC on the cell surface

ERAP1 allotype combinations have been shown to discretely distinguish AS cases from controls, in contrast to individual allotypes that are mostly present in both groups (**Table 4:2**) (6). As with the individual allotypes, it was important to determine whether transfection of different ERAP1 allotype combinations altered the biochemistry of HLA-B27 at the cell surface. Previously, it was shown, in the context of 293T ERAP1$^{-/-}$ B*2705^{+} cells and ERAAP$^{-/-}$ fibroblasts, that AS associated ERAP1 allotype combinations did not increase HLA-B27 expression while control associated pairs did (6).

Table 4:2: ERAP1 allotype combinations

	Allotype combination	Frequency	
		Controls (n=19) n (%)	Cases (n=17) n (%)
C1	*001 + *002	7 (37)	0
C2	*002 + *005	3 (16)	0
C3	*002 + *002	2 (11)	0
C4	*002 + *011	2 (11)	0
C5	*010 + *011	2 (11)	0
C6	*001 + *008	1 (5)	0
C7	*002 + *003	1 (5)	0
C8	*005 + *013	1 (5)	0
A1	*001 + *005	0	9 (53)
A2	*001 + *001	0	2 (12)
A3	*001 + *007	0	2 (12)
A4	*002 + *006	0	1 (6)
A5	*004 + *006	0	1 (6)
A6	*005 + *009	0	1 (6)
A7	*003 + *012	0	1 (6)

HeLa ERAP1$^{-/-}$ cells were transiently transfected with HLA-B*2705 and either a control pair (C1-8) or an AS-associated case pair (A1-7) of ERAP1; these designations were assigned in table 1. These cells were then surface stained for their HLA-B27 and FHC expression (**Figure 4.3**). The results are shown with case and control pairs grouped and then with each pair shown individually. There was no significant difference in the expression of HLA-B27 in cases compared to controls,

however, some slight variability could be seen when the pairs were separated, although these changes were still non-significant (**Figure 4.3a-b**). FHC expression is significantly decreased in AS cases compared to both HeLa ERAP1$^{-/-}$ B*2705 cells ($p<0.001$) and controls ($p<0.0001$) (**Figure 4.3c**). When separated into individual pairs there is a general trend for controls to express higher levels of FHC than AS case-associated pairs (**Figure 4.3d**). In particular, C1 is significantly higher than A2, A3 & A7 ($p<0.05$), and A6 ($p<0.01$). A6 is also significantly lower than C2, C3 and C6 ($p<0.05$).

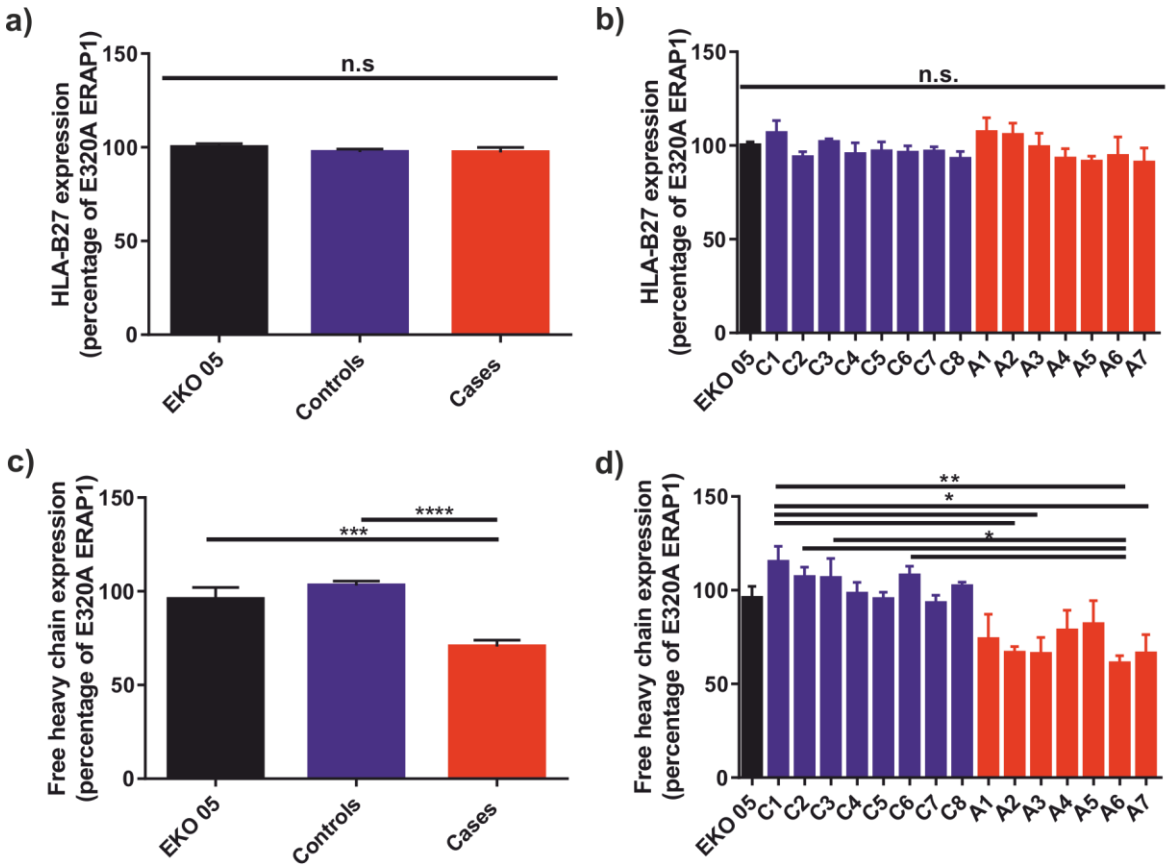

Figure 4.3: ERAP1 allotype combinations alter FHC expression but not HLA-B27 expression

HeLa ERAP1$^{-/-}$ cells were transiently transfected with HLA-B*2705 (EKO 05) and an ERAP1 allotype combination either associated with controls (C1-8) or AS cases (A1-7). (a) The HLA-B27 cell surface expression was measured using ME.1 antibody staining. When controls and AS cases are grouped, there is no significant difference between cell surface HLA-B27 expression with either group. (b) When these groups are separated into individual pairs, there are still no significant differences but C1, A1 and A2 show the highest levels of ME.1 staining. (c) Cell surface FHC levels were measured using the HC10 antibody. When controls and AS cases are grouped, there is a significant reduction in FHC with cases compared both to controls ($p<0.0001$) and HeLa ERAP1$^{-/-}$ B*2705 cells alone ($p<0.001$). (d) When these groups are separated into individual pairs, FHC in C1 are significantly higher than A2, A3, A7 ($p<0.05$) and A6 ($p<0.01$). A6 also shows significantly less cell surface FHC than C2, C3 and C6 ($p<0.05$). N=3, data analysed by one-way ANOVA and Tukey's multiple comparisons test.

4.4.4 AS-associated ERAP1 allotype combinations induce increased NK cell activation compared to control ERAP1 allotype combinations

The NK cell response to these ERAP1 allotype pairs was tested to see how this reduction in FHC expression affected NK cell activation. HeLa ERAP1$^{-/-}$ B*2705 cells transfected with different ERAP1 allotype combinations were used as target cells in LAMP1 assays (2.4 NK cell degranulation (LAMP1) assay). In the whole NK cell population, there was a significant increase in NK cell activation with cases compared to both HeLa ERAP1$^{-/-}$ cells ($p<0.01$) and controls ($p<0.0001$) (**Figure 4.4a**). When these data are separated into individual pairs there were no significant differences but all controls showed equal or less activation than HeLa ERAP1$^{-/-}$ cells, and cases showed higher activation (**Figure 4.4b**). In the KIR3DL1^{+} NK cell population, the significantly higher NK cell activation was repeated with cases being significantly higher than HeLa ERAP1$^{-/-}$ cells ($p<0.01$) and controls ($p<0.0001$) (**Figure 4.4c**). The pattern seen in the whole NK cell population with individual allotype combinations was also observed in this KIR3DL1^{+} population (**Figure 4.4d**).

In the KIR3DL2^{+} NK cell population, there were no significant differences in NK cell activation, although this appeared to be slightly increased with cases compared to controls (**Figure 4.4e**). There were also no significant differences when the ERAP1 allotype combinations were looked at individually (**Figure 4.4f**). In the KIR3DL1/2^{+} NK cell population, there were no significant differences in NK cell activation; however, there was a slight increase in activation in both cases and controls (**Figure 4.4g**). When these results were separated into individual pairs of ERAP1 there were again no significant differences (**Figure 4.4h**).

Unexpectedly, the significant increase in NK cell activation seen with cases previously in the KIR3DL1^{+} population was also observed in the KIR3DL1/2^{-} NK cell population (**Figure 4.4i**). When these results were displayed as individual ERAP1 allotype combinations the trend for cases to be higher than controls was clearly seen, though did not reach statistical significance (**Figure 4.4j**).

Figure 4:4: ERAP1 allotype combinations alter NK cell activation

HeLa ERAP1$^{-/-}$ cells were transiently transfected with HLA-B*2705 (EKO 05) and an ERAP1 allotype combination either associated with controls (C1-8) or AS cases (A1-7) and these cells were then used as target cells in LAMP1 assays. (a) In the whole NK cell population, AS cases significantly increased NK cell activation compared to both controls ($p<0.0001$) and HeLa ERAP1$^{-/-}$ B*2705 (EKO 05) cells ($p<0.01$). (b) When these results were separated into individual pairs there were no significant differences but most controls induced equal or less NK cell activation than EKO 05 cells and AS cases generally induced more NK cell activation. (c) In the KIR3DL1^{+} NK cell population, the same pattern of activation with AS cases can be seen. (d) When these results were separated into individual pairs there were no significant differences but most controls induced equal or less NK cell activation than EKO 05 cells and AS cases generally induced more NK cell activation. (e) In the KIR3DL2^{+} NK cell population, there were no significant differences in NK cell activation. (f) When these results are separated into individual pairs there are no significant differences. (g) In the KIR3DL1/2^{+} NK cell population, there are no significant differences in NK cell activation. (h) When these results were separated into individual pairs there were no significant differences but all pairs showed some slight increase in NK cell activation compared to EKO 05 cells. (i) In the KIR3DL1/2^{-} NK cell population, AS cases induced significantly higher NK cell activation compared to controls ($p<0.0001$). (j) When these results were separated into individual pairs there were no significant differences but most controls induced equal or less NK cell activation than EKO 05 cells and AS cases generally induced more NK cell activation. N=3, data analysed by one-way ANOVA and Tukey's multiple comparisons test.

Figure 4.4: ERAP1 allotype combinations alter NK cell activation

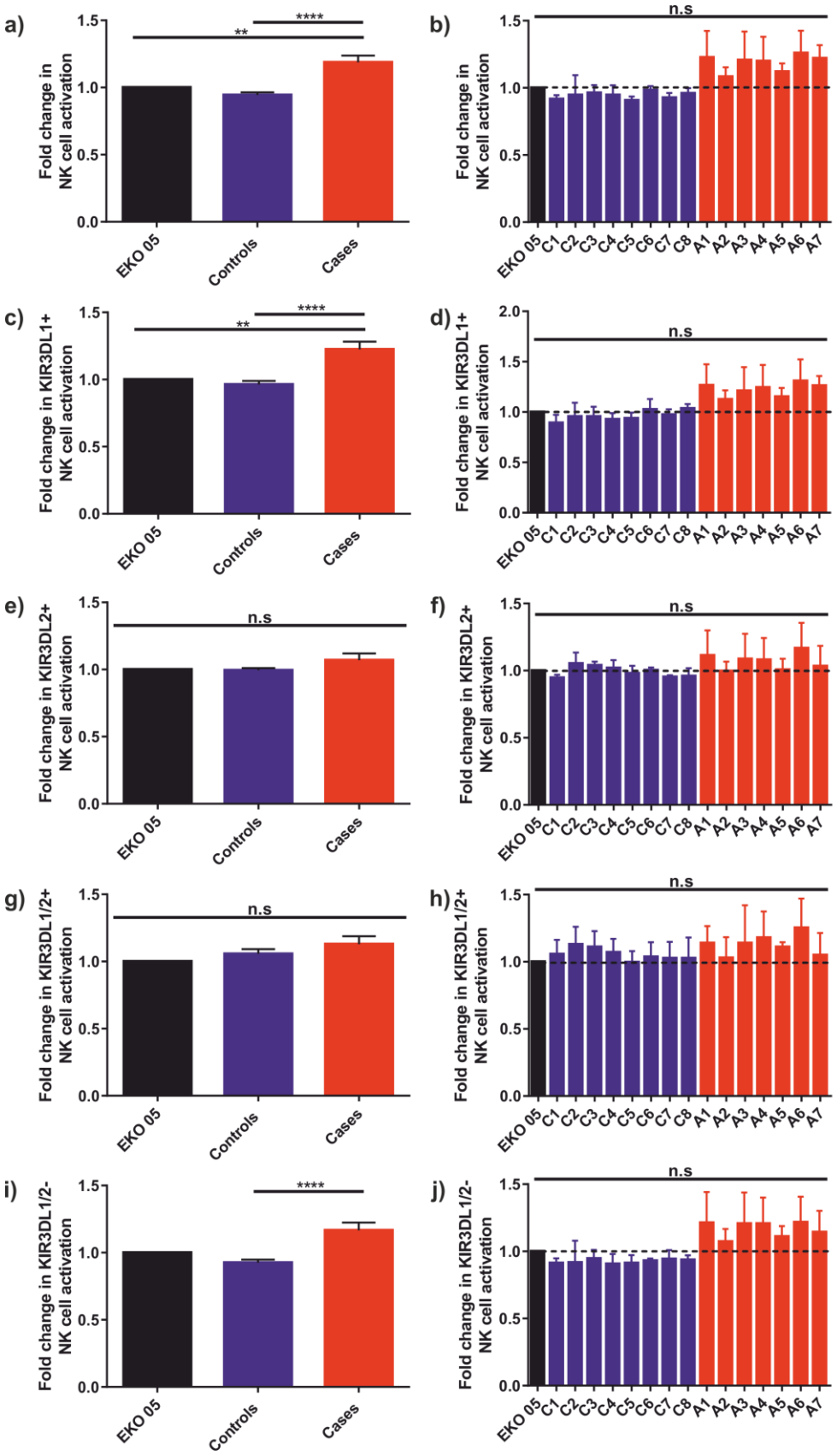

4.4.5 ERAP1 allotype combinations show no significant changes in rhKIR3DL1 binding

The changes in NK cell activation observed in the LAMP1 assay were mostly in KIR3DL1^{+} NK cells and not KIR3DL2^{+} cells. To confirm whether these changes were the result of KIR3DL1 engagement, rhKIR3DL1 bound to ERAP1 allotype combination transfected cells was used to determine whether there were any differences in binding to cases and controls (**Figure 4.5**). rhKIR3DL1 was conjugated to fluorescent protein A overnight which binds up to 4 rhKIR molecules, allowing direct detection of rhKIR3DL1 bound to cells as well as representing physiological conditions by simulating receptor clustering at the cell surface. No significant differences were seen between cases and controls, although there was a slight decrease in binding of rhKIR3DL1 with cases compared to controls (**Figure 4.5a**). When these results were separated into individual pairs the majority of control pairs showed increased binding of rhKIR3DL1 compared to HeLa ERAP1$^{-/-}$ B*2705 cells (with the exception of C5 and C6), while most cases showed reduced rhKIR3DL1 engagement (with the exception of A5) (**Figure 4.5b**). Correct transfection of ERAP1 into HeLa ERAP1$^{-/-}$ cells was confirmed by Western blot (**Figure 4.5c**). The differences in rhKIR3DL1 binding did not appear to be on account of changing levels of ERAP1 or HLA-B27.

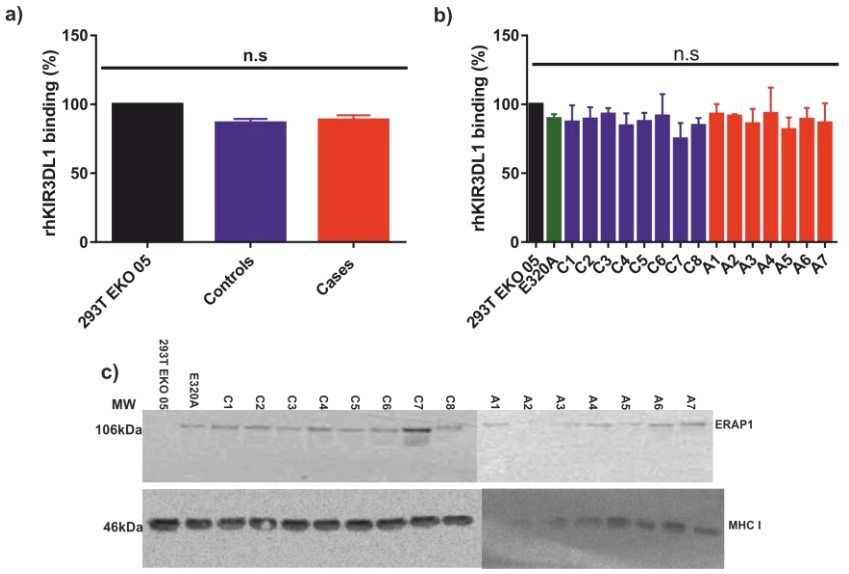

Figure 4.5: Binding of rhKIR3DL1 to ERAP1 allotype pairs

HeLa ERAP1$^{-/-}$ cells were transiently transfected with HLA-B*2705 (EKO 05) and ERAP1 allotype combinations either associated with cases on controls before being used in an rhKIR3DL1 binding assay. (a) When cases and controls were grouped there were no significant differences in the binding of rhKIR3DL1, although there is a slight reduction in cases. (b) When the allotype pairs were separated into individual pairs, most control pairs showed higher rhKIR3DL1 binding than EKO 05 and most cases showed less binding than EKO 05. (c) ERAP1 transfection was confirmed by western blot, with an anti-MHC I antibody as a loading control. N=2, data analysed by one-way ANOVA and Tukey's multiple comparisons test.

4.4.6 Blocking of KIR3DL1 increases NK cell activation

To further investigate the contribution of KIR3DL1, the DX9 anti-KIR3DL1 blocking antibody was used to block the PBMC population for one hour prior to incubation with target cells for LAMP1 assays (**Figure 4.6**). DX9 blocking significantly increased NK cell activation in all groups in the whole NK cell population (**Figure 4.6a**). This increase in NK cell activation was also seen in the KIR3DL1^{+} NK cell population, although as the increase was not as great there was less significance (**Figure 4.6b**). Blocking with IgG control antibody increased NK cell activation in the control group but had little effect on the case group.

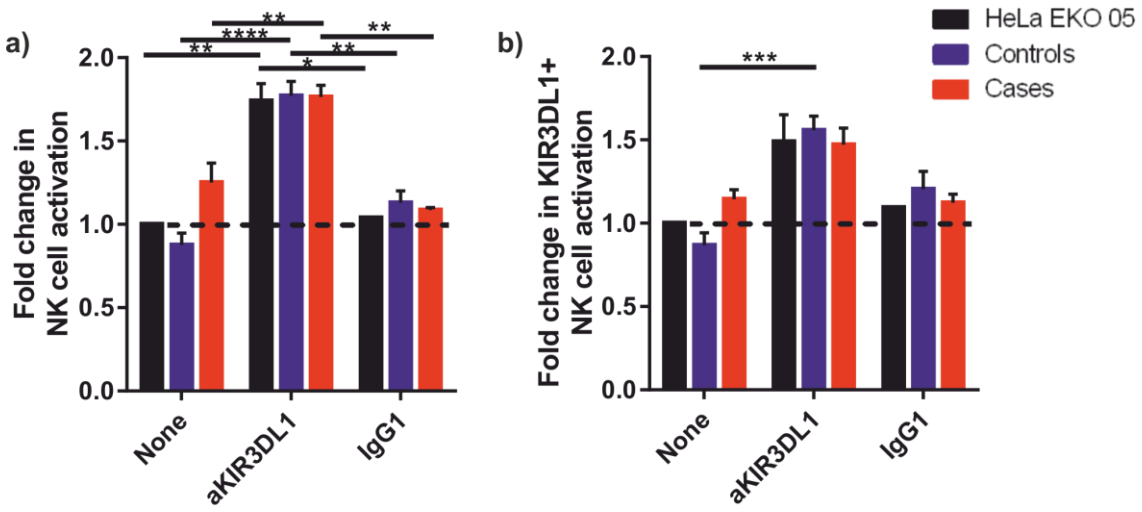

Figure 4.6: KIR3DL1 blocking increases NK cell activation

Before use in LAMP1 assays, PBMCs were incubated for 1 hour at 37°C in the presence of anti-KIR3DL1 blocking antibody (DX9 Clone). These PBMCs were then combined with case or control ERAP1 transfected HeLa ERAP1$^{-/-}$ B*2705 cells. (a) In the whole NK cell population, NK cell activation was increased significantly in the presence of HeLa EKO 05 cells and case ERAP1 transfectants ($p<0.01$) and even more so in the presence of control ERAP1 ($p<0.0001$) (b) In the KIR3DL1^{+} NK cell population, there was an increase in NK cell activation across all groups but this was not as significant as was seen in the whole NK cell population, with only a significant difference noted for the control ERAP1 group($p<0.001$). N=3, data analysed by two-way ANOVA and Tukey's multiple comparisons test.

4.4.7 Blocking of HLA-B27 or FHC shows that pB27 complexes generated by AS-associated ERAP1 allotype combinations do not engage KIR3DL1

The increase in NK cell activation following KIR3DL1 blocking suggests that KIR3DL1 engagement usually occurs to minimise NK cell activation in response to HLA-B27 expressed on transfected target cells. In addition, it is possible that the DX9 antibody is activating ADCC, particularly in the

KIR3DL1/2$^-$ population. HLA-B27 can be found on the cell surface in three forms; peptide and β2m associated heavy chain (pB27), FHCs or $B27_2$ (13, 134). pB27, FHC and $B27_2$ can engage KIR3DL1 (133), while only FHC and $B27_2$ are thought to bind to KIR3DL2 (14). To determine whether it is pB27 or FHC binding to KIR3DL1 that prevents NK cell activation, HeLa ERAP1$^{-/-}$ B*2705 cells transfected with ERAP1 allotype pairs were incubated with the pB27 blocking antibody ME.1 or the FHC and $B27_2$ blocking antibody HC10 (135) for one hour prior to incubation with PBMCs for LAMP1 assays (**Figure 4.7**).

In the whole NK cell population, ME.1 blocking increased NK cell activation in HeLa ERAP1$^{-/-}$ B*2705 and control ERAP1 transfected cells to the same level as previously seen with case ERAP1 pairs (**Figure 4.7a**). There was no change in NK cell activation following ME.1 block with AS-associated case pairs. HC10 block increased NK cell activation to a higher level in all groups than was seen with ME.1 block. Control ERAP1 induced significantly higher NK cell activation following HC10 ($p<0.05$). In the KIR3DL1$^+$ NK cell population, ME.1 block increased NK cell activation slightly in HeLa ERAP1$^{-/-}$ B*2705 and control ERAP1 transfected cells to roughly the same level as previously seen with case ERAP1 pairs (**Figure 4.7b**). HC10 block increased this NK activation in all groups, with controls being significantly higher than in the absence of any blocking antibodies ($p<0.01$).

In the KIR3DL2$^+$ population, there were slight increases in all groups with both ME.1 and FHC block, but none of these changes were significant and these results were highly variable across repeats (**Figure 4.7c**). In the KIR3DL1/2$^+$ NK cell population, ME.1 block clearly increased NK cell activation in response to HeLa ERAP1$^{-/-}$ B*2705 cells and there was a slight increase in controls, but these results were not significant (**Figure 4.7d**). HC10 block increased NK cell activation in response to HeLa ERAP1$^{-/-}$ B*2705 and controls slightly (n.s). But the greatest difference was seen with case ERAP1 pairs where HC10 block significantly increased NK cell activation compared to both no block and ME.1 block ($p<0.0001$).

As seen in the previous LAMP1 assays, significant differences were also seen in the KIR3DL1/2$^-$ NK cell population. ME.1 block increased NK cell activation slightly in response to HeLa ERAP1$^{-/-}$ B*2705 cells and controls slightly (n.s) but had no effect on cases (**Figure 4.7e**). HC10 block increased NK cell activation in both groups further than that seen with ME.1 block and this was significant between controls with no block ($p<0.05$) and cases with both no block and ME.1 block ($p<0.05$).

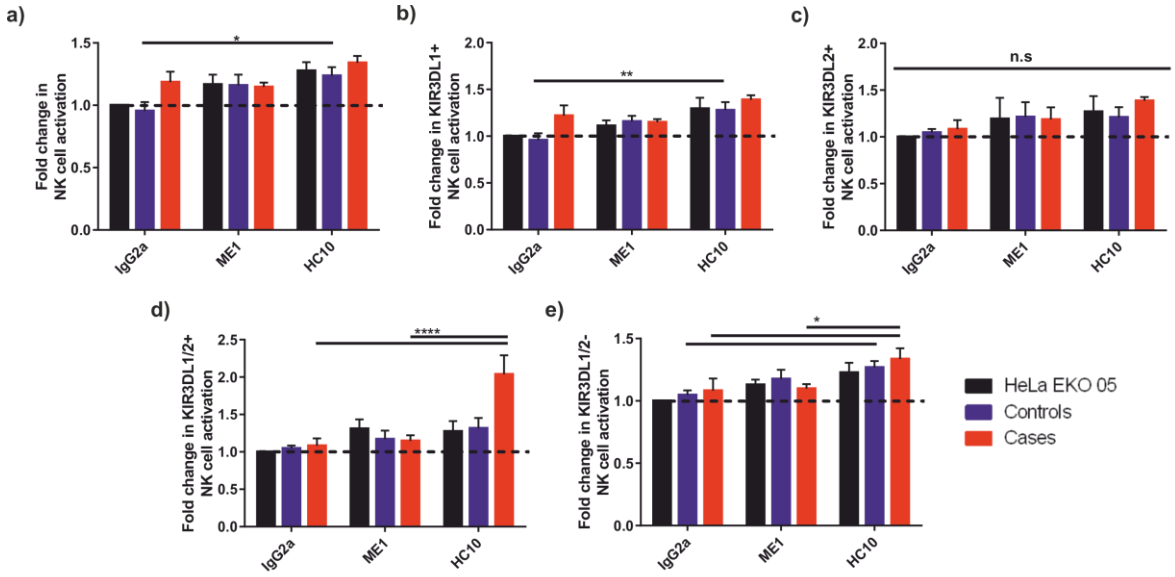

Figure 4.7: Blocking HLA-B27 and FHC increases NK cell activation

HeLa ERAP1$^{-/-}$ cells transfected with HLA-B*2705 (EKO 05) and control or case-associated ERAP1 were incubated at 37°C for 1 hour with IgG2a control, anti-HLA-B27 (ME.1) or anti-FHC (HC10) blocking antibodies, before addition to PBMCs for a LAMP1 assay. (a) In the whole NK cell population, ME.1 block increased NK cell activation in HeLa ERAP1$^{-/-}$ B*2705 cells and controls to the same level as cases. HC10 increased NK cell activation in all groups further than ME.1 block. (b) In the KIR3DL1^{+} population, ME.1 block slightly increased NK cell activation, but this was more pronounced with HC10 block. (c) In the KIR3LD2^{-} population, there were slight increases in NK cell activation with both ME.1 and HC10 but these differences were not significant. (d) In the KIR3DL1/2^{+} population, all groups were slightly increased with ME.1 block but this was largest in the EKO 05 group (n.s). HC10 block slightly increased NK cell activation in the EKO 05 and controls groups, and dramatically increased this in the cases group ($p<0.0001$). (e) In the KIR3DL1/2^{-} NK cell population, ME.1 block slightly increased NK cell activation in EKO 05 and controls, but had little effect on cases. HC10 block increased NK cell activation further in all groups. N=3, data analysed two-way ANOVA and Tukey's multiple comparisons test.

4.4.8 AS-associated ERAP1-induced NK cell activation alters the cytokine & chemokine profile compared to control ERAP1

Having shown that ERAP1 allotype combinations can significantly alter NK cell activation we investigated whether this affected other cells present in the PBMC population. For the LAMP1 assay the whole PBMC population is incubated with target cells but when it comes to the analysis we identify only the NK cells from this vast population. Within the PBMC population there will also be several other immune cells, including macrophages, dendritic cells, T cells, B cells and granulocytes which could have synergistic effects in concert with the NK cell activation seen. To determine whether any differences were present, the cytokine and chemokine profiles in the presence of different ERAP1 variants was assessed to investigate whether there was an increase in pro-inflammatory cytokines in the presence of AS-associated ERAP1 allotype combinations.

Initially, cytokine profiles were determined using the Proteome profiler kit (2.10 RnD Sytems Proteome profiler kit) following incubation of target cells with IL-15 stimulated PBMCs for 24 hours. Supernatants were collected and loaded onto the array overnight before detection the following day. Four cultures were tested: PBMC only, HeLa ERAP1$^{-/-}$ B*2705 target cells, HeLa ERAP1$^{-/-}$ B*2705 + *002 (WT) ERAP1 and HeLa ERAP1$^{-/-}$ B2705 + *001 ERAP1 (**Figure 4.8**). The *001 ERAP1 variant is also known as the 5SNP allotype as it has the five most characterised SNPs associated with AS within its sequence (rs27044, rs17482078, rs10050860, rs30187 and rs2287987) making this the prototypical AS-associated variant. Within the control (C) and case (A) designations *002 is the equivalent of C3 and *001 is the equivalent of A2.

Baseline production of cytokines or chemokines was very low as determined from PBMC cultures without the presence of target cells, despite the overnight IL-15 stimulation these cells were subjected to (**Figure 4.8a**). Both HeLa ERAP1$^{-/-}$ B*2705 cells and those with the *001 allotype visibly induced more cytokines and chemokines than cells with the *002 allotype. Within the blots each analyte is present in duplicate. The density of both dots was calculated using ImageJ software (ImageJ) and the analytes that showed differences between target cell conditions are shown (**Figure 4.8b**). HeLa ERAP1$^{-/-}$ B*2705 cells and those with the *001 allotype induced more expression of CCL2, MIP-1αβ, CCL5, CXCL1 and CXCL10 than *002-transfected cells. These cytokines are involved in inflammation and some act as chemoattractants, attracting other immune cells to sites of infection or inflammation.

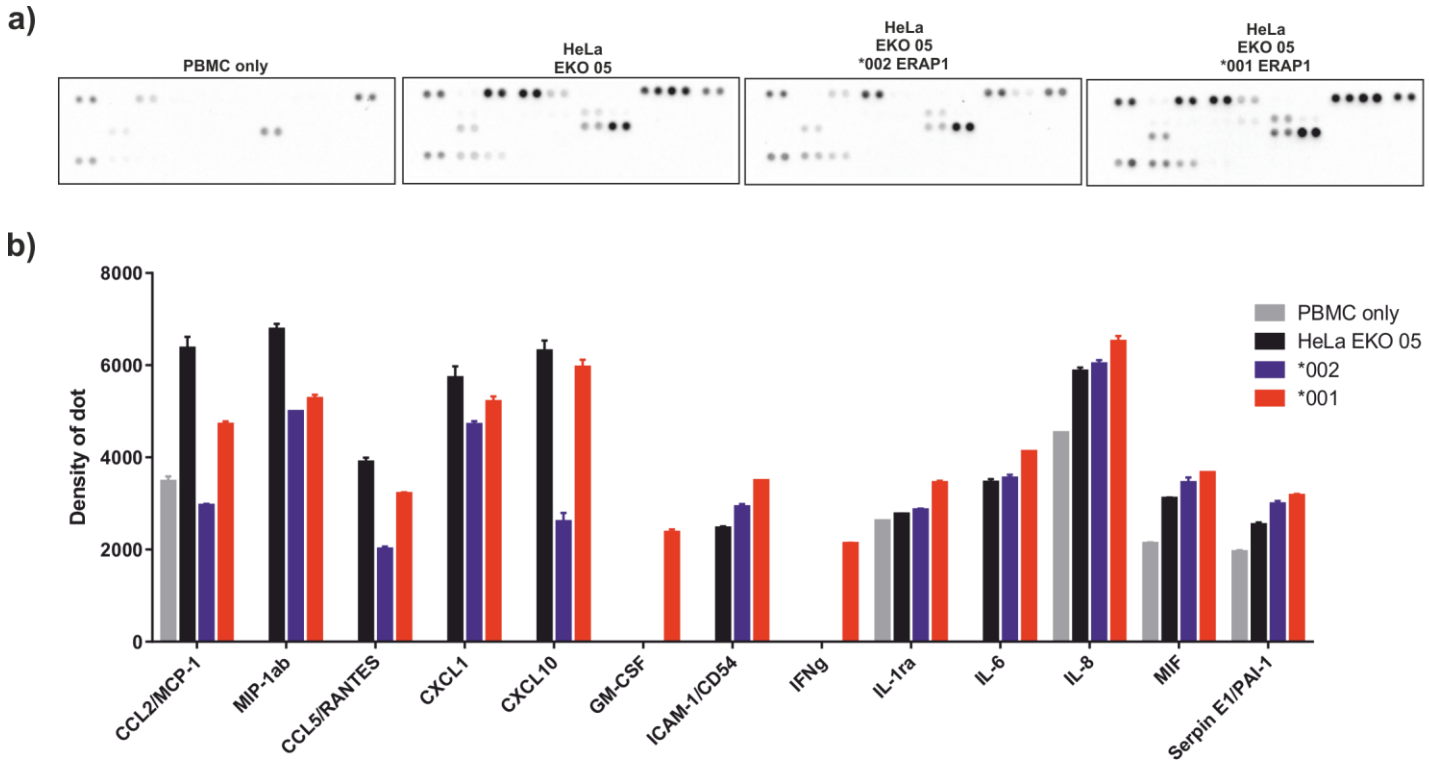

Figure 4.8: Proteome profiler kit shows differences in cytokine release with ERAP1 variants

The RnD Systems Proteome profiler kit was used to simultaneously analyse 32 chemokine and cytokine levels following incubation of PBMCs with HeLa ERAP1$^{-/-}$ cells transfected with HLA-B*2705 (HeLa EKO 05) and a control ERAP1 variant (*002) or case-associated variant (*001). PBMCs and HeLa cells were incubated together overnight before the supernatant was added to the pre-prepared dot blots. (a) Very few cytokines are produced by PBMCs in the absence of target cells. More dots are visible on the blots for HeLa EKO 05 and *001-transfected cells compared to *002-transfected cells. (b) The density of the dots (all of which are in duplicate) was calculated and plotted for each cell line. Only cytokines and chemokines that showed a difference compared to PBMC only are shown here. HeLa EKO 05 and *001-transfected cells produce more CCL2, MIP-1αβ, CCL5, CXCL1 and CXCL10 than *002-transfected cells.

4.4.9 Presence of target cells increases expression of cytokines and chemokines from PBMCs

Next, a panel of 14 analytes was designed for use in Luminex multiplex assays (2.11 RnD Systems Luminex multiplex assay). Luminex assays can simultaneously analyse multiple analytes through the use of fluorescent beads and provide a concentration of each through. This allows detection of multiple analytes in the same way as an ELISA can look at one analyte, providing a robust method for identifying the range of cytokines and chemokines released from the PBMC population.

The aim of the Luminex assay was to further investigate the changes seen in the Proteome profiler kit (**Figure 4.8**): the panel examined CCL2 (MCP-1), MIP-1α, MIP-1β, CCL5, CXCL1 (GROα) and CXCL10 (IP-10). In addition, despite minimal changes in the Proteome profiler analysis the following cytokines and chemokines were altered or increased in the presence of HeLa ERAP1$^{-/-}$ B*2705 cells and were thus included in the panel: GM-CSF, IFNγ, IL-6 and IL-8. IFNγ, IL-6, IL-8, IL-10 and TNFα have been implicated in the pathogenesis of AS and so were included in the panel for this reason (136-139). Changes in the levels of IL-1Rα were visible in the proteome profiler analysis and so this was also included, along with its ligand IL-1α as this cytokine and TNFα have frequently been found to work synergistically as both are acute phase cytokines that promote fever and inflammation (140). The full list of analytes looked at can be found in **Table 4:3**.

The luminex assay determines the concentration of each analyte based on where the detection value sits in the concentration curve produced by dilution of the standards provided with the kit. If any detection values appear out of the range of this standard curve they are not analysed. This led to the exclusion of IL-8, MIP-1α, IL-6, IP-10 and IL-1Rα from analysis. Less than 20% of values were received for MIP-1α, IP-10 and IL-1Rα, but the values for IL-6 and IL-8 were very high and therefore out of the range of the standard curve. This high expression was true across all experimental conditions, but without a repeat experiment or validation of these values by standard ELISA the results could not be validated and were therefore excluded for further analysis.

Table 4:3: Luminex analyte panel	
TNFα	GM-CSF
IFNγ	GROα (CXCL1)
MIP-1α	IL-8
MIP-1β	IL-10
IP-10 (CXCL10)	IL-6
MCP-1 (CCL2)	IL-1α
CCL5	IL-1Rα

Cytokines that showed the greatest differences between HeLa ERAP1$^{-/-}$ or HeLa ERAP1$^{-/-}$ B*2705 cultures in the array assay (**Figure 4.8**) were confirmed and quantitated by multiplex (**Figure 4.9**). Significant increases in IFNγ, MIP-1β, IL-1α and GM-CSF were seen following addition of target cells to PBMCs. The PBMC population alone produced very low levels of cytokines for all of the analytes shown, or undetectable levels for the other analytes.

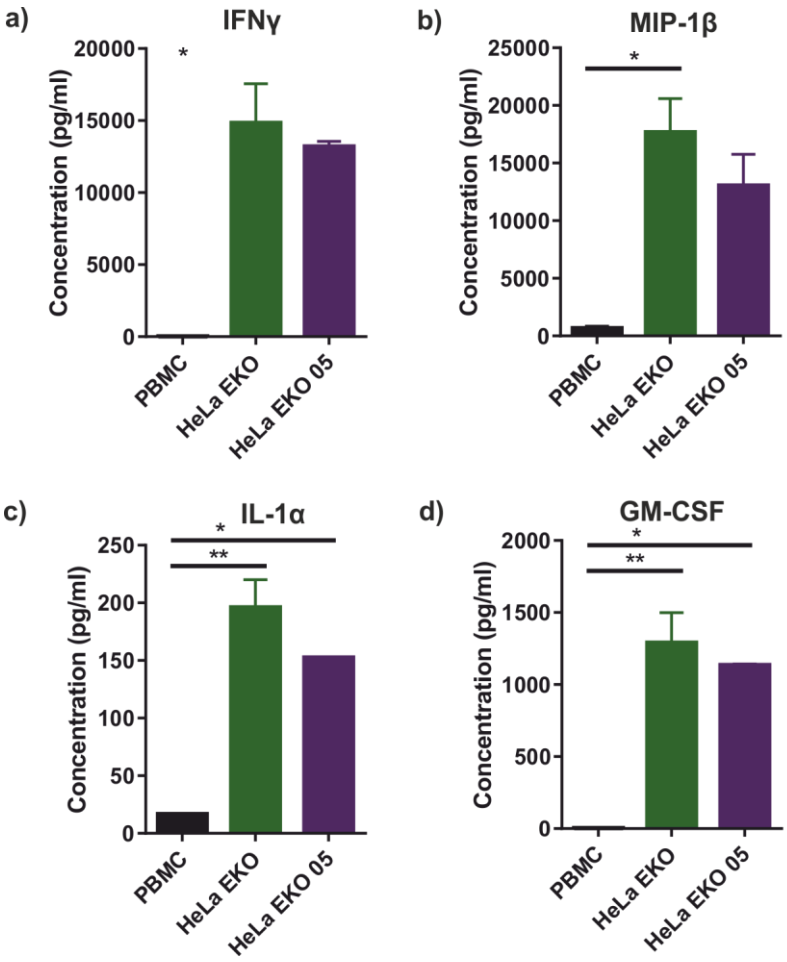

Figure 4.9: Target cells induce cytokine & chemokine release from PBMCs

The release of cytokines and chemokines from PBMCs was measured in a Luminex assay. PBMCs previously stimulated overnight with IL-15 were incubated with HeLa ERAP1$^{-/-}$ (green) or HeLa ERAP1$^{-/-}$ B*2705 (purple) cells for 24 hours before the supernatant was collected. (a) IFNγ was significantly induced in the presence of both HeLa cell lines ($p<0.05$). (b) MIP-1β was significantly induced in the presence of HeLa ERAP1$^{-/-}$ cells ($p<0.05$) but not HeLa ERAP1$^{-/-}$ B*2705 cells despite a large increase compared to PBMC alone.(c) IL-1α was significantly induced by both cell lines: $p<0.01$ for HeLa ERAP1$^{-/-}$ and $p<0.05$ for HeLa ERAP1$^{-/-}$ B*2705 cells. (d) GM-CSF was significantly induced by both cell lines: $p<0.01$ for HeLa ERAP1$^{-/-}$ and $p<0.05$ for HeLa ERAP1$^{-/-}$ B*2705 cells. Data analysed by one-way ANOVA and Tukey's multiple comparisons test.

4.4.10 Control ERAP1 allotype combinations induce increased release of IL-10, IFNγ, CCL5 and IL-1a

HeLa ERAP1$^{-/-}$ cells were transiently transfected with HLA-B*2705 and an ERAP1 allotype combination either associated with healthy controls (C1-8) or AS cases (A1-7) (6) before addition to PBMCs. Data is shown with control and case pairs grouped and individually (**Figure 4.10**). There was a significant reduction in IL-10 production with cases compared to controls ($p<0.05$). IFNγ production was significantly lower with case ERAP1 pairs than in the presence of control ERAP1 ($p<0.05$) (**Figure 4.10b**). C5 and C6 showed lower IFNγ production than other control pairs. A2 and A4 showed the highest IFNγ production of the case group by a long way. This result was the opposite of that previously seen in the Proteome Profiler kit (**Figure 4.8**) and so unexpected.

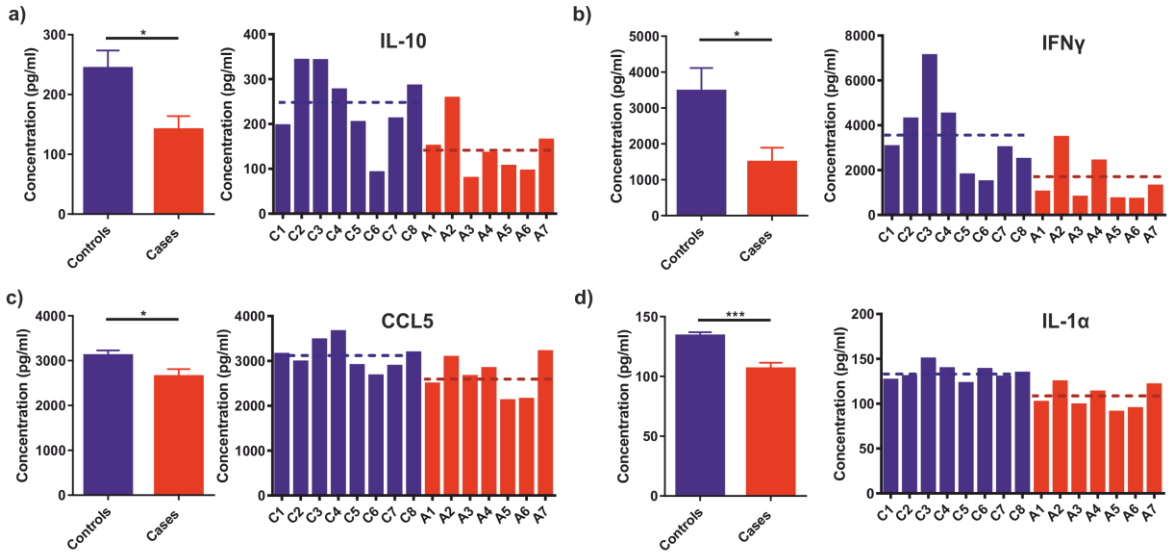

Figure 4.10: AS-associated ERAP1 allotypes reduce the release of cytokines and chemokines

HeLa ERAP1$^{-/-}$ cells were transiently transfected with HLA-B*2705 and an ERAP1 allotype combination, either AS-associated (red) or control (blue), for 24 hours before being combined with IL-15 stimulated PBMCs. The supernatant was collected after 24 hours and analysed in a Luminex assay. Data is presented with control and case ERAP1 combinations grouped and shown individually, with the grouped mean represented by a dotted line for each group. (a) IL-10 production was significantly inhibited by case ERAP1 allotype combinations ($p<0.05$). C6-transfected cells showed one of the lowest levels of IL-10 and A2-transfected cells displayed unusually high IL-10 expression, both of which reduce the significance. (b) IFNγ was significantly reduced with AS-associated ERAP1 allotype combinations ($p<0.05$). Most control ERAP1 pairs induced higher IFNγ production with the exception of C5 and C6, while most AS-associated pairs showed low IFNγ production with the exception of A2 and A4. (c) CCL5 was significantly reduced following transfection with AS-associated ERAP1 allotype combinations ($p<0.05$). (d) IL-1α showed the largest and most consistent reduction in production with AS-associated ERAP1 allotype combinations compared to controls ($p<0.001$). Data analysed by one-way ANOVA and Tukey's multiple comparisons test.

CCL5 expression was also significantly reduced with case ERAP1 pairs ($p<0.05$) (**Figure 4.10c**). Again this result with CCL5 was opposed to the result seen in the Proteome Profiler kit (**Figure 4.8**). IL-1α showed the most significant decrease in expression with AS-associated ERAP1 pairs ($p<0.001$) (**Figure 4.10d**). Little variation in expression of IL-1α was seen across control or case pairs, but a clear reduction was seen with cases. No other significant differences were seen in the release of MIP-1β, MCP-1, GM-CSF or GROα.

4.4.11 AS-associated ERAP1 allotype combinations induce TNFα expression

Release of TNFα was also non-significant, but there was a slight increase in production with case ERAP1 pairs compared to controls (**Figure 4.11**). When these groups were separated into individual pairs, the highest production of TNFα came in the presence of the control ERAP1 pair C5 (**Figure 4.11a**).

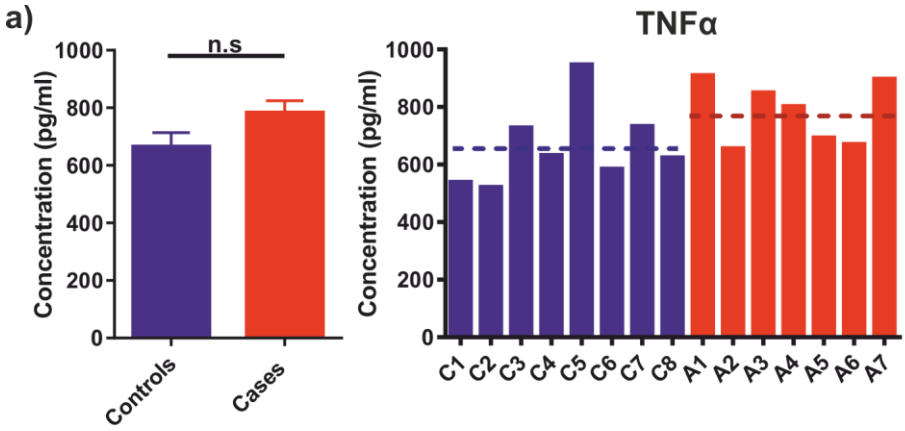

Figure 4.11: AS-associated ERAP1 allotype combinations increase TNFα release from PBMCs

HeLa ERAP1$^{-/-}$ cells were transiently transfected with HLA-B*2705 and an ERAP1 allotype combination, either AS-associated (red) or control (blue), for 24 hours before being combined with IL-15 stimulated PBMCs. The supernatant was collected after 24 hours and analysed in a Luminex assay. Data is presented with control and case ERAP1 combinations grouped and shown individually, with the grouped mean represented by a dotted line for each group. (a) There was no significant difference in expression of TNFα with either group, despite a slight increase with cases compared to controls. C5 showed an unexpectedly high induction of TNFα. Data analysed by one-way ANOVA and Tukey's multiple comparisons test.

All of the data comparing control and case ERAP1 allotype combinations is shown in **Figure 4.12** as a heat map of the fold change of each analyte compared to the control group C1. Low expression is shown in blue, while high expression is shown in red.

a)

	TNFα	MIP-1β	CCL5	IL-1α	MCP-1	GM-CSF	IL-10	GROα	IFNγ
Controls	0.23	0.27	-0.01	0.06	0.06	0.02	0.24	-0.12	0.14
Cases	0.45	0.21	-0.16	-0.16	-0.13	-0.17	-0.28	-0.41	-0.51

b)

	TNFα	MIP-1β	CCL5	IL-1α	MCP-1	GM-CSF	IL-10	GROα	IFNγ
C1	0.00	0.00	0.00	0.00	0.00	0.00	0.00	0.00	0.00
C2	-0.03	0.40	-0.05	0.03	0.17	0.09	0.74	0.03	0.40
C3	0.35	0.44	0.10	0.19	0.83	0.86	0.74	1.04	1.33
C4	0.17	0.23	0.16	0.10	0.12	0.02	0.41	-0.05	0.48
C5	0.76	0.39	-0.08	-0.03	-0.12	-0.18	0.04	-0.48	-0.41
C6	0.09	-0.16	-0.15	0.09	-0.56	-0.62	-0.53	-0.68	-0.51
C7	0.36	0.24	-0.08	0.03	0.15	-0.04	0.08	-0.46	-0.01
C8	0.16	0.65	0.01	0.06	-0.09	0.06	0.45	-0.39	-0.19
A1	0.69	0.36	-0.21	-0.20	-0.11	-0.27	-0.23	-0.51	-0.66
A2	0.22	0.49	-0.02	-0.02	0.19	0.42	0.31	0.32	0.14
A3	0.58	0.08	-0.16	-0.22	-0.21	-0.38	-0.60	-0.52	-0.74
A4	0.49	0.28	-0.10	-0.11	0.21	0.23	-0.31	-0.27	-0.21
A5	0.29	0.05	-0.33	-0.28	-0.34	-0.42	-0.46	-0.66	-0.76
A6	0.24	-0.03	-0.32	-0.25	-0.36	-0.49	-0.51	-0.68	-0.77
A7	0.66	0.24	0.02	-0.04	-0.31	-0.28	-0.16	-0.56	-0.58

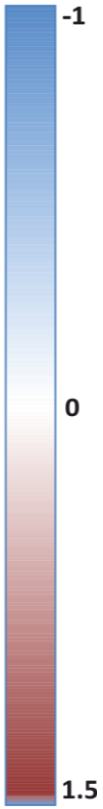

Figure 4.12: Heat map showing fold changes in cytokine levels

HeLa ERAP1$^{-/-}$ cells were transiently transfected with HLA-B*2705 and an ERAP1 allotype combination, either AS-associated or control, for 24 hours before being combined with IL-15 stimulated PBMCs. The supernatant was collected after 24 hours and analysed in a Luminex assay. All data was analysed as a fold change of the value seen for the control group, C1. Fold changes were grouped into cases and controls (a) or displayed individually (b). Red represents high expression, while blue shows low expression levels.

4.4.12 IFNγ and GM-CSF expression is NK cell dependent

To identify the cytokines and chemokines that were released in an NK cell dependent manner, and therefore potentially as a consequence of the increased NK cell activation seen with AS-associated ERAP1 allotype combinations. The NK cell population was deleted using magnetic bead separation (MACS Miltenyl) prior to incubation with HeLa ERAP1$^{-/-}$ transfected target cells for use in the Luminex assay (2.11.2 NK cell depletion).

IFNγ expression was strongly dependent on the NK cell population, with NK cell depletion leading to a highly significant decrease in IFNγ with control ERAP1 pairs ($p<0.0001$) (**Figure 4.13a**). As IFNγ expression was already considerably lower with case ERAP1 pairs (**Figure 4.10b**), there was no significant difference in the NK depleted condition despite a clear reduction. GM-CSF expression was also critically dependent on NK cells with a significant reduction in production from both groups: $p<0.0001$ with the control group and $p<0.001$ with the case group (**Figure 4.13b**).

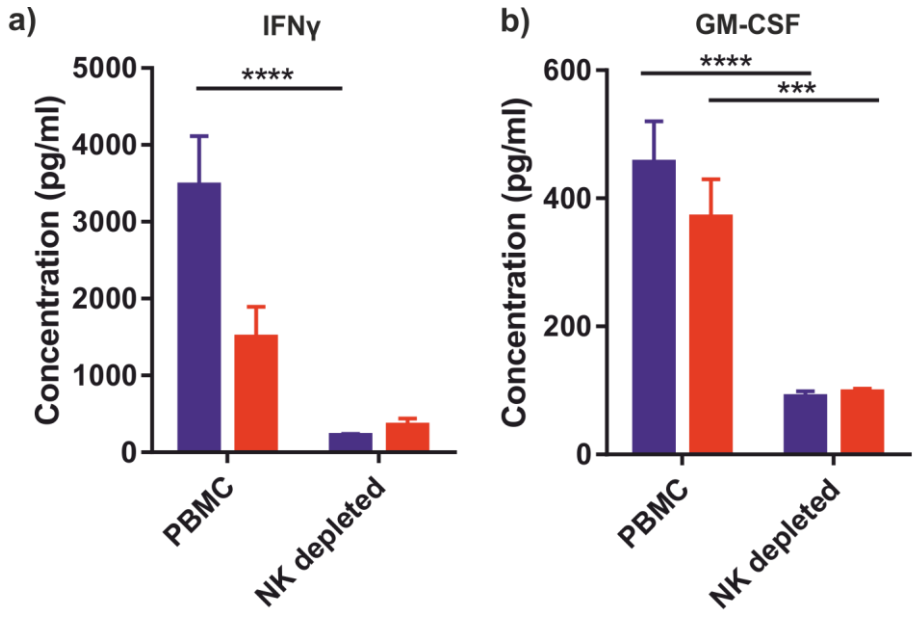

Figure 4.13: IFNγ and GM-CSF release is dependent on NK cells

HeLa ERAP1$^{-/-}$ cells were transiently transfected with HLA-B*2705 and an ERAP1 allotype combination, either AS-associated (red) or control (blue), for 24 hours before being combined with IL-15 stimulated PBMCs or NK-cell depleted PBMCs. The supernatant was collected after 24 hours and analysed in a Luminex assay. (a) IFNγ production was significantly reduced in control transfected cells following NK cell depletion ($p<0.0001$). No significant difference was seen in cases but there was a reduction in IFNγ production. (b) GM-CSF production was also significantly reduced following NK cell depletion with both control ERAP1 pairs ($p<0.0001$) and AS-associated pairs ($p<0.001$). Data analysed by one-way ANOVA and Tukey's multiple comparisons test.

4.4.13 Increased release of IL-1a and CCL5 by control transfected cells was NK cell dependent

Additional analytes reduced by NK cell depletion were IL-1α and CCL5 (**Figure 4.14**). IL-1α levels were reduced in the control group following NK cell depletion ($p<0.05$), while no changes were seen in the case group with NK cell depletion although a slight increase was visible following depletion (**Figure 4.14a**). CCL5 expression was also significantly reduced in the control group following NK cell depletion ($p<0.05$) with no changes in the case group (**Figure 4.14b**). These results suggest that inhibition of NK cells seen with control ERAP1 allotype combinations results in the release of ICAM-1, IL-1α and CCL5 into the milieu.

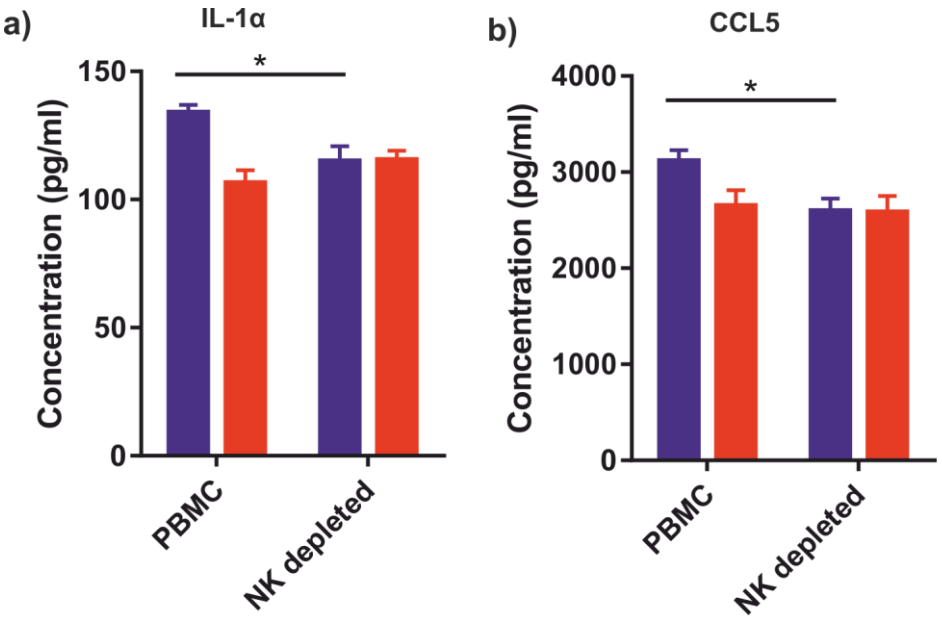

Figure 4.14: IL-1α and CCL5 expression is reduced in the absence of NK cells

HeLa ERAP1$^{-/-}$ cells were transiently transfected with HLA-B*2705 and an ERAP1 allotype combination, either AS-associated (red) or control (blue), for 24 hours before being combined with IL-15 stimulated PBMCs or NK cell depleted PBMCs. The supernatant was collected after 24 hours and analysed in a Luminex assay. (a) IL-1α levels were also significantly reduced in response to control ERAP1 pairs ($p<0.05$), but again no significant changes were seen with AS-associated pairs despite a slight increase in IL-1α levels. (b) CCL5 levels were slightly, but significantly, reduced in the absence of NK cells with control ERAP1 pairs. No differences were seen in the presence of case ERAP1 pairs. Data analysed by one-way ANOVA and Tukey's multiple comparisons test.

4.4.14 TNFα, IL-10 and MIP-1β levels were increased following NK cell depletion

While the previously shown analytes were decreased following NK cell depletion, TNFα, IL-10 and MIP-1β levels were increased (**Figure 4.15**). TNFα levels were significantly increased with control ERAP1 pairs following NK cell depletion ($p<0.01$), but no difference was seen in the AS-associated group (**Figure 4.15a**). MIP-1β levels were increased in the control group following NK cell depletion ($p<0.05$), while no differences were seen with the case group (**Figure 4.15b**). Levels of the anti-inflammatory cytokine IL-10 were significantly increased in the case ERAP1 group following NK cell depletion ($p<0.001$) (**Figure 4.15c**). There was no significant difference in expression of IL-10 in the control group following NK cell depletion, despite a small increase.

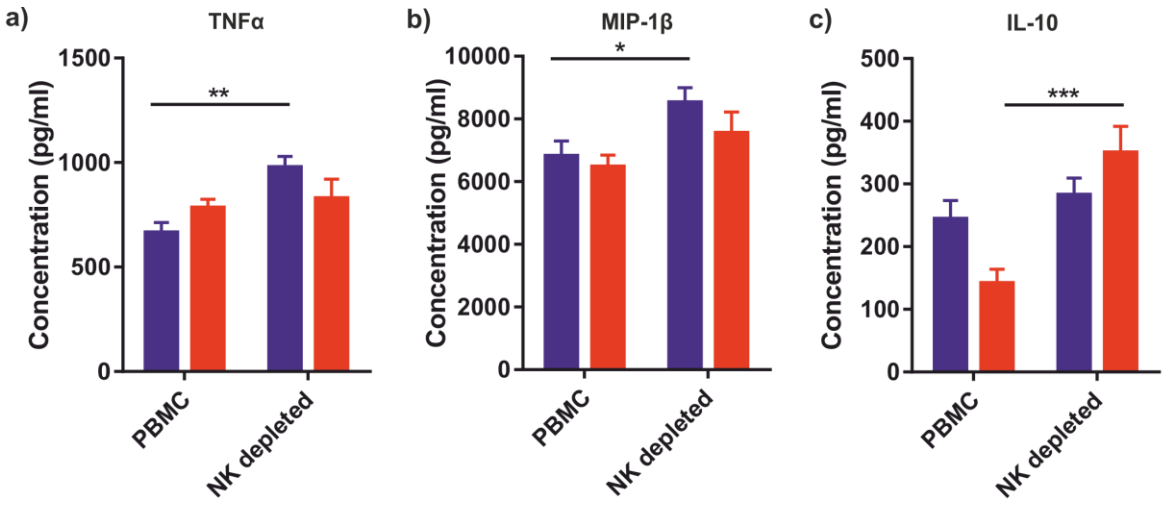

Figure 4.15: TNFα, MIP-1β and IL-10 levels were increased following NK cell depletion

HeLa ERAP1$^{-/-}$ cells were transiently transfected with HLA-B*2705 and an ERAP1 allotype combination, either AS-associated (red) or control (blue), for 24 hours before being combined with IL-15 stimulated PBMCs or NK cell depleted PBMCs. The supernatant was collected after 24 hours and analysed in a Luminex assay. (a) In the presence of control ERAP1 pairs, TNFα expression was increased following NK cell depletion ($p<0.01$), while no differences were seen in the presence of AS-associated pairs. (b) MIP-1β expression was increased with both control and case ERAP1 pairs, but this was only significant with control ERAP1 pairs ($p<0.05$). (c) IL-10 levels were increased in the presence of case pairs ($p<0.001$), while no significant differences were seen with control pairs. Data analysed by one-way ANOVA and Tukey's multiple comparisons test.

4.4.15 Blocking of pHLA-B27 complexes increases TNFα, MIP-1β and IL-1a release

To determine whether cytokine release was dependent on pHLA-B27 complexes, these complexes were blocked using the ME.1 HLA-B27 specific antibody. Following ME.1 block TNFα levels were significantly increased in both groups ($p<0.0001$) (**Figure 4.16a**). MIP-1β levels were also highly significantly increased following ME.1 block ($p<0.0001$) (**Figure 4.16b**). The level of IL-1α was significantly increased in the case ERAP1 group following ME.1 block to the same level as seen consistently with the control group ($p<0.0001$) in both no blocking and ME.1 blocking conditions (**Figure 4.16c**). These results suggest that pB27 complexes can strongly inhibit TNFα and MIP-1β expression, most likely in an NK cell independent manner, as NK cell depletion did not increase the level of these factors to the same level as seen with ME.1 block. While changes in IL-1α expression is likely to be attributable to NK cells as only differences in the case group were seen.

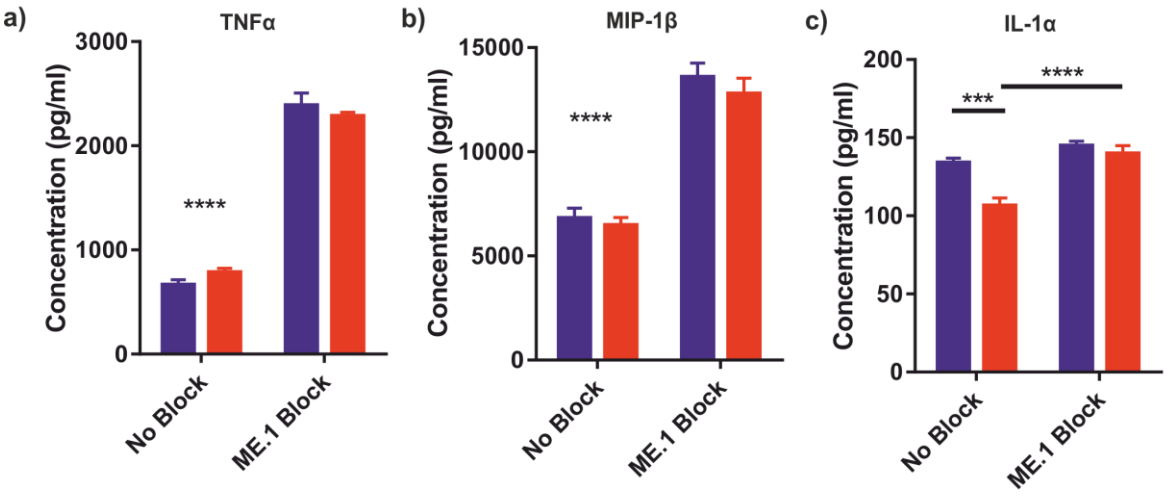

Figure 4.16: ME.1 blocking increases TNFα, MIP-1β and IL-1α expression

HeLa ERAP1$^{-/-}$ cells were transiently transfected with HLA-B*2705 and an ERAP1 allotype combination, either AS-associated (red) or control (blue), for 24 hours before being blocked with ME.1 blocking antibody for one hour combined with IL-15 stimulated PBMCs. The supernatant was collected after 24 hours and analysed in a Luminex assay. (a) TNFα expression was significantly increased in both groups following ME.1 blocking of pB27 complexes ($p<0.0001$). (b) MIP-1β expression was significantly increased in both groups following ME.1 blocking ($p<0.0001$). (c) ME.1 block increased IL-1α expression in the presence of AS-associated ERAP1 pairs ($p<0.0001$) to the same level as was seen with control pairs. Data analysed by one-way ANOVA and Tukey's multiple comparisons test.

4.4.16 Blocking of pHLA-B27 complexes decreases the release of IL-10, IFNγ, GM-CSF and GROα

In contrast, decreases in the levels of IL-10, IFNγ, GM-CSF and GROα were seen following ME.1 block of pHLA-B27 complexes (**Figure 4.17**). ME.1 block reduced IFNγ levels to the same as those seen with NK cell depletion in both groups ($p<0.0001$ for controls) (**Figure 4.17a**). IL-10 levels were significantly reduced in the ERAP1 control group following ME.1 block ($p<0.0001$) (**Figure 4.17b**). No significant difference was seen in the case group due to the already low level of expression seen in this group. GM-CSF levels were reduced in both groups following ME.1, but this was only significant in the control group ($p<0.05$) (**Figure 4.17c**). In contrast to IFNγ, this reduction was not as large as that seen with NK cell depletion. GROα was also reduced following ME.1 block but this was only significant in the control group ($p<0.05$) due to the already lower expression seen with cases in the absence of any blocking antibodies (**Figure 4.17d**).

4.4.17 Blocking FHC increases expression of TNFα, IL-10, MIP-1β, CCL5 and IL-1a

Blocking with HC10 in the previous LAMP1 assays provided some interesting changes in NK cell activation (**Figure 4.7**) and so it was also included here to determine whether blocking FHC or $B27_2$ complexes affected cytokine release. HC10 blocking significantly increased release of TNFα, IL-10, MIP-1β, CCL5 and IL-1α (**Figure 4.18**). TNFα was significantly increased following HC10 block in both groups ($p<0.0001$), with case ERAP1 pairs inducing slightly increased levels than control ERAP1 pairs (**Figure 4.18a**). HC10 blocking increased IL-10 production in the presence of case ERAP1 pairs to the same level as controls ($p<0.01$) (**Figure 4.18b**). The control group did not significantly change despite a small increase in IL-10 production. MIP-1β expression was significantly increased in both groups ($p<0.01$ for controls, $p<0.05$ for cases) with both groups expressing the same levels following HC10 block (**Figure 4.18c**). CCL5 expression was significantly increased following HC10 block in the cases group ($p<0.01$) while no difference was seen in the control group (**Figure 4.18d**). Finally, IL-1α expression was significantly increased in both groups following HC10 block ($p<0.01$ for controls, $p<0.0001$ for cases), with cases showing slightly higher levels of expression than controls following blocking (**Figure 4.18e**).

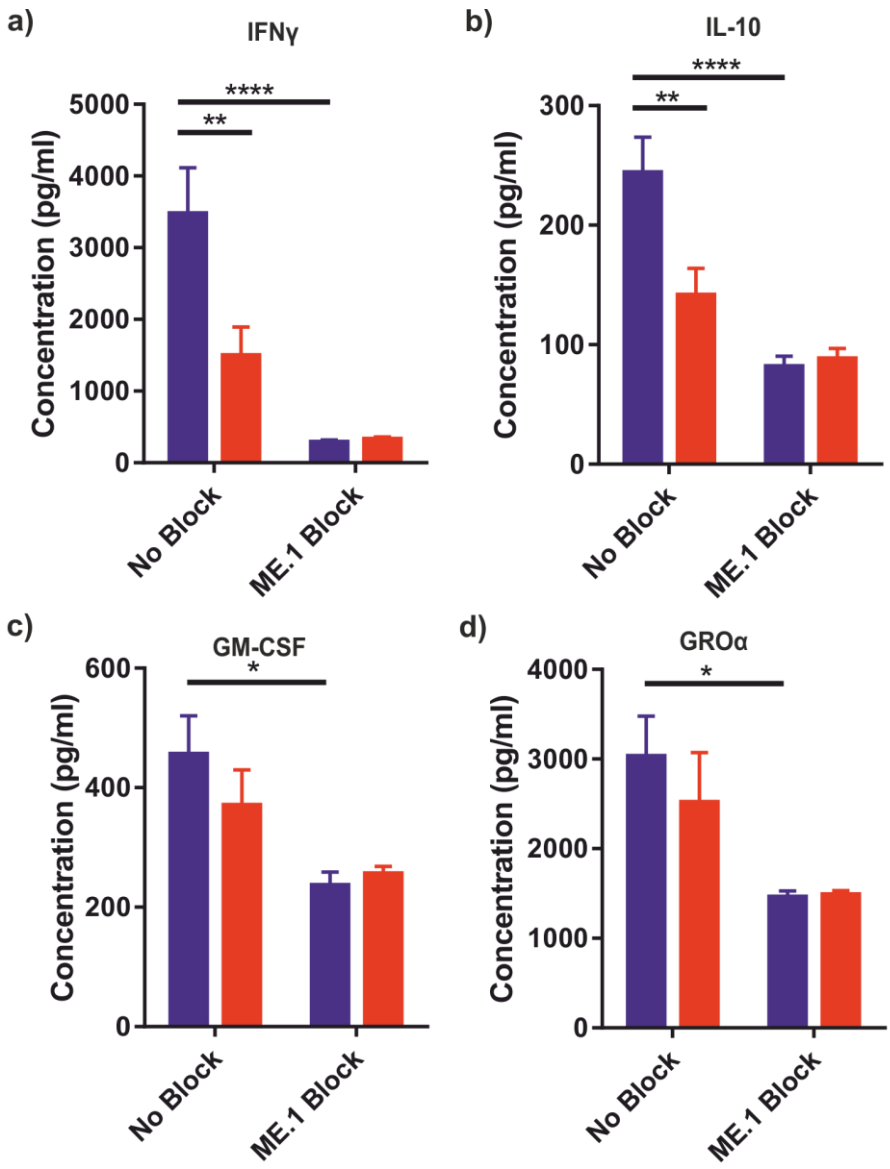

Figure 4.17: ME.1 block decreases IFNγ, IL-10, GM-CSF and GROα levels

HeLa ERAP1$^{-/-}$ cells were transiently transfected with HLA-B*2705 and an ERAP1 allotype combination, either AS-associated (red) or control (blue), for 24 hours before being blocked with ME.1 blocking antibody for one hour combined with IL-15 stimulated PBMCs. The supernatant was collected after 24 hours and analysed in a Luminex assay. (a) IFNγ secretion was also significantly decreased in the presence of control ERAP1 pairs ($p<0.0001$) with ME.1 block. A reduction was seen with AS-associated pairs following ME.1 block but this was not significant. (b) IL-10 levels were significantly reduced following ME.1 block in the presence of control ERAP1 pairs ($p<0.0001$). A reduction was also seen in the presence of case ERAP1 pairs, but this difference was not significant compared to the absence of blocking antibody. (c) ME.1 block induced a significant reduction in GM-CSF levels with control ERAP1 pairs ($p<0.05$), but no significant difference was seen in the presence of AS-associated ERAP1 pairs following ME.1 block, despite a slight decrease. (d) GROα levels were significantly decreased following ME.1 block in the presence of control ERAP1 pairs ($p<0.05$). There was a slight reduction in the presence of case associated pairs following ME.1 block, but this was not significant. Data analysed by one-way ANOVA and Tukey's multiple comparisons test.

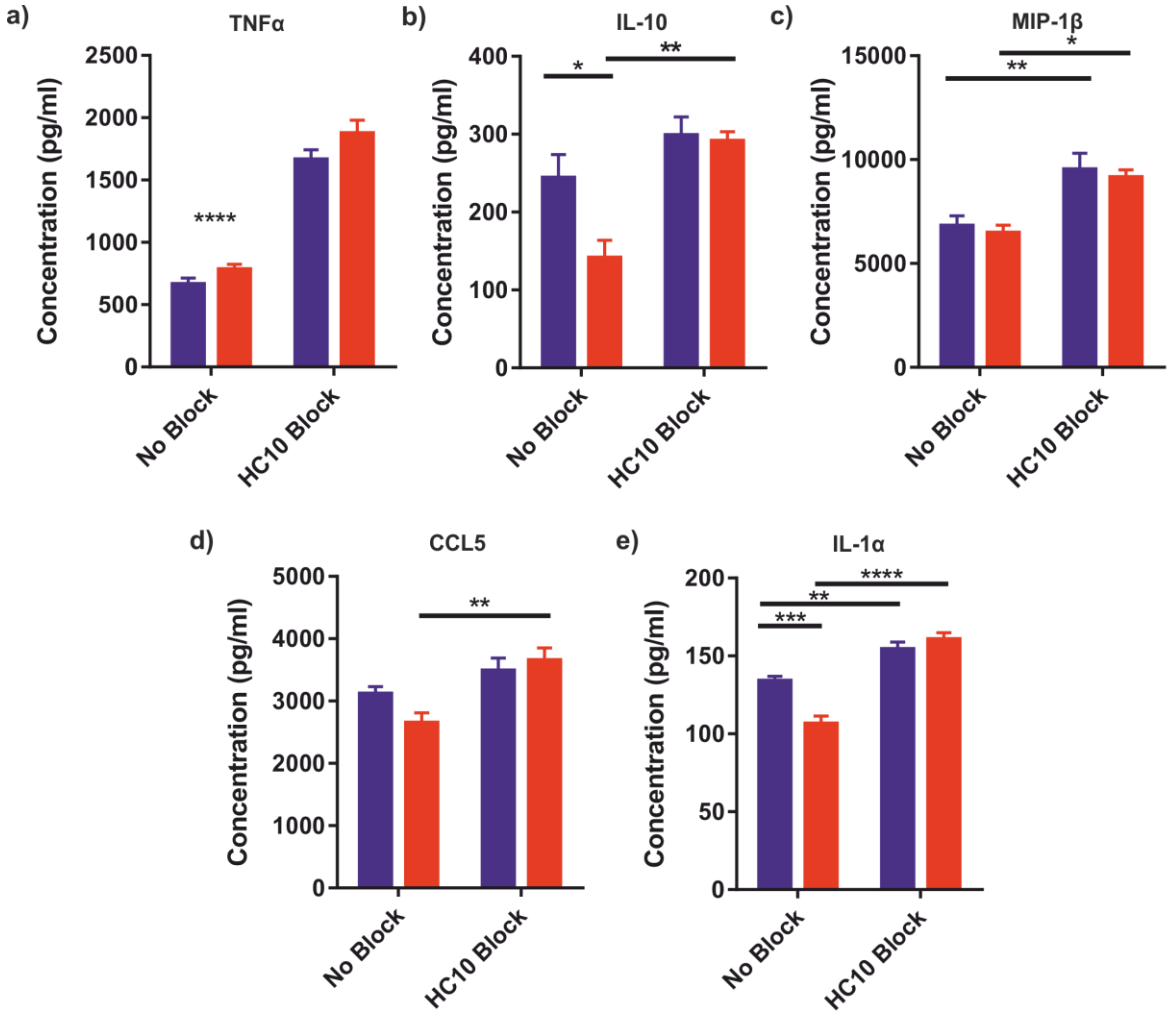

Figure 4.18: HC10 block increases expression of TNFα, IL-10, MIP-1β, CCL5 and IL-1α

HeLa ERAP1$^{-/-}$ cells were transiently transfected with HLA-B*2705 and an ERAP1 allotype combination, either AS-associated (red) or control (blue), for 24 hours before being blocked with HC10 blocking antibody for one hour combined with IL-15 stimulated PBMCs. The supernatant was collected after 24 hours and analysed in a Luminex assay. (a) TNFα expression was significantly increased following HC10 block with both ERAP1 groups ($p<0.0001$). (b) IL-10 expression was significantly increased in AS-associated pairs following HC10 block ($p<0.01$). There was a slight increase with control ERAP1 pairs, but this was not significant, (c) HC10 blocking of FHC increased MIP-1β expression in both groups: $p<0.01$ for control ERAP1 pairs and $p<0.05$ for AS-associated ERAP1 pairs. (d) HC10 blocking slightly increased CCL5 expression in both groups but this was only significant in the case ERAP1 pair group ($p<0.01$). (e) IL-1α expression was increased in both groups following HC10 blocking: $p<0.01$ for control and $p<0.0001$ for case ERAP1 pairs. Data analysed by one-way ANOVA and Tukey's multiple comparisons test.

4.5 Discussion

The highly polymorphic protein ERAP1 is genetically linked with AS disease (4, 11), with clear separation between AS-associated ERAP1 allotype combinations and healthy controls (6). Although this association has been clearly described, the way that ERAP1 polymorphisms lead to, or are associated with, AS disease is still unknown. Previous work has shown that ERAP1 variants can alter the expression of pB27 complexes on the cell surface, with AS-associated pairs inducing less pB27 complex expression at the cell surface (6). How ERAP1 polymorphic variants differentially trim peptides for presentation to $CD8^+$ T cells and the T cell response to these variants has been previously determined (6, 29), but as AS is not thought to be a $CD8^+$ T cell driven disease (141) other cellular causes of the disease need to be investigated. Following reports that NK cells may be important in AS disease (86), the NK cell response to peptide repertoires generated by ERAP1 variants was examined.

In this work we have shown that AS-associated ERAP1 allotype combinations lead to less FHC structures on the cell surface and this reduction induces greater NK cell activation. The luminex data shown here begins to paint a picture of how this increased NK cell activation alters the chemokine and cytokine expression of the PBMC population. AS disease is characterised by chronic inflammation, which is supported by the data shown here showing increased release of pro-inflammatory factors and decreased released of anti-inflammatory IL-10 following transfection of HeLa $ERAP1^{-/-}$ B*2705 target cells. This work suggests that, as well as providing a potential diagnostic method for AS, polymorphisms in ERAP1 have a functional consequence in contributing to the inflammatory environment seen in AS patients through NK cells. However, further work to fully elucidate the role of NK cells in AS disease and to confirm the data seen here is needed.

Individual ERAP1 allotypes identified from both AS patients and healthy controls, and distributed between cases and controls (6) did not significantly alter the pB27 cell surface expression or FHC expression. In addition, there were no significant differences in NK cell activation with any allotype in every NK cell population, apart from $KIR3DL1/2^-$ NK cells. In this population, *013 significantly increased NK cell activation compared to allotypes *001, *002, *003 and *004. This was unexpected based on the lack of results in the other populations, particularly the whole NK cell population, which showed no increase in NK cell activation. However, this may reflect the fact

that in the KIR3DL2^{+} NK cell population allotype *013 showed one of the lowest NK cell activation states creating a balanced level of activation in the whole NK cell population. This allotype may also be altering the repertoire of peptides at the cell surface significantly to prevent engagement of another KIR, such as KIR2DL2/3, with the natural MHC I present on HeLa cells. Looking at the individual allotypes was important as it confirmed that minimal differences are seen with individual allotypes. Adding to the argument proposed by Reeves *et al*, that ERAP1 polymorphisms must be considered as the allotype combination present within an individual, rather than looking at individual allotypes (6).

Examination of ERAP1 allotype combinations previously identified from controls (C1-8) and cases (A1-7) showed no significant differences in pB27 cell surface expression. However, C1, A1 and A2 showed higher cell surface expression of pB27 complexes compared to other allotype combinations. In the grouped analysis, AS-associated cases showed decreased FHC expression compared to both HeLa ERAP1$^{-/-}$ B*2705 cells and control-associated allotype pairs. This reduction was reflected when the groups were separated into individual pairs with all AS-associated pairs showing less FHC expression than controls. In particular, C1 showed the highest expression of FHC and A6 showed the lowest expression. Minimal differences in FHC expression were seen with C4, C5 and C7 allotype combinations compared to HeLa ERAP1$^{-/-}$ B*2705 cells. A1, A4 and A5 showed the highest expression of FHC, but this was still lower than that of HeLa ERAP1$^{-/-}$ B*2705 cells. This reduction in FHC in case-associated allotype combinations, translated into an increase in NK cell activation in the whole NK cell and KIR3DL1^{+} populations. This suggests that FHC engage KIR3DL1 in an inhibitory fashion, and loss of some FHC expression prevented engagement of this inhibitory KIR.

A2 and A5 showed the lowest NK cell activation. In the case of A5 this corresponds with a higher expression of FHC compared to other AS-associated allotypes, however, A2 shows one of the lowest levels of FHC and low NK cell activation. Perhaps the repertoire of peptides produced by the A2 allotype combination is a good repertoire with a lot of peptides that can engage KIR3DL1; this idea is supported by high pB27 expression with this allotype combination. This could lead to more KIR3DL1 engagement through pB27 complexes, which can compensate for the loss of FHC engagement.

We do not have access to a $B27_2$-specific antibody, but the antibody used to identify FHC (HC10) is thought to recognise these homodimer structures as well (13). Therefore, it is expected

that AS-associated ERAP1 allotype combinations also create a reduction in homodimer expression, which would lead to a reduction in KIR3DL2 engagement and potentially NK cell activation. However, no differences in KIR3DL2$^+$ NK cell activation were seen with any allotype, despite some increase with the AS-associated pairs A1, A2, A3 and A4. The increases seen with these pairs were not consistent across experiments resulting in non-significant differences when analysed, suggesting that this increase could be the result of experimental variation.

The KIR3DL1/2$^+$ population appears to respond to target cells in a much more exaggerated manner with a higher general activation level (i.e. higher LAMP1$^+$ population) than in other NK cell populations. There was some variability in this activation with different ERAP1 allotype combinations, with C2, C3, A1, A3, A4 and A6 showing the highest level of activation while C5, A2 and A7 showed the lowest level. There was a lot of variability in these activation levels across repeats, particularly with AS-associated allotype combinations. When the results were grouped together there was a slight increase in NK cell activation with the case group. These results suggest that the presence of both of these inhibitory KIRs overcomes the loss of engagement seen in the KIR3DL1$^+$ population to prevent a significant increase in NK cell activation with case ERAP1 pairs in this population.

Most surprisingly the large increase in NK cell activation seen with cases in the KIR3DL1$^+$ population was also repeated in the KIR3DL1/2$^-$ NK cell population in both the grouped data and the individual pair data. This was surprising as the results up until this point supported the idea that the loss in FHC expression in cases led to a reduction in KIR3DL1 engagement and therefore NK cell activation. Potentially this population may include some KIR3DL1$^+$ and/or KIR3DL2$^+$ NK cells which were not stained. This idea is supported by the fact that when the anti-KIR3DL1 (DX9) antibody was titrated for the blocking experiments some slight increases in the percentage of KIR3DL1$^+$ cells could be seen. However, these increases were so small that, on balance, the use of extra antibody to involve the additional 1-2% of NK cells seemed unnecessary. The number of KIR3DL2$^+$ NK cells may also be under-represented as this antibody was also titrated for potential use in blocking experiments and was found to stain an increasing percentage of NK cells with increasing concentration even at a 1:1 ratio. At this concentration it was decided that it was not feasible to use this antibody for blocking experiments. This shows that the affinity of these KIR antibodies is potentially quite low and so we cannot rule out the possibility that this KIR3DL1/2$^-$ population does not express these KIRs.

Alternatively, as ERAP1 polymorphisms will alter the whole peptide repertoire, and not just those bound to HLA-B27, peptides bound to the natural MHC I on the HeLa cells could alter the

engagement of additional KIRs. There are conflicting reports for the HLA expression of HeLa cells, but they have been serologically typed as HLA-A3, -A28, -Bw15 and –Bw35 expressing (128) and genetically typed as HLA-A68 (a subtype of A28), -B75 (a subtype of B15) and negative for B35 (129). HLA-A3 engages KIR3DL2 in a weaker interaction than that seen with $B27_2$ (90). None of the HLA-B alleles potentially expressed by HeLa cells are part of the HLA-Bw4 group, meaning that they will not engage KIR3DL1 and their KIR ligand is unknown. No HLA-C expression on HeLa cells has been confirmed so the engagement of KIR2DL1/2/3 cannot be confirmed.

HeLa cells do express the ligands for NKG2D (137). NKG2D is an activating NCR that engages the non-classical MHC molecules, MICA and MICB, to induce cytotoxicity by NK cells. MIC molecules bind to induced self-proteins that are usually absent or expressed at low levels on the cell surface, but in the context of infection, transformation, senescence or stress these complexes can be dramatically increased on the cell surface to increase NKG2D engagement and NK cell activation. In fact, NKG2D engagement is capable of overriding signals provided by inhibitory receptors (142). Potentially, addition of AS-associated ERAP1 allotype pairs increases cellular stress inducing increased expression of non-classical MHC I molecules and NKG2D engagement (143). It has previously been suggested that AS-associated ERAP1 polymorphisms can increase cellular stress and UPR, leading to the UPR theory of AS pathogenesis (138). However, this theory was recently put into question by Kenna *et al*, who showed no increase in ER stress with the AS-associated SNP rs30187 (K528R) ERAP1 polymorphism (144).

The use of rhKIR3DL1 showed the same issues as was previously seen in Chapter 3, with no significant differences visible, potentially due to a limit on the level of HLA-B27 expression on the cell surface. However, with the exception of C5, C6 and A5, control ERAP1 allotype combinations showed higher and case ERAP1 allotype combinations showed lower rhKIR3DL1 binding. This higher binding of A5 to rhKIR3DL1 corresponds with the previous results showing higher pB27 expression, the highest FHC of all the AS-associated pairs and lower NK cell activation. The reduction of rhKIR3DL1 binding to C5 and C6 is harder to explain. There were no obvious differences in pB27 expression, but a slight increase in FHC expression was seen with C6. This increase in FHC expression would be expected to decrease NK cell activation, but in fact C6 consistently showed the highest level of NK cell activation of all the control ERAP1 allotype combinations. This ties in more with the reduction in rhKIR3DL1 binding, suggesting that the C6 allotype combination may not produce a peptide repertoire optimised for KIR3DL1 engagement. However, the C5 allotype combination showed none of these characteristics and so the reduction

in rhKIR3DL1 binding remains unexplained. The fact that this assay was only repeated twice means that these results cannot be fully trusted and this experiment would need to be repeated at least once more to improve the power of the experiment.

Blocking experiments were used to confirm the interactions important for the increase in activation of NK cells in the presence of AS-associated ERAP1. Blocking KIR3DL1 with the DX9 antibody resulted in activation across all groups showing that engagement of this KIR must occur by all groups, which is to be expected in the presence of HLA-B27. Slight increases in NK cell activation were seen in the KIR3DL2^{+} NK cell population but this was variable across repeats and may just represent experimental variation.

Surprisingly, despite slight increases there were no significant changes in NK cell activation following DX9 blocking in the KIR3DL1/2^{+} population. As mentioned previously, this population of NK cells usually show higher NK cell activation than any other population. Perhaps this increased activation state shows a lack of, or minimal, KIR3DL1 engagement and so blocking of this receptor has little effect on activation. Even more surprisingly, the largest effect of DX9 blocking was seen in the KIR3DL1/2^{-} NK cell population with DX9 blocking inducing at least two-fold increase in NK cell activation. This activation was significantly smaller in the case group compared to the control group and may be the result of some KIR3DL1^{+} NK cells that were not stained as suggested before, but this is more unlikely in this experiment as the NK cells are blocked with DX9 antibody for one hour before the LAMP1 assay. The use of control IgG for these blocking experiments was not possible because these antibodies can induce ADCC in NK cells (145). Potentially, NK cells without KIR3DL1 expression for the DX9 antibody to bind to could be binding to CD16 via the Fc portion to induce ADCC, leading to the large increase in NK cell activation.

Blocking with the pB27 binding antibody ME.1 increased NK cell activation in the HeLa ERAP1$^{-/-}$ B*2705 cells and control groups to the same raised level as was seen with cases; a result seen in all NK cell populations. This suggests that pB27 complexes in control groups are involved in the inhibition of NK cells seen with control ERAP1 allotype combinations. This is in line with the prediction that AS-associated ERAP1 allotype combinations will produce a peptide repertoire with a lower affinity for MHC I than control ERAP1 allotype combinations. Blocking of FHC with the HC10 antibody further increased NK cell activation in all groups above the levels seen with ME.1 blocking in the whole NK cell population. NK cell activation in the presence of case ERAP1 allotypes was additionally increased compared to the other cell lines. This same pattern was seen in every NK cell population; although in the KIR3DL1/2^{+} population HC10 blocking induced nearly

two-fold increase in NK cell activation with cases. This data suggests that FHC interaction with KIR3DL1 is necessary for inhibition and loss of this interaction can increase NK cell activation.

Taken together this blocking data supports the idea that control ERAP1 allotype combinations engage KIR3DL1 through a good peptide repertoire bound to HLA-B27 and HLA-B27 FHC. This inhibitory interaction is reduced with AS-associated ERAP1 allotypes due to a reduction in high affinity pB27 complexes, as shown by the increase of the control group to the same level as cases following ME1 block. FHC engagement of NK cells also seems to be important, suggesting that the reduction with case ERAP1 pairs may have a strong effect on NK cell activation.

One limitation of these blocking experiments is the fact that not all 15 allotype combinations were included in the experiments. Instead only two control allotype combinations, C2 and C3, and two case allotype combinations, A2 and A6, were chosen. C3 was chosen because it is homogeneous for the wild-type allotype *002, while A2 was chosen because it is homogeneous for the strongly AS-associated hypo-active *001 (5SNP) allotype. C2 was chosen as it induced a median level of NK cell activation and A6 was chosen as it represented a higher level of NK cell activation, which, along with A2, gave a median level of NK cell activation that was still lower than controls. The inclusion of only two allotype pairs as opposed to seven or eight, will obviously limit the conclusions we can make from these experiments, but the data shown here should be enough to determine the interactions important for the increased NK cell activation seen with AS-associated ERAP1 allotypes.

Table 4:4: Effect of NK cell depletion, ME.1 or HC10 block on Luminex analytes

Analyte	NK cell depletion	ME.1 Block	HC10 Block
TNFα	+	+	+
IFNγ	-	-	n.s
IL-10	+	-	+
MIP-1β	+	+	+
IL-1α	-	+	+
CCL5	-	n.s	+
GM-CSF	-	-	n.s
GROα	n.s	-	n.s

In the Luminex multiplex assay, higher levels of IL-10, IFNγ, CCL5 and IL-1α were seen with control ERAP1 pairs suggesting that, in this context, these cytokines and chemokines may be protective. TNFα expression was higher in AS-associated ERAP1 pairs, in line with previous studies showing high TNFα levels in AS patients (136, 137, 139) and the success of α-TNFα treatment for AS for several years (9, 10). The results from the Luminex analysis allow us to make some interesting conclusions, however as each cytokine is released from multiple immune cells further investigation would be required to fully characterise the cytokine profile seen in the presence of AS-associated ERAP1 allotype combinations (**Figure 4.19**).

Analysis of the results seen with NK cell depletion, ME.1 block and HC10 block must be combined with these initial results in order to determine whether the differences in NK cell activation seen with ERAP1 allotype combinations is responsible for the changes seen in the cytokine profile. A summary of how these experimental conditions altered each cytokine can be seen in **Table 4:4**.

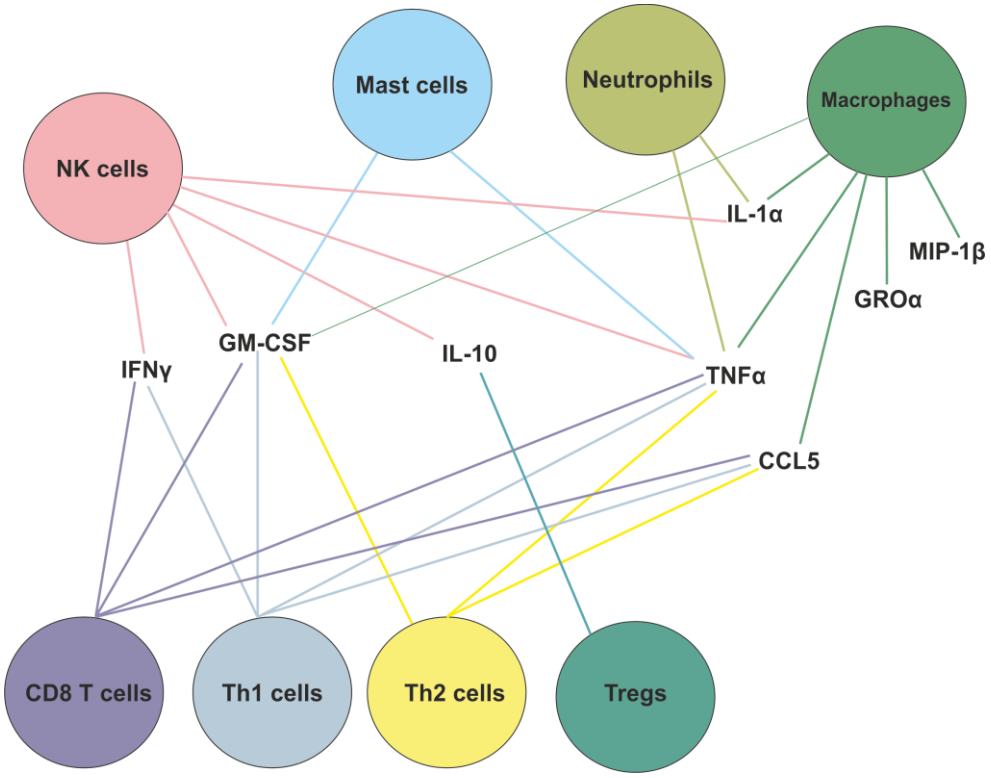

Figure 4.19: Release of cytokines of interest from immune cells

All cytokines investigated in the Luminex assay can be secreted from a range of immune cells. Coloured lines connected to the coloured cells represent expression of the cytokine by that cell line.

Taken altogether the Luminex and the NK cell activation results suggests how the many elements previously associated with AS tie in together. AS-associated ERAP1 allotype combinations (6) induce increased NK cell activation compared to control ERAP1 allotype combinations as a result of a reduction of FHC structures on the cell surface. This increased NK cell activation potentially leads to an environment with higher TNFα and lower IFNγ, CCL5 and IL-10 levels.

There was a trend for higher TNFα expression following case ERAP1 transfection although this was variable across conditions. These differences with various control and case allotype combinations may provide an explanation for the conflicting data showing an increase in TNFα in AS patients (146, 147). If the patients expressed an ERAP1 allotype combination that induced

TNFα at a level only minimally different to control ERAP1 pairs, i.e. A2, A5 or A6, or the control group expressed the allotype combinations C3, C5 or C7, the differences in TNFα expression seen with this cohort would be minimal. In addition, these differences in TNFα production may provide some insight into why anti-TNFα treatment is only successful in ~50% of AS patients (9); if a patient does not exhibit higher than normal TNFα levels, treatment may have little effect and another mechanism of disease may be more dominant in these cases.

A role for IFNγ in anti-inflammatory mechanisms has been found, with IFNγ suppressing IL-1 production and increasing production of IL-1Rα, which sequesters IL-1 to prevent IL-1 signalling (148). In particular, IL-1β production by macrophages was inhibited by IFNγ in the synovial fluid of RA patients (149). In addition, IFNγ-dependent induction of apoptosis may be a mechanism of limiting inflammation (150). It has also been found that IFNγ-producing NK cells have lower cytotoxic function than NK cells that produce low levels of IFNγ (151), and in a study by Scrivo *et al* this reduction in IFNγ production was seen with NK cells from AS patients but not healthy controls (91). This anti-inflammatory role for IFNγ helps to explain the Luminex results, which showed that IFNγ levels were higher in the presence of control associated ERAP1 allotype combinations compared to AS-associated ERAP1.

CCL5 levels were slightly higher in the presence of control ERAP1 allotype combinations compared to case allotype combinations, with this difference being neutralised by NK cell depletion suggesting that this population is necessary for this increased CCL5 expression. ME.1 block had no effect on expression levels but HC10 block induced increased CCL5 expression to slightly higher levels in both groups than previously seen controls. These results together suggest that FHC induce CCL5 production as a result of NK cell interaction.

IL-10 is the only anti-inflammatory cytokine detected in the Luminex assay. While IL-10 has been conclusively shown to suppress TNFα and IL-1 production (152), key cytokines thought to be important in the pathogenesis of AS, no conclusive link between these three cytokines and disease have been confirmed with conflicting results published. Vazquez *et al* showed that AS patients had higher levels of IL-1β, with no change in TNFα and IL-10 levels between cases and controls (147). Conversely, Chou *et al* have previously found increased TNFα and IL-1β expression and decreased IL-10 expression in AS cases compared to controls (146). The results seen here are more consistent with those seen by Chou *et al*, with increased TNFα and decreased IL-10 levels with AS-associated ERAP1 allotype combinations compared to controls, however, IL-1β was not investigated in this study.

This data potentially ties in with previously published data suggesting a role for Th17 cells in AS pathogenesis (89, 153). Th17 cells are a subset of $CD4^+$ T helper cells induced by IL-1, IL-6 and IL-23 to produce IL-17, IL-23, IL-1 and IL-6. Their differentiation is inhibited by IL-12 and IFNγ (94). Potentially the cytokines that are altered in the presence of AS-associated ERAP1 allotype combinations are either generated as a result of Th17 cell differentiation or induce their differentiation (**Figure 4.20**). In support of this, IL-6 levels were found to be very high in the Luminex assay, but no validation of this result could be run to confirm. Previously published data for IL-1 and IL-6 showed an upregulation in AS patients (136, 137, 139). These cytokines induce Th17 cell differentiation under the proviso that IFNγ levels are low (94), a condition which was found with our AS-associated ERAP1 allotype combinations.

In addition, Th17 cells inhibit CCL5 and IL-10 expression (94, 154), both of which were reduced in AS-cases compared to controls. In addition, Th17 cells have previously been shown to reduce the levels of CCL5 and CCL2 (MCP-1) within the context of Autoimmune Anti-Myeloperoxidase Glomerulonephritis (154). Again the data for IL-1Rα was unavailable for the Luminex assay but potentially an increase in this receptor would be expected in the control group due to the high levels of IFNγ, an inducer of IL-1Rα expression. IL-1Rα reduces the effects of IL-1 by sequestering it and preventing downstream signalling (148); thus providing another mechanism for the prevention of Th17 differentiation in healthy people. Without the IL-1Rα data it is impossible to tell but the increase in IL-1 in controls may be balanced with an increase in IL-1Rα, which would cancel out any effect of IL-1.

In the AS-associated condition the net result of the potential changes in cytokines is osteoclastogenesis, the process by which osteoclasts are formed. Osteoclasts are important in the breaking down of bone tissues, but they have also been implicated in the formation of new bone (155). A hallmark of AS disease is the formation of new bone between the vertebrae (2). TNFα, along with IL-17-induced IL-1, has been shown to induce osteoclastogenesis (156). Osteoclastogenesis has been shown to be more common in the PBMCs of AS patients compared to healthy controls (157), potentially as a result of cytokine levels in the milieu. In contrast, IFNγ and IL-10 can inhibit osteoclastogenesis (158, 159), potentially showing that the high IFNγ and IL-10 levels seen in controls are protective against bone destruction. Together this data presents a mechanism by which ERAP1-induced NK cell activation can lead to a pro-inflammatory response, differentiation of Th17 cells and osteoclastogenesis; all of which are potentially key steps in the pathogenesis of AS.

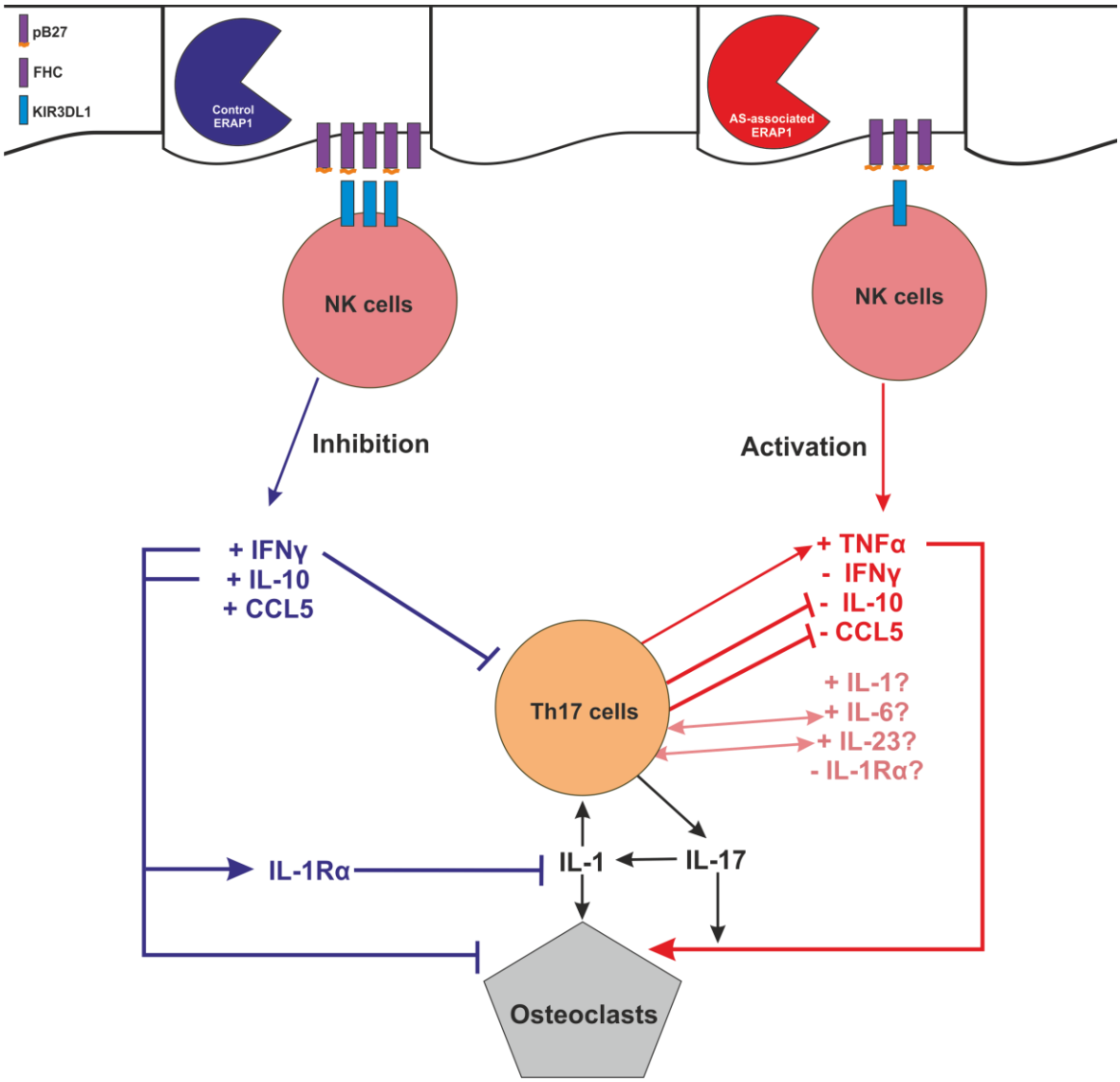

Figure 4.20: Mechanism of the link between ERAP, Th17 cells and osteoclastogenesis

Based on the luminex data and previously published studies, this mechanism suggests how cytokines and chemokines can link the AS-associated factors ERAP1 and Th17 cells, as well as how this leads to osteoclastogenesis. Control ERAP1 induces expression of pB27 and FHC structures on the cell surface, which leads to strong inhibition of NK cell activation through KIR3DL1. AS-associated ERAP1 allotype combinations induce less FHC expression on the cell surface leading to less KIR3DL1 engagement and NK cell activation. These differences in KIR engagement and NK cell activation can alter the cytokine profile generated by the PBMC population. With control ERAP1 allotype combinations there is high IFNγ, IL-10 and increased CCL5 levels, which can inhibit Th17 cell differentiation and osteoclastogenesis, as well as increasing IL-1Rα levels to inhibit IL-1 functions. With AS-associated ERAP1 allotype combinations, there is increased TNFα and decreased IFNγ, IL-10 and CCL5 expression. This increased TNFα can promote osteoclastogenesis and may be present as a consequence of Th17 differentiation, most likely from increased IL-1 induction. This increased IL-1 can also induce osteoclastogenesis. Th17 cells can inhibit IL-10 and CCL5 expression. Th17 cells produce IL-6, IL-23 and IL-17, which can increase TNFα expression.

4.6 Future Directions

To further validate the results observed it would be important to use PBMCs from a new donor to confirm that the changes in NK cell activation seen with ERAP1 allotype combinations could be replicated in another context. Additionally, the blocking experiments were only done using two control and two AS-associated ERAP1 allotype combinations; these experiments would have to be repeated and expanded to include all allotype combinations in order to confirm the results shown here. In addition, further examination of cytokines and chemokines produced following expression of different ERAP1 allotypes by Luminex is required, probing the Th17 axis (including IL-23 and IL-1) and its role in disease. Finally, as the results presented here point to a major role of KIR3DL1 in the difference seen between normal and AS-associated ERAP1 allotype combinations, it would be important to confirm these results using a stripped down assay to examine KIR3DL1 interactions in isolation using KIR3DL1-expressing Jurkat cells. These cells produce IL-2 following KIR engagement and so are a good tool to determine the strength of KIR3DL1 binding to target cells without the confounding effect of other NCRs, and have previously been used to analyse KIR3DL2 engagement (90).

In order to further this work it would be interesting to analyse the PBMC population following long term incubation with ERAP1-transfected target cells. In particular, to observe whether the proportion of Th17 cells is increased in the presence of AS-associated ERAP1 compared to controls. In addition, the analysis of TNFα, IFNγ, IL-10, IL-1 and potentially IL-17 levels following incubation of target cells and PBMCs across a time course ranging from 4 hours to 36 hours would be important. This data would help to show the order of production for each cytokine, thereby helping to further elucidate the interaction of these cytokines with one another. Finally, I would like to expand the assay to include patient samples and use HLA-B27^{+} AS-patient PBMCs to determine a) whether they respond in the same way as our HLA-B27^{-} donor and b) whether they are prone to higher expression of cytokines or NK cell activation.

While this assay works well enough to show significant differences in NK cell activation and cytokine profile, the use of HeLa target cells is less than ideal due to the presence of other HLA molecules. These additional receptors mean that HeLa ERAP1$^{-/-}$ B*2705^{+} cells inhibit NK cell activation relatively strongly already, meaning that any difference in NK cell activation we see is

minimal, although remaining consistent. The use of another target cell line that maximises the differences in NK cell activation would be ideal, however, assessment of 293T, mouse ERAAP$^{-/-}$ fibroblasts, K89 and HeLa cells, has so far failed to achieve this. An alternative would be to transduce the existing HeLa ERAP1$^{-/-}$ cells with an activating receptor such as MICA. MICA is a non-classical MHC I molecule that engages the activating receptor NKG2D to induce NK-mediated lysis (160). This would increase the activation of NK cells in response to these cells but engagement of KIR3DL1 should still be strong enough to inhibit the NK cell in the same way as we see now.

Another limitation of the work here is the fact that the PBMCs are stimulated overnight with IL-15 for the Luminex assay. This was done to ensure that the interaction between target cells and PBMCs occurred in the same manner as was seen in the NK cell activation assays, with the only difference being the length of time for incubation. However, it has previously been shown that incubation of PBMCs in different cytokines such as IL-2, IL-12, IL-18 or IL-15 can sometimes alter the cytokines released from the PBMC population (161). As this stimulation may have an effect on the cytokine profile, it may be worth trying different combinations of cytokines for this stimulation and determining the effect of each. Additionally, or alternatively, we could determine the concentration of IL-2, IL-15 and/or IL-18 in the peripheral blood of AS patients and then use as close to these conditions as possible to stimulate our PBMCs.

Following on from the Luminex data it would be interesting to look at the presence of both NK cells and Th17 cells in biopsies taken from AS patients. If possible, biopsies taken from different stages of the disease could be used to identify changes in the immune infiltrate of the spine across time. However, it is likely that if NK cells are involved in disease pathogenesis their contribution will be restricted to an early stage of disease before any symptoms or conclusive diagnosis for AS is assigned.

Chapter 5: Differences in the AS-associated HLA-B*2705 and non-associated HLA-B*2709 alleles

5.1 Introduction

The association between AS and HLA-B27 has been known for over 40 years, however the mechanisms underpinning this association have not been elucidated (162, 163). HLA-B27 is present in around 95% of AS patients, but only around 5% of the HLA-B27$^+$ population of the world develop the disease (1, 164). In HLA-B27$^+$ disease there is a significantly lower age of onset and a higher prevalence of episodes of eye inflammation (acute anterior uveitis) and hip joint involvement (165). Interestingly, HLA-B27 homozygosity does not affect the patient clinically, but does triple the risk of developing the disease (166). HLA-B27 alleles all derived initially from HLA-B*2705 (4) but display different characteristics for both cell surface expression and tapasin-dependence.

There are 106 known subtypes of HLA-B27, 16 of which have been shown to be present in AS patients, with HLA-B*2705, -B*2702 and –B*2704 being the most widely associated and studied (167, 168). HLA-B*2706, common in Southeast Asia, and HLA-B*2709, a rare subtype found mainly in Sardinia, lack association with AS (169-171). HLA-B*2709 differs from –B*2705 at only one amino acid position in the F pocket of the peptide-binding groove: D116H. This single amino acid change significantly effects the repertoire of bound peptides, with HLA-B*2705 sharing ~79% of its peptide repertoire with HLA-B*2709 and HLA-B*2709 sharing ~88% with –B*2705 (125).

To investigate how these differences in peptide repertoire induce differential association with AS, the activation of NK cells in response to both of these alleles of HLA-B27 as well as the NK cell response to specific peptides bound to these alleles will be looked at. NK cells have been implicated in the pathogenesis of AS with higher numbers of NK cells in the peripheral blood of AS patients (86). In previous chapters, it was shown that the activation of NK cells is altered by peptide sequence and ERAP1 polymorphisms, suggesting that, if the peptide repertoire is an important factor in the pathogenesis of AS, NK cells may have a role to play. With ERAP1 alone altering NK cell activation in the context of HLA-B*2705 it will be interesting to determine whether these changes are reflected in the context of HLA-B*2709.

5.2 Hypothesis

*Peptides bound to HLA-B*2705 will induce more NK cell activation than those bound to HLA-B*2709 due to the way peptides sit in the peptide binding groove being altered by the D116H amino acid change.*

5.3 Aims

- Determine the cell surface composition of HLA-B27 in HLA-B*2705 and –B*2709 positive cells through measurement of pB27 and FHC structure presence and stability
- Determine NK cell activation in response to natural ligands bound to both HLA-B*2705 and –B*2709
- Determine whether HLA-B*2705 or –B*2709 are more affected by changes in ERAP1
- Generate crystal structures for HLA-B*2705 and –B*2709 bound to a natural ligand and its N-terminal extended pre-cursor to show how peptides differentially sit in the peptide-binding groove

5.4 Results

5.4.1 HLA-B*2705 expression is increased compared to HLA-B*2709 on .221 cells

Given the likelihood the HLA-B27 molecules are sensed at the cell surface by NK cells as pB27, FHC and $B27_2$ structures ((133) and chapter 4), the extent to which the single amino acid change between HLA-B*2705 and –B*2709, D116H, altered the relative levels of these species at the cell surface was investigated. .221 cells stably transduced with HLA-B*2705 or –B*2709 were surface stained for pHLA-B27 (ME.1), FHC (HC10) and total MHC I (W6/32) (**Figure 5.1**). .221-B*2705 cells expressed more HLA-B27, FHC and MHC I compared to .221-B*2709, however, this reduction was generally equal resulting in a similar ME.1:HC10 ratio between cell lines.

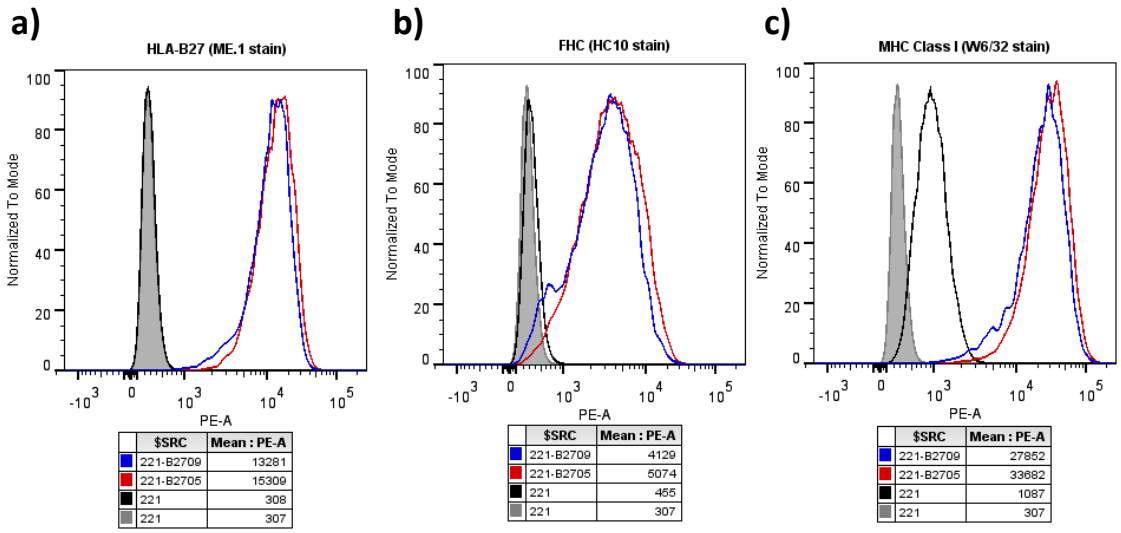

Figure 5.1: MHC I cell surface staining of .221 cells

.221 cells, and their stably transfected sister cell lines .221-B*2705 & .221-B*2709, were surface stained for HLA-B27 (ME.1 stain, a), FHC (HC10 stain, b) and MHC class I expression (W6/32 stain, c). There is higher expression of all three forms in .221-B*2705 cells (red line) compared to .221-B*2709 cells (blue line).

To determine the average stability of peptide cargo bound to each HLA-B27 allele, a BFA peptide stabilisation assay (2.5 Brefeldin A Peptide stabilisation assay) was used to determine the stability of HLA-B27 on the cell surface across 6 hours (**Figure 5.2**). As seen in the previous figure, there was an increase in HLA-B27 expression with .221-B*2705 compared to .221-B*2709, although when expressed as a percentage of maximal binding, at time zero, there was minimal difference between the two alleles. After four hours, there were no significant differences in expression of either HLA (**Figure 5.2a-c**). There was also increased expression of FHC with HLA-B*2705 compared to –B*2709, however, when this was expressed as a percentage of the maximal binding there was more FHC expression with HLA-B*2709 compared to HLA-B*2705. After four hours there was a significant increase in HLA-B*2709 FHC expression compared to HLA-B*2705 ($p<0.05$) (**Figure 5.2d-f**).

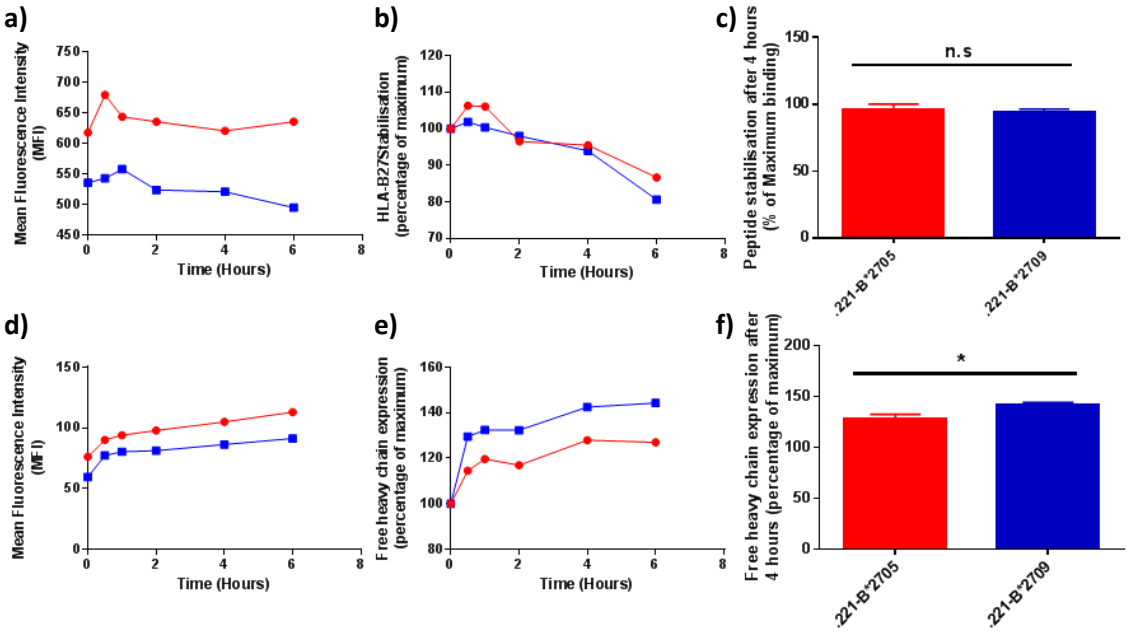

Figure 5.2: Stability of HLA-B*2705 and -B*2709 on the cell surface of .221 cells

The cell surface stability of HLA-B*2705 and –B*2709 was measured across 6 hours in a BFA peptide stabilisation assay. .221-B*2709 cells have lower HLA-B27 expression than .221-B*2705 cells (a). When these MFI values are calculated as a percentage of total binding (i.e. binding at 0 hours) there was minimal difference between –B*2705 and –B*2709 expression (b). After 4 hours there was no significant difference in the cell surface expression between both alleles of HLA-B27 (c). The MFI for FHC expression was higher in .221-B*2705 cells (d). However, when these results are expressed as a percentage of maximal binding, there was increased FHC expression in .221-B*2709 cells compared to .221-B*2705 (e). After 4 hours this increase in FHC with .221-B*2709 cells was significant ($P<0.05$) (f). (a, b, d, e) are a representative experiment of n=3, data analysed by paired t-test.

5.4.2 HLA-B*2705 and –B*2709 induce the same level of NK cell inhibition through KIR3DL1

The .221-B*2705 and .221-B*2709 cells were next used as target cells in LAMP1 assays to determine whether the changes in cell surface expression or allele sequence affected NK cell activation (**Figure 5.3**). In the whole NK cell population, there was significant inhibition of NK cell activation with both cell lines ($p<0.001$) (**Figure 5.3a**). In the KIR3DL1^{+} population, this inhibition was increased ($p<0.0001$) (**Figure 5.3b**). There was no difference in inhibition between the two cell lines in this system.

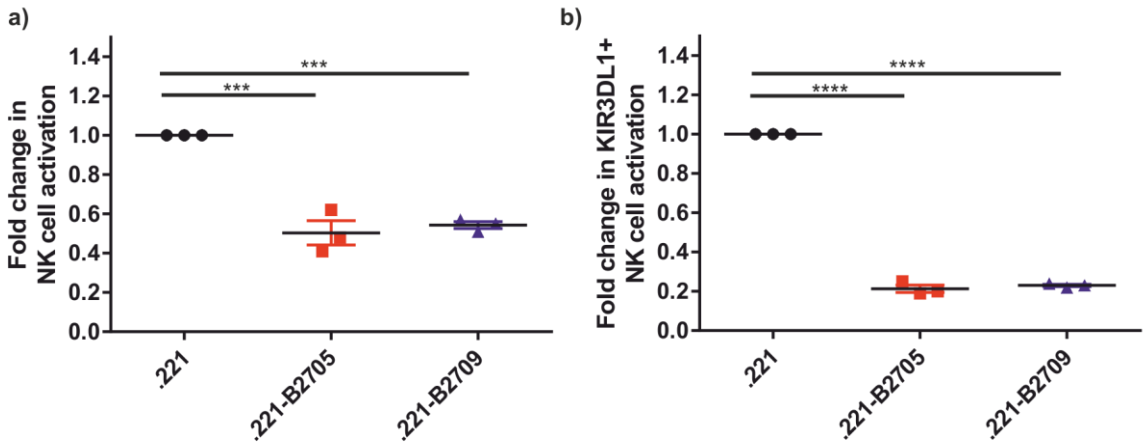

Figure 5.3: .221-B*2705 and .221-B*2709 cells induce NK cell inhibition

.221 cells were used as target cells in a LAMP1 assay to determine whether there were differences in NK cell inhibition with –B*2705 and –B*2709. (a) In the whole NK cell population, .221-B*2705 and .221-B*2709 both significantly inhibited NK cell activation ($p<0.001$). (b) In the KIR3DL1^{+} population, this inhibition was increased with both cell lines ($p<0.0001$). n=3, data analysed by one-way ANOVA and Tukey's multiple comparisons test.

5.4.3 HLA-B*2705 binding to rhKIR3DL1 is more stable that HLA-B*2709 binding

In corroboration with the results of the LAMP1 assay, there was little difference between the binding of recombinant KIR3DL1 with .221-B2705 cells compared to .221-B*2709 (**Figure 5.4a**). Binding to these cells was significantly increased compared to .221 cells ($p<0.05$ for –B*2705, $p<0.01$ for –B*2709). The binding of rhKIR3DL1 to .221-B*5801 cells showed the highest binding, and this was highly significant compared to all other cell lines ($p<0.0001$). HLA-B*5801 has previously been shown to bind more strongly to KIR3DL1 than HLA-B27 (172).

In a competition assay to determine whether the strength of KIR3DL1 binding, HLA-B*2705 binding to rhKIR3DL1 was stronger than to HLA-B*2709, with the MFI of rhKIR3DL1 binding to .221-B*2709 cells reduced compared to .221-B*2705 cells (**Figure 5.4b**). rhKIR3DL1 binding was only slightly reduced after two hours but dramatically reduced after three hours, suggesting that ~2 hours is the length of time rhKIR3DL1 engages HLA-B27. When these MFI results were expressed as a percentage of the maximal binding at time zero, rhKIR3DL1 binding to .221-B*2709 appeared to be less stable than binding to .221-B*2705 (**Figure 5.4c**). This agrees with data previously published that suggested that HLA-B*2705 binding by KIR3DL1 was stronger than HLA-B*2709 binding (172).

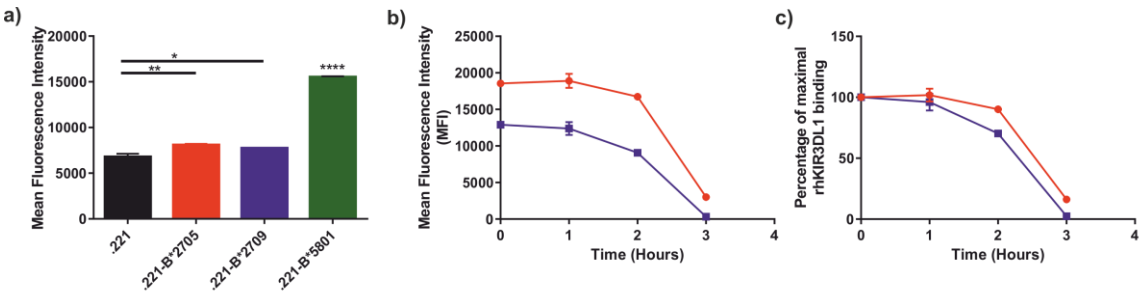

Figure 5.4: Binding of rhKIR3DL1 to .221 cells

rhKIR3DL1 complexed to fluorescent protein A was loaded onto .221 cells for one hour before being analysed by flow cytometry. (a) The mean fluorescence of binding shows significantly more binding of rhKIR3DL1 to .221-B*2705 cells ($p<0.01$) and .221-B*2709 cells ($p<0.05$) compared to .221 cells alone. .221-B*5801 cells showed the largest MFI that was significant compared to all cell lines ($p<0.0001$). N=3, data analysed by one-way ANOVA and Tukey's multiple comparisons test. (b) .221-B*2705 and .221-B*2709 cells were used as target cells in a rhKIR3DL1 binding competition assay. The MFI of rhKIR3DL1 binding at each time point is shown. (c) When these MFI values are expressed as a percentage of maximal binding .221-B*2705 bind rhKIR3DL1 in a more stable reaction than .221-B*2709. N=2.

5.4.4 HLA-B*2709 induces NK cell inhibition in an ERAP1-dependent mechanism

To assess the differences in HLA-B*2705 and –B*2709 expression in the context of a different cell line and under changes in MHC I antigen presentation machinery several HeLa cell lines with changes in antigen presentation machinery were investigated. HeLa cells do not express any HLA-B27 alleles naturally and so were made to stably express either HLA-B*2705 or -B*2709 (**Figure 5.5**). As was seen with the .221 cells, there was higher expression of HLA-B27 on –B*2705 transfected cells compared to –B*2709 transfected cells; however, unlike the .221 cells this was concurrent with more FHC expression with –B*2705 instead of –B*2709 cells.

HeLa B*2705 and HeLa B*2709 cells were then stably transfected with another plasmid containing the Herpes Simplex Virus (HSV) protein ICP47, a TAP inhibitor, which prevents the entry of proteasome-derived peptides into the ER from the cytoplasm. Addition of this viral protein, drastically reduces the cell surface expression of MHC I, as can be seen in the HeLa ICP47^{+} cell line, due to a dramatic reduction in the available pool of peptides for MHC I binding (173). The HeLa B*2705 ICP47^{+} and HeLa B*2709 ICP47^{+} cell lines both had reduced MHC I expression, with a more marked difference in the –B*2705^{+} cells (**Figure 5.5**).

Transiently transfected HeLa ERAP1$^{-/-}$ cells were next used to assess the contribution of ERAP1 to generation of the peptide repertoire for each HLA-B27 allele. These cells were transiently transfected with either HLA-B*2705 of HLA-B*2709 and for every experiment 50-70% transfection efficiency was achieved. The MFI of the HLA-B27 positive population was measured to allow accurate comparisons of the B27 expression. Equal HLA-B27 expression was seen with both HLA-B*2705 and –B*2709, but the MFI of the FHC population was much higher in the –B*2705 cells (**Figure 5.5**).

Further examination of the MFI of HLA-B27 and FHC expression on HeLa cells expressing alleles of HLA-B27, showed B*2705 was expressed better than B*2709 ($p>0.001$) in both HeLa and HeLa ERAP1$^{-/-}$ cells (**Figure 5.6a**). Similarly, B*2705 FHC was generally expressed better than B*2709 FHC (**Figure 5.6b**).

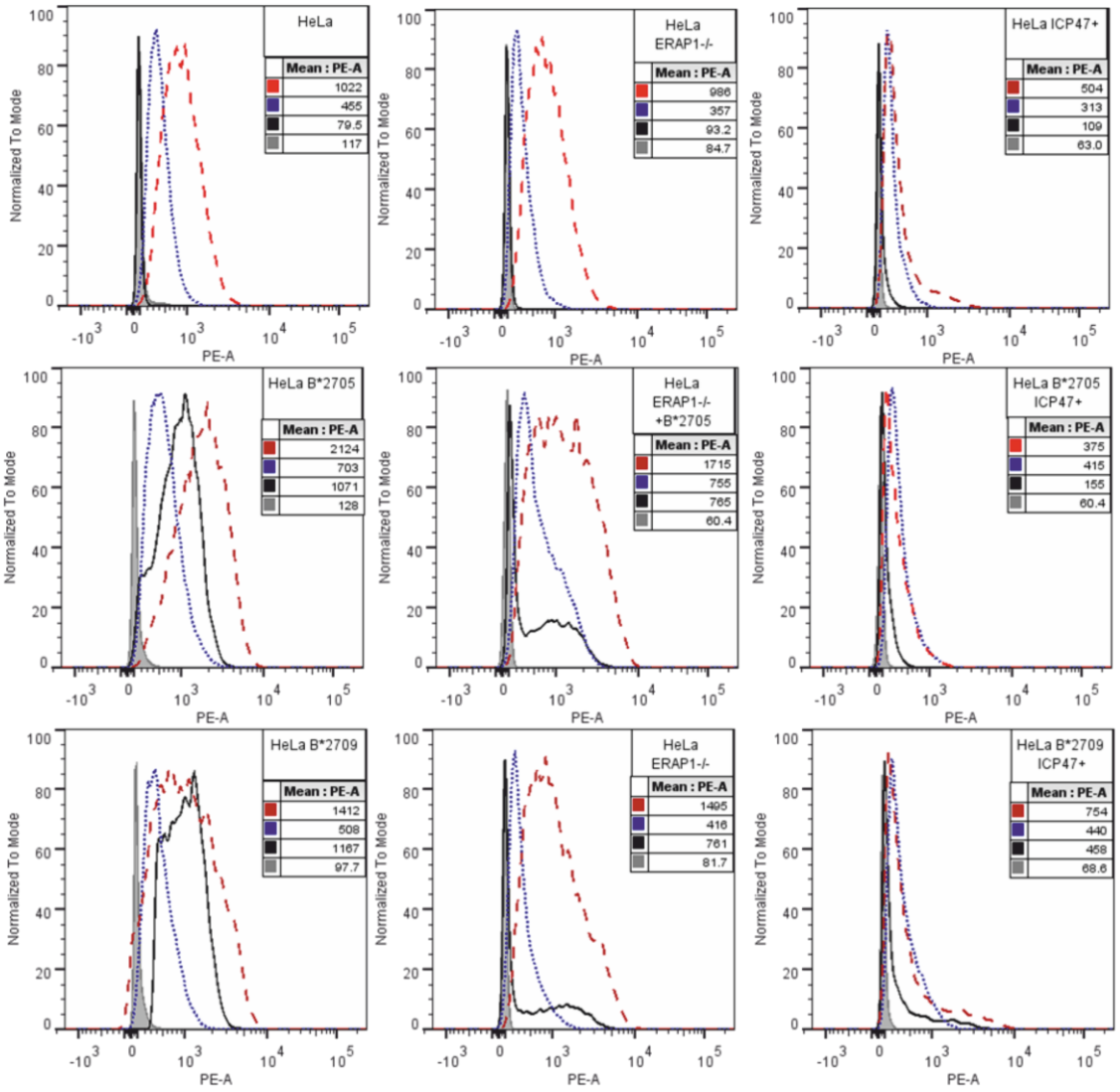

Figure 5.5: MHC I expression on HeLa cell lines

The native HeLa cell line was taken and made to stably express HLA-B*2705 or HLA-B*2709. These three cell lines were then made to stably express the TAP inhibitor ICP47, to create HeLa ICP47^{+}, HeLa B*2705 ICP47^{+} and HeLa B*2709 ICP47^{+} cells. The HeLa ERAP1$^{-/-}$ cell line previously made in our lab through CRISPR could not be made to stably express either HLA-B*2705 or –B*2709, so instead these cells were transiently transfected for each experiment. HeLa cells express no ME.1 binding MHC I (black line), but have high levels of other MHC I (red line) and low levels of FHC (blue line). The MHC I expression of HeLa ERAP1$^{-/-}$ is unchanged from that of HeLa, while in HeLa ICP47^{+} cells there is a clear reduction in MHC I levels on the cell surface, and a slight reduction in FHC expression. HeLa B*2705 and HeLa B*2709 show good ME.1 staining (black line), and addition of ICP47 reduces all MHC I expression as before. HeLa ERAP1$^{-/-}$ B*2705 and HeLa ERAP1$^{-/-}$ B*2709 show good ME.1 staining (black line) in the transfected cells; usually an average of 50-70% of the cells.

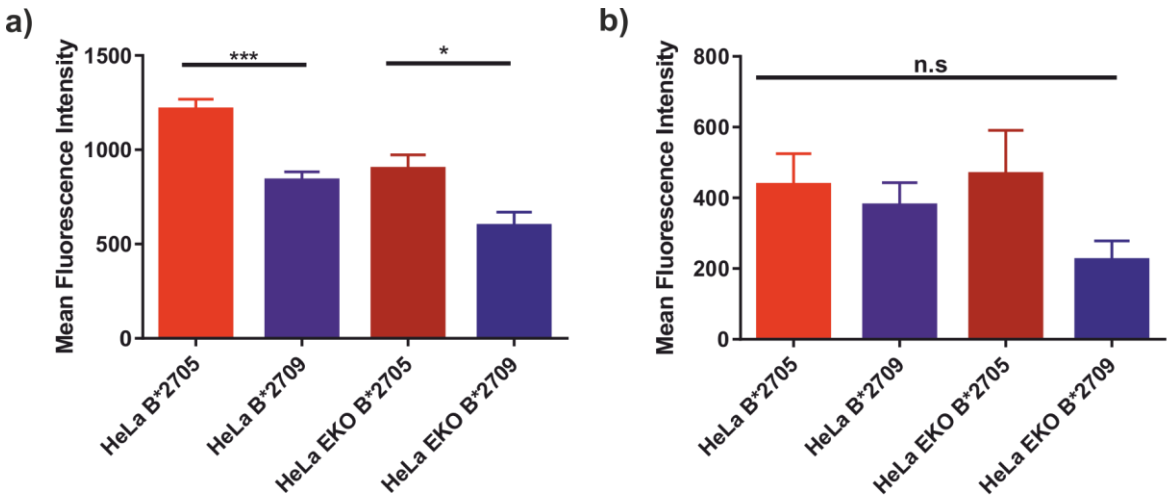

Figure 5.6: Expression of HLA-B27 and FHC on -B*2705 cells compared to -B*2709

HeLa cells stably expressing HLA-B*2705 or –B*2709 and HeLa ERAP1$^{-/-}$ cells transiently transfected with HLA-B*2705 or –B*2709 were surface stained for HLA-B27 (a) and FHC (b). There was a significant increase in HLA-B*2705 expression compared to –B*2709 in both HeLa cell lines ($p<0.001$) and HeLa ERAP1$^{-/-}$ cell lines ($p<0.05$). There were no significant differences in FHC expression with any cell line. N=3, Data analysed by one-way ANOVA and Tukey's multiple comparisons test.

The NK cell response to the different HeLa cell lines described above was determined by LAMP1 assay (2.4 NK cell degranulation (LAMP1) assay) (**Figure 5.7**). In the whole NK cell population there was significant inhibition with HeLa B*2705 compared to HeLa only and HeLa B*2709. HeLa B*2709 showed no difference compared to HeLa only, in fact showing a slight increase in NK cell activation. In the KIR3DL1^{+} population there were no significant differences in NK cell activation, although there was some inhibition with HeLa B*2705 and slight activation with HeLa B*2709 (**Figure 5.7a-b**).

HeLa ICP47 cells showed increased NK cell activation as expected due to the reduction of MHC I on the cell surface. In the whole NK cell population, HeLa B*2709 ICP47^{+} cells induced significant activation of the NK cells compared to HeLa only ($p<0.01$) and HeLa B*2705 ICP47^{+} ($p<0.05$). In the KIR3DL1^{+} population, HeLa ICP47^{+} cells significantly induced increased activation compared to all other cell lines, showing the highest level of activation. HeLa B*2705 ICP47^{+} cells showed the lowest activation level but this was still significantly higher than HeLa only. HeLa B*2709 ICP47^{+} cells showed an intermediate level of activation (**Figure 5.7c-d**).

HeLa ERAP1$^{-/-}$ cells showed slight inhibition of NK cells in both populations compared to HeLa cells; this unexpected result is likely due to the fact that the natural ERAP1 of HeLa cells is predicted to be a hypo-trimmer and wouldn't be expected to produce good ligands for MHC I, instead producing longer peptides and more unstable complexes (personal communication with

Dr Emma Reeves). This cell line was used in previous experiments in chapters 3 and 4, with loss of ERAP1 increasing NK cell inhibition surprisingly. Addition of B*2705 to HeLa ERAP1$^{-/-}$ cells caused significant inhibition compared to HeLa in the whole NK cell population ($p<0.05$) and the KIR3DL1^{+} population ($p<0.01$). In the KIR3DL1 population this addition of B*2705 also significantly reduced NK cell activation compared to HeLa ERAP1$^{-/-}$ ($p<0.05$). Addition of B*2709 had no significant effect in the whole NK cell population but significantly inhibited NK cell activation in the KIR3DL1^{+} population compared to HeLa cells ($p<0.01$) and HeLa ERAP1$^{-/-}$ cells ($p<0.05$) (**Figure 5.7e-f**).

Upon examination of NK cell activation compared to HeLa ERAP1$^{-/-}$ instead of HeLa cells, there is almost equal inhibition upon addition of HLA-B*2705 and –B*2709 (non-significant). In the KIR3DL1^{+} population, this inhibition was significant with –B*2709 ($p<0.01$), but not with –B*2705 (**Figure 5.7g-h**).

Taken together, these results indicate that pHLA-B*2709 complexes are recognised by NK cells in an ERAP1-dependent manner, as loss of the hypo-trimming ERAP1 native to HeLa cells increased NK cell inhibition whereas no inhibition was seen in the presence of the peptide repertoire generated by the HeLa ERAP1. ERAP1 had little effect on HLA-B*2705 cells with similar inhibition seen with and without ERAP1 (**Figure 5.7a&g**).

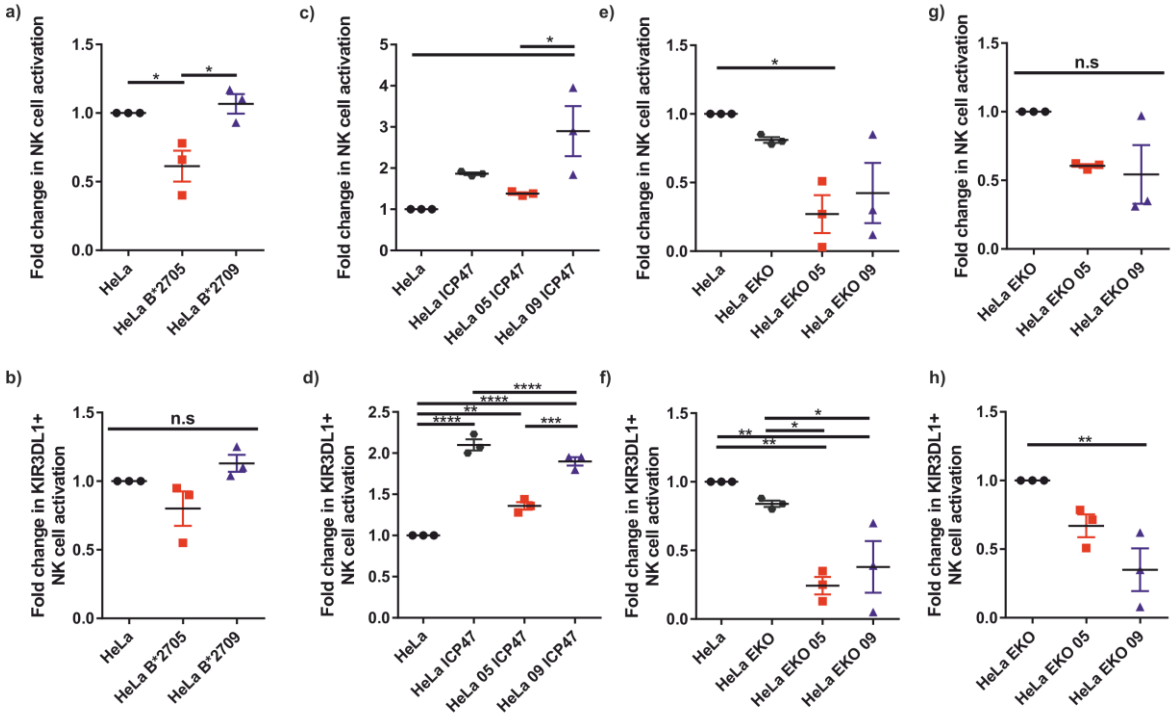

Figure 5.7: NK cell activation in response to different HeLa cell lines

NK cell activation, as measured in a LAMP1 assay, was determined in response the HeLa target cells with different MHC I expression. (a) HeLa B*2705 significantly inhibited NK cell activation compared to HeLa and HeLa B*2709 cells ($p<0.05$) in the whole NK cell population. (b) While this pattern was repeated in the KIR3DL1^{+} NK cell population, there was no significance. (c) As expected due to a reduction in MHC I on the cell surface, HeLa ICP47 cells increased NK cell activation compared to HeLa cells. Addition of HLA-B*2705 reduced this activation slightly, but addition of HLA-B*2709 increased NK cell activation in the whole NK cell population. (d) All cells lines significantly increased KIR3DL1^{+} NK cell activation compared to HeLa cells alone. However, the large activation in response to HeLa B*2709 ICP47 cells in the whole NK cell population was not repeated. (e) Addition of HLA-B*2705 to HeLa ERAP1$^{-/-}$ (EKO) cells significantly reduced NK cell activation in both populations compared to HeLa cells. This was only significant with HLA-B*2705. (f) In the KIR3DL1^{+} NK cell population, loss of ERAP1 significantly reduced NK cell activation in both HLA-B*2705 and –B*2709 transfected cells. (g) When the NK cell activation following addition of HLA-B*2705 or –B*2709 is compared to HeLa EKO cells there is no significant difference in the whole NK cell population. (h) In the KIR3DL1 population, loss of ERAP1 expression significantly reduced NK cell activation in HeLa ERAP1$^{-/-}$ B*2709 cells ($p<0.01$). n=3, Data analysed by one-way ANOVA and Tukey's multiple comparisons test.

5.4.5 Changes in the amino acid at P8 alters NK cell activation when bound to HLA-B*2705 but not HLA-B*2709

In chapter 3, the model peptide FRYNGLIHR was used to show that changes in P7 or P8 of this peptide could alter KIR3DL1 binding. To determine whether this differential KIR3DL1 could be attributed to the structure of the peptide binding in the peptide binding groove, and therefore altered by changes in the area of the MHC I molecule, HLA-B*2705 and HLA-B*2709 were loaded with FRY-IH (inhibitory) and FRY-IK (non-inhibitory) (**Figure 5.8**) and the NK cell activation was determined by LAMP1 assay (2.4 NK cell degranulation (LAMP1) assay). With the amino acid change between these alleles of HLA-B27 being located in the F-pocket of the peptide binding groove the binding of peptide by these two alleles may lead to altered KIR3DL1 engagement.

As previously seen (**Figure 3.5**), FRY-IK significantly induced NK cell activation compared to FRY-IH in the whole NK cell population ($p<0.05$) and in the KIR3DL1$^+$ NK cell population ($p<0.001$) when bound to HLA-B*2705. This activation was also significant compared to the no peptide addition in the KIR3DL1$^+$ NK cell population ($p<0.01$). However, these differences were not clearly repeated in the context of HLA-B*2709. There were no significant differences in HLA-B27 or FHC expression with any condition (**Figure 5.8c-d**).

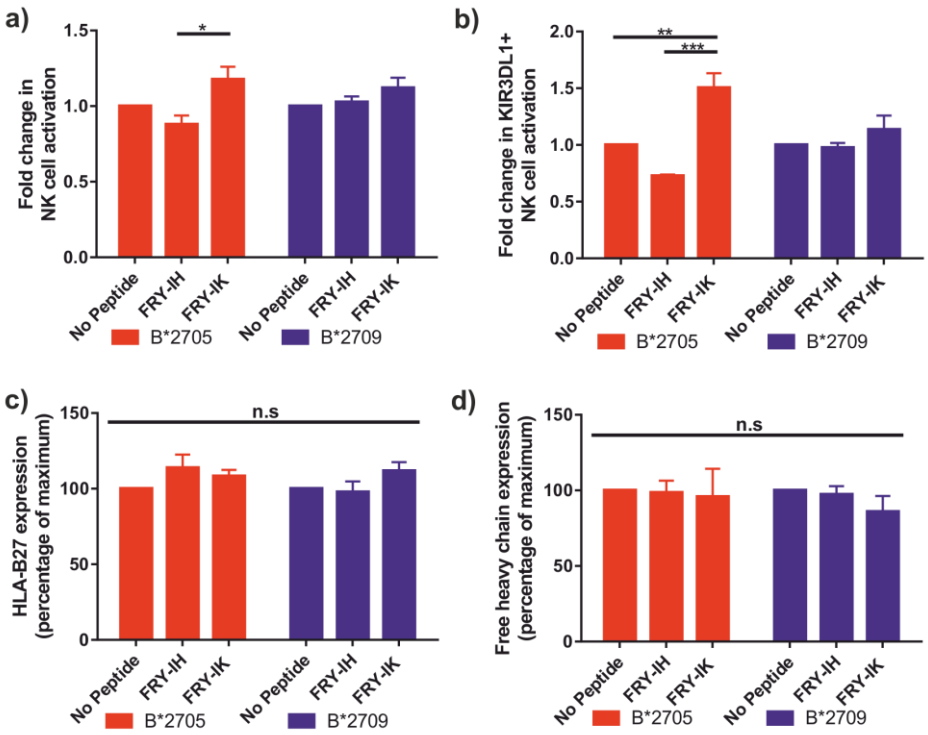

Figure 5.8: FRY-IH and FRY-IK have no effect on B*2709 induced NK cell activation

HeLa ERAP1$^{-/-}$ cells were transiently transfected with HLA-B*2705 or –B*2709 and the inhibitory peptide FRY-IH or activating peptide FRY-IK. These cells were then used as target cells in LAMP1 assays. (a) In the whole NK cell population there was a significant increase in NK cell activation with FRY-IK compared to FRY-IH ($p<0.05$). No significant differences were seen in HLA-B*2709 cells. (b) In the KIR3DL1 population, FRY-IK was significantly activating compared to FRY-IH ($p<0.001$) and no peptide ($p<0.01$). Again no differences were seen with HLA-B*2709. (c) There were no significant changes in HLA-B27 expression following transfection with either peptide or HLA. (d) There were also no significant changes in FHC expression. N=3, data analysed by two-way ANOVA and Tukey's multiple comparisons test.

5.4.6 N-terminal extension of a 9mer peptide has little effect on NK cell activation

In the previous data, HLA-B*2709 was shown to be more ERAP1 dependent than HLA-B*2705 when it comes to KIR3DL1 engagement (**Figure 5.7**). To confirm this association further, a new model peptide, LRNQSVFNF (LF9), was chosen as this peptide has been previously eluted from both alleles of HLA-B27 (125) and found to be N-terminally extended to SRLRNQSVFNF (SF11) following ERAP1 silencing (174). These new peptides were made on minigenes (2.3 Plasmid minigene construction), loaded onto HLA-B*2705 or HLA-B*2709 on HeLa ERAP1$^{-/-}$ cells and the NK cell activation was determined by LAMP1 assay (2.4 NK cell degranulation (LAMP1) assay**)** (**Figure 5.9**). There were no significant differences upon addition of any peptide compared to the no peptide controls in both the whole NK cell population and the KIR3DL1^{+} population.

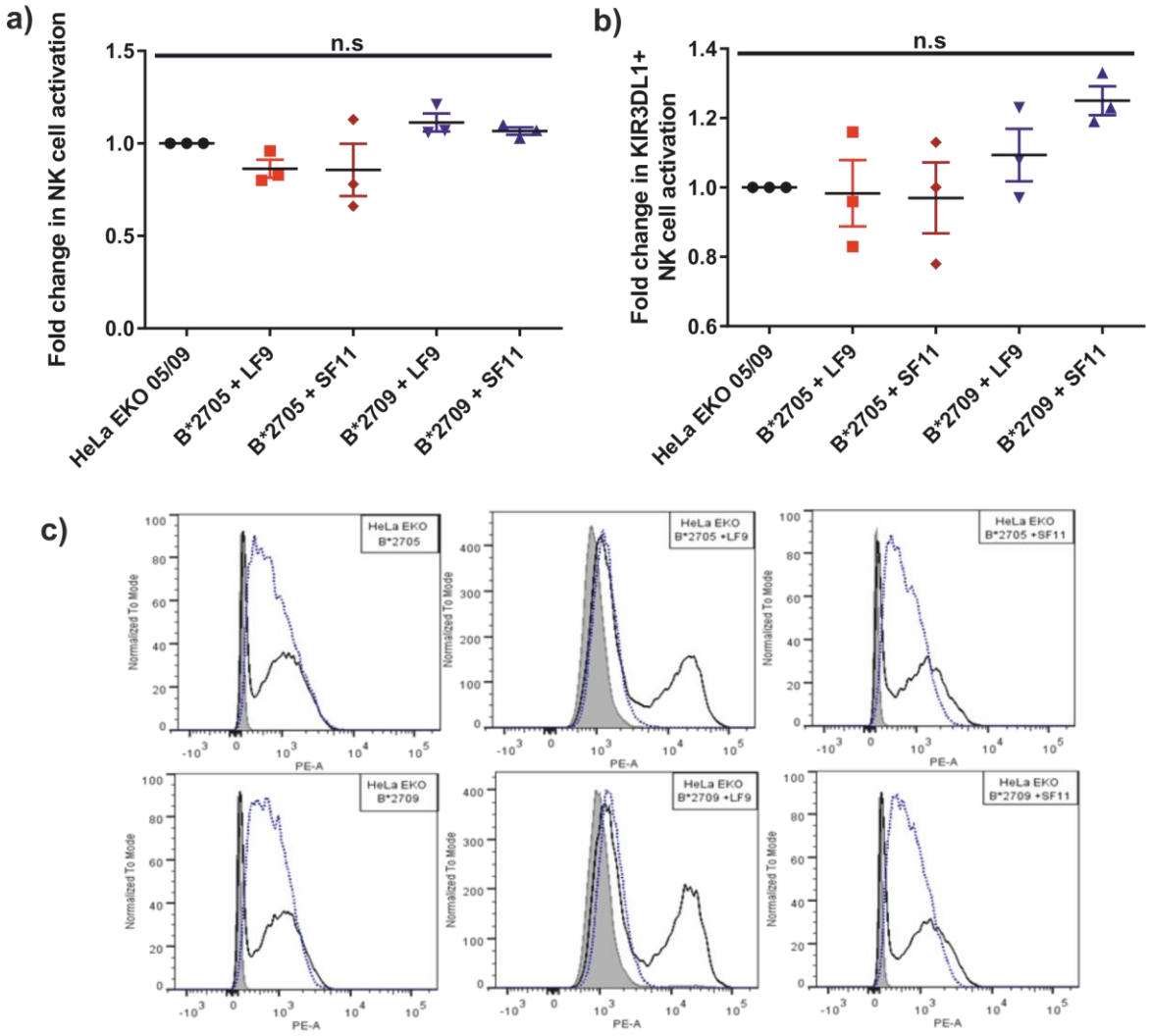

Figure 5.9: NK cell response to LF9 & SF11 in HeLa ERAP1$^{-/-}$ cells

The LF9 and SF11 model peptides were transiently transfected into HeLa ERAP1$^{-/-}$ along with HLA-B*2705 or –B*2709 and then these cells were used as target cells in a LAMP1 assay. (a) In the whole NK cell population there were no significant differences under any conditions. (b) This non-significance was repeated in the KIR3DL1^{+} population. C) Good transfection of HLA-B27 was seen with all conditions. The addition of LF9 in the presence of HLA-B*2705 and –B*2709 reduced the amount of FHC staining on the cell surface, while SF11 had no effect. N=3, data analysed by one-way ANOVA and Tukey's multiple comparisons test.

5.4.7 Limiting the existing peptide repertoire increases model peptide effects

The addition of peptide minigenes in ERAP1$^{-/-}$ HeLa cells may not result in significant amounts of cell surface peptide presentation as there are many high affinity competing peptides. To reduce the peptide competition, HeLa ERAP1$^{-/-}$ ICP47^{+} cells were used as targets in LAMP1 assays (2.4 NK cell degranulation (LAMP1) assay) (**Figure 5.10**). Addition of ICP47 to the system, induced inhibition of NK cells with LF9 bound to HLA-B*2709 (non-significant), while SF11 did not. In addition to this reduction in NK cell activation, there was significantly less cell surface HLA-B27 expression with LF9-B*2709 ($p>0.05$). However, there was little difference in HLA-B*2705 cells following addition of any peptide (**Figure 5.10**). These results are conflicting with less pB27 expression leading to increased NK cell inhibition, potentially suggesting that LF9 bound to HLA-B*2709 is a highly inhibitory complex. However, further repeats of this experiment would be required to confirm this.

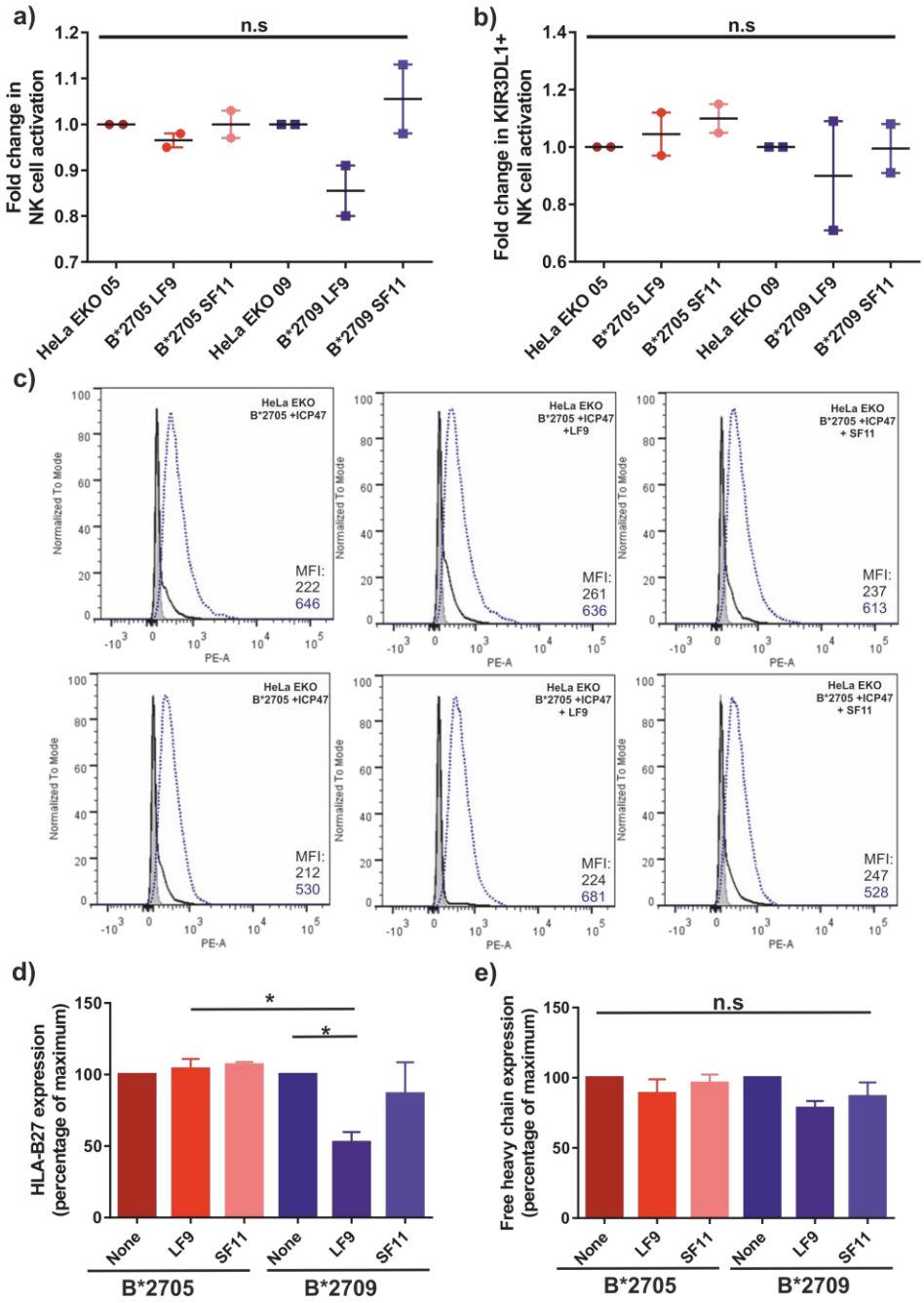

Figure 5.10: NK cell response to LF9 & SF11 in the presence of a TAP inhibitor

In the previous experiment there was a lack of difference upon addition of peptide to the target cells, to overcome this, target cells were transfected with the TAP inhibitor, ICP47, to reduce the pool of high affinity peptides readily available in the cell. These transfected target cells were then used in a LAMP1 assay of NK cell activation. (a) In the whole NK cell population, there was inhibition in response to LF9 peptide bound to HLA-B*2709. No other condition altered the NK cell activation. (b) In the KIR3DL1+ population the pattern was similar but no significant differences could be seen. (c) The ME.1 and HC10 staining for each cell line following transfection. (d) When the data from the ME.1 staining is grouped there is a significant reduction in HLA-B27 expression with LF9 bound to HLA-B*2709 compared to no peptide addition or LF9 bound to HLA-B*2705 ($p<0.05$). (e) No significant differences are seen in the FHC expression on the cell surface. n=2, Data analysed by one-way ANOVA and Tukeys multiple comparisons test.

5.5 Discussion

The association between HLA-B27 and AS has been known for over 40 years without any clear explanation (117, 118). More interestingly, despite the fact that all alleles of HLA-B27 are derived from HLA-B*2705 (4), there is a lack of association between disease and the alleles, HLA-B*2706 and –B*2709 (169-171). This study investigated whether there are any differences in the MHC expression, NK cell activation or structure in response to peptides bound to either HLA-B*2705 and –B*2709.

HLA-B*2705 was expressed on the cell surface in a higher abundance than HLA-B*2709 corresponding to both previous studies (175) and higher FHC staining on the cell surface. When stability of these HLA complexes on the cell surface across 6 hours was examined only a significant increase in FHC expression in HLA-B*2709 compared to HLA-B*2705 after 4 hours was observed. This suggests that, despite lower levels being presented at the cell surface, FHC in HLA-B*2709 cells is more stable and its expression increases across 6 hours slightly more dramatically than HLA-B*2705.

Although there were slight changes in cell surface MHC expression, no differences in NK cell activation in response to .221-B*2705 or .221-B*2709 were found. This suggests that there is a minimum level of cell surface expression required for inducing NK cell inhibition, which is achieved by both .221 cell lines. A slight difference in rhKIR3DL1 engagement could be seen with HLA-B*2705 and –B*2709, but this was minimal and very close to the binding of rhKIR3DL1 to .221 cells alone. The competition assay showed a greater difference in rhKIR3DL1 binding with .221-B*2709 showing less binding than .221-B*2705 cells. While rhKIR3DL1 binding to .221-B*2705 cells seemed to be slightly stronger than binding to .221-B*2709, both cell lines lost rhKIR3DL1 engagement after 2 hours suggesting that this is the lifespan of KIR3DL1-HLA-B27 interactions at the cell surface. Khakoo *et al* previously identified a hierarchy of HLA alleles that induce greater KIR3DL1 engagement with HLA-B*5801 showing the highest engagement and HLA-B*2705 binding to KIR3DL1 more strongly than HLA-B*2709 (172).

As was seen in the .221 cells, there was a reduction in HLA-B27 cell surface expression with HeLa B*2709 and HeLa ERAP1$^{-/-}$ B*2709 cells compared to their HLA-B*2705^{+} counterparts. There was also a reduction in FHC levels, but this was not significant. HeLa cells are strongly adherent and require EDTA for removal from the surface of tissue culture dishes. This use of EDTA can affect

the cell surface expression of HLA; following harvest, these cells are usually left at 37°C for 1.5 hours to allow the MHC levels to return to 'normal'. As such it is difficult to use these cells in a BFA decay so we cannot determine whether HLA-B27 behaves the same in these cells as it does in the .221 cells, however, following corroboration of the MHC expression results, it is expected that the results would be similar.

Some interesting differences were seen in the LAMP1 assays using various HeLa cell lines expressing either HLA-B*2705 or –B*2709. Firstly, HeLa B*2709 cells were not inhibitory in any way compared to HeLa cells in both the whole NK cell population and the KIR3DL1^{+} population. HeLa B*2705 cells were inhibitory but only slightly and this was only significant in the whole NK cell population. Potentially, these results are due to low expression of these HLA on the cell surface in comparison to other MHC I molecules, because HeLa cells express several other native HLA alleles that will interact with NK cells as well as preventing high expression of our transfected HLA through competition for space on the cell surface. Perhaps the difference in cell surface expression seen in HeLa B*2705 versus HeLa B*2709 is the amount required for KIR3DL1 engagement, and thus an effect on NK cell activation.

However, the more interesting explanation is that pB*2709 complexes cannot engage NK cells in the presence of a hypotrimming allotype of ERAP1, as is present in HeLa cells. This idea is supported by the result that when ERAP1 is absent from HeLa cells HeLa ERAP1$^{-/-}$ B*2709^{+} cells can induce inhibition. These results again suggest that the natural ERAP1 in HeLa cells generates a peptide repertoire that prevents KIR engagement as loss of this protein has increased the inhibition of NK cells suggesting that, in its absence, there is a better peptide repertoire for KIR engagement on the cell surface. We know that loss of ERAP1 from cells can lead to an altered peptide repertoire with some usual peptides absent, increase in expression of others and presentation of novel peptides (25). However, the ERAP1 present in HeLa cells is thought to be a hypo-trimmer that cannot trim peptides well leading to presentation of longer peptides and a more unstable peptide repertoire (personal communication with Dr Emma Reeves). This data supports that idea as loss of this hypo-trimming ERAP1 allowed the generation of a more stable peptide repertoire, potentially through generation of peptides by ERAP2.

This suggests that ERAP1 generates pB27 complexes on HLA-B*2709 that can engage NK cells, and loss of ERAP1 or a hypo-trimming allotype prevents the formation of these complexes preventing NK cell inhibition. Conversely, it seems that ERAP1 presence has little effect on the

pB27 complexes expressed by HLA-B*2705^{+} cells, with similar inhibition of NK cells seen in the presence and absence of ERAP1. This may be important in the context of NK cell education with HLA-B*2705^{+} individuals potentially being less susceptible to peptide changes affecting KIR3DL1 engagement as they are used to seeing peptides that do not engage well anyway. Whereas, HLA-B*2709^{+} individuals are educated correctly through KIR3DL1 meaning that changes in peptide repertoire have profound effects on their NK cell activation.

When the pool of available peptides was reduced using the TAP inhibitor ICP47, HeLa B*2709 ICP47^{+} cells induced greater NK cell activation than HeLa ICP47^{+} cells in the whole NK cell population and greater than HeLa B*2705 ICP47^{+} in the KIR3DL1^{+} population. There was a slight increase in the staining for all MHC on the cell surface of HeLa B*2709 ICP47^{+} cells compared to HeLa B*2705 ICP47^{+} cells, which would suggest that these cells would be more inhibitory. Perhaps these extra pMHC complexes are highly unstable and prevent correct KIR engagement or are in some way engaging activating receptors instead. Following the lack of NK cell inhibition seen with HeLa B*2709 it is not unsurprising that these cells will create more activated NK cells following addition of ICP47. Previously, it has been found that HLA-B*2709 does not induce as strong CTL responses against a self-peptide induced by inflammation, pVIPR1 (176), as HLA-B*2705 despite binding and presenting the peptide in much the same way. This was in contrast to the activation of CTLs following encounter with an EBV peptide, which generated the same strength of CTL response when bound to both HLA-B*2705 and –B*2709 (177). These results suggest that while the CTL, and therefore potentially NK cell response, to infectious peptides will be equal the response to induced self-peptides may be different.

Following the use of model peptides in chapter 3, model peptides were used to determine whether there were any differences in the engagement in each allele were dependent on peptide sequence or length. However, while FRY-IH was inhibitory and FRY-IK was activating in HeLa ERAP1$^{-/-}$ B*2705 cells, FRY-IH was not inhibitory when bound to HLA-B*2709. FRY-IK was slightly activating but this was non-significant. This data suggests that changes in the amino acid at P8 of this peptide are important in disrupting engagement KIR3DL1 and HLA-B*2705, but not HLA-B*2709. This may be due to the amino acid change in the peptide binding groove which may alter the contacts and interactions between KIR and MHC.

The addition of either LF9 or SF11 peptide to either allele made no real impact on NK cell inhibition, although both peptides bound to HLA-B*2705 showed slightly less NK cell activation than those bound to HLA-B*2709. The lack of result seen here may reflect the fact that the

results are compared to the activation of the NK cells in response to HeLa ERAP1$^{-/-}$ B*2705 or B*2709, which we already know to be quite inhibitory. Potentially, the addition of these peptides has little effect on cell surface pMHC as the expressed peptide repertoire is already made up of high affinity complexes. Addition of ICP47 into the system to reduce the pool of already available peptides still showed no significant effects, but LF9 bound to HLA-B*2709 showed some inhibition. Unexpectedly, this inhibition was associated with a significant decrease in HLA-B27 expression on the cell surface. This suggests that despite low expression levels the pMHC expressed are highly inhibitory.

Taken together, the results from these peptide experiments and the HeLa cell line LAMP1 assays could be postulated to suggest that HLA-B*2709 is an ERAP1-dependent molecule with alterations in the presence or absence of ERAP1 creating large changes in NK cell activation. In addition, the 9mer LF9 peptide potentially inhibits NK cell activation when bound to HLA-B*2709 but not HLA-B*2705, while the N-terminally extended SF11 peptide does not. This suggests that in the presence of HLA-B*2709 ERAP1 polymorphisms that alter the peptide repertoire may induce large changes in NK cell activation which the NK cells may be able to compensate for through education.

Conversely, HLA-B*2705 effects on NK cells appear to be ERAP1-independent with loss of ERAP1 having no effect on NK cell activation and changes in the length of LF9 having little effect. However, peptide sequence seems to be more important in the context of this allele suggesting that this allele may induce a more exaggerated response to peptides similar to host peptides, as occurs in molecular mimecry.

The generation of crystal structures showing a model peptide bound to both HLA-B*2705 and –B*2709 would provide insight into whether the amino acid change in the F-pocket of the peptide binding groove has any effect on how the peptide sits in the groove, helping to clear up the idea of whether it is peptide sequence or structure that affects KIR3DL1 engagement. Previously, HLA-B27 crystal structures have been generated using separate refolding of HLA-B27 HC, β2m and peptide (178, 179), but no SCT crystal structures have been made for this MHC I. We aimed to make four different SCT constructs to investigate the difference between how a 9mer and 11mer peptide sit in the binding groove of each HLA-B27 allele and whether there were any differences between how the peptides bind to each allele. There are currently no crystal structures available

for an 11mer peptide bound to HLA-B27, although there are structures available for HLA-B*2705 and –B*2709 bound to the same peptide (178). In this investigation they showed some flexibility in the binding of the peptide with slight differences in conformation when bound to HLA-B*2705 or –B*2709.

Initially, these SCTs were intended for use in LAMP1 assays as then we could be sure that all of the HLA-B27 complexes on the cell surface expressed the peptide of interest. However, despite good transfection of each SCT into HeLa ERAP1$^{-/-}$ cells, there were no differences between the addition of no SCT to these cells and transfection of any SCT in LAMP1 assays. While it is tempting to assume that this lack of difference may be because these cells are already inhibitory, it is important to remember that while HeLa ERAP1$^{-/-}$ B27 cells were highly inhibitory HeLa ERAP1$^{-/-}$ only inhibited NK cell activation by ~20% less than HeLa cells. Colleagues from Prof. Salim Khakoo's group have previously generated KIR2DL2/3 SCTs and transfected these into cells for use in LAMP1 assays and found that minimal inhibition of NK cells occurred. They have postulated that this lack of difference is probably due to a lack of flexibility within the SCT. For correct KIR engagement there must be some flexibility within the pMHC complex. Due to the disulphide trap and linker regions connecting each chain of the SCT, this flexibility is absent and thus correct engagement cannot occur (personal communication with Prof. Salim Khakoo). This supports the lack of result seen here with HLA-B27 and KIR3DL1 in the LAMP1 assays.

Purification of SCT protein for crystallisation trials was found to be highly problematic and, unfortunately, ultimately unsuccessful. Chromatograms from purification attempts by FPLC showed the presence of several higher order aggregates and dimers of SCT in each attempt. Bondos and Bicknell have shown several condition alterations that can prevent protein aggregation during concentration and purification that we could try but none of these have been tried for HLA previously (180). Additionally, Middelberg has reviewed three methods of on column refolding, potentially this would avoid the concentration step thereby preventing the chance of aggregation (181).

Without the generation of crystal structures it is impossible to determine whether the D116H change can alter peptide binding although, as it was previously shown that the same peptide bound to both alleles showed some changes in peptide-binding and flexibility (178), we would expect this to be the case.

5.6 Future directions

Taken together, these results suggest that the quality of peptide repertoire may have different effects on HLA-B*2705 and –B*2709. In particular it may be useful to determine the NK cell response to HeLa ERAP1$^{-/-}$ cells transfected with different ERAP1 variants in the presence of HLA-B*2705 and –B*2709. Evidence for this comes from the result showing that loss of ERAP1 from HeLa cells induces greater NK cell inhibition in HLA-B*2709 transfected cells than –B*2705^{+} cells. This work would tie in with current work by our collaborators in Israel who are working to determine the peptidome of HLA-B*2705 following ERAP1 variant transfection.

To determine whether PBMCs from HLA-B*2705 and –B*2709 individuals act differently, or are more prone to activation or induction of inflammatory pathways, it would be good to conduct these experiments in the presence of PBMCs from a –B*2705 and –B*2709 donor. This work may provide insight into the natural activation state of NK cells educated in the presence of differing HLA-B27 alleles.

Identifying a method of SCT purification without inducing aggregation is a priority as there is a wealth of knowledge that could be gleaned from the solving of these four crystal structures. Colleagues with more experience in protein purification are working on new recipes for the refold solution and methods of concentration, which might solve the aggregation issues. In addition, a colleague is working on expressing SCT protein in mammalian insect cells, as opposed to the bacterial system usually used. He has previously used this system to minimise purification issues seen with other proteins and is hopeful this may be a useful method for purifying SCT protein in this case.

Chapter 6: Concluding Remarks

Ankylosing Spondylitis is an autoimmune disease of the sacro-iliac region with an unknown pathogenesis despite strong genetic links with HLA-B27 and ERAP1. The contribution of both of these factors provide the greatest disease risk with 95% of AS patients expressing one or more HLA-B27 allele (182). However, how these factors initiate or contribute to disease has yet to be described. This body of work has aimed to show how ERAP1 polymorphisms may contribute to disease through alteration of the peptide repertoire and HLA-B27 complexes at the cell surface. Additionally, why the HLA-B*2705 allele is disease associated whereas –B*2709 is protective despite differing by only a single amino acid was examined.

Following previous reports that the amino acids at positions 7 and 8 of a 9 amino acid peptide alter KIR3DL1 engagement (115), the preference for KIR3DL1 engagement was investigated. Interestingly, new preferences for KIR3DL1 engagement were uncovered showing that the combinations P7V:P8A and P7I:P8S were inhibitory while P7H:P8S and P7R:P8S prevented inhibition, but further investigation is required to fully elucidate these. With the ability to investigate the effect of peptide differences on NK cell responses, the model system of using peptide minigenes to load peptides onto HeLa cells may be expanded to examine the role of peptide and KIR engagement in disease such as HIV-1 infection and AS.

Indeed, in HIV-1 infection, an interaction between KIRs and HLA-B has been implicated (81) with slower disease progression and better control of viral replication in patients with HLA-Bw4 epitope alleles (183). In addition, certain combinations of KIR3DL1 and HLA-Bw4 alleles have been shown to be protective in HIV-1 infection (82). It would be interesting to investigate whether particular viral epitopes from HIV-1 preferentially engage inhibitory KIRs preventing NK cell mediated killing of infected cells. In the context of AS, the knowledge of KIR3DL1/peptide engagement preferences may be important to examine the peptide repertoire presented in cells expressing different ERAP1 allotype combinations once elucidated. From this analysis we would be able to predict the NK response to each repertoire and potentially predict how different ERAP1 allotype combinations would affect NK cell activation to establish a link between the ERAP1 combinations identified in patients and pathogenesis.

So far there have been no reported incidences of AS is people who are HLA-B*2706^{+} or –B*2709^{+} (184). This is strange as all other alleles of HLA-B27 found in AS patients seems to be associated and these unassociated alleles only differ from the strongly associated HLA-B*2705 by one or two amino acids. In this work, we have shown that HLA-B*2709 seems to be more ERAP1-dependent requiring a good functioning ERAP1 in order to produce a peptide repertoire capable of inhibiting NK cell activation. On the other hand, HLA-B*2705 interaction with KIR3DL1 seemed unaltered by the presence or absence of ERAP1, other than in the comparison between AS-associated and control ERAP1 allotype combinations. This differential need for "normal" ERAP1 may explain why this allele is not associated with AS disease, suggesting that HLA-B*2709 may exhibit more dramatic changes in KIR3DL1 engagement leading to different education of NK cells.

Here, AS-associated ERAP1 allotype combinations were shown to induce greater NK cell activation than control ERAP1 allotype combinations, which induced the secretion of pro-inflammatory cytokines and an altered cytokine profile compared to that seen with control ERAP1 allotype combinations. This data suggests that PBMCs in AS patients may be prone to greater NK cell activation and release an altered cytokine profile, indicating the establishment/presence of a more pro-inflammatory response in PBMC compared to healthy controls. This idea is supported by the study by Fiorillo *et al* showing that the CTL response to a self-peptide was more dramatic with PBMCs from AS patients compared to PBMCs from healthy controls. Interestingly this study also showed that the response to a self-peptide bound to HLA-B*2705 induced a stronger CTL response than the same peptide bound to HLA-B*2709 (177); a difference that may be replicated in NK cell activation through KIR interaction with self-peptide.

An important aspect to consider is that ERAP1 SNPs are germline, meaning that any peptide repertoire differences will always be present in individuals. Despite these ever-present differences, age of onset for disease is ~28 years (although this is the age at which symptoms generally start so disease onset will likely occur sooner), suggesting that an additional trigger event is required to initiate disease. Based on the data presented here, an altered peptide repertoire resulting from different ERAP1 allotype combinations may result in NK cells that have higher basal activation levels in AS patients compared to the general population. This increase in NK cell activation is slight and insufficient to induce an immune response or inflammation on its own but, as demonstrated by the Luminex results and previous cytokine data for AS patients (136, 138, 139), is enough to alter the cytokine profile towards a more pro-inflammatory response. Therefore increased NK cell activation together with a potential propensity of NK cells and CTL to

respond more strongly to self-peptides (177), may mean that a minor trauma or injury occurring in the sacro-iliac region or a more distal site such as the gut may result in the presentation of a novel or infrequently observed self-peptide inducing a strong, inflammatory response that pushes an individual from exhibiting a low level of NK cell activation to a full, and eventually, chronic inflammatory state. This is supported by AS symptoms being localised to the spine with patients also exhibiting other auto-inflammatory disorders with 70% of AS patients showing symptoms of IBD and 10% of IBD patients having AS (3).

It has been proposed that $B27_2$ engagement of KIR3DL2 on Th17 cells can induce their proliferation and extend their lifespan potentially explaining the presence of high numbers of these cells in AS patients (89). This idea suggests that the presence of HLA-B27 will promote the life of these cells but does not explain how this rare Th17 CD4 T cell population is induced initially. In this study I have proposed a mechanism by which Th17 cell differentiation is promoted by the cytokine profile seen with AS-associated ERAP1 allotypes and inhibited with control allotypes; the activation of NK cells by AS-associated ERAP1 allotype combinations led to the release of TNFα and decreases in IFNγ and IL-10, conditions that favour the generation of Th17 cells (94). In this way, the work shown here combined with the previous study by Fiorillo *et al* (177) promotes the idea that NK cells educated on an AS-associated ERAP1 allotype combination background are more activated and respond more strongly to self-peptides further increasing NK cell activation. This leads to a cytokine profile of increased TNFα, IL-1 and IL-6, with decreased IFNγ (this study and (136, 139). These Th17 cells and the cytokines produced may also promote osteoclastogenesis and leading to both bone destruction and generation of new bone (155).

The difference in generation of TNFα by AS-associated ERAP1 allotype combinations may provide insight into why anti-TNFα treatment is only effective in around 50% of patients (9). The AS-associated ERAP1 allotype combinations A2, A5 and A6 showed TNFα levels similar to that of some control ERAP1 allotype combinations. At the moment there is no test used to determine the ERAP1 allotype combination status in patients. However, this identification may allow non-responder patients to be identified. In the non-responder patients there may be another disease mechanism that by passes the need for TNFα to induce inflammation. Evidence that non-responders to anti-TNFα treatment have increased Th17 cell levels and these cells produce more IL-17 and IL-23 but not TNFα support this idea (185). Therefore these patients may have a

difference in Th17 cells by which they produce less TNFα and more IL-17 and IL-23, which will be important to investigate.

This idea, plus the difference seen in NK cell activation to different ERAP1 allotype combinations, further supports the idea proposed by Reeves *et al* that sequencing of ERAP1 could be used as a diagnostic marker for the disease (6). Currently the process of sequencing both copies of the full ERAP1 gene is very labour intensive and takes at least 3 weeks per sample. Further optimisation, and the use of new sequencing techniques, may help to make this process more streamlined and hopefully lead to a diagnostic test for AS in the future.

One limitation of this work is the absence of isotype controls for several experiments. The flow cytometry data presented here was optimised to make use of the four available lasers on the Fortessa X-20 Flow cytometer with minimal overlap. However, the use of isotype controls would validate this data further. Isotype controls were included in the blocking experiments seen in chapter 4 (**Figure 4.6** & **Figure 4.7**) but this was not continued into the subsequent Luminex experiments as these isotype control conditions showed evidence of ADCC induction. With hindsight, this ADCC induction by isotype control antibodies could have also altered the cytokine profile released from the PBMCs and thus should have been included as control conditions within these experiments. While the lack of correct controls may skew the readers view of the data it is the author's belief that the differences in NK cell activation between the isotype control and without antibody were not great enough to have a major impact on the cytokine profile. It is the author's opinion that the Luminex results presented here should be viewed as a preliminary data suggesting an altered cytokine profile can be seen in the presence of AS-associated ERAP1 allotype combinations. As such, and as mentioned previously, several subsequent experiments, including the appropriate controls, would be required to confirm any of the data shown here.

The altered peptide repertoire presented by different ERAP1 combinations may have a significant effect on NK cell education, which is likely to be important in disease pathogenesis. According to the licensing hypothesis, NK cells need to engage the ligand of their inhibitory receptors in order to acquire responsiveness to appropriate targets (186). In agreement with this hypothesis, Parsons *et al* showed that KIR3DL1^{+} NK cells from Bw4^{+} donors were more responsive with increased IFNγ production and cytotoxicity than those isolated from Bw6^{+} donors (187). The disarming model proposes that NK cells which lack the cognate KIR for the expressed MHC class I

molecules are anergic or disarmed, while those with the corresponding KIR and MHC class I molecules are armed (188). The rheostat model, proposed by Brodin *et al*, suggests that stronger inhibitory signalling through more interactions between KIR and corresponding ligands leads to greater functional responsiveness of NK cells (189).

KIR expression in the most part is randomly determined by the KIR gene content, polymorphism and stochastic epigenetic regulation at the promoter level (72). This random acquisition of KIRs means that in some individuals there will be no inhibitory KIR expressed for the MHC I present, i.e. the KIRs expressed will not interact with any MHC I expressed by the individual (190, 191). Interactions between KIRs on NK cells and MHC I complexes will help to determine levels of KIR expression, limiting expression so that not too many inhibitory receptors are present on one NK cell (192).

In the context of this work it is possible that in control ERAP1 conditions, or HLA-B*2709^{+} individuals, the peptide repertoire presented to KIR3DL1 engages well leading to a strong response during NK cell education (according to the licensing hypothesis). Whereas AS associated ERAP1 allotypes may not engage so strongly meaning that the NK cells are not educated properly through KIR3DL1. If this is the case, then changes in the abundance of FHC or $B27_2$ at the cell surface due to cellular stress or presentation of a novel peptide could induce a greater NK cell response than anticipated. Evidence for this comes from the data showing that HeLa B*2709 cells do not inhibit NK cell activation, whereas HeLa ERAP1$^{-/-}$ B*2709 cells do suggesting that the repertoire of peptides is crucial for the engagement of KIR3DL1.

Alternatively, according to the rheostat model of NK cell education, there could be less strong engagement of KIR3DL1 than is seen with AS ERAP1 allotypes or in HLA-B*2705 individuals meaning that the NK cells are functionally less responsive, potentially making them less prone to involvement in autoimmune conditions. Furthermore, while it is true that FHC and $B27_2$ will always be present on the cell surface, it is not known whether NK cell education can occur through these molecules or if the interaction between FHC and KIR3DL1 is as strong as that of pB27 with KIR3DL1. For example, if FHC binding to KIR3DL1 is weaker this interaction may not be enough to license the NK cells during education.

Indeed the activation of NK cells observed in these experiments may not be due to KIR/MHC interactions but due to an up-regulation of NKG2D ligands such as MICA and MICB that induces an increase in NK cell activation leading to an altered cytokine profile. These ligands are up-regulated when the cell is stressed which may occur as a result of $B27_2$ accumulation in the cell

leading to UPR, which can also lead to a reduction of MHC I presentation at the cell surface, instead retaining pMHC complexes in the ER (193).

The question of how NK cell education plays a role in the pathogenesis of AS remains unclear and further investigation needed to elucidate. The identification of potential high-risk AS patients early in life may allow their NK cell activation levels and responses to self-peptides and infectious antigens to be determined. This may also establish whether a trigger event is required in NK cells to break their tolerance or whether this is a consequence of their education resulting in a more activated phenotype compared to healthy controls.

Whatever the mechanism of NK cell education, based on the data presented here I propose a model of AS pathogenesis whereby NK cells present in AS patients are more prone to activation, or already in a more activated state, than those from healthy controls and this prior 'arming' of NK cells induces a more exaggerated response to self-peptides that are novel or cryptic, as could occur following a minor injury in the sacro-iliac region or at a distal site. An exaggerated response to a self-peptide may induce the release of pro-inflammatory cytokines such as TNFα, IL-1 and IL-6. This cytokine environment would then promote the generation of both Th17 cells and osteoclasts, potentially aiding in creating a chronic inflammatory environment and new bone formation (**Figure 6.1**).

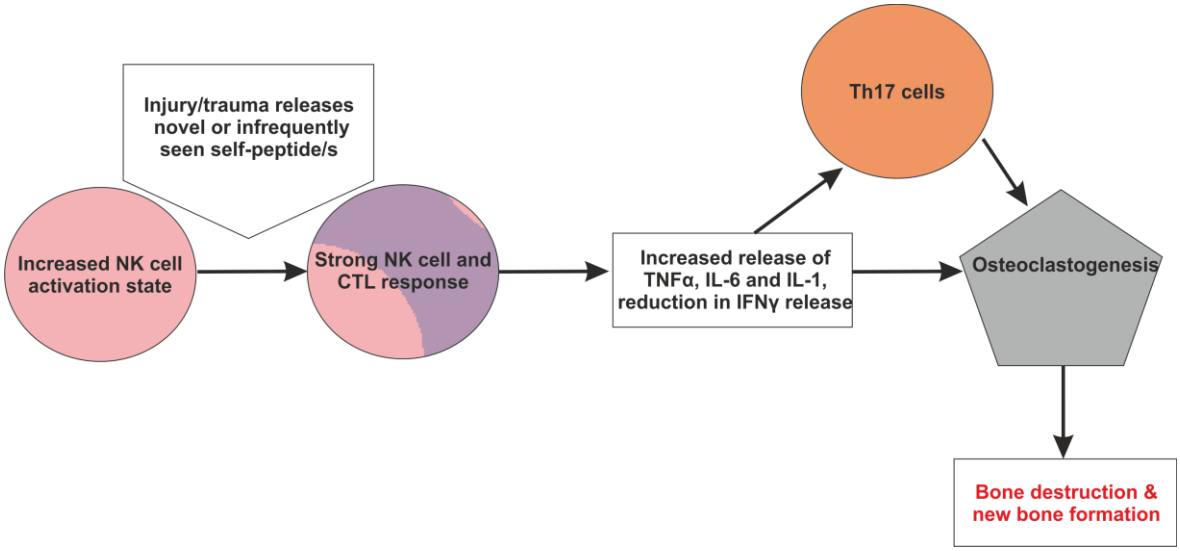

Figure 6.1: Schematic of how NK cells induce osteoclastogenesis

NK cells from AS patients are potentially at an increased activation state than those from healthy controls. Following an injury the release of novel or not commonly seen self-peptides could induce a strong, and unnecessary, CTL and NK cell response leading to increases in the release of TNFα, IL-6 and IL-1. This cytokine release, along with a reduction in IFNγ release could induce both the formation of Th17 $CD4^+$ T cells and osteoclasts. Th17 cells produce cytokines that can also induce osteoclastogenesis such as IL-1. Osteoclasts can destroy bone but have also been implicated in the formation of new bone – a key feature of AS disease.

Appendix A Antibody information

Antigen	Fluorophore	Clone (Cat. Number)	Company
CD107a	eFluor 660 (APC)	eBioH4A3	eBioscience
CD56 (NCAM)	AF488 (FITC)	HCD56	Biolegend
CD3	PerCP	UCHT1	Biolegend
CD158e1 (KIR3DL1)	PE	DX9	Biolegend
CD158e1 (KIR3DL1)	BV421	DX9	Biolegend
CD158k (KIR3DL2)	PE	DX31, FAB2878P	R&D Systems
Anti-Mouse IgG	PE	Goat, ab7002	Abcam
Streptavidin	PE	554061	Pharmingen
MHC class I	Unconjugated	W632	Made in house
HLA-B7, -B22, -B27, -B42, -B67, -B73	Unconjugated	ME.1	Made in house
Free heavy chains	Unconjugated	HC10	Made in house
CD158b	FITC	559784	BD Biosciences
CD56 (NCAM)	PeCy7	HCD56	Biolegend

Appendix B Peptide database analysis

Cell Line	Peptide Sequence	Amino acid			References
		P7	P8	P9	
C1R05	ARAPAPYKR	Y	K	R	(12)
	ARDNTINLI	N	L	I	(5)
	ARFVNVLGY	L	G	Y	(2), (12)
	ARHPSFFLY	F	L	Y	(12)
	ARLKEVLEY	L	E	Y	(8), (14)
	ARLLMPSQL	S	Q	L	(2)
	ARLQTALLV	L	L	V	(1), (7), (8), (11), (13)
	ARLTDYVAF	V	A	F	(8), (9)
	ARYSHVSQH	S	Q	H	(12)
	ERLEKFFHR	F	H	R	(2), (12)
	FRYQGHVGA	V	G	A	(2), (12)
	GRALQASAL	S	A	L	(5)
	GRFEDVYQL	Y	Q	L	(5)
	GRFEGTSTK	S	T	K	(3), (8), (11), (12)
	GRHEQVVER	V	E	R	(12)
	GRIGPNIRL	I	R	L	(8), (11)
	GRLGSTVFV	V	F	V	(2)
	GRMPFPVNH	V	N	H	(2), (12)
	GRNSNICHY	C	H	Y	(12)
	GRSGYNYFF	Y	F	F	(12)
	GRSLPRFQV	F	Q	V	(12)
	GRSLPVLGL	L	G	L	(2), (12)
	GRSPLHLAV	L	A	V	(5)
	GRTELAIKL	I	K	L	(5)
	GRTFIQPNM	P	N	M	(3), (8), (9), (12)
	GRWDQQYVI	Y	V	I	(12)
	GRWFGGRQI	R	Q	I	(12)
	GRWPGSSLY	S	L	Y	(8), (9)
	GRYDGLVGM	V	G	M	(2)
	GRYRGSVHF	V	H	F	(5)
	HRDSHITNL	T	N	L	(2), (12)
	HRHGKPFVF	F	V	F	(12)
	HRIGQQNEV	N	E	V	(8), (12), (13)
	HRIGQTKTV	K	T	V	(8), (12), (13)
	HRLPHVLLL	L	L	L	(12)
	IRCIPSQAV	Q	A	V	(12)
	IRGAIILAK	L	A	K	(8), (9)
	IRHGATHVF	H	V	F	(12)
	IRNDVLDSL	D	S	L	(5)
	IRNIPIPTL	P	T	L	(12)
	IRNSRPLVK	L	V	K	(12)
	IRYPDSHQL	H	Q	L	(5)
	KRFKEANNF	N	N	F	(1), (7), (8), (10), (11), (12), (13)
	KRLEEIPLI	P	L	I	(12)
	KRNDYVHAL	H	A	L	(8)
	LRARVRPLF	P	L	F	(12)
	LRFQSSAVM	A	V	M	(3), (8)
	LRHPGIVNL	V	N	L	(8), (11)
	LRHPNIVSL	V	S	L	(5)
	LRNHMAVAF	V	A	F	(2), (12)
	LRVDPVNFK	N	F	K	(1), (8), (11), (12)

	MRMATPLLM	L	L	M	(8), (9)
	NRIVYLYTK	Y	T	K	(8), (9)
	QRDDILINR	I	N	R	(5)
	QRGPVRVGF	V	G	F	(8), (12)
	QRIGPLAFL	A	F	L	(12)
	QRLKEYRSK	R	S	K	(12)
	QRNVNVFKF	F	K	F	(12)
	QRVNVQPEL	P	E	L	(8), (9)
	RRAPHLHTL	H	T	L	(12)
	RRARGKVKV	V	K	V	(5)
	RRDFNHINV	I	N	V	(8), (12)
	RRDPNNYRP	Y	R	P	(12)
	RRFDPKLFL	L	F	L	(12)
	RRFKGQILM	I	L	M	(12)
	RRFWQGDTF	D	T	F	(12)
	RRGEFIQEI	Q	E	I	(8), (13)
	RRGEIQHRM	H	R	M	(12)
	RRGFFFSHV	S	H	V	(12)
	RRGPPPRRY	R	R	Y	(12)
	RRIALGNNV	N	N	V	(5)
	RRIATGSFL	S	F	L	(8), (12), (13)
	RRKDGVFLY	F	L	Y	(12)
	RRLGVQQSL	Q	S	L	(5)
	RRNEKIAVH	A	V	H	(12)
	RRNGNLTAF	T	A	F	(12)
	RRNPEPLRF	L	R	F	(12)
	RRSGPPASY	A	S	Y	(12)
	RRSQPLISL	I	S	L	(12)
	RRYQKSTEL	T	E	L	(4), (6), (8), (12), (13)
	RRYVRKFVL	F	V	L	(4)
	SRAFLAQAL	Q	A	L	(5)
	SRANSLFAF	F	A	F	(12)
	SRASTLAKF	A	K	F	(12)
	SRAVQEFGL	F	G	L	(5)
	SRFGKFIQL	I	Q	L	(12)
	SRFGKFVEI	V	E	I	(12)
	SRFIKFQEM	Q	E	M	(2), (12)
	SRFNFDNKY	N	K	Y	(12)
	SRHGIQKKL	K	K	L	(12)
	SRHGSSVTR	V	T	R	(12)
	SRLPQLVGV	V	G	V	(5)
	SRSVIRPPF	P	P	F	(12)
	SRTPPVTRR	T	R	R	(12)
	SRTPYHVNL	V	N	L	(1), (7), (8), (11), (12)
	SRVGFVRGY	R	G	Y	(12)
	SRYSQKQHY	Q	H	Y	(12)
	TRSELLPFL	P	F	L	(12)
	VRFLEQQTL	Q	T	L	(5)
	VRLPYPLQM	L	Q	M	(12)
	YRVYQPVRY	V	R	Y	(12)
HeLa	ARAGVLAER	A	E	R	(2)
	ARAVVEKRL	K	R	L	(2)
	ARDALAKNL	K	N	L	(2)
	ARFEQLISR	I	S	R	(8), (11)
	ARFGLIQSM	Q	S	M	(8), (9), (13)
	ARFKERVGY	V	G	Y	(2)
	ARGMFVFGY	F	G	Y	(2)

ARHGLYEKK	E	K	K	(2)
ARHKLQHHL	H	H	L	(2)
ARIALLPLL	P	L	L	(2)
ARIDEVVSR	V	S	R	(2)
ARIGEAEAK	E	A	K	(2)
ARIGQTGTK	G	T	K	(2)
ARIGSTVNM	V	N	M	(2)
ARILQQHGY	H	G	Y	(2)
ARIMQIHSR	H	S	R	(2)
ARIPPVAVR	A	V	R	(2)
ARLDHKFDL	F	D	L	(2)
ARLFGIRAK	R	A	K	(6), (8), (11)
ARLGVISKV	S	K	V	(8)
ARLGVVTGL	T	G	L	(2)
ARLKDALVR	L	V	R	(2)
ARLKLSEEL	E	E	L	(2)
ARLQIVLGH	L	G	H	(2)
ARNLIYFGF	F	G	F	(2)
ARNPNNMQV	M	Q	V	(2)
ARSASAAAR	A	A	R	(2)
ARSEQFINL	I	N	L	(2)
ARSGEKITV	I	T	V	(1), (8), (11)
ARSGMKIGR	I	G	R	(2)
ARTPVTSTY	S	T	Y	(2)
ARTSPVTAR	T	A	R	(2)
ARVAEQLRA	L	R	A	(2)
ARVDAVAAR	A	A	R	(2)
ARVGQALEL	L	E	L	(8), (13)
ARVSIVNQY	N	Q	Y	(8), (14)
ARYLVNEGF	E	G	F	(2)
CRTFHTIGF	I	G	F	(8)
DRELCQLLL	L	L	L	(2)
DRLQLFIAK	I	A	K	(2)
ERIEKLWKR	W	K	R	(2)
FRHPHIIKL	I	K	L	(2)
FRKAQIQGL	Q	G	L	(8)
FRKKLNAGY	A	G	Y	(2)
FRNIPGITL	I	T	L	(8), (11), (13)
FRYPQDYQF	Y	Q	F	(2)
GRAPVLVAL	V	A	L	(2)
GRASYGVSK	V	S	K	(2)
GRDVHTFAF	F	A	F	(2)
GRFADSHEL	H	E	L	(8), (11)
GRFDVKIEV	I	E	V	(8)
GRFEGDTGL	T	G	L	(2)
GRFFLSSGL	S	G	L	(2)
GRFHMYEGY	E	G	Y	(2)
GRFPQVQAF	Q	A	F	(2)
GRFSEPHAR	H	A	R	(2)
GRHAVVVGR	V	G	R	(2)
GRIEILSGF	S	G	F	(2)
GRILSQVSY	V	S	Y	(2)
GRIPFTVSL	V	S	L	(2)
GRIPSAVGY	V	G	Y	(2)
GRKEIDIKK	I	K	K	(2)
GRLAAIVAK	V	A	K	(8), (11)
GRLEGGSAR	S	A	R	(2)
GRLLGIITK	I	T	K	(2)

GRLSNISHL	S	H	L	(8), (11)
GRLVKDMKI	M	K	I	(2)
GRNQGGYDR	Y	D	R	(2)
GRQKELVSR	V	S	R	(2)
GRQKIHISK	I	S	K	(2)
GRSEYVEKF	E	K	F	(2)
GRSPVVLSL	L	S	L	(2)
GRTGGSWFK	W	F	K	(2)
GRTLSDYNI	Y	N	I	(8), (11)
GRTPEAVQK	V	Q	K	(2)
GRTYPVQEY	Q	E	Y	(2)
GRVDFAYKF	Y	K	F	(2)
GRVDVVKAL	K	A	L	(2)
GRVKESITR	I	T	R	(2)
GRVLIGVGK	V	G	K	(2)
GRVLYAYGY	Y	G	Y	(2)
GRVNVVEAL	E	A	L	(2)
GRVPLILNL	L	N	L	(2)
GRVRPGETL	E	T	L	(8), (13), (14)
GRWKDILTH	L	T	H	(2)
GRYGEDLLF	L	L	F	(2)
GRYGSTNAR	N	A	R	(2)
GRYIPPHLR	H	L	R	(2)
HRAPPIIGY	I	G	Y	(2)
HRIKDYHSY	H	S	Y	(2)
HRLEELYTK	Y	T	K	(2)
HRTELETKL	T	K	L	(2)
IRFEVSPSY	P	S	Y	(2)
IRFILIQNR	Q	N	R	(2)
IRKLIKDGL	D	G	L	(8), (11)
IRNDEELNK	L	N	K	(8), (9)
IRQAGGIGK	I	G	K	(2)
IRTITVVQR	V	Q	R	(2)
KRADLQSTF	S	T	F	(2)
KRAEEVVVR	V	V	R	(2)
KREPGTKTK	K	T	K	(2)
KRFDDKYTL	Y	T	L	(8)
KRFEELTNL	T	N	L	(2)
KRFEGLTAR	T	A	R	(2)
KRFEKVYTH	Y	T	H	(2)
KRGEPAIYR	I	Y	R	(2)
KRGILTLKY	L	K	Y	(8), (10)
KRIDIIHNL	H	N	L	(8)
KRIHGVGFK	G	F	K	(2)
KRKVLILTL	L	T	L	(2)
KRLDEKLGI	L	G	I	(2)
KRLEIEKSL	K	S	L	(2)
KRLKVTELR	E	L	R	(2)
KRLPDGLTR	L	T	R	(2)
KRLPPFETF	E	T	F	(2)
KRMAEERRK	R	R	K	(2)
KRSFLLDIL	D	I	L	(2)
KRTPDFHDK	H	D	K	(2)
KRVEEIKQK	K	Q	K	(2)
KRVQVDVKM	V	K	M	(2)
LRAVTLTAK	T	A	K	(2)
LRFPEILQK	L	Q	K	(2)
LRLEAGLNR	L	N	R	(2)

LRLSASALF	A	L	F	(2)
MRANITAIR	A	I	R	(2)
MRFDGRLGF	L	G	F	(2)
MRFLAATFL	T	F	L	(2)
MRLELDALR	A	L	R	(2)
MRLGSIFGL	F	G	L	(2)
MRLLPRLLL	L	L	L	(2)
MRMSVGLSL	L	S	L	(2)
MRTSYLLLF	L	L	F	(2)
MRYVASYLL	Y	L	L	(2)
NRFKGVKYF	K	Y	F	(2)
NRHEGVFKF	F	K	F	(2)
NRHKEVIVK	I	V	K	(2)
NRIAETHSK	H	S	K	(2)
NRIKGIPKL	P	K	L	(8), (11), (13)
NRLSFFFDF	F	D	F	(2)
NRLTKIEGL	E	G	L	(8), (11)
NRSDYMFQR	F	Q	R	(2)
NRTTIVVAH	V	A	H	(2)
NRYEKIVKK	V	K	K	(2)
QRDPPHNNF	N	N	F	(8), (11)
QRGALFLLF	L	L	F	(2)
QRHEIVQTL	Q	T	L	(2)
QRMTTQLLL	L	L	L	(2)
QRNELNAKV	A	K	V	(8), (11)
QRNVNIFKF	F	K	F	(8), (9)
QRSSGLVQR	V	Q	R	(2)
QRTDVLTGL	T	G	L	(2)
RRFKEPWFL	W	F	L	(2)
RRIYDLIEL	I	E	L	(8), (13)
RRKQEEEAR	E	A	R	(2)
RRLGLALGL	L	G	L	(8)
RRRWRRLTV	L	T	V	(8), (13)
RRSSSLKER	K	E	R	(2)
RRVEKHWRL	W	R	L	(1), (8)
RRVPLPLLL	L	L	L	(2)
SRAGPLSGK	S	G	K	(2)
SRAKPAVGR	V	G	R	(2)
SRAYPTPLR	P	L	R	(2)
SRFGGAVVR	V	V	R	(2)
SRFLIINAM	N	A	M	(2)
SRFLNKQPY	Q	P	Y	(2)
SRFQGTLYL	L	Y	L	(2)
SRFSNVYHL	Y	H	L	(2)
SRFVHGEGL	E	G	L	(2)
SRIGTSTSF	T	S	F	(2)
SRIHPVSTM	S	T	M	(8), (11)
SRIPMPVNF	V	N	F	(2)
SRKFGQLRL	L	R	L	(8), (13), (14)
SRLATLNEK	N	E	K	(2)
SRLIGGISK	I	S	K	(2)
SRLKASESF	E	S	F	(2)
SRLPSYFVR	F	V	R	(2)
SRLQEVFGH	F	G	H	(2)
SRLQPFLQR	L	Q	R	(2)
SRLTLLTLL	T	L	L	(2)
SRNAGAFGF	F	G	F	(2)
SRNAQSLGF	L	G	F	(2)

	SRNEGVATY	A	T	Y	(2)
	SRNPRGFFL	F	F	L	(2)
	SRNPTFMGL	M	G	L	(2)
	SRSFPFVSK	V	S	K	(2)
	SRSPPPVSK	V	S	K	(2)
	SRSWLSYSY	Y	S	Y	(2)
	SRTEGRPTV	P	T	V	(2)
	SRTEISSSR	S	S	R	(2)
	SRTEVASSR	S	S	R	(2)
	SRTEVISSR	S	S	R	(2)
	SRTVGPTQR	T	Q	R	(2)
	SRVKFSPSL	P	S	L	(2)
	SRVLIFSQM	S	Q	M	(2)
	SRVNIPKVL	K	V	L	(2)
	SRWEEYISK	I	S	K	(2)
	SRWEKVVQR	V	Q	R	(2)
	SRYKDTINK	I	N	K	(2)
	TRDPIVKEK	K	E	K	(2)
	TRFTGATGR	T	G	R	(2)
	TRHGSFVNK	V	N	K	(2)
	TRIPKIQQL	Q	Q	L	(2)
	TRIPKVQKL	Q	K	L	(2)
	TRLFAVLRF	L	R	F	(2)
	TRWNKIVLK	V	L	K	(2)
	VRAGVLKEK	K	E	K	(2)
	VRLGSLSTK	S	T	K	(2)
	VRNEPTVSR	V	S	R	(2)
	VRNPSVVVK	V	V	K	(2)
	VRWVGGPEI	P	E	I	(2)
	YRIGDLQAF	Q	A	F	(2)
	YRIPLNPYL	P	Y	L	(2)
	YRKGHFTSL	T	S	L	(2)
	YRYPGGESY	E	S	Y	(2)
	YRYPIVLGY	L	G	Y	(2)
LG2	ARFQHGHSR	H	S	R	(12)
	ARFYKLHER	H	E	R	(12)
	ARKERQLHM	L	H	M	(12)
	GRFSGLLGR	L	G	R	(8), (9), (12)
	GRIGVFPSV	P	S	V	(12)
	GRTKIFIRF	I	R	F	(12)
	GRTKPIPKK	P	K	K	(12)
	GRWQYPLIY	L	I	Y	(2), (12)
	GRYLRRELL	E	L	L	(12)
	GRYSGRKAV	K	A	V	(8), (12)
	HRAQLQIRI	I	R	I	(12)
	IRSSLLLGF	L	G	F	(12)
	KRFGKAYNL	Y	N	L	(1), (8), (12)
	KRHFRRDSF	D	S	F	(12)
	KRHRIQFKY	F	K	Y	(12)
	KRLHQEERM	E	R	M	(12)
	KRLKTVLEL	L	E	L	(12)
	KRLQQFLEF	L	E	F	(12)
	KRVFPKWTY	W	T	Y	(12)
	KRYHIAKVY	K	V	Y	(12)
	KRYKNRPGL	P	G	L	(12)
	LRAGLVLGF	L	G	F	(12)
	RRAPVPRTK	R	T	K	(12)

	RRAPVVVRL	V	R	L	(12)
	RRFARAPSL	P	S	L	(12)
	RRFDRKAAM	A	A	M	(12)
	RRFFKAKKL	K	K	L	(12)
	RRFGGPVHH	V	H	H	(12)
	RRFGIQAQM	A	Q	M	(12)
	RRFRASPLF	P	L	F	(12)
	RRFRPRSEF	S	E	F	(12)
	RRFTRPEHL	E	H	L	(12)
	RRGNNGPPK	P	P	K	(12)
	RRGVISPNF	P	N	F	(12)
	RRHYNGEAY	E	A	Y	(12)
	RRKGEQIYY	I	Y	Y	(12)
	RRKQLQNYL	N	Y	L	(12)
	RRKQPFTHF	T	H	F	(12)
	RRLDPIPQL	P	Q	L	(12)
	RRLERIKQK	K	Q	K	(12)
	RRLPHVVSH	V	S	H	(12)
	RRLPILPTL	P	T	L	(12)
	RRLRVLSGH	S	G	H	(12)
	RRMAEEFRL	F	R	L	(12)
	RRNPYFRNK	R	N	K	(12)
	RRTRGPVER	V	E	R	(12)
	RRVARQAQL	A	Q	L	(12)
	RRVEHNQSY	Q	S	Y	(12)
	RRYPQVVTR	V	T	R	(12)
	RRYQGPRTK	R	T	K	(12)
	SRWPAFPAF	P	A	F	(12)
	VRIGLTLLL	L	L	L	(12)
	YRFFLGNQF	N	Q	F	(12)
	YRYNPRPRL	P	R	L	(12)
P50	ARIYHTIAY	I	A	Y	(12)
	ARLPKPKAK	K	A	K	(12)
	ARLPLRLFL	L	F	L	(12)
	ARNPVSRNF	R	N	F	(12)
	ARQKLALRR	L	R	R	(12)
	GRCGSVLVR	L	V	R	(12)
	GRFPRLLTR	L	T	R	(12)
	GRIGRLVTR	V	T	R	(12)
	GRVAPRSGL	S	G	L	(8), (12), (13)
	GRVKGRTGL	T	G	L	(8), (12), (13)
	GRYAGGQGY	Q	G	Y	(12)
	GRYTIKVLF	V	L	F	(12)
	HRHFQHHAK	H	A	K	(12)
	IRNGHIATR	A	T	R	(12)
	KRAYIPRTL	R	T	L	(12)
	KRFQVAVNL	V	N	L	(12)
	KRNLPRRGL	R	G	L	(12)
	KRTTVVAQL	A	Q	L	(3), (8), (12)
	MRQKAVSLF	S	L	F	(2)
	NRLPLVVSF	V	S	F	(12)
	QRYPNPYSK	Y	S	K	(1), (8), (12)
	RRAARQWQL	W	Q	L	(12)
	RRAGIKVTV	V	T	V	(1), (8), (12)
	RRILRLSTF	S	T	F	(12)
	RRIQPPLGF	L	G	F	(12)
	RRLPVPRAK	R	A	K	(12)
	RRMYPPPLI	P	L	I	(12)

RRQQQQLRY	L	R	Y	(12)
RRYAHVVLR	V	L	R	(12)
SRFARLQKL	Q	K	L	(12)
SRIALKSGY	S	G	Y	(12)
SRIRKLFNL	F	N	L	(8), (12)
SRLAIRNEF	N	E	F	(12)
SRLGSVFPF	F	P	F	(12)
SRLPLARVK	R	V	K	(12)
SRMIRKMKL	M	K	L	(12)
SRNGSVFVR	F	V	R	(12)
SRNQQIFLR	F	L	R	(12)
SRVKLILEY	L	E	Y	(7), (8), (11), (12)
SRVQVQKAF	K	A	F	(12)
SRYRPQYGY	Y	G	Y	(12)
TRNGKIIGK	I	G	K	(12)
TRYQGVNLY	N	L	Y	(8), (9), (12)
VRAKWFPEV	P	E	V	(12)
VRFKHRYLL	Y	L	L	(12)
YRIKFKESF	E	S	F	(12)

Peptide Database References

1 **Alvarez I**, *et al.* The Cys-67 residue of HLA-B27 influences cell surface stability, peptide specificity, and T-cell antigen presentation. The Journal of biological chemistry. **2001 Dec 28;276(52):48740-7**

2 **Ben Dror L**, Barnea E, Beer I, Mann M, Admon A. The HLA-B*2705 peptidome. Arthritis Rheum. **2010 Feb;62(2):420-9**.

3 **Fiorillo MT**, *et al*. Susceptibility to ankylosing spondylitis correlates with the C-terminal residue of peptides presented by various HLA-B27 subtypes. Eur J Immunol. **1997 Feb;27(2):368-73**

4 **García F**, *et al*. HLA-B27 (B*2701) specificity for peptides lacking Arg2 is determined by polymorphism outside the B pocket. Tissue Antigens. **1997;49(6):580-7.**

5 **Gomez P**, *et al*. B*2707 differs in peptide specificity from B*2705 and B*2704 as much as from HLA-B27 subtypes not associated to spondyloarthritis. Eur J Immunol. **2006 Jul;36(7):1867-81**.

6 **Jardetzky T**, *et al* . Identification of self peptides bound to purified HLA-B 27. Nature. **1991;353(6342):326-9.**

7 **Lamas JR,** *et al*. Modulation at multiple anchor positions of the peptide specificity of HLA-B27 subtypes differentially associated with ankylosing spondylitis. Arthritis Rheum. **1999 Sep;42(9):1975-85**.

8 **Lopez de Castro JA**, *et al*. HLA-B27: a registry of constitutive peptide ligands. Tissue Antigens. **2004 May;63(5):424-45.**

9 **Luckey CJ**, *et al*. Differences in the expression of human class I MHC alleles and their associated peptides in the presence of proteasome inhibitors. Journal of immunology. **2001 Aug 1;167(3):1212-21.**

10 **Marti M**, *et al*. Large sharing of T-cell epitopes and natural ligands between HLA-B27 subtypes (B*2702 and B*2705) associated with spondyloarthritis. Tissue Antigens. **2001 Dec;58(6):351-62.**

11 **Ramos M**, *et al*. Differential association of HLA-B*2705 and B*2709 to ankylosing spondylitis correlates with limited peptide subsets but not with altered cell surface stability. The Journal of biological chemistry. **2002 Aug 9;277(32):28749-56.**

12 **Sanz-Bravo A**, *et al*. Dominant role of the ERAP1 polymorphism R528K in shaping the HLA-B27 peptidome through differential processing determined by multiple peptide residues. Arthritis & rheumatology. **2014 Dec 2.**

13 **Sesma L**, *et al*. The peptide repertoires of HLA-B27 subtypes differentially associated to spondyloarthropathy (B*2704 and B*2706) differ by specific changes at three anchor positions. The Journal of biological chemistry. **2002 May 10;277(19):16744-9.**

14 **Sesma L**, *et al*. Species-specific differences in proteasomal processing and tapasin-mediated loading influence peptide presentation by HLA-B27 in murine cells. The Journal of biological chemistry. **2003 Nov 21;278(47):46461-72.**

List of References

1. Evans DM, Spencer CC, Pointon JJ, Su Z, Harvey D, Kochan G, et al. Interaction between ERAP1 and HLA-B27 in ankylosing spondylitis implicates peptide handling in the mechanism for HLA-B27 in disease susceptibility.[Erratum appears in Nat Genet. 2011 Sep;43(9):919 Note: Opperman, Udo [corrected to Oppermann, Udo]; Moutsianis, Loukas [corrected to Moutsianas, Loukas]]. Nature Genetics. 2011;43(8):761-7.

2. Sieper J, Braun J, Rudwaleit M, Boonen A, Zink A. Ankylosing spondylitis: an overview. Annals of the Rheumatic Diseases. 2002;61(suppl 3):iii8-iii18.

3. Reveille JD, Sims AM, Danoy P, Evans DM, Leo P, Pointon JJ, et al. Genome-wide association study of ankylosing spondylitis identifies non-MHC susceptibility loci. Nat Genet. 2010;42(2):123-7.

4. Reveille J. Recent studies on the genetic basis of ankylosing spondylitis. Current Rheumatology Reports. 2009;11(5):340-8.

5. Rudwaleit M, Jurik AG, Hermann KGA, Landewé R, van der Heijde D, Baraliakos X, et al. Defining active sacroiliitis on magnetic resonance imaging (MRI) for classification of axial spondyloarthritis: a consensual approach by the ASAS/OMERACT MRI group. Annals of the Rheumatic Diseases. 2009;68(10):1520-7.

6. Reeves E, Colebatch-Bourn A, Elliott T, Edwards CJ, James E. Functionally distinct ERAP1 allotype combinations distinguish individuals with Ankylosing Spondylitis. Proc Natl Acad Sci U S A. 2014;111(49):17594-9.

7. Saric T, Chang SC, Hattori A, York IA, Markant S, Rock KL, et al. An IFN-gamma-induced aminopeptidase in the ER, ERAP1, trims precursors to MHC class I-presented peptides. Nat Immunol. 2002;3(12):1169-76.

8. York IA, Chang SC, Saric T, Keys JA, Favreau JM, Goldberg AL, et al. The ER aminopeptidase ERAP1 enhances or limits antigen presentation by trimming epitopes to 8-9 residues. Nat Immunol. 2002;3(12):1177-84.

9. Braun J, Brandt J, Listing J, Zink A, Alten R, Golder W, et al. Treatment of active ankylosing spondylitis with infliximab: a randomised controlled multicentre trial. The Lancet. 2002;359(9313):1187-93.

10. Braun J, Baraliakos X, Brandt J, Listing J, Zink A, Alten R, et al. Persistent clinical response to the anti-TNF-alpha antibody infliximab in patients with ankylosing spondylitis over 3 years. Rheumatology (Oxford). 2005;44(5):670-6.

11. Harvey D, Pointon JJ, Evans DM, Karaderi T, Farrar C, Appleton LH, et al. Investigating the genetic association between ERAP1 and ankylosing spondylitis. Human Molecular Genetics. 2009;18(21):4204-12.

12. Hampton RY. ER stress response: Getting the UPR hand on misfolded proteins. Current Biology. 2000;10(14):R518-R21.

13. Allen RL, O'Callaghan CA, McMichael AJ, Bowness P. Cutting edge: HLA-B27 can form a novel beta 2-microglobulin-free heavy chain homodimer structure. J Immunol. 1999;162(9):5045-8.

14. Kollnberger S, Bird L, Sun MY, Retiere C, Braud VM, McMichael A, et al. Cell-surface expression and immune receptor recognition of HLA-B27 homodimers. Arthritis Rheum. 2002;46(11):2972-82.

15. Colbert RA, Tran TM, Layh-Schmitt G. HLA-B27 misfolding and ankylosing spondylitis. Molecular immunology. 2014;57(1):44-51.

16. Haroon N, Tsui FW, Uchanska-Ziegler B, Ziegler A, Inman RD. Endoplasmic reticulum aminopeptidase 1 (ERAP1) exhibits functionally significant interaction with HLA-B27 and relates to subtype specificity in ankylosing spondylitis. Annals of the Rheumatic Diseases. 2012;71(4):589-95.

17. Tsujimoto M, Hattori A. The oxytocinase subfamily of M1 aminopeptidases. Biochim Biophys Acta. 2005;1751(1):9-18.

18. Hattori A, Matsumoto H, Mizutani S, Tsujimoto M. Molecular cloning of adipocyte-derived leucine aminopeptidase highly related to placental leucine aminopeptidase/oxytocinase. J Biochem. 1999;125(5):931-8.

19. Cui X, Hawari F, Alsaaty S, Lawrence M, Combs CA, Geng W, et al. Identification of ARTS-1 as a novel TNFR1-binding protein that promotes TNFR1 ectodomain shedding. J Clin Invest. 2002;110(4):515-26.

20. Serwold T, Gonzalez F, Kim J, Jacob R, Shastri N. ERAAP customizes peptides for MHC class I molecules in the endoplasmic reticulum. Nature. 2002;419(6906):480-3.

21. York IA, Brehm MA, Zendzian S, Towne CF, Rock KL. Endoplasmic reticulum aminopeptidase 1 (ERAP1) trims MHC class I-presented peptides in vivo and plays an important role in immunodominance. Proc Natl Acad Sci U S A. 2006;103(24):9202-7.

22. Blanchard N, Shastri N. Coping with loss of perfection in the MHC class I peptide repertoire. Curr Opin Immunol. 2008;20(1):82-8.

23. Chang SC, Momburg F, Bhutani N, Goldberg AL. The ER aminopeptidase, ERAP1, trims precursors to lengths of MHC class I peptides by a "molecular ruler" mechanism. Proceedings of the National Academy of Sciences of the United States of America. 2005;102(47):17107-12.

24. Kanaseki T, Blanchard N, Hammer GE, Gonzalez F, Shastri N. ERAAP synergizes with MHC class I molecules to make the final cut in the antigenic peptide precursors in the endoplasmic reticulum. Immunity. 2006;25(5):795-806.

25. Hammer GE, Gonzalez F, James E, Nolla H, Shastri N. In the absence of aminopeptidase ERAAP, MHC class I molecules present many unstable and highly immunogenic peptides. Nat Immunol. 2007;8(1):101-8.

26. Yan J, Parekh VV, Mendez-Fernandez Y, Olivares-Villagomez D, Dragovic S, Hill T, et al. In vivo role of ER-associated peptidase activity in tailoring peptides for presentation by MHC class Ia and class Ib molecules. J Exp Med. 2006;203(3):647-59.

27. Blanchard N, Kanaseki T, Escobar H, Delebecque F, Nagarajan NA, Reyes-Vargas E, et al. Endoplasmic reticulum aminopeptidase associated with antigen processing defines the composition and structure of MHC class I peptide repertoire in normal and virus-infected cells. J Immunol. 2010;184(6):3033-42.

28. Nagarajan NA, Gonzalez F, Shastri N. Nonclassical MHC class Ib-restricted cytotoxic T cells monitor antigen processing in the endoplasmic reticulum. Nature Immunology. 2012;13(6):579-86.

29. Reeves E, Edwards CJ, Elliott T, James E. Naturally Occurring ERAP1 Haplotypes Encode Functionally Distinct Alleles with Fine Substrate Specificity. J Immunol. 2013;191(1):35-43.

30. Fung EY, Smyth DJ, Howson JM, Cooper JD, Walker NM, Stevens H, et al. Analysis of 17 autoimmune disease-associated variants in type 1 diabetes identifies 6q23/TNFAIP3 as a susceptibility locus. Genes Immun. 2009;10(2):188-91.

31. Strange A, Capon F, Spencer CC, Knight J, Weale ME, Allen MH, et al. A genome-wide association study identifies new psoriasis susceptibility loci and an interaction between HLA-C and ERAP1. Nat Genet. 2010;42(11):985-90.

32. Guerini FR, Cagliani R, Forni D, Agliardi C, Caputo D, Cassinotti A, et al. A functional variant in ERAP1 predisposes to multiple sclerosis. PLoS One. 2012;7(1):e29931.

33. Mehta AM, Jordanova ES, Corver WE, van Wezel T, Uh HW, Kenter GG, et al. Single nucleotide polymorphisms in antigen processing machinery component ERAP1 significantly associate with clinical outcome in cervical carcinoma. Genes Chromosomes Cancer. 2009;48(5):410-8.

34. Chen R, Yao L, Meng T, Xu W. The association between seven ERAP1 polymorphisms and ankylosing spondylitis susceptibility: a meta-analysis involving 8,530 cases and 12,449 controls. Rheumatology International. 2012;32(4):909-14.

35. Martin-Esteban A, Gomez-Molina P, Sanz-Bravo A, Lopez de Castro JA. Combined effects of ankylosing spondylitis-associated ERAP1 polymorphisms outside the catalytic and peptide-binding sites on the processing of natural HLA-B27 ligands. J Biol Chem. 2013.

36. Evnouchidou I, Kamal RP, Seregin SS, Goto Y, Tsujimoto M, Hattori A, et al. Cutting Edge: Coding single nucleotide polymorphisms of endoplasmic reticulum aminopeptidase 1 can affect antigenic peptide generation in vitro by influencing basic enzymatic properties of the enzyme. J Immunol. 2011;186(4):1909-13.

37. Taurog JD, Lowen L, Forman J, Hammer RE. HLA-B27 in inbred and non-inbred transgenic mice. Cell surface expression and recognition as an alloantigen in the absence of human beta 2-microglobulin. J Immunol. 1988;141(11):4020-3.

38. Hammer RE, Maika SD, Richardson JA, Tang JP, Taurog JD. Spontaneous inflammatory disease in transgenic rats expressing HLA-B27 and human beta 2m: an animal model of HLA-B27-associated human disorders. Cell. 1990;63(5):1099-112.

39. DeLay ML, Turner MJ, Klenk EI, Smith JA, Sowders DP, Colbert RA. HLA-B27 misfolding and the unfolded protein response augment interleukin-23 production and are associated with Th17 activation in transgenic rats. Arthritis Rheum. 2009;60(9):2633-43.

40. Braem K, Lories RJ. Insights into the pathophysiology of ankylosing spondylitis: Contributions from animal models. Joint Bone Spine. 2012;79(3):243-8.

41. Medzhitov R, Janeway Jr CA. Innate immunity: impact on the adaptive immune response. Current opinion in immunology. 1997;9(1):4-9.

42. Beutler B. Innate immunity: an overview. Molecular Immunology. 2004;40(12):845-59.

43. Witko-Sarsat V, Rieu P, Descamps-Latscha B, Lesavre P, Halbwachs-Mecarelli L. Neutrophils: Molecules, Functions and Pathophysiological Aspects. Lab Invest. 0000;80(5):617-53.

44. Kucuk A, Uslu AU, Ugan Y, Bagcaci S, Karahan AY, Akarmut A, et al. Neutrophil-to-lymphocyte ratio is involved in the severity of ankylosing spondylitis. Bratisl Lek Listy. 2015;116(12):722-5.

45. Robertson M. Innate immunity. Current Biology. 1998;8(17):R595-R7.

46. Taylor P, Botto M, Walport M. The complement system. Current Biology. 1998;8(8):R259-R61.

47. Cowling P, Ebringer R, Ebringer A. Association of inflammation with raised serum IgA in ankylosing spondylitis. Annals of the Rheumatic Diseases. 1980;39(6):545-9.

48. Kinsella TD, Espinoza L, Vasey FB. Serum complement and immunoglobulin levels in sporadic and familial ankylosing spondylitis. J Rheumatol. 1975;2(3):308-13.

49. Krauledat PB, Krapf FE, Manger B, Kalden JR. Evaluation of plasma C3d and immune complex determinations in the assessment of disease activity of patients with rheumatoid arthritis, systemic lupus erythematosus, and spondylitis ancylopoetica. Rheumatol Int. 1985;5(3):97-101.

50. Brinch L, Vinje O, Teisberg P, Mellbye OJ, Aakesson I. The in-vivo metabolism of C3 in ankylosing spondylitis. Ann Rheum Dis. 1982;41(1):86-9.

51. Ebringer A. The relationship between Klebsiella infection and ankylosing spondylitis. Baillieres Clin Rheumatol. 1989;3(2):321-38.

52. Yang C, Ding P, Wang Q, Zhang L, Zhang X, Zhao J, et al. Inhibition of Complement Retards Ankylosing Spondylitis Progression. Scientific Reports. 2016;6:34643.

53. Foley B, Felices M, Cichocki F, Cooley S, Verneris MR, Miller JS. The biology of NK cells and their receptors affects clinical outcomes after hematopoietic cell transplantation (HCT). Immunol Rev. 2014;258(1):45-63.

54. Mousavi T, Poormoghim H, Moradi M, Tajik N, Shahsavar F, Asadifar B. Inhibitory Killer Cell Immunoglobulin-Like Receptor KIR3DL1 in Combination with HLA-B Bw4(iso) Protect against Ankylosing Spondylitis. Iranian Journal of Immunology. 2010;7(2):88-95.

55. Warren HS, Smyth MJ. NK cells and apoptosis. Immunol Cell Biol. 1999;77(1):64-75.

56. Zhang Y, Wallace DL, de Lara CM, Ghattas H, Asquith B, Worth A, et al. In vivo kinetics of human natural killer cells: the effects of ageing and acute and chronic viral infection. Immunology. 2007;121(2):258-65.

57. Beziat V, Descours B, Parizot C, Debre P, Vieillard V. NK cell terminal differentiation: correlated stepwise decrease of NKG2A and acquisition of KIRs. PLoS One. 2010;5(8):e11966.

58. Laouar Y, Sutterwala FS, Gorelik L, Flavell RA. Transforming growth factor-β controls T helper type 1 cell development through regulation of natural killer cell interferon-γ. Nature Immunology. 2005;6(6):600-7.

59. Ghiringhelli F, Menard C, Terme M, Flament C, Taieb J, Chaput N, et al. CD4+CD25+ regulatory T cells inhibit natural killer cell functions in a transforming growth factor-beta-dependent manner. J Exp Med. 2005;202(8):1075-85.

60. Smyth MJ, Teng MWL, Swann J, Kyparissoudis K, Godfrey DI, Hayakawa Y. CD4+CD25+ T Regulatory Cells Suppress NK Cell-Mediated Immunotherapy of Cancer. The Journal of Immunology. 2006;176(3):1582-7.

61. Presnell SR, Chan HW, Zhang L, Lutz CT. IL-2/IL-15 activate the human clonally restricted KIR3DL1 reverse promoter. Genes and Immunity. 2013;14(2):107-14.

62. Chan AT, Kollnberger SD, Wedderburn LR, Bowness P. Expansion and enhanced survival of natural killer cells expressing the killer immunoglobulin-like receptor KIR3DL2 in spondylarthritis. Arthritis Rheum. 2005;52(11):3586-95.

63. Campbell KS, Hasegawa J. Natural killer cell biology: An update and future directions. Journal of Allergy and Clinical Immunology. 2013;132(3):536-44.

64. Long EO, Rajagopalan S. HLA class I recognition by killer cell Ig-like receptors. Semin Immunol. 2000;12(2):101-8.

65. Koch J, Steinle A, Watzl C, Mandelboim O. Activating natural cytotoxicity receptors of natural killer cells in cancer and infection. Trends in Immunology. 2013;34(4):182-91.

66. Moretta A, Biassoni R, Bottino C, Mingari MC, Moretta L. Natural cytotoxicity receptors that trigger human NK-cell-mediated cytolysis. Immunology Today. 2000;21(5):228-34.

67. Lazetic S, Chang C, Houchins JP, Lanier LL, Phillips JH. Human natural killer cell receptors involved in MHC class I recognition are disulfide-linked heterodimers of CD94 and NKG2 subunits. J Immunol. 1996;157(11):4741-5.

68. Cheent KS, Jamil KM, Cassidy S, Liu M, Mbiribindi B, Mulder A, et al. Synergistic inhibition of natural killer cells by the nonsignaling molecule CD94. Proc Natl Acad Sci U S A. 2013;110(42):16981-6.

69. Long EO, Rajagopalan S. Stress Signals Activate Natural Killer Cells. J Exp Med. 2002;196(11):1399-402. doi:10.084/jem.20021747.

70. Falco M, Moretta L, Moretta A, Bottino C. KIR and KIR ligand polymorphism: a new area for clinical applications? Tissue Antigens. 2013;82(6):363-73.

71. Wang S, Li GX, Ge R, Duan ZH, Zeng Z, Zhang TC, et al. Association of KIR genotype with susceptibility to HLA-B27-positive ankylosing spondylitis. Modern Rheumatology. 2013;23(3):538-41.

72. Beziat V, Traherne JA, Liu LL, Jayaraman J, Enqvist M, Larsson S, et al. Influence of KIR gene copy number on natural killer cell education. Blood. 2013;121(23):4703-7.

73. Christensen MD, Geisler C. Recruitment of SHP-1 protein tyrosine phosphatase and signalling by a chimeric T-cell receptor-killer inhibitory receptor. Scand J Immunol. 2000;51(6):557-64.

74. Campbell KS, Purdy AK. Structure/function of human killer cell immunoglobulin-like receptors: lessons from polymorphisms, evolution, crystal structures and mutations. Immunology. 2011;132(3):315-25.

75. O'Connor GM, Guinan KJ, Cunningham RT, Middleton D, Parham P, Gardiner CM. Functional polymorphism of the KIR3DL1/S1 receptor on human NK cells. J Immunol. 2007;178(1):235-41.

76. Middleton D, Gonzelez F. The extensive polymorphism of KIR genes. Immunology. 2010;129(1):8-19.

77. Foley BA, De Santis D, Van Beelen E, Lathbury LJ, Christiansen FT, Witt CS. The reactivity of Bw4+ HLA-B and HLA-A alleles with KIR3DL1: implications for patient and donor suitability for haploidentical stem cell transplantations. Blood. 2008;112(2):435-43.

78. McCappin J, Harvey D, Wordsworth BP, Middleton D. No association of KIR3DL1 or KIR3DS1 or their alleles with ankylosing spondylitis. Tissue Antigens. 2010;75(1):68-73.

79. Trundley A, Frebel H, Jones D, Chang C, Trowsdale J. Allelic expression patterns of KIR3DS1 and 3DL1 using the Z27 and DX9 antibodies. European Journal of Immunology. 2007;37(3):780-7.

80. Morvan M, Willem C, Gagne K, Kerdudou N, David G, Sebille V, et al. Phenotypic and functional analyses of KIR3DL1+ and KIR3DS1+ NK cell subsets demonstrate differential regulation by Bw4 molecules and induced KIR3DS1 expression on stimulated NK cells. J Immunol. 2009;182(11):6727-35.

81. Martin MP, Gao X, Lee JH, Nelson GW, Detels R, Goedert JJ, et al. Epistatic interaction between KIR3DS1 and HLA-B delays the progression to AIDS. Nat Genet. 2002;31(4):429-34.

82. Martin MP, Qi Y, Gao X, Yamada E, Martin JN, Pereyra F, et al. Innate partnership of HLA-B and KIR3DL1 subtypes against HIV-1. Nat Genet. 2007;39(6):733-40.

83. Hansasuta P, Dong T, Thananchai H, Weekes M, Willberg C, Aldemir H, et al. Recognition of HLA-A3 and HLA-A11 by KIR3DL2 is peptide-specific. European Journal of Immunology. 2004;34(6):1673-9.

84. Pende D, Biassoni R, Cantoni C, Verdiani S, Falco M, di Donato C, et al. The natural killer cell receptor specific for HLA-A allotypes: a novel member of the p58/p70 family of inhibitory receptors that is characterized by three immunoglobulin-like domains and is expressed as a 140-kD disulphide-linked dimer. J Exp Med. 1996;184(2):505-18.

85. Hatano H, Shaw J, Marquardt K, Zhang Z, Gauthier L, Chanteux S, et al. The D0 Ig-like domain plays a central role in the stronger binding of KIR3DL2 to B27 free H chain dimers. J Immunol. 2015;194(4):1591-601.

86. Azuz-Lieberman N, Markel G, Mizrahi S, Gazit R, Hanna J, Achdout H, et al. The involvement of NK cells in ankylosing spondylitis. International Immunology. 2005;17(7):837-45.

87. Diaz-Pena R, Vidal-Castineira JR, Alonso-Arias R, Suarez-Alvarez B, Vicario JL, Solana R, et al. Association of the KIR3DS1*013 and KIR3DL1*004 Alleles With Susceptibility to Ankylosing Spondylitis. Arthritis Rheum. 2010;62(4):1000-6.

88. Tajik N, Shahsavar F, Poormoghim H, Radjabzadeh MF, Mousavi T, Jalali A. KIR3DL1+HLA-B Bw4(Ile80) and KIR2DS1+HLA-C2 combinations are both associated with ankylosing spondylitis in the Iranian population. International Journal of Immunogenetics. 2011;38(5):403-9.

89. Bowness P, Ridley A, Shaw J, Chan AT, Wong-Baeza I, Fleming M, et al. Th17 cells expressing KIR3DL2+ and responsive to HLA-B27 homodimers are increased in ankylosing spondylitis. J Immunol. 2011;186(4):2672-80.

90. Wong-Baeza I, Ridley A, Shaw J, Hatano H, Rysnik O, McHugh K, et al. KIR3DL2 binds to HLA-B27 dimers and free H chains more strongly than other HLA class I and promotes the expansion of T cells in ankylosing spondylitis. J Immunol. 2013;190(7):3216-24.

91. Scrivo R, Morrone S, Spadaro A, Santoni A, Valesini G. Evaluation of Degranulation and Cytokine Production in Natural Killer Cells from Spondyloarthritis Patients at Single-Cell Level. Cytometry Part B-Clinical Cytometry. 2011;80B(1):22-7.

92. Iwakura Y, Ishigame H. The IL-23/IL-17 axis in inflammation. The Journal of Clinical Investigation. 2006;116(5):1218-22.

93. Murphy CA, Langrish CL, Chen Y, Blumenschein W, McClanahan T, Kastelein RA, et al. Divergent pro- and antiinflammatory roles for IL-23 and IL-12 in joint autoimmune inflammation. J Exp Med. 2003;198(12):1951-7.

94. McGeachy MJ, Cua DJ. Th17 cell differentiation: the long and winding road. Immunity. 2008;28(4):445-53.

95. Miceli MC, Parnes JR. The roles of CD4 and CD8 in T cell activation. Semin Immunol. 1991;3(3):133-41.

96. Schirmer M, Goldberger C, Würzner R, Duftner C, Pfeiffer K-P, Clausen J, et al. Circulating cytotoxic CD8+ CD28-T cells in ankylosing spondylitis. Arthritis Research & Therapy. 2001;4(1):1.

97. Atagunduz P, Appel H, Kuon W, Wu P, Thiel A, Kloetzel PM, et al. HLA-B27-restricted CD8+ T cell response to cartilage-derived self peptides in ankylosing spondylitis. Arthritis Rheum. 2005;52(3):892-901.

98. Duftner C, Goldberger C, Falkenbach A, Würzner R, Falkensammer B, Pfeiffer KP, et al. Prevalence, clinical relevance and characterization of circulating cytotoxic CD4+ CD28-T cells in ankylosing spondylitis. Arthritis Res Ther. 2003;5(5):1.

99. Yang PT, Kasai H, Zhao LJ, Xiao WG, Tanabe F, Ito M. Increased CCR4 expression on circulating CD4+ T cells in ankylosing spondylitis, rheumatoid arthritis and systemic lupus erythematosus.

100. Wang C, Liao Q, Hu Y, Zhong D. T lymphocyte subset imbalances in patients contribute to ankylosing spondylitis. Exp Ther Med. 2015;9(1):250-6. Epub 2014 Nov 4 doi:10.3892/etm.2014.46.

101. Liao HT, Lin YF, Tsai CY, Chou CT. Regulatory T cells in ankylosing spondylitis and the response after adalimumab treatment. Joint Bone Spine. 2015;82(6):423-7. doi: 10.1016/j.jbspin.2015.03.003. Epub Jul 15.

102. Wu Y, Ren M, Yang R, Liang X, Ma Y, Tang Y, et al. Reduced immunomodulation potential of bone marrow-derived mesenchymal stem cells induced CCR4+ CCR6+ Th/Treg cell subset imbalance in ankylosing spondylitis. Arthritis research & therapy. 2011;13(1):1.

103. Vilches C, Castano J, Gomez-Lozano N, Estefania E. Facilitation of KIR genotyping by a PCR-SSP method that amplifies short DNA fragments. Tissue Antigens. 2007;70(5):415-22.

104. Gardiner CM, Guethlein LA, Shilling HG, Pando M, Carr WH, Rajalingam R, et al. Different NK cell surface phenotypes defined by the DX9 antibody are due to KIR3DL1 gene polymorphism. J Immunol. 2001;166(5):2992-3001.

105. Shimizu Y, DeMars R. Production of human cells expressing individual transferred HLA-A,-B,-C genes using an HLA-A,-B,-C null human cell line. The Journal of Immunology. 1989;142(9):3320-8.

106. Alter G, Malenfant JM, Altfeld M. CD107a as a functional marker for the identification of natural killer cell activity. J Immunol Methods. 2004;294(1-2):15-22.

107. Betts MR, Brenchley JM, Price DA, De Rosa SC, Douek DC, Roederer M, et al. Sensitive and viable identification of antigen-specific CD8+ T cells by a flow cytometric assay for degranulation. J Immunol Methods. 2003;281(1-2):65-78.

108. Dushek O, van der Merwe PA. An induced rebinding model of antigen discrimination(). Trends Immunol. 2014;35(4):153-8.

109. Misumi Y, Miki K, Takatsuki A, Tamura G, Ikehara Y. Novel blockade by brefeldin A of intracellular transport of secretory proteins in cultured rat hepatocytes. Journal of Biological Chemistry. 1986;261(24):11398-403.

110. Ljunggren HG, Stam NJ, Ohlen C, Neefjes JJ, Hoglund P, Heemels MT, et al. Empty MHC class I molecules come out in the cold. Nature. 1990;346(6283):476-80.

111. Grandea AG, 3rd, Van Kaer L. Tapasin: an ER chaperone that controls MHC class I assembly with peptide. Trends Immunol. 2001;22(4):194-9.

112. Salter RD, Howell DN, Cresswell P. Genes regulating HLA class I antigen expression in T-B lymphoblast hybrids. Immunogenetics. 1985;21(3):235-46.

113. Yu YYL, Netuschil N, Lybarger L, Connolly JM, Hansen TH. Cutting Edge: Single-Chain Trimers of MHC Class I Molecules Form Stable Structures That Potently Stimulate Antigen-Specific T Cells and B Cells. The Journal of Immunology. 2002;168(7):3145-9.

114. Truscott SM, Lybarger L, Martinko JM, Mitaksov VE, Kranz DM, Connolly JM, et al. Disulfide Bond Engineering to Trap Peptides in the MHC Class I Binding Groove. The Journal of Immunology. 2007;178(10):6280-9.

115. Peruzzi M, Parker KC, Long EO, Malnati MS. Peptide sequence requirements for the recognition of HLA-B*2705 by specific natural killer cells. J Immunol. 1996;157(8):3350-6.

116. Vivian JP, Duncan RC, Berry R, O'Connor GM, Reid HH, Beddoe T, et al. Killer cell immunoglobulin-like receptor 3DL1-mediated recognition of human leukocyte antigen B. Nature. 2011;479(7373):401-5.

117. Brewerton DA, Hart FD, Nicholls A, Caffrey M, James DC, Sturrock RD. Ankylosing spondylitis and HL-A 27. Lancet. 1973;1(7809):904-7.

118. Schlosstein L, Terasaki PI, Bluestone R, Pearson CM. High association of an HL-A antigen, W27, with ankylosing spondylitis. N Engl J Med. 1973;288(14):704-6.

119. Luft T, Rizkalla M, Tai TY, Chen Q, MacFarlan RI, Davis ID, et al. Exogenous peptides presented by transporter associated with antigen processing (TAP)-deficient and TAP-competent cells: intracellular loading and kinetics of presentation. J Immunol. 2001;167(5):2529-37.

120. Goldsmith K, Chen W, Johnson DC, Hendricks RL. Infected cell protein (ICP)47 enhances herpes simplex virus neurovirulence by blocking the CD8+ T cell response. J Exp Med. 1998;187(3):341-8.

121. Garcia-Medel N, Sanz-Bravo A, Dung Van N, Galocha B, Gomez-Molina P, Martin-Esteban A, et al. Functional Interaction of the Ankylosing Spondylitis-associated Endoplasmic Reticulum Aminopeptidase 1 Polymorphism and HLA-B27 in Vivo. Molecular & Cellular Proteomics. 2012;11(11):1416-29.

122. Sanz-Bravo A, Campos J, Mazariegos MS, LopezdeCastro JA. Dominant role of the ERAP1 polymorphism R528K in shaping the HLA-B27 peptidome through differential processing determined by multiple peptide residues. Arthritis Rheumatol. 2014.

123. Zemmour J, Little AM, Schendel DJ, Parham P. The HLA-A,B "negative" mutant cell line C1R expresses a novel HLA-B35 allele, which also has a point mutation in the translation initiation codon. Journal of immunology (Baltimore, Md : 1950). 1992;148(6):1941-8.

124. Parker KC, Biddison WE, Coligan JE. Pocket mutations of HLA-B27 show that anchor residues act cumulatively to stabilize peptide binding. Biochemistry. 1994;33(24):7736-43.

125. Lopez de Castro JA, Alvarez I, Marcilla M, Paradela A, Ramos M, Sesma L, et al. HLA-B27: a registry of constitutive peptide ligands. Tissue Antigens. 2004;63(5):424-45.

126. Fadda L, O'Connor GM, Kumar S, Piechocka-Trocha A, Gardiner CM, Carrington M, et al. Common HIV-1 peptide variants mediate differential binding of KIR3DL1 to HLA-Bw4 molecules. J Virol. 2011;85(12):5970-4.

127. Fadda L, Borhis G, Ahmed P, Cheent K, Pageon SV, Cazaly A, et al. Peptide antagonism as a mechanism for NK cell activation. Proc Natl Acad Sci U S A. 2010;107(22):10160-5.

128. Espmark JA, Ahlqvist-Roth L, Sarne L, Persson A. Tissue typing of cells in culture. III. HLA antigens of established human cell lines. Attempts at typing by the mixed hemadsorption technique. Tissue Antigens. 1978;11(3):279-86.

129. Benham AM, Gromme M, Neefjes J. Allelic differences in the relationship between proteasome activity and MHC class I peptide loading. Journal of immunology (Baltimore, Md : 1950). 1998;161(1):83-9.

130. Smyth MJ, Cretney E, Kelly JM, Westwood JA, Street SEA, Yagita H, et al. Activation of NK cell cytotoxicity. Molecular Immunology. 2005;42(4):501-10.

131. Abdullah H, Zhang Z, Yee K, Haroon N. KIR3DL1 interaction with HLA-B27 is altered by ankylosing spondylitis associated ERAP1 and enhanced by MHC class I cross-linking. Discovery medicine. 2015;20(108):79-89.

132. Martin-Esteban A, Gomez-Molina P, Sanz-Bravo A, Lopez de Castro JA. Combined effects of ankylosing spondylitis-associated ERAP1 polymorphisms outside the catalytic and peptide-binding sites on the processing of natural HLA-B27 ligands. J Biol Chem. 2014;289(7):3978-90.

133. Kollnberger S, Chan A, Sun MY, Chen LY, Wright C, di Gleria K, et al. Interaction of HLA-B27 homodimers with KIR3DL1 and KIR3DL2, unlike HLA-B27 heterotrimers, is independent of the sequence of bound peptide. Eur J Immunol. 2007;37(5):1313-22.

134. Antoniou AN, Ford S, Taurog JD, Butcher GW, Powis SJ. Formation of HLA-B27 Homodimers and Their Relationship to Assembly Kinetics. Journal of Biological Chemistry. 2004;279(10):8895-902.

135. Marroquin Belaunzaran O, Kleber S, Schauer S, Hausmann M, Nicholls F, Van den Broek M, et al. HLA-B27-Homodimer-Specific Antibody Modulates the Expansion of Pro-Inflammatory T-Cells in HLA-B27 Transgenic Rats. PLoS One. 2015;10(6):e0130811. doi:10.1371/journal.pone..

136. Bal A, Unlu E, Bahar G, Aydog E, Eksioglu E, Yorgancioglu R. Comparison of serum IL-1β, sIL-2R, IL-6, and TNF-α levels with disease activity parameters in ankylosing spondylitis. Clinical Rheumatology. 2007;26(2):211-5.

137. Alessandro Moretta, Cristina Bottino, Massimo Vitale, Daniela Pende, Claudia Cantoni, Maria Cristina Mingari, et al. ACTIVATING RECEPTORS AND CORECEPTORS INVOLVED IN HUMAN NATURAL KILLER CELL-MEDIATED CYTOLYSIS. Annual Review of Immunology. 2001;19(1):197-223.

138. Dong W, Zhang Y, Yan M, Liu H, Chen Z, Zhu P. Upregulation of 78-kDa glucose-regulated protein in macrophages in peripheral joints of active ankylosing spondylitis. Scand J Rheumatol. 2008;37(6):427-34. doi: 10.1080/03009740802213310.

139. Gratacos J, Collado A, Filella X, Sanmarti R, Canete J, Llena J, et al. Serum cytokines (IL-6, TNF-alpha, IL-1 beta and IFN-gamma) in ankylosing spondylitis: a close correlation between serum IL-6 and disease activity and severity. Br J Rheumatol. 1994;33(10):927-31.

140. Caldwell J, Emerson SG. IL-1 alpha and TNF alpha act synergistically to stimulate production of myeloid colony-stimulating factors by cultured human bone marrow stromal cells and cloned stromal cell strains. J Cell Physiol. 1994;159(2):221-8.

141. Taurog JD, Dorris ML, Satumtira N, Tran TM, Sharma R, Dressel R, et al. Spondylarthritis in HLA-B27/human beta2-microglobulin-transgenic rats is not prevented by lack of CD8. Arthritis Rheum. 2009;60(7):1977-84.

142. Zafirova B, Wensveen FM, Gulin M, Polić B. Regulation of immune cell function and differentiation by the NKG2D receptor. Cell Mol Life Sci. 2011;68(21):3519-29. Epub 2011 Sep 6 doi:10.1007/s00018-011-0797-0.

143. Regunathan J, Chen Y, Wang D, Malarkannan S. NKG2D receptor-mediated NK cell function is regulated by inhibitory Ly49 receptors. Blood. 2005;105(1):233-40. Epub 2004 Aug 24.

144. Kenna TJ, Lau MC, Keith P, Ciccia F, Costello ME, Bradbury L, et al. Disease-associated polymorphisms in ERAP1 do not alter endoplasmic reticulum stress in patients with ankylosing spondylitis. Genes Immun. 2015;16(1):35-42. doi: 10.1038/gene.2014.62. Epub Nov 6.

145. Jewett A, Bonavida B. Peripheral blood monocytes derived from HIV+ individuals mediate antibody-dependent cellular cytotoxicity (ADCC). Clin Immunol Immunopathol. 1990;54(2):192-9.

146. Chou CT, Huo AP, Chang HN, Tsai CY, Chen WS, Wang HP. Cytokine production from peripheral blood mononuclear cells in patients with ankylosing spondylitis and their first-degree relatives. Arch Med Res. 2007;38(2):190-5.

147. Vazquez-Del Mercado M, Garcia-Gonzalez A, Munoz-Valle JF, Garcia-Iglesias T, Martinez-Bonilla G, Bernard-Medina G, et al. Interleukin 1beta (IL-1beta), IL-10, tumor necrosis factor-alpha, and cellular proliferation index in peripheral blood mononuclear cells in patients with ankylosing spondylitis. J Rheumatol. 2002;29(3):522-6.

148. Muhl H, Pfeilschifter J. Anti-inflammatory properties of pro-inflammatory interferon-gamma. Int Immunopharmacol. 2003;3(9):1247-55.

149. Ruschen S, Lemm G, Warnatz H. Spontaneous and LPS-stimulated production of intracellular IL-1 beta by synovial macrophages in rheumatoid arthritis is inhibited by IFN-gamma. Clin Exp Immunol. 1989;76(2):246-51.

150. Dellacasagrande J, Ghigo E, Raoult D, Capo C, Mege JL. IFN-gamma-induced apoptosis and microbicidal activity in monocytes harboring the intracellular bacterium Coxiella burnetii require membrane TNF and homotypic cell adherence. J Immunol. 2002;169(11):6309-15.

151. Caligiuri MA. Human natural killer cells. Blood. 2008;112(3):461-9. doi: 10.1182/blood-2007-09-077438.

152. Antoniv TT, Ivashkiv LB. Dysregulation of interleukin-10-dependent gene expression in rheumatoid arthritis synovial macrophages. Arthritis Rheum. 2006;54(9):2711-21.

153. Chen L, Ridley A, Hammitzsch A, Al-Mossawi MH, Bunting H, Georgiadis D, et al. Silencing or inhibition of endoplasmic reticulum aminopeptidase 1 (ERAP1) suppresses free heavy chain expression and Th17 responses in ankylosing spondylitis. Ann Rheum Dis. 2015.

154. Gan P-Y, Steinmetz OM, Tan DSY, O'Sullivan KM, Ooi JD, Iwakura Y, et al. Th17 Cells Promote Autoimmune Anti-Myeloperoxidase Glomerulonephritis. Journal of the American Society of Nephrology. 2010;21(6):925-31.

155. Tanaka Y, Nakayamada S, Okada Y. Osteoblasts and osteoclasts in bone remodeling and inflammation. Curr Drug Targets Inflamm Allergy. 2005;4(3):325-8.

156. Zhao B, Grimes SN, Li S, Hu X, Ivashkiv LB. TNF-induced osteoclastogenesis and inflammatory bone resorption are inhibited by transcription factor RBP-J. The Journal of Experimental Medicine. 2012;209(2):319-34.

157. Colina M, Penolazzi L, di Ciano M, Lambertini E, Ciancio G, Orzincolo C, et al. Osteoclasts from peripheral blood mononuclear cells culture of ankylosing spondylitis subjects are resistant to apoptosis. Biomedicine & Preventive Nutrition. 2013;3(3):253-9.

158. Takayanagi H, Ogasawara K, Hida S, Chiba T, Murata S, Sato K, et al. T-cell-mediated regulation of osteoclastogenesis by signalling cross-talk between RANKL and IFN-gamma. Nature. 2000;408(6812):600-5.

159. Owens JM, Gallagher AC, Chambers TJ. IL-10 modulates formation of osteoclasts in murine hemopoietic cultures. J Immunol. 1996;157(2):936-40.

160. Bottino C, Castriconi R, Moretta L, Moretta A. Cellular ligands of activating NK receptors. Trends in Immunology. 2005;26(4):221-6.

161. Lauwerys BR, Garot N, Renauld J-C, Houssiau FA. Cytokine Production and Killer Activity of NK/T-NK Cells Derived with IL-2, IL-15, or the Combination of IL-12 and IL-18. The Journal of Immunology. 2000;165(4):1847-53.

162. Brewerton DA, Hart FD, Nicholls A, Caffrey M, James DC, Sturrock RD. Ankylosing spondylitis and HL-A 27. Lancet (London, England). 1973;1(7809):904-7.

163. Schlosstein L, Terasaki PI, Bluestone R, Pearson CM. High Association of an HL-A Antigen, W27, with Ankylosing Spondylitis. New England Journal of Medicine. 1973;288(14):704-6.

164. van der Linden SM, Valkenburg HA, de Jongh BM, Cats A. The risk of developing ankylosing spondylitis in HLA-B27 positive individuals. A comparison of relatives of spondylitis patients with the general population. Arthritis Rheum. 1984;27(3):241-9.

165. Khan MA, Kushner I, Braun WE. Comparison of clinical features in HLA-B27 positive and negative patients with ankylosing spondylitis. Arthritis & Rheumatism. 1977;20(4):909-12.

166. Kim TJ, Na KS, Lee HJ, Lee B, Kim TH. HLA-B27 homozygosity has no influence on clinical manifestations and functional disability in ankylosing spondylitis. Clinical and experimental rheumatology. 2009;27(4):574-9.

167. Gomez P, Montserrat V, Marcilla M, Paradela A, de Castro JA. B*2707 differs in peptide specificity from B*2705 and B*2704 as much as from HLA-B27 subtypes not associated to spondyloarthritis. Eur J Immunol. 2006;36(7):1867-81.

168. TAUROG JD. The Role of HLA-B27 in Spondyloarthritis. The Journal of Rheumatology. 2010;37(12):2606-16.

169. Lopez-Larrea C, Sujirachato K, Mehra NK, Chiewsilp P, Isarangkura D, Kanga U, et al. HLA-B27 subtypes in Asian patients with ankylosing spondylitis. Evidence for new associations. Tissue Antigens. 1995;45(3):169-76.

170. Nasution AR, Mardjuadi A, Kunmartini S, Suryadhana NG, Setyohadi B, Sudarsono D, et al. HLA-B27 subtypes positively and negatively associated with spondyloarthropathy. J Rheumatol. 1997;24(6):1111-4.

171. D'Amato M, Fiorillo MT, Carcassi C, Mathieu A, Zuccarelli A, Bitti PP, et al. Relevance of residue 116 of HLA-B27 in determining susceptibility to ankylosing spondylitis. Eur J Immunol. 1995;25(11):3199-201.

172. Khakoo SI, Geller R, Shin S, Jenkins JA, Parham P. The D0 domain of KIR3D acts as a major histocompatibility complex class I binding enhancer. J Exp Med. 2002;196(7):911-21.

173. Furukawa L, Brevetti LS, Brady SE, Johnson D, Ma M, Welling TH, et al. Adenoviral-mediated gene transfer of ICP47 inhibits major histocompatibility complex class I expression on vascular cells in vitro. Journal of vascular surgery. 2000;31(3):558-66.

174. Chen L, Fischer R, Peng Y, Reeves E, McHugh K, Ternette N, et al. Critical role of endoplasmic reticulum aminopeptidase 1 in determining the length and sequence of peptides bound and presented by HLA-B27. Arthritis Rheumatol. 2014;66(2):284-94.

175. Cauli A, Shaw J, Giles J, Hatano H, Rysnik O, Payeli S, et al. The arthritis-associated HLA-B*27:05 allele forms more cell surface B27 dimer and free heavy chain ligands for KIR3DL2 than HLA-B*27:09. Rheumatology (Oxford, England). 2013;52(11):1952-62.

176. Sreedharan SP, Huang JX, Cheung MC, Goetzl EJ. Structure, expression, and chromosomal localization of the type I human vasoactive intestinal peptide receptor gene. Proc Natl Acad Sci U S A. 1995;92(7):2939-43.

177. Fiorillo MT, Maragno M, Butler R, Dupuis ML, Sorrentino R. CD8(+) T-cell autoreactivity to an HLA-B27-restricted self-epitope correlates with ankylosing spondylitis. J Clin Invest. 2000;106(1):47-53.

178. Hulsmeyer M, Hillig RC, Volz A, Ruhl M, Schroder W, Saenger W, et al. HLA-B27 subtypes differentially associated with disease exhibit subtle structural alterations. J Biol Chem. 2002;277(49):47844-53.

179. Stewart-Jones GB, di Gleria K, Kollnberger S, McMichael AJ, Jones EY, Bowness P. Crystal structures and KIR3DL1 recognition of three immunodominant viral peptides complexed to HLA-B 2705. Eur J Immunol. 2005;35(2):341-51.

180. Bondos SE, Bicknell A. Detection and prevention of protein aggregation before, during, and after purification. Anal Biochem. 2003;316(2):223-31.

181. Middelberg AP. Preparative protein refolding. Trends Biotechnol. 2002;20(10):437-43.

182. Bowness P. HLA B27 in health and disease: a double-edged sword? Rheumatology. 2002;41(8):857-68.

183. Flores-Villanueva PO, Yunis EJ, Delgado JC, Vittinghoff E, Buchbinder S, Leung JY, et al. Control of HIV-1 viremia and protection from AIDS are associated with HLA-Bw4 homozygosity. Proc Natl Acad Sci U S A. 2001;98(9):5140-5.

184. Ramos M, Paradela A, Vazquez M, Marina A, Vazquez J, Lopez de Castro JA. Differential association of HLA-B*2705 and B*2709 to ankylosing spondylitis correlates with limited peptide subsets but not with altered cell surface stability. J Biol Chem. 2002;277(32):28749-56.

185. Xueyi L, Lina C, Zhenbiao W, Qing H, Qiang L, Zhu P. Levels of circulating Th17 cells and regulatory T cells in ankylosing spondylitis patients with an inadequate response to anti-TNF-alpha therapy. J Clin Immunol. 2013;33(1):151-61. doi: 10.1007/s10875-012-9774-0. Epub 2012 Aug 29.

186. Kim S, Poursine-Laurent J, Truscott SM, Lybarger L, Song Y-J, Yang L, et al. Licensing of natural killer cells by host major histocompatibility complex class I molecules. Nature. 2005;436(7051):709-13.

187. Parsons MS, Zipperlen K, Gallant M, Grant M. Killer cell immunoglobulin-like receptor 3DL1 licenses CD16-mediated effector functions of natural killer cells. Journal of Leukocyte Biology. 2010;88(5):905-12.

188. Fernandez NC, Treiner E, Vance RE, Jamieson AM, Lemieux S, Raulet DH. A subset of natural killer cells achieves self-tolerance without expressing inhibitory receptors specific for self-MHC molecules2005 2005-06-01 00:00:00. 4416-23 p.

189. Brodin P, Lakshmikanth T, Johansson S, Kärre K, Höglund P. The strength of inhibitory input during education quantitatively tunes the functional responsiveness of individual natural killer cells2009 2009-03-12 00:00:00. 2434-41 p.

190. Fernandez NC, Treiner E, Vance RE, Jamieson AM, Lemieux S, Raulet DH. A subset of natural killer cells achieves self-tolerance without expressing inhibitory receptors specific for self-MHC molecules. Blood. 2005;105(11):4416-23. Epub 2005 Feb 22.

191. Yawata M, Yawata N, Draghi M, Partheniou F, Little AM, Parham P. MHC class I-specific inhibitory receptors and their ligands structure diverse human NK-cell repertoires toward a balance of missing self-response. Blood. 2008;112(6):2369-80. doi: 10.1182/blood-2008-03-143727. Epub 2008 Jun 26.

192. Orr MT, Lanier LL. Natural killer cell education and tolerance. Cell. 2010;142(6):847-56. doi: 10.1016/j.cell.2010.08.031.

193. Granados DP, Tanguay P-L, Hardy M-P, Caron É, de Verteuil D, Meloche S, et al. ER stress affects processing of MHC class I-associated peptides. BMC Immunology. 2009;10(1):1-15.